



HAL
open science

Haptic Rendering in Virtual Reality During Interaction with Tangibles

Xavier de Tinguy

► **To cite this version:**

Xavier de Tinguy. Haptic Rendering in Virtual Reality During Interaction with Tangibles. Computer Science [cs]. INSA Rennes, 2020. English. NNT: . tel-03299362

HAL Id: tel-03299362

<https://theses.hal.science/tel-03299362v1>

Submitted on 26 Jul 2021

HAL is a multi-disciplinary open access archive for the deposit and dissemination of scientific research documents, whether they are published or not. The documents may come from teaching and research institutions in France or abroad, or from public or private research centers.

L'archive ouverte pluridisciplinaire **HAL**, est destinée au dépôt et à la diffusion de documents scientifiques de niveau recherche, publiés ou non, émanant des établissements d'enseignement et de recherche français ou étrangers, des laboratoires publics ou privés.

THESE DE DOCTORAT DE

L'INSA DE RENNES

ECOLE DOCTORALE N° 601
*Mathématiques et Sciences et Technologies
de l'Information et de la Communication*
Spécialité : *Informatique*

Par

Xavier de TINGUY

Haptic Rendering in Virtual Reality During Interaction with Tangibles

Thèse présentée et soutenue à Rennes, le 14/12/2020

Unité de recherche : IRISA

Thèse N° : 20ISAR 29 / D20 - 29

Rapporteurs avant soutenance :

Jeremy Cooperstock Professeur, Univ. McGill, Canada
Matthias Harders Professeur, Univ. Innsbruck, Austria

Composition du Jury :

Président :	Paolo Robuffo Giordano	Directeur de Recherche, HDR, CNRS, Univ Rennes, Inria, IRISA
Examineurs :	Francesco Chinello Paolo Robuffo Giordano	Associate Professor, Univ. Aarhus, Denmark Directeur de Recherche, HDR, CNRS, Univ Rennes, Inria, IRISA
Dir. de thèse :	Maud Marchal	Maître de Conférences, HDR, Univ Rennes, INSA, IRISA
Co-encadrant :	Claudio Pacchierotti	Chargé de Recherche, CNRS, Univ Rennes, Inria, IRISA

Acknowledgments

First, I would like to thank my advisors, Maud Marchal and Claudio Pacchierotti for supervising me during these three years. They taught me everything about conducting research, from having an idea, a concept, to the writing of a scientific article. Maud provided a lot of support on the experimental design and data analysis of the various experiments that I conducted, while Claudio found ways to simplify and clarify the overly detailed draft that I wrote. I thank them for spending with me all these all-nighters to correct and complete an article, a video, a presentation which turned into plenty successfully accepted works.

I would also like to thank the members of the PhD committee for reading this manuscript, for their participation to the virtual defense and for their patience discussing this piece of work despite all the last-minute technical issues.

Then, I would thank the various professors and advisors I had and which guide me toward this PhD. Especially two professors I had during my first year of preparatory class at Condorcet, Mr Benlhajlahsen and Mr Lafitte who I sincerely thank for their rigorous teachings. They set me on the right tracks and taught me to always work harder without giving up which helped me to overcome various hardships. But also, Simon who was my advisor during my first internship and who taught me a lot about programming, research, and to always question things and search for answers. And I would also thank Anatole Lecuyer for hosting this PhD within his Hybrid team and for always providing efficient advices.

I particularly want to thank my colleague and dear friend Thomas Howard with whom we discussed crazy ideas and end up developing the WeATaViX in a single month. I would like to also thank Sarah Viguier, my family and friends for proofreading this manuscript.

Finally, I thank all researchers, PhD students, engineers and postdocs that I met at Inria, especially in Hybrid and Mimetic, all the very good friend that I met in Rennes, the ones from Paris, and those who identify themselves as being asked "to roast a piglet".

Special mention to Mushu for sleeping below my desk.

Contents

List of Figures	vii
List of Tables	xi
Résumé Long en Français	xiii
1 Introduction	1
2 Related Work	13
2.1 Haptics: a General Overview	15
2.1.1 Haptic Sense	15
2.1.2 Haptic Interfaces	16
2.1.3 Haptic Rendering	30
2.1.4 Haptic Illusions	33
2.2 Tangible Props in VR	34
2.2.1 Tangible Objects	35
2.2.2 Tangible Surroundings	42
2.3 Application of Tangibles in Virtual Environment	47
2.3.1 Passive Haptics	47
2.3.2 Beyond Passive Haptics	52
2.4 Discussion on the Role of Tangibles in VR Interaction	63
I Improving the Rendering of Virtual Objects using Tangibles	69
3 Enhancing the Stiffness Perception of Tangible Objects in Mixed Reality Using Wearable Haptics	71
3.1 Proof of concept: augmenting tangible objects stiffness using a finger wearable tactile device	73
3.1.1 Motivation and Concept	73
3.1.2 2-DoF Wearable Haptic Device	74
3.1.3 Demonstrator: Increasing the Stiffness of a Foam as It Is Pressed	75
3.2 Perceptual evaluation	75
3.2.1 Experimental Apparatus and Participants	76
3.2.2 Procedure	76
3.2.3 Conditions and Plan	77
3.2.4 Collected Data	78
3.2.5 Results	78
3.3 Use cases	81
3.3.1 Setup	82
3.3.2 Use Cases Descriptions	82

3.4	Discussion	84
3.5	Conclusion	86
4	How Different Tangible and Virtual Objects Can Be While Still Feeling the Same?	87
4.1	Methods	88
4.1.1	Experimental setup	89
4.1.2	Experimental task and procedure	89
4.2	User study #1: Width	90
4.2.1	Procedure Description	90
4.2.2	Experimental Design and Participants	91
4.2.3	Results	91
4.3	User study #2: Local Orientation	92
4.3.1	Procedure Description	92
4.3.2	Experimental Design and Participants	92
4.3.3	Results	93
4.4	User study #3: Local Curvature	94
4.4.1	Procedure Description	94
4.4.2	Experimental Design and Participants	94
4.4.3	Results	94
4.5	Subjective Questionnaire	95
4.6	Discussion	96
4.7	Conclusions	97
5	Toward Universal Tangible Objects: Optimizing Haptic Pinching Sensations in 3D Interaction	99
5.1	Description of the Algorithm	102
5.1.1	Object description: a set of pinch poses	103
5.1.2	Cost Function: rating the association	106
5.1.3	Algorithm Implementation	113
5.2	User Study	116
5.2.1	Experiment Description	117
5.2.2	Conditions	119
5.2.3	Collected Data	120
5.2.4	Results	121
5.3	Discussion	124
5.4	Conclusion	125
II	Improving the Registration between Tangibles and Virtual Objects	127
6	Capacitive Sensing for Improving Contact Rendering with Tangible Objects in VR	129
6.1	Capacitive Sensing for Tangibles in Virtual Reality	130
6.1.1	Context of Application	130
6.1.2	Prior Capacitive Sensing Applications	131
6.1.3	Motivation: Embedding Tangibles with Proximity Capacitive Sensing	132
6.2	Method	134
6.2.1	Capacitive Sensitivity to Human Hand	134
6.2.2	Apparatus	135
6.2.3	Capacitive Sensing	135
6.2.4	Signal Characterization	141

6.2.5	Visuohaptic Retargeting	141
6.3	User Study	144
6.3.1	Experimental Methods	144
6.3.2	Experimental Results	147
6.4	Discussion	149
6.5	Conclusion	151
7	WeATaViX: WEarable Actuated TAngibles for VIRTUAL reality eXperiences	153
7.1	The WeATaViX haptic interface	154
7.1.1	Motivation and Consideration	154
7.1.2	Design and description	155
7.1.3	Evaluation of the device performance	157
7.2	Interaction technique in VR	158
7.2.1	Command of the Servomotor	158
7.2.2	States of the Grasp Interaction	159
7.3	User study	160
7.3.1	Static task	161
7.3.2	Dynamic Task	161
7.3.3	Results and Discussion	162
7.4	Use case	163
7.5	Conclusion and perspectives	164
8	Conclusion	165
	Conclusion	165
	Appendices and Bibliography	172
A	Author's publications	I
B	Tracking Solution	III
	Bibliography	XI

List of Figures

1	Notre Approche Implementée Dans un Scénario Virtuel de Palpation Médicale.	xvi
2	Objectif : Induire un Décalage Entre le Tangible et le Virtuel.	xvii
3	Un Carrousel d’Objets Virtuels.	xviii
4	Divergences au Contact Tangible.	xix
5	Structure du WeATaViX.	xx
1.1	Perception-Action Loop in Virtual Environment.	2
1.2	Haptic Devices Used in this Manuscript.	5
1.3	Using tangibles in Virtual Reality.	5
1.4	Perception-Action Loop When Using <i>Tangibles</i> in Virtual Environment.	7
2.1	Encounter-Type with Robotic Arm, Part 1.	18
2.2	Encounter-Type with Robotic Arm, Part 2.	19
2.3	Encounter-Type using Drones.	20
2.4	Encounter-Type using Robots.	21
2.5	Encounter-Type using Encasing Structure.	21
2.6	Reference grasps for hand-held devices.	22
2.7	Hand-Held Passive Devices.	23
2.8	Hand-Held Self-Reconfigurable Devices.	23
2.9	Active Hand-Held Devices Providing Feedback Non-Limited to the Hand.	25
2.10	Active Hand-Held Devices Providing Feedback Within Medium Warp Grasp.	26
2.11	Active Hand-Held Devices Providing Feedback Within Writing Tripod Grasp.	26
2.12	Active Hand-Held Devices Providing Feedback For Index Finger Extention Grasp.	27
2.13	Active Hand-Held Devices Providing Feedback and Actuation for Pinching.	28
2.14	Wearable Devices for Contact and Orientation Display.	29
2.15	Wearable Devices for Pressure and Skin Stretch Display.	29
2.16	Compact Wearable Devices.	31
2.17	Simple Haptic Rendering Algorithm.	32
2.18	Tangible Objects: Passive Objects.	36
2.19	Tangible Objects: Everyday Life Passive Objects.	37
2.20	Tangible Objects: Frameworks Around Everyday Life Objects.	38
2.21	Tangible Objects: Custom Built.	39
2.22	Tangible Objects: Reconfigurable.	40
2.23	Tangible Objects: Embedded with Sensors.	41
2.24	Tangible Objects: Actuated, Part 1.	42
2.25	Tangible Objects: Actuated, Part 2.	43
2.26	Tangible Surroundings: Tangible Furniture.	43
2.27	Tangible Surroundings: Tangible Surfaces, Part I.	44
2.28	Tangible Surroundings: Tangible Surfaces, Part II.	45

2.29 Tangible Surroundings: Floor Elements.	46
2.30 Tangible Surroundings: Structural Elements.	47
2.31 Passive Haptics: Recreational Virtual Scenario.	49
2.32 Passive Haptics: Virtual Working, Part I.	50
2.33 Passive Haptics: Virtual Working, Part II.	51
2.34 Passive Haptics: Risk Minimization Virtual Environments.	52
2.35 Passive Haptics: Data Manipulation.	53
2.36 Beyond Passive Haptics: Re-registration.	54
2.37 Beyond Passive Haptics: Reconfiguration.	56
2.38 Beyond Passive Haptics: Similitude and Discrepancy between Tangibles and Virtuals.	57
2.39 Beyond Passive Haptics: Enhanced Haptics Property of Tangible, Stiffness.	58
2.40 Beyond Passive Haptics: Enhanced Haptics Property of Tangibles, Weight.	59
2.41 Beyond Passive Haptics: Enhanced Haptics Property of Tangibles, Texture.	59
2.42 Beyond Passive Haptics: Enhanced Haptics Property of Tangibles, Shape.	60
2.43 Beyond Passive Haptics: Enhanced Haptics Property of Tangibles, Added or Subtracted Parts.	60
2.44 Beyond Passive Haptics: Encounter-Type Haptic Devices.	61
2.45 Beyond Passive Haptics: Generic Enhanced Controllers.	63
2.46 Beyond Passive Haptics: Toward New Life-Like Paradigms.	63
3.1 Approach Implemented in a VR Medical Palpation Simulator.	73
3.2 The hRing, a Tactile Wearable Device.	74
3.3 Proof-of-concept Demonstrator.	75
3.4 Experimental Setup of the Perceptual Evaluation.	77
3.5 True Discovery Rate in Function of the Difference of Stiffness.	79
3.6 Psychometric Curves: JND and PSE.	80
3.7 Bar-graph of the Subjective Questionnaire.	81
4.1 Objective: Induced Discrepancy between Tangible and Virtual.	88
4.2 Experimental Setup.	89
4.3 Tangibles Reference of the Experiment.	90
4.4 User Study #1: Width - Virtual Objects.	91
4.5 User Study #1: Width - Psychometric Curve.	92
4.6 User Study #2: Local Orientation - Virtual Objects.	93
4.7 User Study #2: Local Orientation - Psychometric Curve.	93
4.8 User Study #3: Curvature - Virtual Objects.	95
4.9 User Study #3: Curvature - Psychometric Curve.	95
4.10 Barplots of the Subjective Questionnaire.	96
5.1 Carousel of virtual objects.	102
5.2 Example of Virtual Object with Patches and Pinches.	104
5.3 Linear Representation of an Object.	104
5.4 Parametrisation of a Pinch Pose.	105
5.5 Parametrisation of a Patch.	105
5.6 Registration Cases With the Projected Distance to Mass Center.	108
5.7 Cost Function: Projected Distance to Mass Center, Close to the Center.	108
5.8 Cost Function: Projected Distance to Mass Center, Away from the Center.	109
5.9 Cost Function: Patch Orientation.	110
5.10 Cost Function: Weight Orientation of patch Curvatures.	112

5.11 Suggested Generation on Valid Pinch Poses.	114
5.12 Setup of the experiment.	118
5.13 Answers to the Subjective Questionnaire.	124
6.1 Exaggerated Examples of Discrepancies upon Tangible Contact.	132
6.2 Capacitive Sensitivity.	135
6.3 Experimental Setup.	136
6.4 Measurement Principle of the Capacitive Sensing.	137
6.5 Conditioning acquisition units.	138
6.6 Conditioned Signal Image of the Proximity.	138
6.7 Fitting of the Proximity Signal.	142
6.8 Visuohaptic retargeting.	143
6.9 Grid of Contact Points.	144
6.10 3D-printed calibration prop.	146
6.11 Mean score for each condition.	148
6.12 Mean Error at Contact for each condition.	149
6.13 Bar-graph of Subjective Questionnaire.	149
7.1 Structure of the WeATaViX.	156
7.2 Schematic of Electronics Structure for Sensing and Control.	157
7.3 VR Setup.	157
7.4 State Machine of the Grasp Interaction.	159
7.5 Release Interaction.	160
7.6 Task Environments.	162
7.7 Virtual Orchard.	164
B.1 Tracking Setup.	IV
B.2 Calibrated Support.	V
B.3 Connection Between the Support and the Tangible.	V
B.4 3D-printed Attachments With Constellations of Markers.	VI
B.5 Attachments sets.	VI
B.6 Varying parameters of the sets.	VII
B.7 Calibration Procedure of the Virtual Fingers for Pinching.	VIII
B.8 Calibration Procedure of the Virtual Hand for Touching.	IX

List of Tables

3.1	Use Cases in VR.	83
3.2	Use Cases in AR.	84
5.1	Examples of How Criteria Are Evaluated.	107
5.2	Tangible and Virtual Object of the Experiment.	120
5.3	Ratings for the static task.	122
5.4	Ratings of the Dynamic Task.	123
6.1	Ratings of Contact Coherency and Error at Contact	148
B.1	Measurements Index Set	VII
B.2	Measurements Thumb Set	VIII

Résumé Long en Français

Introduction

Dans ce manuscrit, nous présentons plusieurs contributions sur l'utilisation d'objets réels et tangibles pour la réalité virtuelle (RV), en particulier avec des visiocasques de RV. Les objets tangibles peuvent servir de supports physiques pour l'interaction avec des objets virtuels tout en fournissant un contact naturel et familier fort aux utilisateurs, augmentant ainsi considérablement leur expérience de l'environnement virtuel.

Ces dernières années, la RV a gagné en popularité avec le développement de nombreux visiocasques, rendant la technologie plus accessible et plus abordable par rapport au premier prototype construit en 1968 par Sutherland, qui était alors suspendu au plafond. Sutherland a décrit sa fonction comme étant de "présenter à l'utilisateur une image en perspective qui change en fonction de ses mouvements" [1]. En d'autres termes, alors que l'utilisateur porte un visiocasque et se déplace dans une pièce réelle, le mouvement de sa tête est capté et utilisé pour afficher, dans son champ de vision, une succession d'images calculées d'un mouvement similaire au sein de l'environnement virtuel. De nos jours, les visiocasques de RV substituent complètement la vue de la pièce réelle à celle calculée de l'environnement virtuel, rendant ainsi les utilisateurs *aveugles du monde réel*. Cependant, la RV ne se limite pas à fournir une représentation visuelle de l'environnement virtuel lorsque les utilisateurs se déplacent, elle doit également engager activement ces derniers en leur donnant les moyens d'interagir avec l'environnement virtuel et d'observer les résultats de leur interaction par le biais d'interfaces multisensorielles pouvant stimuler la vue, l'audition et le toucher.

Fournir un retour sensoriel à la main est un défi majeur de l'haptique. Il s'agit d'un vaste domaine de recherche où de nombreux dispositifs sont développés pour fournir un retour cutané ou kinesthésique, afin de recréer les sensations auxquelles les utilisateurs sont habitués lorsqu'ils manipulent des objets ou des outils dans la vie réelle. Toutefois, ces interfaces doivent être aussi transparentes que possible afin d'offrir une bonne *immersion* aux utilisateurs. Elles doivent leur permettre d'agir avec l'environnement virtuel aussi naturellement qu'ils le feraient dans le monde réel. Mais elles doivent aussi leur faire même oublier qu'elles se trouvent en réalité entre eux et l'environnement virtuel. Dans ce manuscrit, nous nous concentrerons sur l'utilisation d'objets tangibles, car ils peuvent fournir un retour haptique riche et complet pour un moindre coût. Hoffman [2] a affirmé que la manipulation d'objets réels superposés à des objets virtuels identiques peut procurer une sensation convaincante de forme, de poids et de textures qu'il serait difficile de restituer avec des dispositifs actifs. En conséquence, le réalisme de tout l'environnement virtuel s'en trouve accru. Plus tard, Insko [3] a montré que cette technique peut également augmenter la sensation de *présence*.

Objectifs et contributions de la thèse

L'objectif de cette thèse consiste à ce que l'utilisateur reçoive un retour haptique convaincant en manipulant avec ses mains un objet tangible, alors qu'il est le pendant physique d'un élément virtuel affiché dans le visiocasque. Le but de cette thèse est donc d'aborder les questions sous-jacentes de ce paradigme selon deux axes de recherche principaux : (I) *améliorer le rendu haptique des objets virtuels en utilisant des objets tangibles* et (II) *améliorer la superposition des objets virtuels et tangibles*.

Alors qu'un objet tangible fournit un retour haptique d'un élément de l'environnement virtuel, nous avons étudié comment et dans quelle mesure une divergence entre les deux peut être introduite sans dégrader l'immersion de l'utilisateur. Nous avons proposé trois objectifs : 1) altérer la perception que l'utilisateur a de l'objet tangible, 2) induire intentionnellement des différences imperceptibles entre la représentation physique et virtuelle, et 3) associer un même objet tangible à plusieurs éléments de l'environnement virtuel.

Au chapitre 3, nous proposons de combiner des objets tangibles avec des dispositifs haptiques portables afin d'améliorer le rendu haptique de sensations de raideur en RV. Un objet tangible passif permettra de rendre à l'utilisateur des sensations fortes sur la forme générale des objets, tandis qu'un dispositif haptique portable permettra d'augmenter - dans une certaine mesure - la raideur perçue de l'objet tangible en fournissant des stimuli tactiles adaptés au niveau des doigts. Nous avons développé une preuve de concept permettant de simuler des sensations de raideur variables lors de l'interaction avec des objets tangibles en utilisant des haptiques portables à retour cutané sur les doigts. Nous avons ensuite réalisé une étude utilisateur montrant que l'ajout d'une pression cutanée permet bien d'augmenter la raideur perçue des objets réels, alors même que les stimuli tactiles ne sont pas délivrés au point de contact. Nous avons illustré notre approche à la fois en RV et en RA, avec plusieurs cas d'utilisation et différents objets tangibles.

Dans le chapitre 4, nous avons étudié dans quelle mesure un objet tangible et sa représentation virtuelle doivent être similaires. Pour obtenir une illusion convaincante, il doit y avoir une bonne correspondance entre les caractéristiques haptiques de l'objet tangible et celles évaluées à partir de l'élément virtuel correspondant. En d'autres termes, ce que les utilisateurs voient dans l'environnement virtuel doit correspondre autant que possible à ce qu'ils touchent dans le monde réel. Pour comprendre dans quelle mesure nous pouvons intentionnellement induire des différences sans que l'utilisateur s'en rende compte, nous avons mené des études utilisateurs pour déterminer la différence juste perceptible (JND) lors d'une saisie à deux doigts d'un objet tangible qui diffère d'un objet virtuel sur l'une de trois caractéristiques haptiques importantes : la largeur, l'inclinaison des surfaces et la courbure.

Le chapitre 5 propose un concept dans lequel il est suggéré à l'utilisateur de saisir un endroit spécifique d'un objet virtuel tout en lui faisant saisir un objet tangible ayant des caractéristiques haptiques similaires au point de saisie, comme la largeur, l'inclinaison des surfaces, la masse ou la courbure locale. Pour obtenir une illusion convaincante, il doit y avoir une bonne correspondance entre ce que l'utilisateur voit de l'environnement virtuel et ce qu'il touche du monde réel, même si l'objet tangible est globalement différent de la représentation virtuelle associée. Nous avons développé un algorithme qui calcule la correspondance entre diverses poses de saisie sur les objets tangibles et virtuels pour trouver des paires qui possèdent des propriétés similaires et qu'il est alors possible de superposer. Cette méthode recherche dans un premier temps de potentielles poses de saisie à deux doigts sur les objets, et en extrait ensuite leurs propriétés haptiques afin de calculer le meilleur appariement. Cette approche a été testée dans le cadre d'une étude utilisateur.

Comme la superposition d'un objet tangible et d'un objet virtuel est affectée par des limitations en termes de précisions et de contraintes spatiales dans l'espace de travail, nous proposons d'améliorer les méthodes de superpositions à deux échelles différentes : 1) à petite échelle, en *compensant les erreurs de positionnement pour réaliser une synchronisation des contacts* entre la main virtuelle (respectivement physique) et l'objet virtuel (respectivement physique), et, 2) à une échelle plus large, en *donnant à l'utilisateur un tangible à saisir et à relâcher n'importe où dans l'espace de travail*, sans aucune restriction spatiale.

Dans le chapitre 6, nous abordons la question de l'erreur de positionnement résultantes qui est assez courante lorsque des systèmes de captures classiques sont utilisés. L'objectif est de compenser cette erreur en instrumentant des objets tangibles à l'aide de capteurs capacitifs. Ceux-ci permettent d'estimer la proximité entre la surface de l'objet et la main de l'utilisateur. Dès lors, cette information peut être utilisée pour rediriger le mouvement de la main virtuelle par rapport à la surface virtuelle afin de reproduire le positionnement relatif de la main physique par rapport à la surface de l'objet tangible. Enfin, une étude utilisateur évalue les performances de la fusion du capteur capacitif avec le système de capture optique ainsi que l'appréciation des utilisateurs sur la qualité de la synchronisation des contacts tangibles et virtuels, et ceci, en utilisant deux solutions différentes de captures de la main : un système de capture de la phalange distale et un système de capture de paume.

Dans le chapitre 7, nous présentons la conception et l'évaluation d'un type inhabituel de dispositif haptique portable pour une manipulation naturelle d'objets tangibles en RV. Ce dispositif est capable d'engager et de désengager un objet tangible de la main de l'utilisateur n'importe où dans l'espace de travail. Il supprime également la nécessité de connaître l'emplacement du tangible puisque ce dernier contrôlé pour se rapprocher de la main de l'utilisateur lorsque la main virtuelle est proche d'un élément virtuel saisissable. En outre, ce dispositif est compatible avec tout système de capture standard capable de fournir une position et une orientation - pas nécessairement précises mais plausibles - de la main réelle. Une technique d'interaction basique est mise en œuvre et testée dans le cadre d'une étude utilisateur afin d'évaluer la capacité du dispositif à fournir un objet tangible partout où l'utilisateur doit saisir un élément virtuel, et, à rendre des interactions de saisie et de relâche convaincantes avec des objets virtuels statiques et à faible vitesse.

Augmenter la perception de raideur d'objets tangibles en Réalité Mixte avec une haptique portable

Dans ce chapitre, nous nous concentrons sur l'altération de la perception que l'utilisateur a d'un objet tangible sans pour autant le modifier : nous proposons d'améliorer le rendu haptique dans les environnements virtuels en tirant partie des avantages respectifs de deux solutions haptiques simples en combinant l'utilisation d'objet tangible et d'haptique portable. L'objet tangible fournit un contact raide, convaincant et des sensations réparties dans la main quant à sa forme, tandis que le dispositif haptique portable, le hRing, peut générer une sensation tactile variable mais localisées et servira à modifier dynamiquement les propriétés mécaniques perçues de l'objet tangible (Fig. 1).

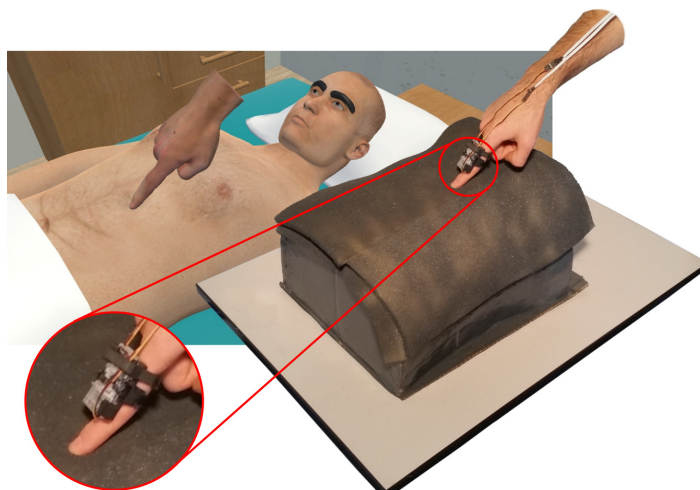


Figure 1: Notre approche implémentée dans un scénario virtuel de palpation médicale

Principe

Le principe est que l'utilisateur touche un objet tangible avec une raideur fixe du bout de l'index de la main droite, tandis qu'il porte sur l'une de ses phalanges, le dispositif haptique portable. Le positionner sur la phalange intermédiaire ou proximale permet de laisser le bout du doigt libre pour interagir directement avec l'objet tangible. Ainsi, en exerçant une pression tactile synchronisée avec les mouvements de l'utilisateur, nous pouvons augmenter la raideur perçue par ce dernier.

Etude utilisateur et résultats

Nous avons effectué une étude perceptuelle qui vise à évaluer la capacité de notre dispositif portable à augmenter la raideur perçue de l'objet tangible. Nous avons également voulu évaluer l'effet de l'éloignement du stimulus cutané du point de contact avec la surface réelle, en plaçant le dispositif alternativement sur chaque phalange de l'index et sur la phalange distale de l'index de la main inactive.

Les résultats de notre évaluation perceptuelle montrent un effet significatif sur l'augmentation de la perception de raideur par cette méthode. La raideur perçue peut être augmentée d'au moins 10% lorsque l'haptique portable est sur la main droite, contre seulement 6,5% lorsqu'il est placé sur la main opposée.

Dans quelle mesure les objets tangibles et virtuels peuvent-ils être différents sans le paraître?

Les objets tangibles sont utilisés en réalité virtuelle et augmentée pour transmettre la sensation haptique de toucher des objets virtuels. Cependant, pour que l'illusion fonctionne, les caractéristiques haptiques des objets tangibles doivent correspondre autant que possible à celles des objets virtuels associés en termes, par exemple, de taille, de forme locale, de texture, de masse. En d'autres termes, il devrait y avoir une *bonne* correspondance entre ce que les utilisateurs voient dans l'environnement virtuel et ce qu'ils touchent dans le monde réel. Cependant, la perception humaine n'est pas parfaite et toute estimation d'un bien matériel est entachée d'erreur. En conséquence, une certaine divergence entre la représentation matérielle et virtuelle devrait être indiscernable pour l'utilisateur.

Principe

Nous allons *intentionnellement induire des différences* entre les deux afin de comprendre à quel point un objet virtuel peut être différent de son homologue tangible sans que l'utilisateur s'en rende compte (voir Fig. 2), ceci pouvant ouvrir des voies intéressantes quant à l'utilisation de quelques objets tangibles dans le rendu de multiples objets virtuels. Nous nous intéresserons en particulier au cas d'une saisie à deux doigts où certaines propriétés locales seront altérées: la largeur, l'inclinaison et la courbure des faces.

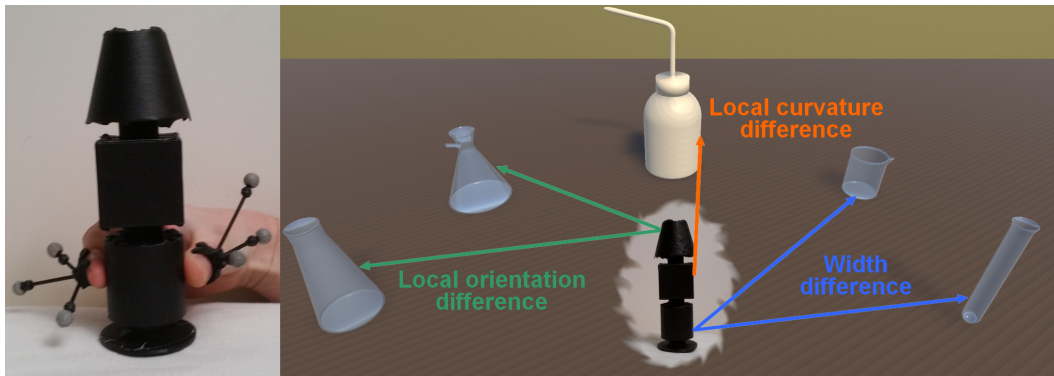


Figure 2: Objectif de notre étude : comprendre à quel point un objet tangible (à gauche) peut être différent d'un objet virtuel (à droite) sans que l'utilisateur ne s'en aperçoive. Nous avons axé notre étude sur trois critères spécifiques : la largeur, l'inclinaison locale et la courbure.

Etudes utilisateur et résultats

Dans le but de quantifier jusqu'à quel point les différences sont acceptables, nous avons mené une étude utilisateur afin de mesurer le seuil de détection (JND) lors de l'introduction de disparité entre un couple d'objets tangibles et virtuels lors de la saisie à deux doigts, et ce, sur les trois dimensions haptiques mentionnées ci-dessus : largeur, inclinaison et courbure des faces. Les résultats ont montré un JND à 75% respectivement de 5,75%, 43,80% et 66,66% pour la perception de la largeur, de l'inclinaison des faces et de la courbure locale lors de la saisie, respectivement autour de valeurs de référence de 4 cm, 10° et 33 m^{-1} . Ces valeurs ont été choisies comme valeurs centrales dans la gamme des valeurs réalistes lors d'une saisie à deux doigts.

Vers des objets tangibles universels : optimisation des sensations lors de la saisie à deux doigts

Dans ce chapitre, nous utiliserons à notre avantage la possibilité d'avoir une différence entre le tangible et le virtuel en *appariant un seul tangible à de multiples éléments de l'environnement virtuel*, dans l'optique d'utiliser peu d'objets tangibles pour rendre de nombreux objets virtuels. Toutefois, pour que l'illusion fonctionne, les caractéristiques haptiques des éléments tangibles doivent correspondre à celles des objets virtuels associés. Nous proposons donc un algorithme qui analyse différents objets tangibles et virtuels afin de trouver la stratégie de saisie entre les deux objets qui correspond le mieux en termes de sensations haptiques. (voir Fig. 3).

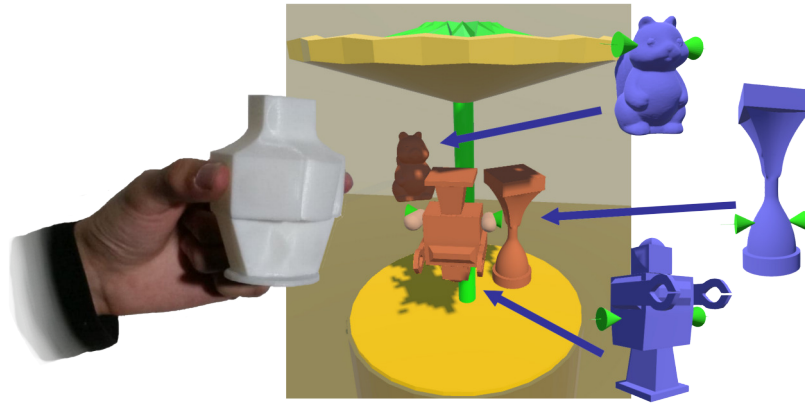


Figure 3: Un carrousel d'objets virtuels qui peuvent être saisis à l'aide d'un seul objet tangible "universel". Ces poses sont suggérées par notre algorithme pour correspondre au mieux aux sensations haptiques de saisies correspondantes sur l'objet tangible.

Algorithme

Ayant en entrée seulement les modèles 3D de tous les objets considérés, notre algorithme se comporte de la manière suivante. Tout d'abord, il identifie différentes poses de saisie à deux doigts possibles sur chaque objet. Ensuite, pour chaque pose et pour chaque objet, l'algorithme évalue une série de caractéristiques haptiques : distance entre les deux bouts des doigts, distance de la pose par rapport au centre de masse, inclinaison entre l'axe des doigts et l'axe principal d'inertie, inclinaison des surfaces saisies et leurs courbures. Ensuite, l'algorithme utilise une fonction de coût pour évaluer toutes les paires possibles afin d'identifier les deux poses de saisie les plus similaires, l'une sur l'objet tangible et l'autre sur l'objet virtuel, évaluées en fonction de caractéristiques évoquées. Enfin, la meilleure association permet de superposer les deux objets et est mise en évidence dans la scène virtuelle afin que l'utilisateur puisse la saisir.

Etude utilisateur et résultats

Nous avons mené une étude préliminaire auprès des utilisateurs pour évaluer l'efficacité de notre algorithme. Il a été demandé aux participants d'évaluer la similarité entre l'objet manipulé et l'objet vu, sachant que les positions de saisie sont obtenues soit par le biais de notre approche, c'est-à-dire optimisées en termes de similarités haptiques, soit par une superposition globale des objets tangibles et des objets virtuels et ceci lors d'une tâche de saisie statique et d'une tâche dynamique de saisie et déplacement. Cette évaluation a montré que notre algorithme a été capable de bien combiner les caractéristiques haptiques considérées et de trouver des poses de saisies convaincantes entre les objets tangibles et virtuels de l'expérience. Nous avons enregistré des améliorations de 48,8% et 45,1% par rapport à la technique de superposition standard pour les tâches statiques et dynamiques, respectivement.

Utilisation de capteurs capacitifs pour améliorer le rendu du contact avec des objets tangibles en RV

L'utilisation d'objets tangibles peut fournir un retour haptique riche et fort. Cependant, la superposition d'un objet tangible et d'un objet virtuel entraîne souvent des erreurs de

positionnement : sa position étant capturée ou calibrée au préalable, l'objet tangible peut ne pas être correctement positionné par rapport à l'objet virtuel en raison de l'imprécision système de capture. Ainsi, lors d'un contact tangible, il peut y avoir un écart résiduel ou une interpénétration, comme le montre la Fig. 4. Nous compenserons cette *erreur de positionnement* à l'aide d'un capteur capacitif afin d'obtenir une meilleure *synchronisation visuohaptique au contact*, et ainsi, préserver l'immersion lors de l'interaction de contact en RV.



Figure 4: Divergences au contact tangible : lorsque l'utilisateur touche l'objet tangible (au milieu), il peut y avoir un écart virtuel (à gauche) ou une interpénétration virtuelle (à droite) entre le doigt virtuel et la surface de l'objet virtuel.

Principe

Nous proposons d'instrumenter un objet tangible avec des capteurs capacitifs en raison de leurs propriétés intéressantes. Premièrement, ils sont sensibles à la proximité d'une main humaine, car celle-ci possède naturellement des propriétés capacitives, et permettent une interaction directe avec la main sans composant intermédiaire. Deuxièmement, il suffit de recouvrir la surface du tangible avec un simple matériau conducteur, comme une fine bande de cuivre ou une peinture conductrice, pour obtenir une sensibilité capacitive. Enfin, lorsqu'ils sont correctement conditionnés, les capteurs capacitifs sont des capteurs de proximité qui peuvent fournir une estimation de la distance générale entre le bout des doigts de l'utilisateur et la surface. Cette information peut ensuite être utilisée pour rediriger, *avant le contact*, le mouvement de l'utilisateur obtenu à partir du système de capture optique, vers la surface de l'objet tangible.

Etude utilisateur et résultats

Nous avons mené une étude utilisateur pour évaluer les performances et la viabilité de notre approche combinant capteur capacitif et système de capture standard. Les participants ont été invités à interagir avec un cube tangible en RV et à évaluer la cohérence des contacts virtuels et tangibles, soit en utilisant uniquement le système de capture optique (approche standard), soit en combinant ce système avec la détection capacitive (notre approche). Les résultats montrent que notre approche augmente considérablement la cohérence et la synchronicité perçues au cours de l'expérience, en corrige les erreurs de positionnement relatives courantes qui surviennent dès lors qu'un système de capture optique est utilisé en même temps que des objets tangibles. Grâce au capteur capacitif, l'erreur au contact est ramenée en dessous du millimètre dans toutes les conditions testées.

WeATaViX : un objet tangible actionné portable pour la RV

Nous avons développé un dispositif qui peut *fournir un objet tangible* à l'utilisateur qu'il peut *saisir et relâcher n'importe où dans l'espace de travail*, permettant de superposer un unique objet tangible à une multitude d'objets virtuels tout en conservant l'espace de travail libre de tout support tangible. Cette interface haptique portable est conçue pour permettre une manipulation naturelle des objets tangibles en réalité virtuelle. Elle permet de positionner l'objet tangible dans la main de l'utilisateur ou de l'en éloigner, ce qui permet rendre la sensation d'établir ou de rompre le contact avec des objets virtuels, permettant de surcroît de les saisir et de les manipuler.

Conception et principe du dispositif

Notre nouvelle solution, "WeATaViX", vise à assurer la présence physique d'objets virtuels tout en restant aussi simple et discrète que possible. L'appareil est maintenu sur l'arrière de la paume, fixé à la peau par une couche de silicone adhésive. Un servomoteur permet de faire pivoter une tige rigide au bout de laquelle se trouve un objet tangible et de l'approcher ou de l'éloigner de la paume de l'utilisateur afin d'engager ou de désengager l'objet tangible de la main de l'utilisateur. Ainsi, celle-ci reste entièrement libre et un objet tangible est rendu disponible dès que l'utilisateur tend la main vers un objet virtuel. Ceci fonctionne n'importe où dans l'espace de travail puisque le dispositif est fixé à la main de l'utilisateur. Par ailleurs, le placement relatif entre l'objet tangible et la main de l'utilisateur imite celui de leurs homologues virtuels, sans qu'il ne soit vraiment nécessaire de suivre séparément la main et l'objet. Si un objet virtuel se trouve à proximité de la main virtuelle, le tangible est engagé, sinon, il est retiré. De plus, l'utilisation d'un capteur de contact capacitif sur le tangible permet de déterminer le moment où l'utilisateur saisit le tangible afin de déclencher une animation d'ouverture ou fermeture de la main. Ce système est par ailleurs compatible avec tout système de capture standard capable de fournir une position et une orientation de la main réelle.

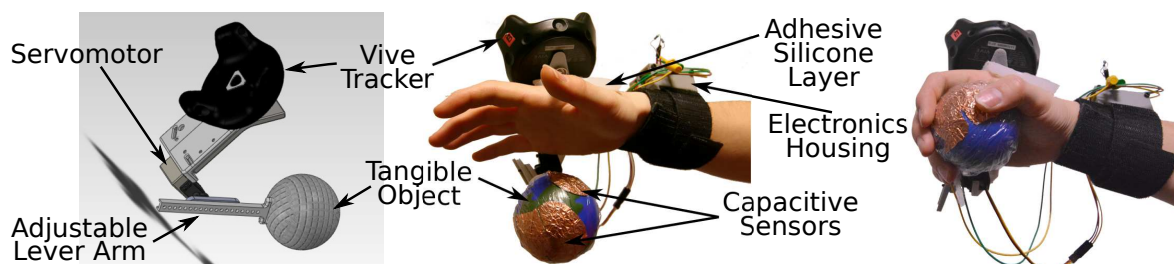


Figure 5: Dispositif haptique composé d'une pièce imprimée en 3D ancrée à une couche de silicone adhésive fixée à la main.

Etude utilisateur et résultats

Notre dispositif offre une solution simple et efficace pour une interaction tangible avec de multiples objets virtuels dans de grands espaces de travail, ainsi qu'une grande adaptabilité aux environnements virtuels. Nous avons mené une étude utilisateur pour évaluer notre dispositif et notre technique d'interaction en RV. Nous avons conçu des tâches couvrant un large éventail d'interactions de saisie et de relâchement avec différentes vitesses et configurations de positionnement des objets par rapport à l'utilisateur afin de déterminer

la gamme d'interactions prises en charge par notre dispositif. Notre dispositif a reçu des réactions positives de la part des utilisateurs lors de sa validation expérimentale et permet de saisir et relâcher des objets virtuels immobiles ou à faibles vitesses sans contraintes de positionnement.

Conclusion

Dans ce manuscrit, nous nous sommes concentrés sur l'utilisation d'objets *tangibles* pour fournir un retour haptique riche et convaincant des objets virtuels auxquels ils sont superposés, pendant une interaction de manipulation avec un visiocasque de RV. Nous avons abordé plusieurs aspects qui peuvent affecter l'immersion de l'utilisateur dans deux axes de recherche principaux. Le premier axe s'est concentré sur l'amélioration du rendu des objets virtuels en utilisant des objets tangibles différents, tandis que le second axe s'est intéressé à l'amélioration de la superposition entre objets tangibles et virtuels.

Dans la partie I de ce manuscrit, nous avons travaillé à l'élaboration de diverses stratégies pour rendre un élément virtuel avec un objet tangible tout en maintenant un niveau d'immersion acceptable. Nous avons proposé trois approches : 1) *altérer la perception* que l'utilisateur a de l'élément tangible, 2) *introduire intentionnellement des divergences imperceptibles* entre l'objet tangible et sa représentation virtuelle, et, 3) *apparier un élément tangible unique à plusieurs éléments de l'environnement virtuel*.

Dans la partie II de ce manuscrit, nous avons abordé le deuxième axe autour des limitations et contraintes courantes survenant lors de la superposition d'objets *tangibles* et virtuels. Nous avons proposé d'aborder ces problèmes, à deux échelles différentes : 1) en *compensant les erreurs de positionnements pour obtenir une synchronisation des contacts* entre les mains et les objets réels et virtuels, et 2) en *fournissant un objet tangible à saisir et à relâcher n'importe où dans l'espace de travail*, sans aucune restriction spatiale.

Chapter 1

Introduction

This PhD manuscript presents various contributions to the use of real, tangible objects for haptic interaction in Virtual Reality (VR). Tangibles can mediate various kinds of interaction with virtual objects while providing a strong natural and familiar contact for the users, thus, greatly increasing the latter's experience of the virtual environment.

In recent years, VR has gained in popularity as many VR HMDs have been developed, making the technology more accessible and affordable compared to the first prototype built in 1968 by Sutherland, which was suspended from the ceiling. Sutherland described its purpose as "to present the user with a perspective image which changes as he moves." [1]. In other words, as users are wearing HMDs and walking within a real room, the motion of their heads are captured and used to display, in their fields of view, a computed succession of images of a similar virtual motion within a virtual environment. Current VR HMDs completely substitute the view of the real room with the computed view of the virtual environment, making the users *blind to the real world*.

Hence, it is possible to display any virtual content to the users and immerse them in a virtual environment totally different to that of the room where they actually are: they can be walking in small and narrow corridors inside a cave behind a waterfall, in a large room with a high ceiling and large windows like Versailles's Hall of Mirrors, or even outdoors in an open field with trees around them, while hearing birds flying above their heads or the sound of cicadas in the grass, simply by adding spatialized sounds. Virtual objects and avatars can fill the environment, and the users are able to walk around them: a reconstructed statue from Ancient Greece, a moving triceratops, or an asynchronous motor engine with highlights on the physical phenomenon involved, which make it spin. These objects are displayed in the space right in front of the users, as if they were actually there, mainly due to this central idea of presenting the users with a view of the virtual environment adjusted to their own movements. This often results in a "wow" effect the first time someone puts on a HMD, and they realize how it feels to be immersed elsewhere, and later, once the HMD is removed, as they realize that they actually forgot about the real room they never left.

In my numerous attempts to convert people to VR by inviting them to try out a HMD, I noticed several times that, as soon as they can see virtual hands reconstructed by a Leap Motion, novices stretch out their hands as if they were trying to reach and touch a virtual object, which obviously fails as there is nothing for them to touch in the real world. Despite being fascinated, they often spoke about how weird it was not being able to touch anything. This observation is not surprising: First, they are trying to use their hands, because of their dexterity and experience on daily basis. Second, they have never had to question the fact that touching something with the hand results in them feeling it.

Providing sensory feedback to the hand is a major challenge of haptics and Virtual Reality. In this regard, this thesis will strive to address this issue by studying how it is possible to provide compelling touch sensations in VR in the most natural and seamless manner, taking advantage of tangible objects and innovative haptic interfaces.

An Apologia of Virtual Reality

Although there is no consensus on the definition of virtual reality, Philippe Fuchs defines its purpose as to make "possible a sensorimotor and cognitive activity for a person (or persons) in a digitally created artificial world, which can be imaginary, symbolic, or a simulation of certain aspects of the real world" ([4], translation of [5]). In that regard, VR not only provides a visual representation of the virtual environment as the users move around it, but, it also has to actively engage them by giving them the means to interact with the virtual environment and observe the results of their interactions, following a perception-action loop displayed in Fig. 1.1.

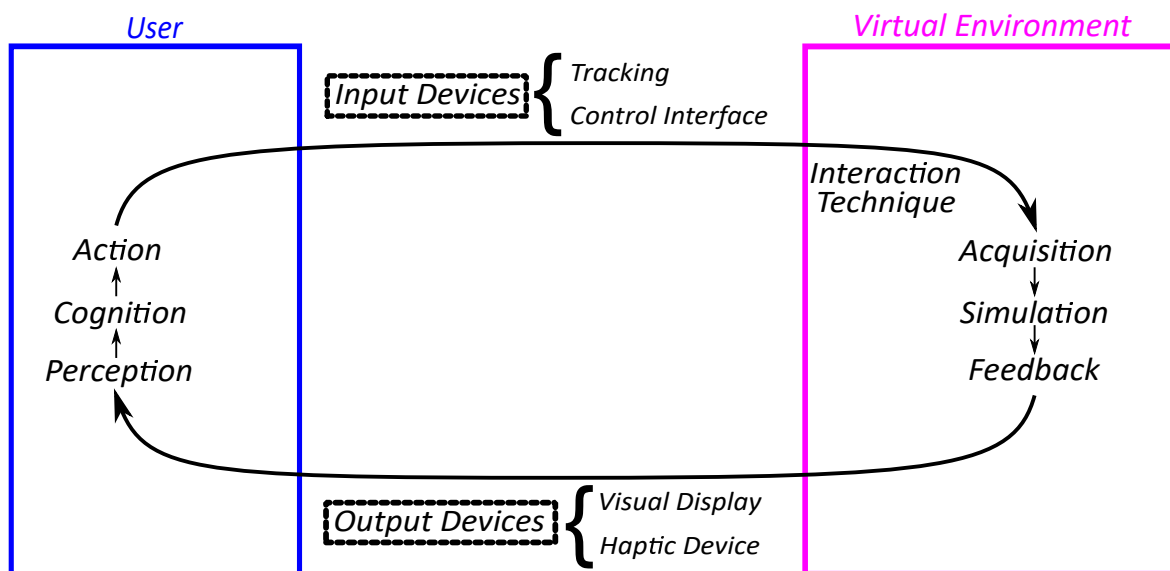


Figure 1.1: Perception-Action Loop in Virtual Environment. The users can act using input interfaces which are often tracking systems meant to capture the users' motion, or intermediate control devices (e.g. joysticks, a robotic arm's handle). They are coupled with software elements to create *interaction techniques* which offers specific ways to interact with the virtual environment and perform valid tasks. The simulation processes the acquired input data and determines their impact on the simulated virtual environment. The necessary feedback for the users is generated by the rendering algorithm which commands the output interfaces: image rendering for the visual display, one image per eye, the sound rendering for the earphones which is spatialized in the virtual environment, and haptic rendering for the haptic devices. The users perceive the virtual environment through the sensory stimulation rendered by the output devices. Their cognitions process what they perceive to push further their action, as they would naturally in the real environment, under the assumption that the loop works at a high enough rate to be natural to the user.

Outside recreational usages, Virtual Reality has already found many applications in training and workplace contexts. It is also a tool that makes it possible to teach expertise with minimum risks, and possibly at a lower cost and more accessibly. In the medical field, VR helps students to learn and understand procedures and make them become automatic reflexes: Rajeswaran et al. [6] developed a scenario to teach students how to correctly

perform an endotracheal intubation to prevent further complications. Additionally, experts can prepare themselves right before performing an intubation on a complex case. Alternatively, Bracq et al. [7] developed a scenario as a situation awareness training for scrub nurses who have to prepare and check the hygiene and security of an operating theater. The scenario was set with many errors the nurses had to check for as any could impair the success of medical operations. Similarly, in the construction field, workers are often exposed to many risks which could be fatal if not handled properly. Dris et al. [8] developed a risk-hunting scenario to raise awareness and train workers on safety procedures. Moreover, as construction companies already have models of the building site to monitor the building process at every step, it is possible to set the training in a virtual representation of the building at the current state of construction, which workers are familiar with. Even in the current pandemic situation, VR is used to help patients to recover their motor functions faster after being in intensive care for extended periods.

However, VR is not just a means to simulate existing experience, it is also a medium that can create new kinds of experiments. For example, it can be a tool to analyze human behavior in psychological experiments. By having participants take part in a self-counseling scenario where they alternately embody first a virtual avatar of themselves explaining their troubles and then a virtual avatar of Sigmund Freud providing counsel, Osimo et al. [9] studied how the embodiment of the virtual avatar can lead to a cognitive change. As a result, participants were able to adjust their ways of thinking and improve the outcome of their own thought process. More recently, Seinfeld et al. [10] conducted an experiment in which male offenders were embodied in an avatar of a woman; the men could see themselves moving in a mirror, and in a room appearing bigger to them, so as to reinforce the illusion of ownership. They were then confronted with a taller male avatar which verbally abused them and invaded their personal space. The offenders actually experienced an abusive situation and understood the perspective of the victim, independently of their motivation to do so or their imaginative capacity to see the situation from the victim's point of view. This last example highlights the need for users to be engaged in the virtual environment, to truly take possession of the virtual avatar given to them, and to agree with the scenario, i.e., to be immersed in the virtual environment.

Immersion in Virtual Reality

For the user to truly take part in the action playing out in virtual environment, two underlying notions are at work together as to achieve a credible illusion [11]: the *presence* which "is the human response to the system" and the *immersion* which is "an objective property of a system".

Slater [12] proposed two concepts to characterize how users realistically respond to a virtual experiment as if it was real: The first component, close to the initial usage of *presence*, is the "place of illusion" (referred as PI), the sensation that the virtual environment displayed is real. The second component is the "plausibility illusion" (referred as Psi), the sensation that the scenario or the events happening in the virtual environment are real. Both are required for the users to respond realistically to virtual events or situations as they would to the real world.

Immersion is an objective property of the system and "refers to the technical capability of the system to deliver a surrounding and convincing environment with which the participant can interact" [11]. The perception-action loop of Fig.1.1, inspired by Fuchs et al. [13], displays the generic key components of a VR setup which may affect the *immersion*. In

order to actively engage the users in the virtual environment, these components provide multi-sensory feedback upon interaction with the virtual environment, by stimulating the users' view, hearing and touch. Several parameters can affect the *immersion* of the whole VR system, e.g., the realism of the displays, the width of field of view, the frame-rate and latency of the visual display, or the precision, complexity and fidelity of the tracking system employed, or even the number of different human sensory receptors stimulated, the fidelity of rendering for each sensory modality [11] of the haptic feedback. Additionally, *immersion* can be described by the interactions enabled for the user to act on the virtual environment, by the "sensorimotor contingencies that they support" [12] (defined as "actions that we know to carry out in order to perceive" [12] or as "the lawful relations" tying together "motor actions and associated sensory stimulations" [14]). Conceivably, other sensory modalities like smell and taste can also be stimulated. However, these are currently marginalized.

Therefore, there are a lot of possible axes to improve *immersion* in Virtual Reality, but the main axis of this manuscript is centered on *haptics*. It is a wide research field where many devices are developed to provide cutaneous or kinesthetic feedback in order to render sensations that the users are accustomed to when manipulating objects or tools in real life. However, these interfaces need to be as transparent as possible to provide an adequate *immersion* to the users. They have to allow the users to act with the virtual environment as naturally as they would in the real tangible world and even make them forget that these interfaces are actually between them and the virtual environment. Haptic devices can be of many kinds: there are force feedback grounded interfaces, which are often robotic end-effectors meant to render force and/or torque on several degrees of freedom (DoF), tactile feedback devices, which stimulate the user's skin with localized cutaneous sensations (vibration, pressure, skin stretch, etc.) and can also come in a very wearable format, tactile displays which are meant to render shape and texture on fixed surfaces (e.g., pin arrays), Encounter-Type Haptic Devices (ETHD) which reposition their end-effector according to the user's movement in order to encounter the users as they are about to interact with virtual elements, mid-air ultrasound devices which can focus the ultrasound onto the users' skin, or even using real object for the user to grasp. Culbertson et al. [15] proposed to split them into three major and representative categories: graspable, wearable and touchable systems which can themselves be broken down into various subcategories.

We used various kind of haptic interfaces shown on Fig. 1.2: grounded force feedback interface which can render virtual elements of variable stiffness by applying simulated forces to the users' hand, wearable haptics which can elicit various kind of tactile stimulus while being lightweight and unobtrusive, and ETHD which can register the tangible end-effector with a virtual element in real time as the users move around the virtual environment.

In this manuscript, we will focus on using tangible objects, as they can provide a complex and compelling feedback at a lesser cost (see Fig. 1.3). Hoffman [2] stated that manipulating real objects superimposed with identical virtual ones can provide compelling sensation over the shape, weight and textures which are difficult to render altogether with actuated devices. Thus, this increases the realism of the whole virtual environment. Later, Insko [3] showed that it can also increase the sensation of *presence*.

Additionally, it is interesting to note that providing the users with a near perfect realistic haptic feedback can also impair their *immersion*. According to Berger et al. [16], when the feedback is almost realistic, small mismatches of any kind are more likely to be noticed and bother the user. Moreover, if some haptic feedback contrasts too realistically with other haptic feedback or any other sensory feedback, the *immersion* drops instead of improving. This introduces the idea of the just necessary haptic feedback: to provide bare sufficient

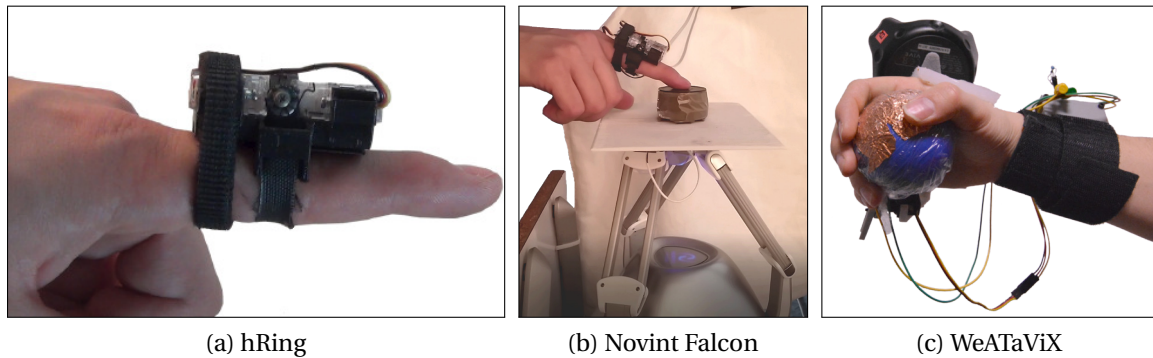


Figure 1.2: Haptic devices used in this manuscript. a) the hRing, a wearable which can provide pressure and skin stretch to any phalanx of the hand, b) the Novint Falcon, a grounded force feedback interface which end-effector has been replaced by a plate with a small cylinder as it renders buttons of variable stiffness, c) the WeATaViX, a wearable encounter-type haptic device which can engage/disengage a tangible sphere from the users' hand.

and meaningful information to the user to allow him to perform the virtual task in a natural way.

In short, to provide the user with a suitable virtual experience two criteria are required:

- To achieve a "good" sense of *presence* (PI and Psi) by providing a credible virtual environment with plausible virtual interaction, a virtual avatar the user can assimilate with and enough control interact naturally with the virtual elements;
- To achieve a "good" *immersion* by using a VR system able to provide various kind of interaction with adapted visual, auditory and haptic feedback.

Furthermore, using tangible elements seems promising in VR as it can provide compelling sensation while increasing the user's *immersion* and sense of *presence*.

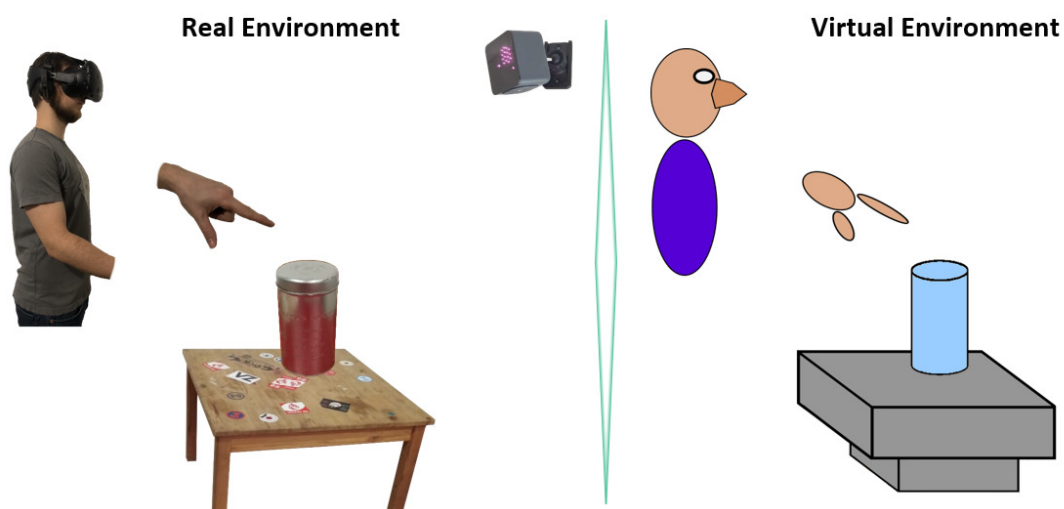


Figure 1.3: Using tangibles in VR: Users receive a haptic feedback as they use their own hands to touch a tangible, the physical counterpart of a virtual element of the virtual environment which is displayed thanks to the HMD.

Tangibility in Virtual Environment

According to Merriam-Webster, Tangibility is defined as something palpable - "capable of being perceived especially by the sense of touch" - and material - "substantially real". Thus, we will use tangible elements so that, whenever users reach for a virtual object of any kind with their virtual hands, they can actually touch a real, palpable and material element with their real hands. This idea of coupling a virtual object with a real one and then manipulating the real one to change the state of the virtual one, is quite similar to the idea of giving "physical form to digital information, employing physical artifacts both as representations and controls for computational media." [17], i.e., the early definition of Tangible User Interface (TUI) of Ullmer and Ishii [18]. As Ullmer and Ishii suggested, we will use the word *tangibles* as a generic designation for tangible artifacts, objects, tools, containers, etc. This definition was then broadened as the TUI framework covered more aspect with various sub-framework [17]. For example, "Tangible Augmented Reality", which makes it possible to "attach" virtual objects or informative displays to the tangibles, "Tangible Tabletop Interaction", which rely on touch-surfaces, or "Embedded User Interfaces", that are characterized by having computing embedded into many separated tangibles. Shear and Hornecker reported in their survey on TUI [17] that there are several unifying perspectives proposed around TUIs. One of them is "Reality-Based Interaction" which supports the idea that interaction should be based on already existing skills to increase the overall efficiency and that the interaction could work around four themes: basic physical understanding, body awareness, environment awareness, and social awareness.

In this regard, the use of Tangibles in VR is part of the TUI framework. However, in the end, the paradigm of TUI is for users to use "their hands to manipulate some physical object(s) via physical gestures; a computer system detects this, alters its state, and gives feedback accordingly." [19]. And such a paradigm seems incomplete from a VR point of view, especially when using an HMD: The users' field of view is completely substituted by a virtual environment, making them blind to the real environment. There is a need to provide them with a meaningful virtual representation of the environment, of their bodies and of the *tangibles*. An effective tracking system needs to be deployed to continuously render and localize virtual elements in the virtual environment, especially because we aim to make the invisible *tangibles* attainable for the users. Furthermore, virtual representation of the *tangibles* in VR might affect the perception the users have of the tangible, as well as any additional haptic feedback provided to the users. All the underlying question related to perception, immersion and presence in VR need to be addressed.

In short, Tangibles in VR are at a crossroads between TUI and VR. This paradigm is derived from the TUI framework, from which it can borrow ideas, concept, technical solutions but needs to be addressed from a VR point of view to solve VR additional constraints.

A generic adaptation of the Perception-Action Loop, for hand manipulation of tangibles in VR is visible on Fig. 1.4. The graph illustrates all the needed components, but for the purpose of simplification and clarity, any modality other than haptic and vision is not represented, neither is the tracking of the user's head.

The tangible, while serving as an intermediate interface between the user and the virtual environment, is associated with a virtual element, just as the user's hand is associated with a virtual hand avatar. Through the tracking system, the virtual hand will interact with the virtual element as the user is interacting with the tangible. This will make it possible to provide plausible visual feedback to the user and possibly command the tangible if it is actuated or any additional haptic interface.

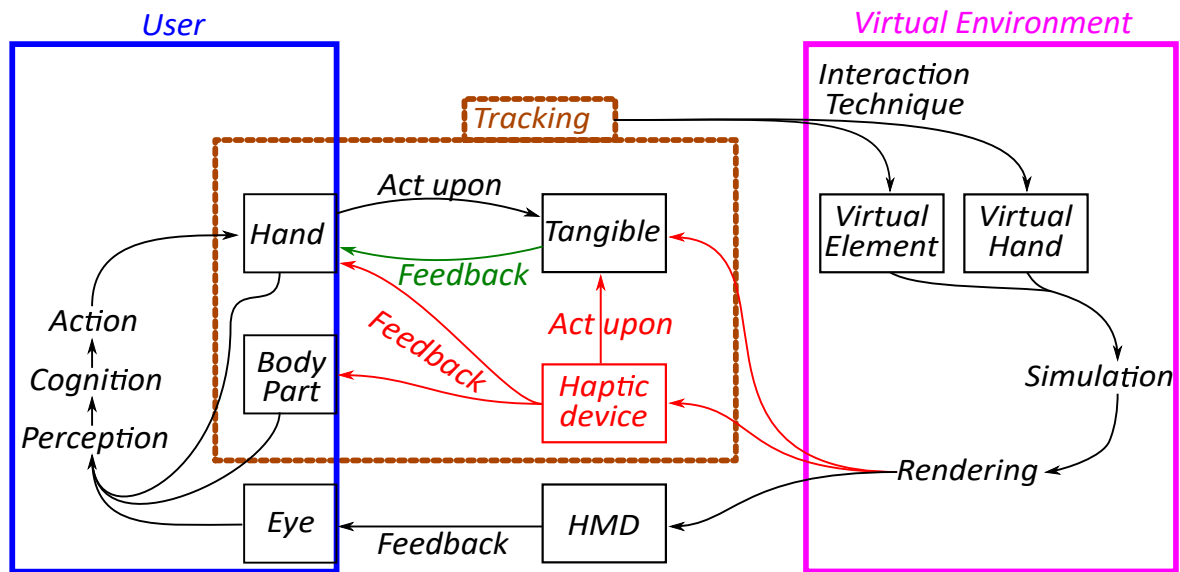


Figure 1.4: Perception-action loop when using *tangibles* in virtual environments. The user is highlighted in blue with his/her head, hand, and possibly an additional body part which can receive feedback. The tangible used in the setup serves as an interface between the user's hand and the virtual environment, and has a counterpart within the virtual environment depicted in purple. In red, is a possible additional haptic device which can provide direct feedback to the user's hand and/or the additional body part or can act upon the tangible (e.g., imposing the motion of the tangible). The tracking system can acquire data (usually position) from the hands and/or the *tangible* (possibly, any other involved haptic device). This data will change the state of the virtual hand and the virtual element according to the interaction technique made for the setup. These changes are spread through the simulation which then computes the rendering for the different outputs: a visual rendering for the HMD and possibly haptic rendering for the tangible (or any additional haptic device) if it is actuated. The feedback is then applied respectively to the eye and the hand (possibly to another body part) for the user to perceive and elaborate the next action to perform with his hands. Feedback from the tangible to the hand is depicted in green, as it can only exist in the case of contact between them.

Thesis objectives

In this thesis, our main objective is to improve haptic interaction while using *tangibles* in VR, as the users receive compelling haptic feedback whilst using their hands to manipulate a *tangible*, the physical counterpart of a virtual element displayed in a HMD. To address the underlying questions, two main axes of research are developed in this thesis.

First, as a tangible object renders part of the virtual environment, we will study how and to what extent a discrepancy between the two can be introduced without flawing the users' immersion. With this objective in mind, the first axis of research is: (I) *improving the rendering of virtual objects using tangibles*.

Second, as registering a *tangible* to a virtual object comes with limitations in term of accuracy or workspace constraints, we will study how and to what extent we can improve the registration of the two in terms of quality of the interaction and availability. With this objective in mind, the second axis of research is: (II) *improving the registration between tangibles and virtual objects*.

Axis I: Improving the Rendering of Virtual Objects using Tangibles

When wearing a VR HMD, users are unable to see the *tangibles* onto which are rendered virtual elements. During interaction, they will naturally confront their vision of the virtual environment with the haptic sensation they get from the *tangibles*. Although the presence of *tangibles* greatly increases presence and immersion, if the visual or haptic information is too different with respect to each other, i.e., the *tangibles* and virtual elements are shaped differently, immersion can be negatively affected. A simple solution would be to have perfect tangible replicas of the virtual elements. This can be possible if the *tangibles* are 3D-printed from virtual models, or if the *tangibles* are captured to reconstruct virtual models. However, these processes are highly constraining and can still end up with mismatches depending on the quality of the technical solution employed. Moreover, this replica-based solution tends to limit the reusability of the tangible and it seems excessive to recreate the virtual environment with different sets of tangibles for each virtual scene of any virtual experience, without mentioning possible tracking issues. Thus, using discrepant *tangibles* would lift these restrictions and increase their reusability.

Human perception is not perfect, the various sensory receptors have inaccuracies [20] which give us leeway for admissible discrepancies between a *tangible* and its virtual representation, which - to a certain extent - will not be perceived by the users or at least will not bother their immersion. Thus, we elaborated different strategies to render a virtual element with a slightly different tangible while maintaining an acceptable level of immersion and proposed three objectives: 1) *altering the perception* the user has of the *tangible*, 2) *intentionally inducing unnoticeable discrepancies* between the tangible and its virtual representation, and, 3) *pairing a single tangible to multiple elements of the virtual environment*.

- 1) When users are manipulating a *tangible* in the real environment, they are able to perceive its properties through visual and haptic cues: when the *tangible* is actuated and can change its properties, it can provide multiple perceptions to the users. However, this is not as straight forward when the *tangible* is passive. From Ernst and Banks' perspective [20], by adding a new cue, a new stimulus, it should be possible to influence the sensory system's estimation of a property, therefore, *altering the perception* the user has of the *tangible* without actually modifying it.
- 2) Human perception admits a range of error. Ernst and Banks [20] showed that human perception integrates visual and haptic cues despite the fact they have provided different estimations, by considering the variance of each source. As a consequence, a certain amount of discrepancy between the tangible and its virtual representation should be indiscernible for the users, or at least, should not bother them. Thus, it should be possible to design either one by *intentionally inducing unnoticeable discrepancies* with respect to the other without impairing the immersion.
- 3) Since some discrepancy is allowed when associating a tangible to a virtual element, it should be possible to match one *tangible* with multiple similar virtual elements. Additionally, when users grasp or touch a tangible on one side, they are not aware of the haptic properties of the other side: the tangible and its virtual representation could be similar only locally while overall being totally different. Thus, we aim to *pair a single tangible to multiple elements of the virtual environment*.

Axis II: Improving the Registration between Tangibles and Virtual Objects

Although there are several methods to use *tangibles* to render virtual object in VR on interaction, these require the virtual objects to be correctly registered to the *tangibles* in order provide a natural and realistic interaction for the users. However, several limitations and constraints commonly interfere with the registration process. First, high accuracy is needed when using *tangibles* in VR. When the users reach for a virtual object, they can only move their real hands according to the movement of the virtual ones towards the virtual element. If the virtual element is not located correctly with respect to the *tangible* (and the virtual hand with respect to the real one), either the users encounter the tangible before the virtual hand reaches the virtual element, thus touch something invisible to them, or they can reach the virtual object without finding the tangible contact. Both cases can occur due to the tracking system's inaccuracy. Second, when not carried by the users, *tangibles* are constrained to the supporting structure onto which they are embedded (e.g., restricted to the surface of a table). Hence, the virtual objects have similar constraints in the virtual environment due to the registration (e.g., restricted to a virtual surface).

In this axis of research, we propose to address these registration issues, on two different scales: 1) on a finer scale, by *compensating setup errors to achieve contact synchronization* between both real and virtual hand/object contacts, and, 2) on a wider scale, by *providing a tangible to grasp and release anywhere in the workspace*, without any spatial restriction.

- 1) When reaching for a pair comprised of a tangible and its virtual representation, the tangible contact (between the users' hand and the tangible) and the virtual contact (between the avatar and the virtual element) might not happen simultaneously due to an error of estimation of the relative positioning of the users' hand and the tangible, e.g., an element may be ill-calibrated, a virtual model can differ from the real counterpart, or the tracking system cannot determine with precision the location of every part of the hand that can make contact with the tangible. Thus, we aim to *compensate* such small-scale *setup errors to achieve better contacts synchronization* between the real and virtual and improve the quality of the interaction.
- 2) *Tangibles* have to be put on supporting structures as they cannot float in air. Thus, they often lay on a table where they can be picked up and put down. However, virtual environments are not always limited to a virtual desk upon which virtual objects are positioned. Sometimes, the users might need to pick an object, then move around in the workspace to perform a task, and finally put the object down elsewhere. This means that there is also a need to position a sufficient amount of supporting structures within reach that are compatible with the virtual environment. Only then can *tangibles* and virtual objects be positioned for the virtual scenario. However, in the end, the virtual elements available for registration with a *tangible* are limited to those in the vicinity of the supporting structures. Thus, the second objective is to *provide a tangible* for the users *to grasp and release anywhere in the workspace*, without any spatial restrictions or need for supporting structures.

Approach and contributions

The remainder of this manuscript is organized as follows. Chapter 2 presents related work on the use of *tangibles* in Virtual Reality, especially when using HMD. To begin with, a

general overview of haptics is drawn up, about the underlying mechanics of human perception, haptic interfaces, rendering and perception in virtual environments. To continue, a categorization of the different kinds of *tangibles* is proposed as well as the various applications of *tangibles* in VR. Finally, a discussion synthesizes the underlying context of *tangibles* in virtual reality and position the following Chapters with respect to the state-of-the-art.

Then, in the remainder of the manuscript, each of our two axes of research is addressed in a separate part. In Part I, we focus on *improving the rendering of virtual objects using discrepant tangibles*.

In Chapter 3, we propose to combine *tangibles* and wearable haptics to improve the display of stiffness sensations in virtual environments. The passive *tangible* makes it possible to feel the general shape of objects, while a wearable haptic device will enable us to augment - to a certain extent - the perceived stiffness of real/tangible objects by providing timely tactile stimuli at the fingers. We developed a proof-of-concept framework to simulate varying elasticity/stiffness sensations when interacting with tangible objects by using wearable tactile modules at the fingertips. We carried out a user study showing that wearable haptic stimulation can significantly increase the perceived stiffness of real objects, even when the tactile stimuli are not delivered at the contact point. We illustrated our approach both in VR and AR, with several use cases and different tangible settings.

In Chapter 4, we study the extent to which a *tangible* and its virtual representation have to be similar. To achieve a compelling illusion, there should be adequate correspondence between the haptic features of the *tangible* and those assessed from the corresponding virtual element, i.e., what users see in the virtual environment should match as much as possible what they touch in the real world. To understand to what extent, we can intentionally induce discrepancies without the users noticing, we conducted user studies to determine the just-noticeable difference (JND) when grasping, with a thumb-index pinch, a *tangible* which differs from a seen virtual one on three important haptic features: width, local orientation, and curvature.

Chapter 5 is about suggesting to the users a grasping pose on the virtual object while making them grasp a *tangible* with compatible haptic features, e.g., size, local shape, mass, local curvature. To achieve a compelling illusion, there should be adequate correspondence between what users see in the virtual environment and what they touch in the real world even if the *tangible* is globally different to the associated virtual representation. We proposed an algorithm which performs a grasp pose matching to suggest compatible places the users can pinch between a *tangible* and a virtual object which are registered adequately. This method searches for possible pinching location on the objects and then extracts their haptic properties in order to compute the best pairing. The effectiveness of our approach was evaluated through a user study.

The second axis of research is addressed in Part II, which broaches several issues that arise when we try to register a virtual object to a tangible, either due to relative mispositioning, or the constrain on the tangible's position, we will focus on *improving the registration between tangibles and virtual objects*.

In Chapter 6, we address the issue of the remaining positioning error which is quite common when classical tracking systems are employed. The objective is to compensate such errors by instrumenting tangible objects with capacitive sensors. This makes it possible to estimate the proximity between the object surface and the users' hand, which can then be used to retarget the motion of the virtual hand with respect to the virtual surface to reproduce the relative positioning on the tangible side on contact. Finally, a user

study evaluates the ability of the combination of capacitive sensing with optical tracking as well as the users' appreciation of the quality of visuohaptic synchronization of tangible and virtual contacts, when two different hand tracking solutions are employed, fingertip tracking and palm tracking.

In Chapter 7, we propose the design and evaluation of an uncommon type of wearable device for the natural manipulation of tangible objects in VR. This body-grounded encounter-type device is able to engage and disengage a tangible from the users' hand anywhere in the workspace. It also removes the need to know the location of the tangible as the device is controlled to get the tangible close to the users' hand when then virtual hand is close to a graspable virtual element. Moreover, the device is compatible with any standard tracking system able to provide a - not necessarily accurate but plausible - position and orientation of the real hand. A basic interaction technique was implemented and tested in a user study to assess the ability of the device to provide a tangible to grasp wherever the users need to grasp a virtual element, and, to render compelling grasp and release interactions with static and slowly-moving virtual objects.

Finally, Chapter 8 concludes this manuscript and discusses short-term future work for each contribution as well as long-term perspectives that relate to the use of tangibles in VR.

Chapter 2

Related Work

Sommaire

2.1 Haptics: a General Overview	15
2.1.1 Haptic Sense	15
2.1.2 Haptic Interfaces	16
2.1.2.1 Encounter-Type Haptic Devices	17
2.1.2.2 Hand-Held Haptic Devices	20
2.1.2.3 Wearable Haptic Devices	28
2.1.3 Haptic Rendering	30
2.1.4 Haptic Illusions	33
2.2 Tangible Props in VR	34
2.2.1 Tangible Objects	35
2.2.1.1 Passive Tangible Objects	35
2.2.1.2 Everyday Life Tangible Objects	35
2.2.1.3 Custom-Built Tangible Objects	37
2.2.1.4 Reconfigurable Tangible Objects	39
2.2.1.5 Tangible Object Embedded with Sensors	40
2.2.1.6 Actuated Tangible Objects	40
2.2.2 Tangible Surroundings	42
2.2.2.1 Tangible Furniture	42
2.2.2.2 Tangible Surfaces	44
2.2.2.3 Floor Elements	45
2.2.2.4 Structural Elements	46
2.3 Application of Tangibles in Virtual Environment	47
2.3.1 Passive Haptics	47
2.3.1.1 Recreational Virtual Scenario	48
2.3.1.2 Virtual Working	49
2.3.1.3 Virtual Training Scenario	50
2.3.1.4 Risk Minimization Virtual Environments	51
2.3.1.5 Data Manipulation	52

2.3.2	Beyond Passive Haptics	52
2.3.2.1	Re-registration to Multiple Virtual Elements	53
2.3.2.2	Reconfiguration of the Physical Environment	54
2.3.2.3	Similitude and Discrepancy between Tangibles and Virtuals	55
2.3.2.4	Enhanced Haptics Property of Tangibles	57
2.3.2.5	Encounter-Type Haptic Devices	60
2.3.2.6	Generic Enhanced Controllers	62
2.3.2.7	Toward New Life-Like Paradigms	62
2.4	Discussion on the Role of Tangibles in VR Interaction	63

This Chapter presents the context of this manuscript, the prior work within the Haptics and Virtual Reality community. It is made of four sections. The first one presents a general overview of Haptics: the haptic sense, which explains the base mechanism of human perception; the haptic interfaces, which are devices commonly used to provide feedback to the users and with a focus on the various kind of devices used in this manuscript; the haptic rendering, which compute in real-time the feedback provided to the user, and the haptic illusions which are alternative means to provide feedback to the user. In the second section, the idea of *tangible props within VR* is displayed as well as several prior works which relies on the use of real object to mediate the interaction with virtual elements. This section does not provide a definition of the concept but rather an overview of the already existing content and interesting thoughts and perspectives which might hint toward a definition in the future as the use of real objects in VR becomes standard.

Then, the third section display the various applications of tangibles in VR and how they went beyond the *Passive Haptics* interaction technique defined by Insko [3].

Although the second and third sections objectively highlights the context of using tangibles in VR, the fourth section positions my own work by analyzing the limitations and constraints in existing systems and how these are alleviated by the contributions of the following chapters.

2.1 Haptics: a General Overview

2.1.1 Haptic Sense

Haptic is relative to the sense of touch, which enables humans to perceive their environment, especially by providing them feedback upon the action they are performing, enabling them to correct themselves on the fly and achieve great precision and accuracy.

The haptic perception comes from various receptors spread across the human body. There are mechanoreceptors of various size and sensitivity spread in the various layer of the skin and stimulated whenever the skin is put under stress, providing feedback to the nervous system [21]. In addition, thermosensory fibers through the body are responding to warmth and cold and serves as the base temperature sensitivity. These mechanoreceptors and fibers are responsible of the cutaneous sensitivity and is fully detailed by McGlone et al. [22]. There also are proprioceptors embedded within muscles and tendons which, in addition to mechanoreceptors around the joints [23], inform the nervous system of the muscles length and joints angles as well as the stress applied on each muscles and tendons. These compose the proprioception and kinesthesia, allowing the human body to know the position and motion of any limb, as well as the undergoing forces applied to them [24]. The higher the density of receptors is, the more precise is the perception, the more accurate is the action. Thus, the cutaneous perception [25] and proprioception are especially developed on the hand, allowing human to perform really fine manipulation with them. These two perceptions are the base mechanisms of the haptic sense and the underlying mechanisms are more detailed in human perception-oriented or neuroscience studies [21, 24].

The cutaneous and kinesthetic sensitivities enable human to perceive various properties of manipulated objects. Each property affects several physical phenomena which can be detected individually, but the estimation of the property is done by combining all the cues together. For example, the stiffness of an object is asserted through the force/displacement relation as well as the growth of the contact area between the finger and the object's surface as both deform against one another [26, 27, 28]. Similarly, both

cutaneous and kinesthetic cues are necessary to assess the weight of a held object, and removing a single cue leads to a loss of accuracy in the weight estimation [29]. Again, both cutaneous cues on the fingertip and proprioception from the shoulder are necessary to estimate the angle of a corner when exploring the the shape of an object [30]. Only three properties were mentioned here while many more are addressed in the literature. Though, an exhaustive list would be outside of the scope of this manuscript. The various studies are assessing human perception over various kinds of haptic stimuli or properties, by following *psychophysics* procedures [31]. The most common quantitative measurement to describe human perception is to find the Just Noticeable Different (JND), i.e., the minimum difference between two stimuli, one being a reference, to apply for the users to unconsciously start perceiving it. Once the JND is obtained for several reference stimuli, the constant of the linear regression of the Weber's law can be computed in order to quantify the perception rate independently to the reference stimulus.

Understanding and quantifying the human perception is mandatory in order to design haptic interface meant to recreate various stimuli in order to render physical phenomenon happening in virtual environment, by eliciting cutaneous and proprioception sensitivity of users in a way which is both perceptible and understandable for them.

2.1.2 Haptic Interfaces

Haptic interfaces are commonly used to mediate the interaction between the users and the virtual environment while providing many kind of feedback. Although there is no universal categorization for the various haptics devices, several keys features are often used to split them: they can be split between passive and/or active feedback devices, between grounded and ungrounded devices, they can be hand-held or wearable, and can provide kinesthetic feedback (e.g., force, torque, etc.) and/or cutaneous feedback (e.g., shape, textures, vibration, skin stretch, indentation, stiffness, etc.).

Culbertson et al. [15] proposed a general overview of the domain and split them in three major and representative categories: touchable, graspable, and wearable systems.

- Touchable interfaces, also referred as tactile display, are often grounded interfaces which users can explore with their hands in order to feel its surface properties such as its shape, texture, roughness, stiffness, temperature, etc. [15, 32, 33]. Some touchable interfaces are Encountert-Type Haptic Device (ETHD) where the device move and position itself according to the users' movement and interaction in the virtual environment, this kind of device will be discussed in Section 2.1.2.1.
- Graspable interfaces are typically devices which can be hand-held or devices with an end-effector users can grasp in order to interact with the simulation. Most common graspable interfaces are grounded force-feedback interfaces onto which users can apply some force to control them and receive force feedback upon the virtual interaction. A taxonomy of grounded force-feedback devices is developed on the Haptipedia database [34] in order to guide future generations of force-feedback devices. In the recent year, Hand-held devices has regained interest in VR as they can provide compelling feedback without restriction to the size of the workspace. They will be discussed in Section 2.1.2.2.
- Wearable interfaces are devices mounted on the hand or any other body part, also referred as body-grounded devices. They are often assimilated to (but not restricted to) cutaneous feedback, as they can easily provide various stimuli on the skin at specific location. These devices will be discussed in Section 2.1.2.3.

Shimoga et al. [32] reported various technical solutions in order to provide various kinds of tactile feedback, independently of the category of the device: pneumatics with air jets, pockets or rings, vibro-tactile with voice-coils, piezoelectric actuators or pin arrays, electrotactile stimulation when electrical pulses are induced through the skin in order to stimulate the mechanoreceptors and neuro-muscular stimulation when pulses are induced in the muscles and tendons. Later, Benali-Khoudja et al. [33] proposed an updated survey.

Despite this separation in three major categories, some subcategories are relevant by themselves and gather a whole aspect of the haptic technologies. For example, Sarac et al. [35] made a whole survey on hand exoskeletons for rehabilitation, assistive or haptic usage where they describe the mobility, mechanical design, actuation solution and operational strategy of the different devices in order to propose design requirement for generic hand exoskeleton. These are a subcategory from the wearables covered by Pacchierotti et al. [36]. Alternatively, Wang et al. [37] made a survey on kinesthetic feedback devices restricted to whole-hand feedback in which they studied the grounding base of the devices which can be the digits, the palm, the back of the hand or even the ground, meaning that, this subset of device is a cross-category from Culbertson et al. [15] perspective.

In this manuscript, the focus are on 4 subcategorizes which might overlap:

- *Encounter-Type Haptic Devices* (ETHD): they are often robotic arm or drone meant to automatically move and present an end-effector to the users as they are about to touch a virtual element.
- *Hand-held haptic devices*: Users hold the entire time by the handle, these can provide many kind of feedback.
- *Wearables*: they are often small and lightweight haptic devices, mostly focusing on tactile stimuli.
- *Tangible props*: they are material, physical props used to physically render a virtual element.

However, we can also consider that, along the tangible props, the end-effectors of the ETHDs, and handles of hand-held devices can be considered as part of a larger category which can be named *Tangibles*: real and material objects, often passive, eventually instrumented, used to provide a complex, compelling and natural feedback of a virtual element to the users.

In the remainder of this section we will focus on the first three subcategorizes which are commonly used in the haptic and VR community. As for the tangible props, they will be discussed later in Section 2.2 as the main focus of this manuscript. We will even split this subcategory between tangible objects which are smaller and mainly graspable props and tangible surroundings which are bigger and mostly touchable props.

2.1.2.1 Encounter-Type Haptic Devices

In the early days of VR and Haptic, William A. McNeely proposed the concept of *Robotic Graphics* [38] which consists of rendering a tangible volume in space by moving an end-effector with a robotic arm wherever the users are about to touch the virtual counterpart. Later, such concepts were referred to as Encounter-Type Haptic Device (ETHD).

In this section, we will expose the various kinds of *Tangibles* which can be embedded on devices in order to control their position and the interaction with the users. We will split them depending on the technical solution employed: robotic arms, drones and grounded mobile robots.

Robotic arms In the early days, Hoshino et al. [39] developed a method relying on Bezier’s curve to propose a large virtual surface for the users to touch while an actuated device beneath moved to render the different surface patches (Fig. 2.1a). Later, Furukawa et al. [40] proposed a system made of a flexible sheet held on both sides by two robotic arms which can apply different kinds of torsion to the sheet to render various shape and surface orientation whilst the users are touching the virtual object displayed onto the sheet (Fig. 2.1b). ETHDs enable the users to keep their hand free as the end-effector is repositioned to prepare the next contact. Thus, Posselt et al. [41] proposed to use a robotic-arm to provide tangible support for the users to explore the passenger compartment of a prototype car in development (Fig. 2.1c). Vonach et al. [42] used a grounded haptic device with a panel at the end coupled with an omni-direction walking device, in order to allow users to move around and touch virtual elements in a large-scale virtual environment (Fig. 2.1d). Similarly, Kim et al. [43] presented to the users an acrylic panel end-effector as to render virtual indoor environment such as wall and doors and developed a method to sample the scene and create Per-Plane Reachability Maps which will be used to position the prop at runtime (Fig. 2.1e).



Figure 2.1: Encounter-Type with Robotic Arm, Part 1. a) A Construction Method of Virtual Haptic Space [39], (b) Encountered-type Using Flexible Sheet [40], (c) Toward virtual touch [41], (d) VR-Robot [42], (e) Per-Plane Reachability Maps [43].

Thus, Encounter-Type can well render tangible surfaces of various sizes and curvatures. However, they can also be used to render more complex tangible elements with finer details: Yafune et al. [44] developed a method to render a virtual control panel using a cubic end-effector with, on each face, a different kind of button or switch (Fig. 2.2c). Araujo et al. [45] developed several kinds of end-effectors for encounter-type haptic devices to enable different kinds of interactions: a cube with various buttons and potentiometers for a virtual panel, another smaller cube with Peltier Pad to display heating and cooling, a smaller cube with pressure plate to detect whenever users are grasping the prop and release any control from the robotic arm, a touchscreen to enable finger/surface interaction, a prop to enable a directional air-flow, and a prop with 6 faces in order to display various textures (Fig. 2.2a). Mercado et al. [46] developed an approach to render unbound tangible surfaces by using a cylindrical prop which rotate as the users are moving. In addition, several textures cover the cylinder as to present to the users various feedback depending on the content of the virtual environment: cork, foam, felt, leather, cardboard and wood (Fig. 2.2b).

Alternatively, some works focused on interaction techniques with ETHD: Ruffaldi et al. [47] worked on the haptic rendering of catching and throwing objects for ETHD and applied it to a juggling use case where two balls were fixed at the end of robotic arms. The system switched between a catching interaction while rendering the inertia of the balls in

the users' hands and a throwing interaction while rendering ballistic trajectories (Fig. 2.2d). Tracking the hands was not mandatory in this example. Whilst, Mercado et al. [48] proposed 5 interaction techniques to control the movement of a robotic arm with a simple circular platform attached to the extremity. They then tested these interaction techniques in a coloring task in which the virtual panel was larger than the tangible circular prop (Fig. 2.2e).

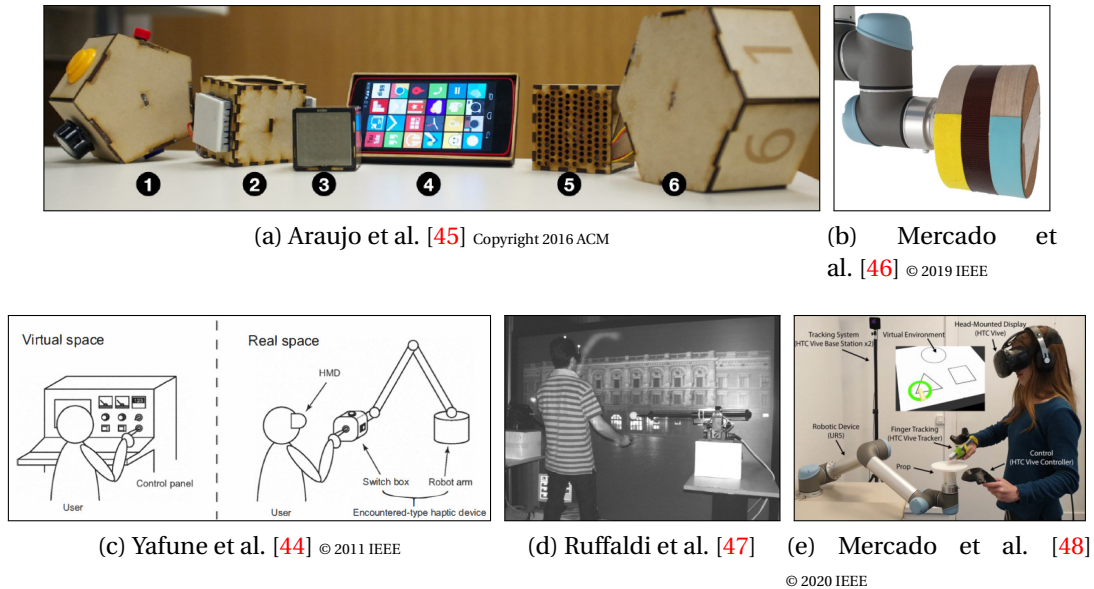


Figure 2.2: Encounter-Type with Robotic Arm, Part 2. (a) Snake Charmer [45], (b) ENTROPiA [46], (c) Haptically Rendering Different Switches [44], (d) Haptic Rendering of Juggling [47], (e) Design and Evaluation of Interaction Techniques [48].

Drones and Grounded Mobile Robots As an alternative to grounded robotic arm, mobile robots (grounded and drones) can be used to embed a tangible end-effector and enlarge the available workspace.

Knierim et al. [49] suggested using drones in order to render virtual elements mid-air. The concept behind was to simply track the users' hand and control the acceleration of the drone in order to render a tangible contact synchronized with the virtual one (Fig. 2.3a). Similarly, Abdullah et al. [50] used a drone with a flat surface or a handle on the top for the users to touch or grasp and experience force feedback as the drone was commanded to render weight or stiffness. To ensure the safety of the users, they put on a safety net cover over the drone's blades (Fig. 2.3b). Whilst, Hoppe et al. [51] embedded various tangible props and render different kinds of contacts. Their system displays 3 different interfaces: a vertical flat surface for the users to touch, a sphere in front of the drone to pock the users or a spherical end-effector for the users to grasp (Fig. 2.3c). Knierim et al. [52] explored the feasibility and acceptability of a system adjusting the position of flying *tangibles* in air. By using a small drone with a cubicle protection, they enabled tangible interactions such as touching, pushing or grabbing/releasing anywhere in mid-air (Fig. 2.3d). Alternatively, Yamaguchi et al. [53] used a drone with a flexible end-effector in order to provide a choc feedback: As the users are slaying a virtual creature with a virtual sword, they actually hit the drone with a stick (Fig. 2.3e).

As an alternative to drones, He et al. [54] proposed to use a small mobile robot in order to render an object manipulated by another user in a remote location. Users can then

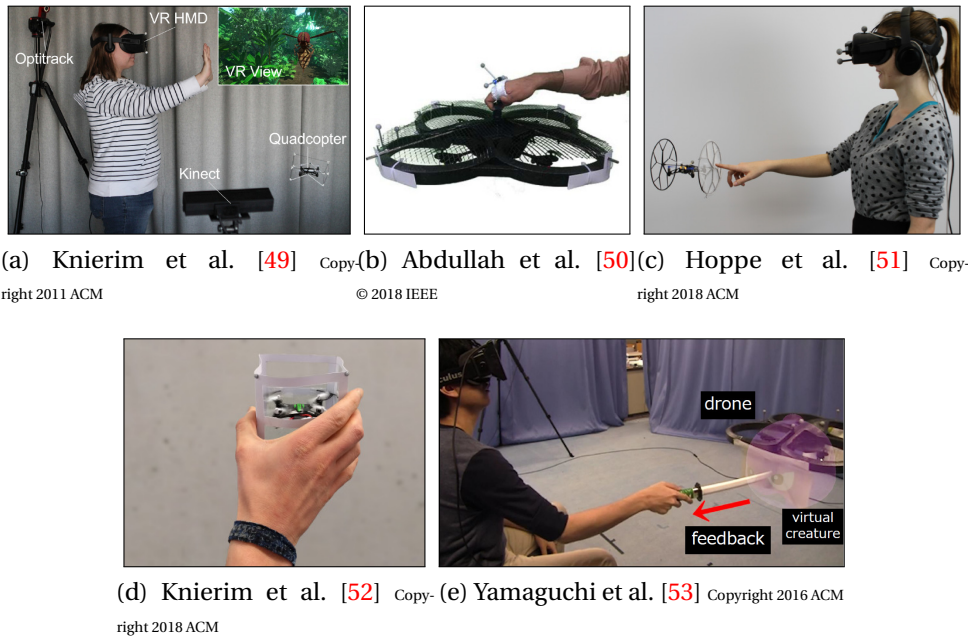


Figure 2.3: Encounter-Type using Drones. (a) Tactile Drone [49], (b) HapticDrone [50], (c) VRHapticDrone [51], (d) Flyables [52], (e) Encountered-type Haptic Display Using a Drone [53].

contact virtual objects with each other as the robot will encounter the real object they are holding (Fig. 2.4a). They [55] also suggested that two users shared a set of virtual objects. As one would move an object on his/her side, the same movement would be rendered on the other side by the moving robot. In addition, they embedded a board onto the robot on the floor as to display a virtual wall for the users to reach (Fig. 2.4b). Similarly, Siu et al. [56] made a tabletop device, shapeShift, which can move and rotate while displaying shapes at the top with a pin array (Fig. 2.4c). On a larger scale, Wang et al. [57] proposed to use a cleaning robot onto which various tangible props can be embedded and enable several interactions between the users and moving virtual entities (dog, fish, human), or simply to display box-like rigid objects for the users to touch and lift (Fig. 2.4d). In the same line of thought, Suzuki et al. [58] used cleaning robots embedded with an actuated scissor structure which can move up and down in order to lift and move pieces of furniture around and reconfigure the tangible space as users progress in the virtual environment (Fig. 2.4e).

Encasing Structure Huang et al. [59] developed a novel kind of ETHD which is a cylindrical structure encasing the users. The idea behind their Haptic-Go-Round is to provide a rotating rack from which users can pick and place or simply touch various kinds of *tangibles*. The structure can support many kinds of tangible end-effectors (handles, knob, steering wheel, etc.) that the users can manipulate and reconfigure according to the virtual task they are doing. Since the structure can rotate, the registration between *tangibles* and virtual objects can be adjusted in real time (Fig. 2.5).

In Chapter

2.1.2.2 Hand-Held Haptic Devices

Hand-held devices are meant to be held by users and often take the shape of tools' handles. Hence, they provide a natural contact within the users' grasp and intrinsically serve as

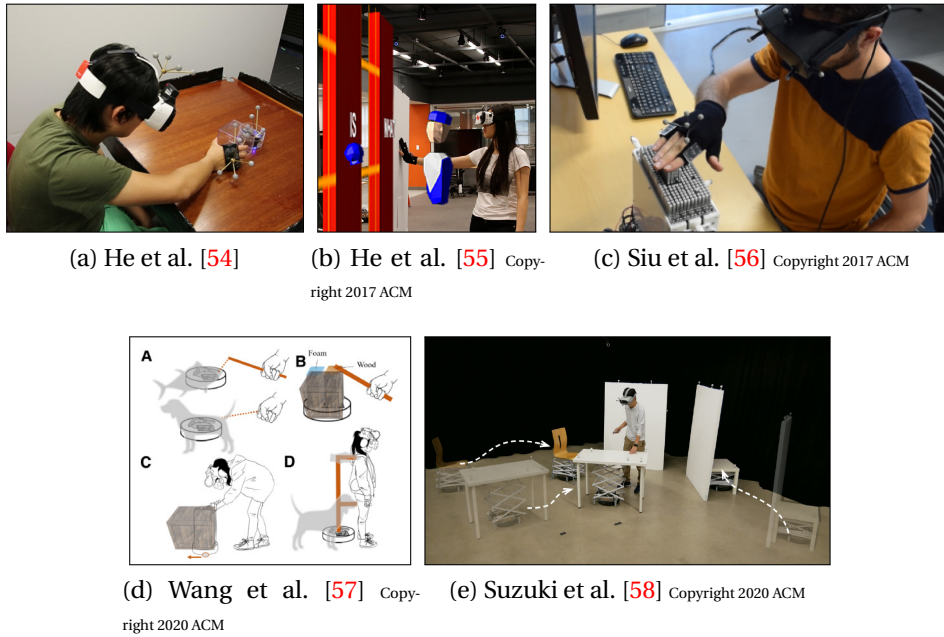


Figure 2.4: Encounter-Type using Robots. (a) Robotic Haptic Proxies [54], (b) PhyShare [55], (c) shapeShift [56], (d) MoveVR [57], (e) RoomShift [58].



Figure 2.5: Encounter-Type using Encasing Structure: Haptic-Go-Round [59] Copyright 2020 ACM.

proxies to mediate the virtual interaction with other virtual elements. Additionally, hand-held devices can be used over a larger workspace compared to classical grounded haptic devices, and are as effective in delivering various kinds of feedback and enabling dedicated interaction for a large variety of VR/AR scenarios.

Hand-held devices can provide passive feedback due to physical properties: users can assess their shape, texture, compliance, and when moving their arms around, perceive the inertia of the device. Moreover, such devices can be actuated either to reconfigure themselves to change some of their geometrical and/or kinetic properties, or even to provide active feedback, be it cutaneous and/or kinesthetic. As they are grasped by the users, the feedback can be applied within the grasp of the users, e.g., skin stretch against the palm or a force feedback on the index specific finger. When applying feedback within the hand from a grasped object, the grasping pose is of importance. Thus, we discriminate the different grasping poses using the human grasp taxonomy of Feix et al. [60]. By opposition, the feedback can also be less localized and non-limited to the hand, for example, it can provide force feedback engaging the proprioception of the whole arm in the process or even another modality like hearing.

In the remaining part of this section, we will describe several hand-held devices into 4 thematic paragraphs using the characteristics exposed above and from the most simple device (passive device with passive feedback) to the most complex one (active device with active feedback); First, the passive devices and self-reconfigurable devices, then the active devices providing feedback non-limited to the hand, and finally, active devices providing feedback within the users' grasp according to the representative grasping poses: medium wrap, writing tripod, index finger extension, and various pinching grasp. These four reference grasps are represented on Fig. 2.6, some variation of these grasps can be targeted by certain hand-held devices.

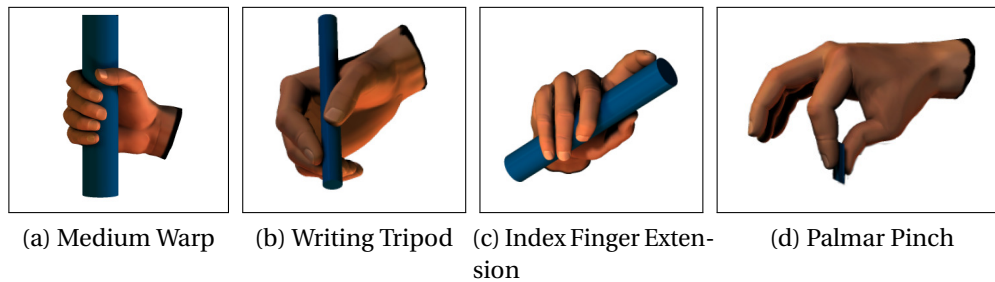


Figure 2.6: Reference grasp from the Human Grasp Taxonomy [60]. © 2016 IEEE

Passive Devices Passive devices provide feedback by their sole properties, be it geometrical (shape, curvature, size, etc.), kinesthetic (stiffness, weight distribution) or surface properties (texture, roughness, compliance) and are often meant to render a virtual object of similar or compatible properties.

Fujinawa et al. [61] proposed a method, the Haptic Shape Illusion (Fig. 2.7a), to design a hand-held device with a weight distribution matching that of the virtual tool while both are held by the handle, the obtained hand-held device can then serve as a tangible substitution or a base design for further development of a hand-held device. Montano-Murillo et al. [62] designed a selection technique, Slicing-Volume, based on rigid proxies by embedding on standard controllers a stylus on one side and a tablet on a 3D-printed support on the other side. They designed an interaction meant to select and manipulate point clouds by simply moving around a virtual cubical volume attached to a virtual tablet's surface and touching the virtual tablet with the virtual stylus. However, the virtual tablet interaction provides a natural and real contact interaction as they are based on an actual tablet and stylus (Fig. 2.7b).

As an alternative to rigid proxy, some works used deformable hand-held devices and measured their deformation in order to then control the virtual interaction. Matsumoto et al. [63] made a non-linear spring sensor warping itself around a curved acrylic support to provide a signal image of the deformation of the spring. They can then render stiffness upon squeezing virtual objects and even several values of stiffness by using pseudo-haptic, as they augment or reduce the visual deformation of the object (Fig. 2.7c).

Similarly, Achibet et al. [64] used a hand-exerciser which can be compressed along a single deformation axis to passively render grasping force with its springs while holding and squeezing virtual objects. In addition, they proposed an interaction technique with a graphical representation of the virtual force occurring during interaction and modulate the perceived forces also using pseudo-haptic (Fig. 2.7d).



Figure 2.7: Passive Devices. (a) Haptic Shape Illusion [61], (b) Slicing-Volume [62], (c) Passive Nonlinear Spring [63], (d) Virtual Mitten [64].

Self-Reconfigurable Devices Although actuated, some devices can only reconfigure themselves in order to change some of their passive properties (e.g. shape or weight distribution) without providing any active feedback to the users. In that regard, Zenner et al. [65] proposed the concept of *Dynamic Passive Haptic Feedback* device, as the device can dynamically reconfigure itself while still providing passive feedback. They also proposed such a device, Shifty, a physical proxy with a 1 Degree of Freedom (DoF) actuator which can slowly shift an internal weight in order to change its overall inertia. Their study showed that it could render many kinds of virtual objects more realistically than passive proxy by adjusting their length and thickness with respect to the translation of the weight (Fig. 2.8a).

Shigeyama et al. [66] pushed the concept further by making a device able to change the mass distribution with 3 Degrees Of Freedom (DoF). Transcalibur possesses two separated arms which can symmetrically spread open, each one possesses a weight which can shift along the arm independently (Fig. 2.8b). The latest version of Transcalibur [67] possesses 4 DoF as it can even rotate each arm independently in order to render asymmetrical virtual shapes.

Alternatively, Liu et al. [68] proposed a device, ShapeSense, with 3 large actuated surfaces which can provide air resistance in addition to the change of mass distribution. With 3 independent translations, it can take any shape between fully retracted with the 3 surfaces overlapping near the hilt or the edge minimizing air resistance, or fully extended while maximizing the exposed surface to air resistance (Fig. 2.8c). Similarly, Zenner et al. [69] also developed a fan-like device, Drag:on, made of two fans which can extend by rotation, in order to increase the air resistance and create a drag force or drag torque when the users move it around (Fig. 2.8d).

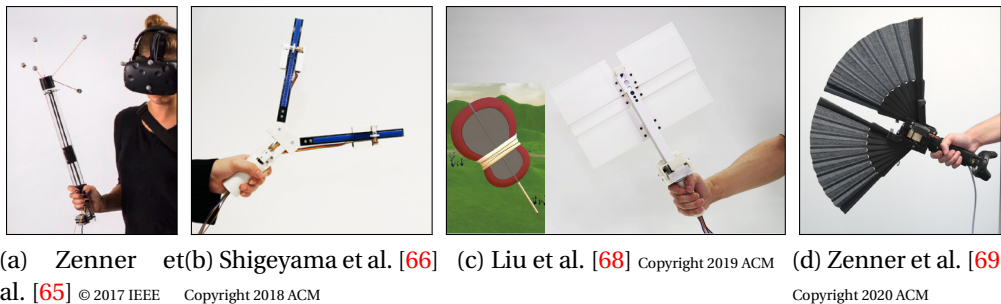


Figure 2.8: Self-Reconfigurable Devices. (a) Shifty [65], (b) Transcalibur [66], (c) ShapeSense [68], (d) Drag:on [69].

Active Devices providing Feedback Non-Limited to the Hand Some hand-held devices are not specifically meant to be used with HMD or VR, but are rather concept of actuation to provide force or torque feedback from an external virtual source, e.g., the virtual contact with another virtual element. Moreover, the feedback is often engaging the proprioception of the whole hand or arm of the users.

Swindells et al. [70] developed the TorqueBAR, a dynamic inertial feedback device. This device is a two-handed device with a mobile mass which can translate along a single axis, from one hand to the other. As a result, the device can change the position of its center of mass, and then dynamically render varying torque around the users' hands by moving the mass or simply relocate the center of mass to passively render a different inertia. It could also be used to spatially guide users' movement (Fig. 2.9a).

Yano et al. [71] developed a hand-held device using the gyro effect: As a wheel is spinning, the flywheel, tilting it in one direction would induce a torque orthogonal to the rotational axis of the flywheel. Thus, as to tilt the flywheel and induce a torque in any direction, they mounted it on a two-axis gimbal driven by motors. The induced force on the handle is not continuous as the reaction torque decreases over time, but it can provide pulses of a few tenth of second width. They evaluated their device in three scenarios. In the first one, by rendering discrete reaction forces with the virtual environment, users were able to bump against walls and find their way through a maze without visual cues. In the second one, the device exerted a pulsing linear force to guide the users toward targets. In the last one, the device is able to cancel itself or augment and alter the users' swing trajectory over a longer time duration (Fig. 2.9b).

Winfrey et al. [72] pushed further the concept of Yano et al. [71] by increasing the range of motion and the precision of the sensors as to implement a closed-loop which negate the residual moment coming from the device as the users are moving and fully command the output torque. As a result, iTorqU 2.0 is an optimized version which can produce torque in any direction (Fig. 2.9c).

Alternatively, Strasnick et al. [73] proposed three versions of Haptic Links to render bimanual force feedback by coupling both VR controllers with mechanical linkage. The first one can lock the relative position of the controller by pulling on the cable of an articulated chain to compress each pair of ball/socket, unlocking allowing free motion between the two controllers. The second and third one can apply opposite forces along the axis between both controllers, with the slight difference that the third one can mechanically lock the relative motion in any direction (Fig. 2.9d).

Instead of providing mid-air force feedback, Kotaoka et al. [74] proposed a stylus-like device meant to interact with a surface. As the users are exploring, with the stylus, a curved surface in VR and a flat surface in the real environment, the tip of the stylus can extend or shorten as to push the users' hand up let it down, rendering the reaction force of a curved surface to the users' arm (Fig. 2.9e).

Lu et al. [75] also targeted surface interaction. The movement of a tracked-stylus onto the surface was enhanced by rendering in real-time the sound of a stylus against surfaces of various textures (Fig. 2.9f).

Active Hand-Held Devices Providing Feedback Within the Grasp

As an alternative to providing kinesthetic feedback to the whole hand and arm of the user, some devices apply feedback within the grasp of the users to elicit different sensations. A first kind of device provides feedback against the palm while the users hold it with a medium warp hand grasp (see Fig. 2.6). Guinan et al. [76] made a device which is meant to make the users perceive force and torque cues simply by applying skin stretch within the

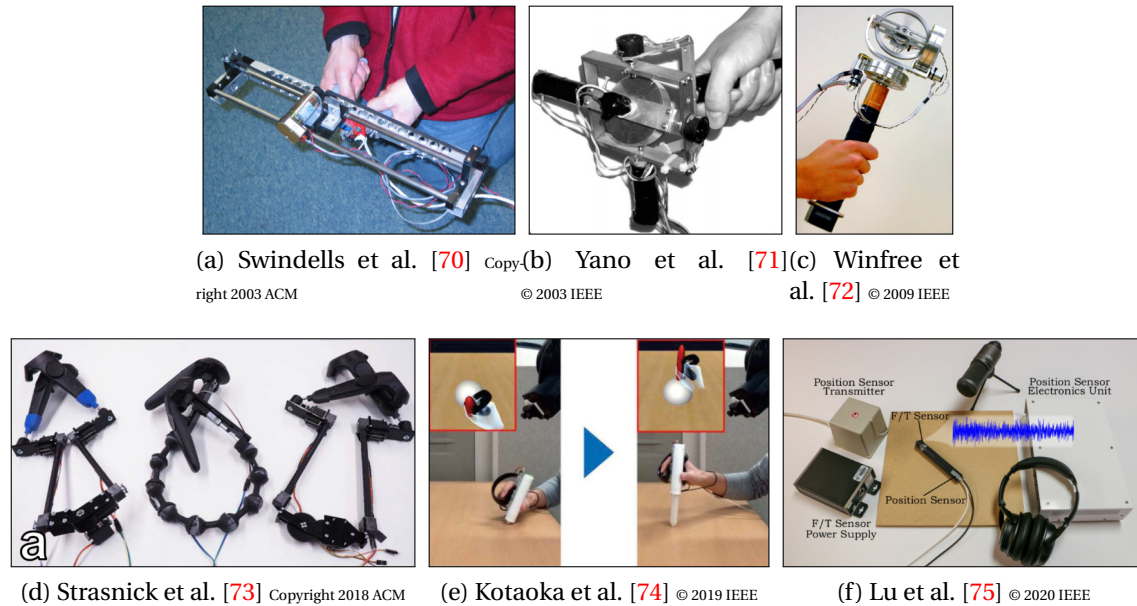


Figure 2.9: Active devices providing feedback non-limited to the hand. (a) TorqueBar [70], (b) Gyro Effect [71], (c) iTorqU 2.0 [72], (d) Haptic Link [73], (e) Physical Contact Feeling of Virtual Objects [74], (f) Rendering Sounds [75].

hand through 4 actuated sliding plates contactors located in a handle and facing different directions. The plates are 1 cm large and 9 cm long as tactile feedback with a large area of stimulus tends to have similar performance than having both tactile and kinesthetic feedback (Fig. 2.10a).

Later, Chen et al. [77] developed a device which handle is a cylindrical 3×5 pin array. Each pin can be engaged through the outer cylinder to contact the users' skin. The device can then provide in-grasp directional pressure in 5 different directions for each hand and 8 considering a bimanual use. Participants of their experiment could well discriminate the direction of the tactile stimuli (Fig. 2.10b). Similarly, Yoshida et al. [78] developed a hand-held device with two 3×6 pin arrays on opposite sides in order to display various shapes within the users' grasp. Each one can display a flat or curved surface in order to render several static shapes (rectangle, sphere, circle), symmetrical or not, and of various width. This device can also render dynamic change like a wiggling snake (Fig. 2.10c).

Alternatively, Sun et al. [79] proposed a device which provides kinesthetic feedback within the users' grasp. PaCaPa is a device similar to pliers' handle which can control the opening angle of two plates, in order to apply forces to open up the user's grasp: a trigger pushing against the users' fingers and a plate pushing on top of the hand between the index and the thumb. The force perceived by the users are similar to forces perceived within the hand while pushing onto a hard surface with a stick. Thus, the device is controlled through an interaction technique which renders the resistive force proportional to the interpenetration of a virtual stick and the virtual object the users are pressing on while displaying the stick just in contact with the object's surface. It is then possible to render virtual objects of different sizes, shapes and stiffness (Fig. 2.10d).

As users are familiar with using and holding pen and stylus, devices assuming such shape can support realistic feedback while providing natural interaction.

Kamuro et al. [80] made a stylus which is able to reproduce the skin stretch users are



Figure 2.10: Active devices providing feedback within medium warp grasp. (a) Differential skin stretch [76], (b) HaptiVec [77], (c) PoCoPo [78], (d) PaCaPa [79].

perceiving on their fingertips when they are pressing onto a rigid or stiff object with the tip of a pen. As the hand-held device is secured to the proximal phalanx of the index, the grip which is held between the fingertips is actuated and can move back and forth. The device provides cutaneous and within-finger kinesthetic feedback without the need of any tangible surface to render the contact with virtual objects (Fig. 2.11a).

Then as well, Culberson et al. [81] developed a stylus with a rolling sphere at the tip onto which a braking force could be applied and with voice coil actuators in the handle. The device could then alter the perceived kinetic friction and roughness of the contact between the stylus and a surface (Fig. 2.11b).

Diversely to stylus, Kato et al. [82, 83] targeted chopsticks and developed an actuated chopsticks device enabling users to grip and lift virtual objects while feeling them and their weight between the two sticks. When users are holding the device, a first motor can actuate the opening angle between the two chopsticks, thus rendering the gripping force of the virtual object. A second motor can actuate a plate below the sticks in order to lift the back end of the sticks as the weight of the gripped object would bring the tip of the sticks down. They conducted a user study which showed that, while using the device without any additional weights, participants could well discriminate virtual weight, despite being worse than real weights discrimination (Fig. 2.11c).

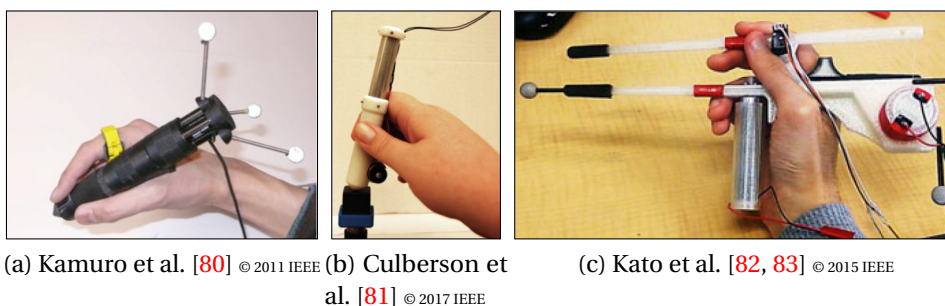


Figure 2.11: Active devices providing feedback within writing tripod grasp. (a) Pen-Shaped Kinesthetic Display [80], (b) Displaying Roughness and Friction [81], (c) HapSticks [82, 83].

Another kind of hand-held device is applying feedback to a single finger, usually the index as it is extended and the device holds with the other fingers. Benko et al. [84] built two hand-held devices meant to provide feedback at the index whilst users are exploring virtual

objects with their virtual index. The first one, NormalTouch is able to tilt a platform with 2 DoF (pitch and roll) as to present to the users' finger the normal of the virtual surface under the virtual index (Fig. 2.12a). The second one, TextureTouch is quite similar with a 4×4 pin array as an end-effector to render the virtual textures of the virtual object (Fig. 2.12b).

Later, Whitmire et al. [85] developed the Haptic Revolver: while users are holding the device with their index extended on a support, a haptic wheel can be engaged and disengaged as to make or break the contact with their fingertip. Additionally, the wheel can spin and present different faces with various kinds of texture or surface on it. As users are exploring the virtual environment with their index finger, the wheel is engaged and presents the corresponding material to the fingertip. The transition between two different textures is handled by briefly disengaging the wheel, preventing users to feel any other texture while not perceiving either that the wheel was being briefly disengaged (Fig. 2.12c).

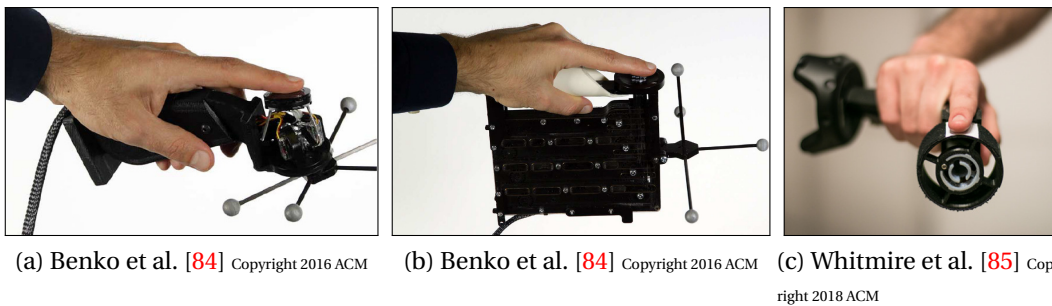


Figure 2.12: Active devices providing feedback to the extended index. (a) NormalTouch [84], (b) TextureTouch [84], (c) Haptic Revolver [85].

Lastly, recent actuated devices are designed in order to enable pinching interaction to the users. Choi et al. [86] developed a hand-held device, Claw, with a spring hinge actuated by a servo in order to render forces to the index. Users can then explore a virtual object and feel its shape with a stiff contact or even pinch virtual objects. In addition, the device has a voice coil actuator to render texture, and buttons and thumbsticks to enable classic controller's inputs (Fig. 2.13a).

Later, Sinclair et al. [87] pushed the concept further in order to allow stronger force feedback. The device has brakes in order to render very stiff contacts (Fig. 2.13b). More recently, Drills et al. [88] proposed another device with a hybrid mix of passive and active actuation for fine pinching (Fig. 2.13c).

Diversely, Walker et al. [89] proposed a device where users pinch two platforms which can both translate as to provide shear stretch to the index and thumb's fingertips. By providing stretch in the same direction, the device can elicit a translation to the user, while stretches of opposite directions elicit rotations. Their experiment showed that participants could well discriminate the different combination of skin stretch as well as the intended cues (Fig. 2.13d).

By opposition to the previous one, Lee et al. [90] proposed a device without any moving parts to increase its durability. Despite having less actuation, this enables pinch interaction through a 2D trackpad below the thumb, which can control the rotation of the grasped virtual object. In addition, a force sensor measures the users' pinching forces applied on the springs between the two plates (Fig. 2.13e).

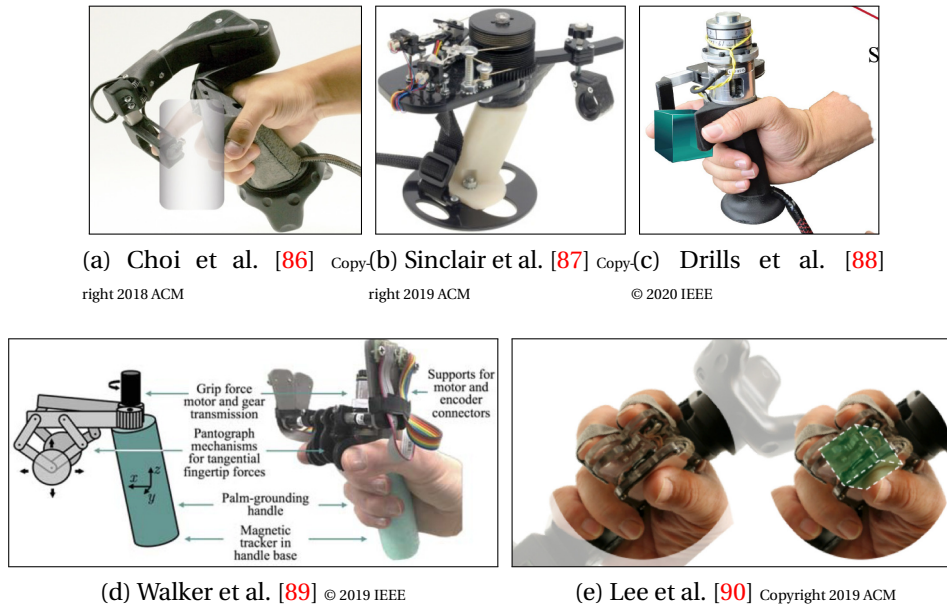


Figure 2.13: Active devices providing feedback and actuation for pinching. (a) Claw [86], (b) Capstan-Crunch [87], (c) Hybrid Active-Passive Actuation [88], (d) Holdable Haptic Device [89], (e) TORC [90].

2.1.2.3 Wearable Haptic Devices

Wearable haptics is gaining more and more interest in VR/AR, being unobtrusive, lightweight, inexpensive, and able to display varying touch sensations when interacting with virtual objects. However, these wearable devices can usually only provide ungrounded tactile stimuli (e.g., local shape, texture) and most kinesthetic sensations (e.g., weight, general shape) are missed [91]. Moreover, wearable devices can only provide stimuli to a reduced number of contact points (e.g., the fingertips), and increasing the number of these points directly affects the wearability and comfort of the system [36].

Several wearable devices have been designed to render to the user the contact and the orientation of a virtual surface: Frisoli et al. [92] were among the first to present a fingertip haptic display for improving curvature discrimination using a moving platform. The device is composed of a parallel platform and a serial wrist; the parallel platform actuates a translation stage for positioning the plate with respect to the fingerpad, while the wrist is in charge of adjusting its orientation. A more portable and improved design solution of the same concept was later on developed by Solazzi et al. [93] whose device worn at the finger had a voice-coil actuator to simulate fast contact transition. The overall system mobility was reduced to 3 DoF: two DoF for the orientation and one linear DoF to control the contact force at the fingertip using motors and Bowden cables. Similarly, Gabardi et al. [94] further improved this device by replacing sheathed tendon actuation with DC motors mounted directly on the joints. They used their wearable haptic device to explore a virtual surface: as the pose of the user's finger wearing the device was tracked through optical sensors, collisions between the finger avatar and the virtual surface were rendered using the wearable device.

Several wearable devices have been designed to render pressure and skin stretch on the fingers: Minamizawa et al. [95] presented a wearable fingertip device consisting of two DC motors that move a belt in contact with the user's fingertip. When the motors spin in opposite directions, the belt presses into the user's fingertip, and when the motors

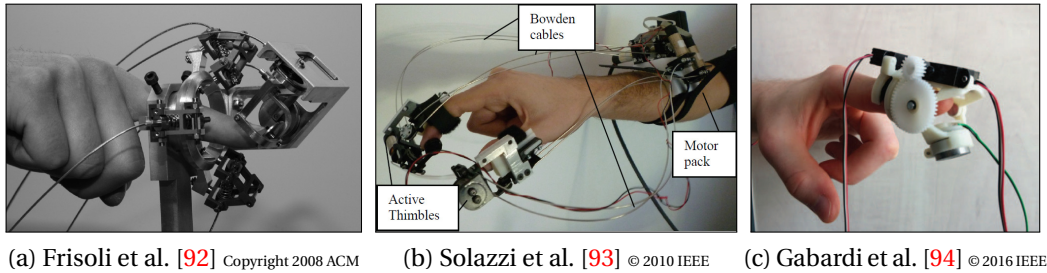


Figure 2.14: Wearable devices for contact and orientation display at the fingertips. (a) Fingertip Haptic Display [92], (b) Active Thimbles [93], (c) Haptic Thimble [94].

spin in the same direction, the belt applies a tangential force to the skin. A device similar to Minamizawa et al. [95] was also used by Pacchierotti et al. [96] in a pick-and-place VR experiment. The fingertips were tracked using a Leap Motion and the device was worn on the proximal finger phalanx to improve the tracking quality. The same device has been also used to render remote tactile experiences [97].

More recently, also Bianchi et al. [98, 99] adopted a similar design for a fabric-based wearable display. Two DC motors move two pulleys attached to an elastic fabric band in contact with the fingertip, varying its stiffness. Moreover, a lifting mechanism can regulate the pressure exerted by the fabric band on the fingertip, enabling the device to render softness information, pressure normal to the fingertip skin, and slipping sensations.

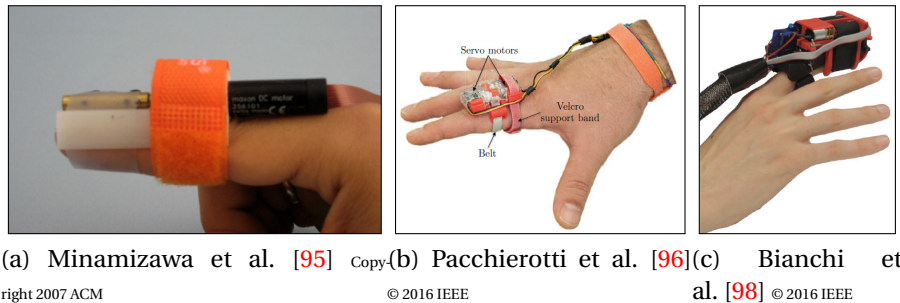


Figure 2.15: Wearable devices for pressure and skin stretch display. (a) Gravity Grabber [95], (b) hRing [96], (c) Wearable Fabric Yielding Display [98].

Several wearable devices have been designed in order to be more compact while still controlling accurately the position of a platform against the users' fingertips: Prattichizzo et al. [100] developed a wearable 3-DoF fingertip device consisting of two platforms: one located on the nail side of the finger, housing three DC motors, and the other one located in contact with the finger pulp. The two platforms are connected by three cables which lengths are controlled with motors to move the platform toward the user's fingertip and re-angle it to simulate contacts with arbitrarily oriented surfaces. Leonardis et al. [101, 102] developed a 3RSR (Revolute-Spherical-Revolute) wearable skin stretch device for the fingertip. It moves a rigid tactor in contact with the skin, providing skin stretch and making/breaking contact sensations. Later, they used two prototypes of their device for a pick-and-place experiment in a virtual environment [102]. The virtual scene was composed of a virtual cube, a table, and two static platforms. Subjects were asked to wear the two haptic devices

on their thumb and index fingers, and the tracking of the fingers was achieved using optical sensors. Chinello et al. [103] developed a similar device with a different mechanical structure which they later combined with a 1-DoF finger kinesthetic exoskeleton [104].

Maisto et al. [105] presented the experimental evaluation of two wearable haptic interfaces [96, 103] for the fingers in AR. They tested three scenarios: writing on a virtual board using a real chalk, where the haptic devices provided the interaction forces between the chalk and the board; pick and place of mixed virtual and real objects, where the haptic devices provided the interaction forces due to the weight of the virtual objects; balancing of a virtual sphere on a real cardboard, where the haptic devices provided the interaction forces due to the weight of the virtual sphere. Meli et al. [106] tested three other tasks in AR with the same wearables: a manipulation task, where participants had to pick an object either real or virtual and place it at another location; a guidance task, where participant had to place an invisible cube at a specific location following the tactile stimuli of the wearable device; a gaming task, a first-person shooter where they had to "air tape" to fire whilst feedback was provided through the wearable device.

Schorr and Okamura [107, 108] presented a wearable device composed of a delta parallel mechanism, capable of making/breaking contact with the fingertip, as well as rendering shear and normal skin deformation stimuli. The device has three translation DoF, enabling normal, lateral, and longitudinal skin deformation. They tested their wearable device in two user studies [108]. Subjects were asked to wear two haptic devices, on their thumb and index fingers. A head-mounted display was used to show the virtual environment, and the pose of the fingers was tracked using a magnetic tracker. In the first experiment, subjects were asked to discriminate the weight of virtual cubes. While in the second, participants could discriminate between modification in mass, stiffness and friction.

Alternatively, Girard et al. [109] developed a wearable fingertip device capable of rendering 2-DoF skin stretch stimuli with great accuracy and proposed several use cases in VR. Two DC motors move a tactor in contact with the finger pulp, achieving a maximum displacement of 2 mm in both directions. Their device was tested in several use cases in VR, like tapping on a virtual bottle, feeling the texture of a virtual surface, and feeling the weight of a virtual object. Later, Feng et al. [110] presented a waterproof wearable fingertip display consisting of four miniature airbags, as well as Wristband version. By inflating the airbags using a miniature speaker, the device can provide a wide range of vibrations as well as normal pressure to the fingertip.

More detailed information can be found in the following surveys: Sarac et al. [35] made a whole survey on hand exoskeletons for rehabilitation, assistive or haptic usage where they describe the mobility, mechanical design, actuation solution and operational strategy of the different devices in order to propose design requirement for generic hand exoskeleton. These are a subcategory from the wearables covered by Pacchierotti et al. [36], whose survey covers the previously developed wearable devices and categorized them upon their mechanical properties, the provided feedback and wearability in order to propose guidelines for future development.

2.1.3 Haptic Rendering

Haptic rendering algorithm are elaborated to compute in real time the command of such devices in order to render to the users the various phenomena resulting from virtual simulations or acquired from a real interaction (e.g., teleoperation). These often rely on physics engines which simulates the physical system of the virtual environment though



Figure 2.16: Compact wearable devices. (a) Towards Wearability in Fingertip Haptics [100], (b) 3-RSR [101], (c) 3-RRS [103], (d) Fingertip Tactile Devices [108], (e) HapTip [109], (f) Submerged Haptics [110].

approximation of Newtonian laws. They compute the dynamics of the various virtual elements as well as the collision and resulting forces between them. Common physics engines only need to render plausible visual representation of the simulation. However, force-feedback interfaces need real time physics with a realistic enough accuracy in order to provide a credible feedback to the users, running around 1 kHz allows to avoid stability issue.

Laycock et al. [111] made a survey on the haptic rendering techniques and exposed the base principle of haptic rendering for force-feedback interfaces which was later improved. Knowing the position and possibly the orientation of a tracked end-effector (such as a handle or a fingertip), the Haptic Interface Point (HIP) is set at the corresponding position and enable the exploration of the virtual environment. When the HIP is not in contact with any virtual element, no force of any kind should be rendered. However, when the HIP is intersecting a virtual element, the haptic device should provide some kind of feedback, like a resistive force. The basic rendering algorithm follows the procedure given by Laycock et al. [111] and highlighted on Fig. 2.17.

1. First, a collision detection flags whenever the HIP intersects the virtual object in order to start rendering feedback right away.
2. Then, the contact features are computed, like the normal to the surface, from which direction and which surface was crossed. As shown on Fig. 2.17a, when the HIP is within the object, there are uncertainties about which surface was actually crossed, and the direction of the rendered force could be ill-computed, resulting in visuo-haptic discrepancies for the users. The God Object algorithm introduced by Zilles et al. [112] allows to solve this issue. Their idea was to create a second haptic point, the Ideal Haptic Interface Point (IHIP), which would superimpose to the HIP in free-space but be constrained to the surface of the virtual object when the HIP interpenetrates it, then, slide onto the surface as the HIP moves within the object.

The IHIP allows then to extract the properties of the correct surface.

3. The penetration depth can then be estimated simply with the distance between the HIP and IHIP and be used in order to compute various kinds of feedback, e.g., rendering stiff contact simply by modeling the reaction force as with a spring model, the friction as the IHIP slide onto the surface with a drag force, or the torque induced by the friction, the texture of the surface, and by construction, the shape of the virtual surface. Many models were developed to render many kinds of contact phenomenon, but also to avoid discontinuities and computational artifacts.

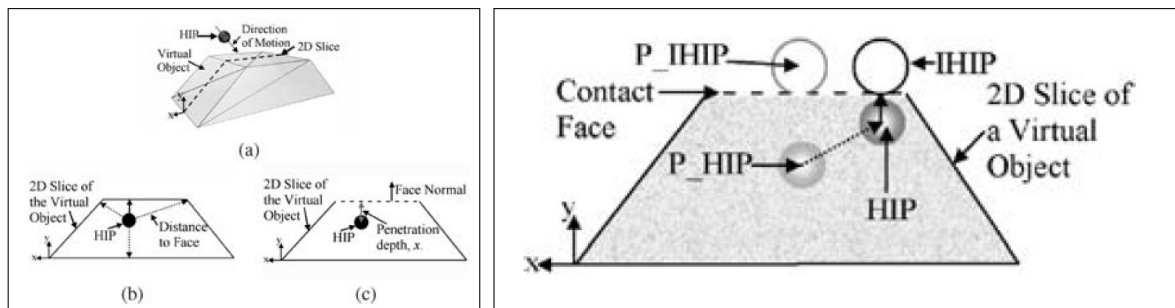


Figure 2.17: Simple HIP Algorithm [111]. Left: (a) HIP above the virtual object. (b) HIP penetrating the virtual object. (c) penetration depth. Right: The IHIP is tracked along the surface of the virtual object (P_ stand for previous). Journal compilation © 2007 The Eurographics Association and Blackwell Publishing Ltd

Even if this simple haptic algorithm is presented as a force rendering algorithm for force feedback interfaces, it can be used to command cutaneous feedback device such as the Gravity Grabber of Minamizawa et al. [95] by mapping the resulting contact forces to the skin displacement: the normal force can control the applied pressure, while the tangential component can control the lateral stretch. A similar method with an increased amount of HIP spread across the virtual finger's surface was elaborated in order to compute the mean surface orientation in order to tilt accordingly the platform of a wearable device [113].

More recently, Young et al. [114] devised a haptic rendering algorithm which adjusts the provided sensations to the physical characteristics of the target user's fingertip. They start with an existing data-driven haptic rendering algorithm that ignores fingertip size, and then they develop two software-based approaches to personalize this algorithm for fingertips of different sizes using either additional data or geometry. Results show that the personalized rendering algorithms performed better than the state-of-the-art generic solutions. Similarly, Pacchierotti et al. [115] presented a haptic rendering algorithm that adjusts the mechanical design of a wearable fingertip device to the target task. Given a set of target tactile interactions to render and a cutaneous device to optimize, they evaluate the minimum number and best configuration of the device's actuators to minimize an estimate of the haptic rendering error.

Instead of simulating physical phenomena with higher complexity and more accuracy, the rendering can be obtained through alternative synthesizing methods by exploiting features extracted from real pre-recorded signals. In that regard, Culbertson et al. [116] recorded the vibrations resulting from the human interaction with surface of various textures and extracted key features in order to render synthetic vibration generated in real time according to the user's motion. Later, Lu et al. [75] applied a similar method for

rendering synthetic sounds of various tool-surface interaction. Similarly, Pacchierotti et al. [117] presented a haptic rendering approach for fingertip cutaneous devices. It maps the stimuli sensed by a remote deformation sensor to the best possible input commands for the device's motors using a data set recorded with the tactile sensor inside the device. As a proof of concept, they considered a custom 3-DoF cutaneous device with a flat contact platform [118], in charge of applying deformations to the user's fingertip.

Another alternative is the use of real and tangible objects for the users to grasp or touch when interacting with virtual ones. Insko [3] defined this technique as *passive haptics* "that incorporates passive physical objects into virtual environments to physically simulate the virtual objects". they intrinsically provide various and distributed sensations over users' hands and address both tactile and kinesthetic sensibility through their shapes, textures, stiffness, mass distributions, etc. Using *Tangibles* increases the realism of the virtual environment [2] as well as the sense of presence [3], while rendering all these intertwined sensations at the same time with any actuated haptic device is challenging. Thus, the computation cost of the rendering is alleviated, and using *tangibles* with Virtual Reality is essentially a matter of registering the tangible and the virtual objects together in terms of positioning and similitude.

As we will see in the remaining sections of this Chapter, which focus will be centered on *Tangibles* in Virtual Reality, more and more works tend to use instrumented *Tangibles* with various kinds of sensors and actuators requiring haptic rendering algorithm similar to the ones previously mentioned.

2.1.4 Haptic Illusions

Sometimes, given in the right condition, some stimuli can be interpreted by the users in a totally different way than what they actually are, making them perceive something which is not happening. Such cases are called perceptual illusions. Two surveys from Hayward et al. [119] and Lederman et al. [120] provide extensive details about common perceptual illusions applied to the haptic perception. Both parties agreed on the fact that there is a wide range of interpretations of what a perceptual illusion is, but Lederman et al. [120] noted that it was commonly accepted to refer to an illusion as "the marked and often surprising discrepancy between a physical stimulus and its corresponding percept". Hayward et al. [119] suggested that a good compromise would be to define an illusion as a "percept arising from a specific stimulus delivered under specific conditions that gives conscious experience when the conditions are changed", focusing on the importance of the conditions and context when an illusion occurs.

Perceptual illusions are quite useful in haptics as it allows to manipulate the human perception to "enhance the display of information" [120] and make users perceive feedbacks which would actually be difficult or even impossible to produce with straight stimulation. A good example is the funneling illusion where two synchronous vibrations are applied at two different spots on the skin while a single vibration is perceived in-between. It is even possible to move the perceived stimuli along the axis between the two actual stimuli by adjusting their relative intensity [121].

However, perceptual illusions are not limited to a single modality (tactile, kinesthetic, visual, auditory, etc.): Biocca et al. [122] studied crossmodal illusion where "users use sensory cues in one modality to "fill in" the "missing" components of perceptual experience", i.e., cues from one modality can affect another modality. Eventually, a transfer can happen from one modality elicited by the system to another one which is actually not addressed at all by the system; for example, a visual feedback can provide haptic sensations to the users.

This exact case is defined as *pseudo-haptics* by Lécuyer [123], "a technique meant to simulate haptic sensations in virtual environments using visual feedback and properties of human visuo-haptic perception". Pseudo-haptic are quite interesting for VR environment as it is easy to create discrepancies between real and virtual, especially when altering the movement of a virtual object. As we will see in the upcoming sections, *pseudo-haptics* also works well when using *tangibles*.

2.2 Tangible Props in VR

The adjective "tangible" is defined by Merriam-Webster as something palpable: "capable of being perceived especially by the sense of touch" and something material: "substantially real". Thus, we will refer to real objects as *tangibles*, which can be used in order to mediate the interaction with virtual elements. As this idea is too broad, we will constrain it at the intersection of Tangible User Interface and Virtual Reality. However, some works may be considered in the following sections even if VR was not a core characteristic, as long as they provide interesting perspectives around *tangibles*.

Tangibility often manifests as real and physical objects or props, be it a plate, a table, a wall, a plank. They are often used in the passive haptic interaction technique described by Insko et al. [3]. However, they are referred under many wordings such as "objects", "props", "containers", "tokens", "artifacts", or even "passive haptics". Ullmer and Ishii [18] studied the terminology in the case of Tangible User Interface and concluded that many terminologies were used depending on the context without clear consensus.

According to the dictionary Merriam-Webster, a prop is defined as "something used in creating or enhancing a desired effect", which would be in our case, providing a real, compelling and complex contact through tangibility to a virtual counterpart. Hence, we will use the wording *tangible props* in this section.

This description of tangible props does not serve as a definition but only proposes hints toward one once the use of tangibles in VR becomes more common and as new ideas highlight complementary perspectives. Here, we suggest that tangible props should be defined on two distinct aspects: the physical affordances of the object and how it is used to render a virtual element. Hence, the tangible prop is also tied to the virtual representation in the virtual environment. For example, we will not consider material parts which are simply meant to elicit tactile stimulus as *tangible props*: a pin from a pin array is not designed to be perceived independently of the other pins, but the full array allows a user to perceive a curved surface that they will associate to the shape of a virtual element; a belt from the wearable device which we use in Chapter 3 is not meant to be perceived individually either as the piece of fabric it is, but is meant for the user to perceive pressure and stretch on his finger. These small end-effectors often provide local tactile stimuli and do not provide distributed sensation through the users' hands as expected from *tangibles*. In addition, despite being *tangible*, we will neither include end-effectors such as handles of grounded force feedback haptic devices or Encounter-Type haptic devices, nor hand-held devices as *tangible props*.

Moreover, props can be elements that users can grasp and manipulate at will like a glass or a plate, or bigger elements that the users can still manipulate to some extent such as a chair or a small table, or even immutable elements like a cupboard, or a wall. Thus, we propose to split this subcategory in two: *tangible objects* which are not too big props and are mostly graspable haptic interfaces [15]; *tangible surroundings* which are bigger props furnishing the real environment and representing the surrounding area in which the users can move and are mostly touchable haptic interfaces [15]. However, the boundary

between the two is blurred, but is sufficient to draw out some distinct characteristics. In the remaining part of this section we will present these two subcategories of tangible props which we will regroup under common thematic.

2.2.1 Tangible Objects

In this section, we describe several tangible objects used in order to mediate the interaction with virtual elements, and split them into 6 thematic subsections; Starting the simplest passive objects, then everyday life and custom-built objects, followed by reconfigurable ones. Finally, we will move toward instrumented objects, which embedded just sensors, then also actuators.

2.2.1.1 Passive Tangible Objects

Tangible object can be as simple as a passive and static cylinder. Ban et al. [124, 125] used one for the users to touch and explore with the index finger whilst displaying in the virtual environment their hand touching cylindrical virtual objects of various radial curvature, calling the technique MagicPot360 (Fig. 2.18a). Sait et al. [126, 127] also used a large cylinder to enable a physical grasp interaction with various virtual elements like a door knob or lever around the virtual environment (Fig. 2.18b), while Han et al. [128] pushed on remapping the users' physical reach with the same tangible prop (Fig. 2.18c).

Similarly, Azmandian et al. [129] used another simple shape, a cube, in a grasp and release VR task where participants would stack virtual blocks by always repositioning the same tangible cube through a haptic retargeting technique (Fig. 2.18d). Meanwhile, Yamaguchi et al. [53] used a stick or a sword prop for the users to touch/hit a real drone to provide a tangible impact anywhere in the work space (Fig. 2.18e).

However, passive tangible objects can assume more complex shape: Spillman et al. [130] used a knee replica for a virtual arthroscopy surgical simulator. The prop is made of bones, ligaments, and menisci of different materials in order to give realistic hard or compliant tactile cues, while manipulating the tools (Fig. 2.18f).

2.2.1.2 Everyday Life Tangible Objects

Everyday life is filled with plenty of object which are commonly accessible and can serve as tangible props for virtual interactions. Moreover, they provide natural and familiar shapes as users are used to them. In the early days of tangible props, Hinckley et al. [131] used a doll head embedded with orientation and position tracking for surgeons to manipulate and visualize a virtual brain before the surgery (Fig. 2.19a). Later, Hoffman et al. [2] simply used a plate to physically touch a virtual plate for their experiment on the realism of a VR scene (Fig. 2.19b). Meanwhile, Oshima et al. [132] made the users grab tangible mallets in order to hit a virtual puck in an AR air hockey game, AR2Hockey (Fig. 2.19c). Then, Sheng et al. [133] proposed an interface to sculpt virtual clay by interacting with a sponge (Fig. 2.19d). And, Miller et al. [134] used a tangible prop made out of building blocks toy (Fig. 2.19e). Alternatively, Billingham et al. [135] used a book, the MagicBook, made out of a ring binder and cardboard pages augmented with AR (Fig. 2.19f); While, Kato et al. [136] used a tracked cup, the MagicCup, to pick and move around virtual element of an AR city planning (Fig. 2.19g); More recently, Kashiwagi et al. [137] proposed to use real tools like screwdriver or spray in order to mediate the interaction while using data gloves to acquire the real action to reproduce in the virtual environment (Fig. 2.19h). Similarly, Strandholt et al. [138] used a real hammer, a screwdriver and a blade-less saw to mediate

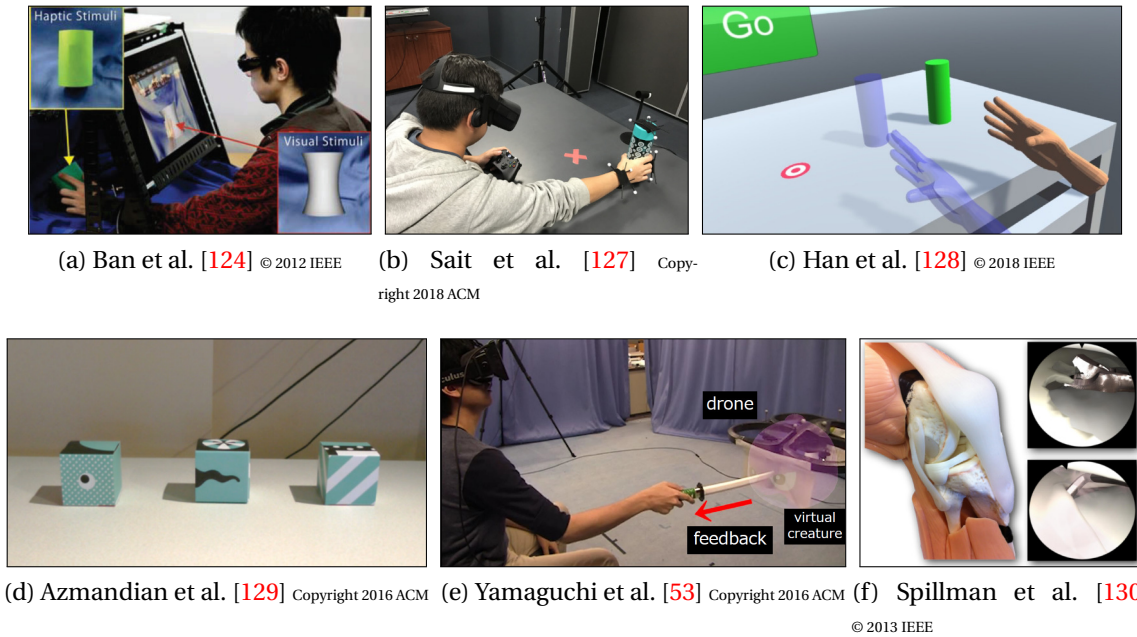


Figure 2.18: Passive Tangible Objects. (a) MagicPot360 [124, 125], (b) Physical Hand Interaction [126, 127], (c) Remapped Physical Reach [128], (d) Haptic Retargeting [129], (e) Haptic Display Using a Drone [53], (f) Arthroscopy Surgical Simulator [130].

the interaction, as the users perform the real task on a bare wooden plank, the virtual interaction is re-targeted as the virtual nail, screw or saw going into the virtual plank 2.19i).

Furthermore, some studies extensively revolve around the use of everyday life objects: Simeone et al. [139] proposed a framework which revolve around using any available tangible objects and tangible furniture in the workspace to substitute tangibles to virtual elements which look similar. They used several real objects: a mug, a wine bottle, a torch, an umbrella and a Force FX replica of Darth Vader’s Lightsaber for the users to grasp, while similar virtual objects are displayed with induced virtual discrepancies such as texture, temperature, missing or additional parts (Fig. 2.20a).

Alternatively, Hettiarachchi et al. [140] propose an AR framework, Annexing Reality, which consist of scanning the real environment in order to find objects with primitive shapes similar to the virtual objects to register them together for the users to grasp and manipulate (Fig. 2.20b).

Later, Yang et al. [141] developed a methodology to track tangible objects and applied it to a chemistry VR scenario in which users can use real chemistry glassware to manipulate virtual solutions (Fig. 2.20c). Similarly, Lowe et al. [142] proposed to use physics lab tools and to augment them as to provide additional information for students (Fig. 2.20d).

More recently, Zhou et al. [143] developed another methodology to use everyday life objects as tangible counterparts but also to turn them into tactile surfaces. By fully tracking the hand using optical tracking and a marked glove, their approach deduces the primitive shape of the object from the hand pose. The primitive is then used to create a virtual tactile surface onto the object, for the other hand (Fig. 2.20e).

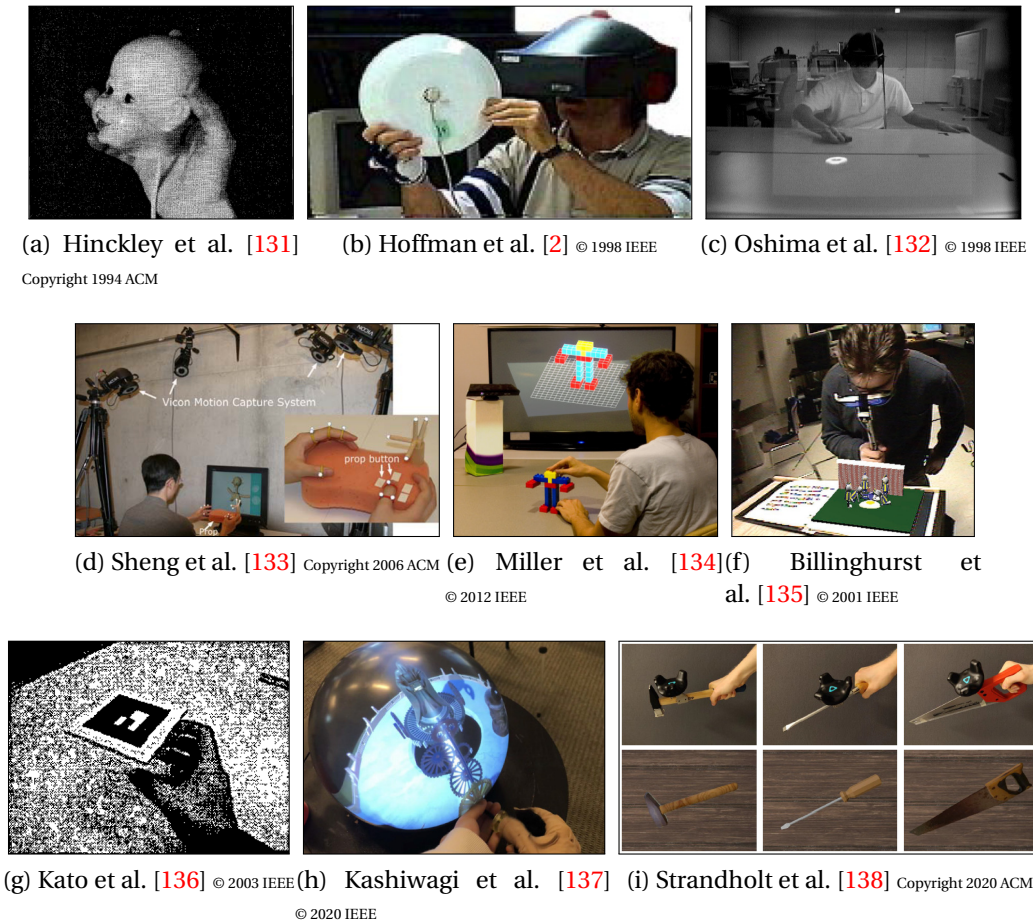
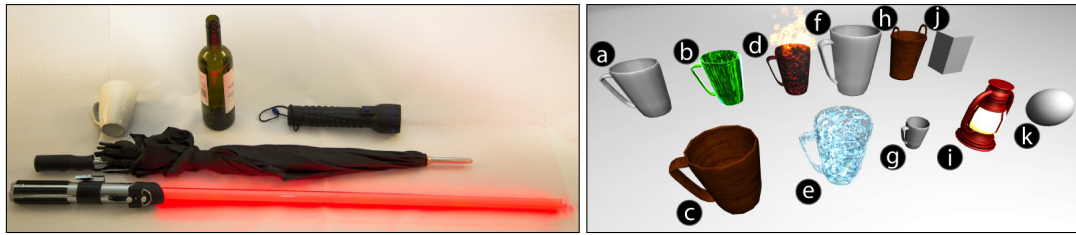


Figure 2.19: Simple Everyday Life Passive Objects. (a) Passive Real-World Interface Props [131], (b) Physically Touching Virtual Objects [2], (c) AR2Hockey [132], (d) Virtual 3D Sculpting [133], (e) MagicCup [136], (f) MagicBook [135], (g) Building Block Structures [134], h) Props in Real-World [137], i) Knock on Wood [138].

2.2.1.3 Custom-Built Tangible Objects

Sometimes, researchers would build themselves tangible objects with specific designs according to their needs and requirements of their studies. A fast and easy solution is to use paper or cardboard: Kwon et al. [144] made boxes of various sizes to grasp AR boxes (Fig. 2.21a), while Song et al. [145] used handicraft such as origami to mediate their AR storytelling environment (Fig. 2.21b).

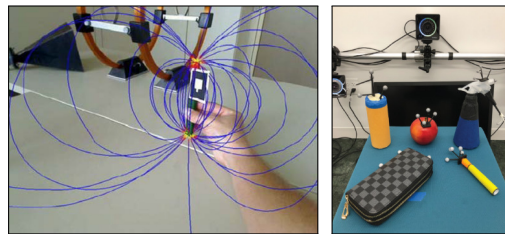
However nowadays, 3D-printing tends to be more common and a good solution whenever the tangibles have more complex designs. In that regard, Kruszynski et al. [146] developed an interface to visualize a virtual model of coral, by holding a 3D-printed one. Similarly, Spence et al. [147] 3D printed replica of museum objects attached to a transparent box containing a marker, for the users to hold the tangible artifact and explore it with the hand (Fig. 2.21i). Clergeaud et al. [148] also used 3D-printed props, but to enable asymmetric collaboration during meeting. Users outside of the virtual environment can interact with the one actually in VR using a large ring which act as a window toward the virtual scene and a cylinder which uses the world-in-miniature technique to see the whole virtual scene (Fig. 2.21d). More recently, Dong et al. [149] 3D-printed tangible props similar to the mechanical part of an expensive and fragile device used for Cryo-Electron



(a) Simeone et al. [139] Copyright 2015 ACM



(b) Hettiarachchi et al. [140] Copyright 2016 ACM (c) Yang et al. [141] © 2016 IEEE



(d) Lowe et al. [142] © 2017 IEEE (e) Zhou et al. [143] Copyright 2020 ACM

Figure 2.20: Frameworks around everyday life objects. (a) Substitutional Reality [139], (b) Annexing Reality [140], (c) Perceptual Issues of MR System [141], (d) Augmenting Laboratories [142], (e) Grip-marks [143].

Microscopy to provide tangible counterpart to their VR formation scenario (Fig. 2.21e). And, Gainer et al. [150] 3D-printed replica of a hazardous material device as to make a scenario in for firefighters in a public safety formation (Fig. 2.21g).

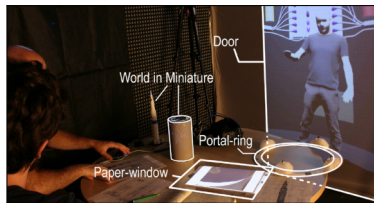
However sometimes 3D-printing is not possible: Zielinski et al. [151] built a transparent cube, the Specimen Box, in order to manipulate the virtual object within the cube (Fig. 2.21c). This tangible prop is meant to be used with a CAVE. As it is transparent, users can see their hands, the cube and the virtual object within the cube while the stereoscopic images are displayed behind it. Similarly, Englmeier et al. [152] built a transparent sphere with a Vive Tracker inside to enable the tracking to work properly (Fig. 2.21h).

Alternatively, Muender et al. [153] used three sets of tangible props with different levels of fidelity objects: wood cylinders, Lego assemblies and 3D-printed props similar to the virtual ones (Fig. 2.21f).

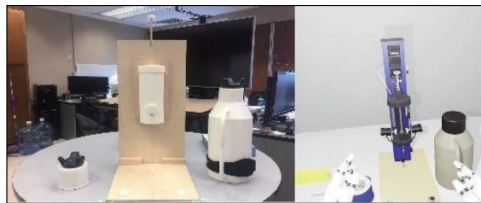
Meanwhile, Villegas et al. [154] created an entire custom tabletop setup for an escape game. It included a red 3D-printed complex shape for a virtual enigma, several tangible flat surfaces with markers, a calculator and a vertical surface (Fig. 2.21j).



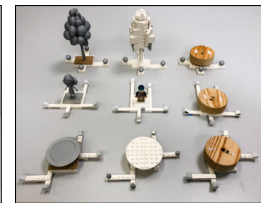
(a) Kwon et al. [144] © 2009 IEEE (b) Song et al. [145] © 2019 IEEE (c) Zielinski et al. [151] © 2017 IEEE



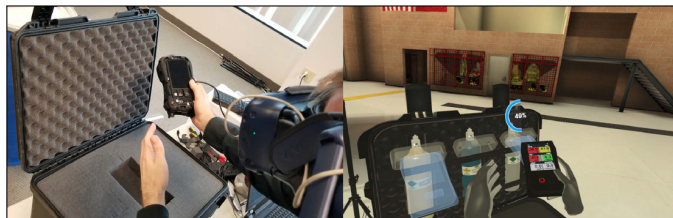
(d) Clergeaud et al. [148] Copyright 2017 ACM



(e) Dong et al. [149] © 2019 IEEE



(f) Muender et al. [153] Copyright 2019 ACM



(g) Gainer et al. [150] © 2020 IEEE



(h) Englmeier et al. [152] © 2020 IEEE



(i) Spence et al. [147] Copyright 2020 ACM



(j) Villegas et al. [154] © 2020 IEEE

Figure 2.21: Custom built tangible objects. (a) Tangible Augmented Reality [144], (b) Mixte Reality Storytelling Environment [145], (c) Specimen Box [151], (d) Asymmetric Collaboration [148], (e) Cryo-EM Sample Preparation [149], (f) Using Tangible with Different Fidelities [153], (g) Detection of Hazardous Material [150], (h) Sphere in Hand [152], (i) VRtefacts [147] (j) Virtual Escape Game [154].

2.2.1.4 Reconfigurable Tangible Objects

In order to increase the reusability of tangible objects and render various virtual objects, they can be reconfigurable by design: Aguerreche et al. [155] built a reconfigurable device made of either three or four telescopic arms of tripods linked together by hinges. Users can then extent or extract each segment (Fig. 2.22a). Similarly, McClelland et al. [156] proposed HaptoBend, a device which could be reconfigured by the users to match virtual objects of various shapes. It is made of 4 plates linked with hinges which users can rotate according to the virtual object they want to manipulate, as rotation sensors are embedded (Fig. 2.22b). Alternatively, such objects can also be self-reconfigurable: Zhao et al. [157] designed small

mobile robots which can assemble themselves in order to shape tangible objects similar to the virtual objects (Fig. 2.22c).

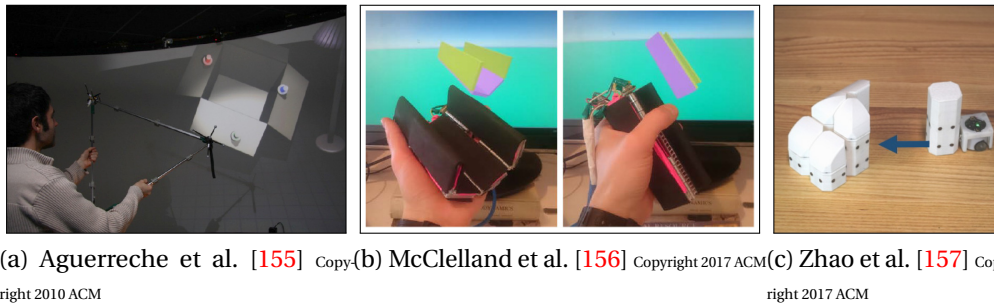


Figure 2.22: Reconfigurable tangible objects. (a) Reconfigurable Tangible Devices [155], (b) Hapto-Bend [156], (c) Robotic Assembly [157].

2.2.1.5 Tangible Object Embedded with Sensors

Tangible objects can be embedded with sensors other than those for rigid position and orientation tracking, as to enable more complex virtual interaction. Wang et al. [158] proposed to use a tablet to track the user's stylus and to sketch on a virtual object, the users can either hold the tablet or the real object behind the tablet (Fig. 2.23a). Alternatively, de Siqueira et al. [159] printed a handle with an actual rotating reel into which, a Microsoft Surface Dial is embedded as to track the rotation of the reel and render virtual fish being reeled in (Fig. 2.23b).

Force sensors are common in order to trigger an interaction: Issartel et al. [160] used a cube with AR markers on each face to display the content of the virtual environment within this volume, and with pressure plates behind the faces to enable the grasping of virtual objects (Fig. 2.23c). Similarly, Callen et al. [161] made a flexible tangible prop out of layers of foam and fabric containing a grid of pressure sensors to detect the users' pressing location and sculpt virtual objects (Fig. 2.23d). Some devices even push the idea further to track interaction up to the third dimension: Panchaphongsaphak et al. [162] developed a 3D interface shaped as a brain which is attached to a base embedded with 6-DoF force/torque sensors. As users touch a part of the brain, an algorithm reconstructs the touching point through the detection of the resulting force and torque at the base (Fig. 2.23e). Similarly, Iwata et al. [163] proposed a concept of deformable device, Volflex, an assembly of small balloons which can individually inflate or deflate with actuated air-cylinder. In addition, pressure sensors enable the system to acquire the amount of force developed by the users (Fig. 2.23f).

In a different way, Otte et al. [164] used a custom keyboard with capacitive sensing on each key in order to allow an immersive text entry within VR (Fig. 2.23g).

2.2.1.6 Actuated Tangible Objects

Tangibles props can also provide various kinds of active feedback by embedded actuators in them, especially vibrotactile feedback: Zhao et al. [165] used a tactile surface in order to track users' finger while providing a virtual counterpart to the finger/tablet interaction as well as electrovibration feedback (Fig. 2.24a). Adilkhaniv et al. [166] proposed a cuboid object, VibeRo, which is made of two plates attached with spring hinges in order

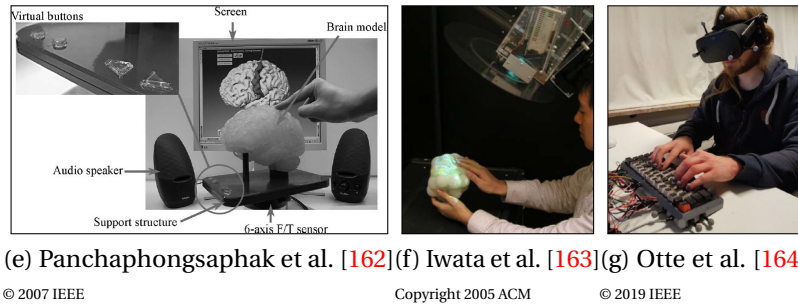
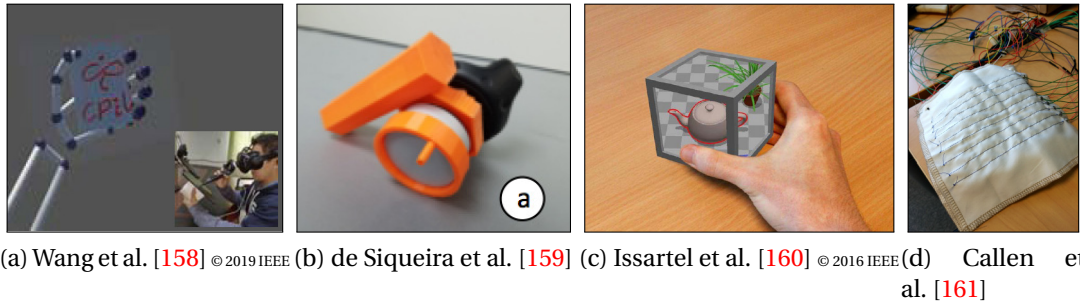


Figure 2.23: Tangible objects embedded with sensors. (a) Tablet for Tangible 3D Sketching [158], (b) Commercially Available Commodity Devices [159], (c) Tangible Volume [160], (d) Digital Sculpting [161], (e) Three-Dimensional Touch Interface [162], (f) Volflex [163], (g) Touch-sensitive Physical Keyboard [164].

to enable users to press and deform it. Force sensors on each plate measure the pinching force of the users. In addition, a voice coil actuator in the middle can generate vibratory feedback (Fig. 2.24b). In another way, Sun et al. [167] embedded 4 eccentric rotating masses actuated with motors to provide vibrotactile feedback within a tangible cube, Smart Haproxy (Fig. 2.24c). Similarly, Harley et al. [168] developed four diegetic tangible objects prototypes for VR storytelling, including a cube, a stuffed animal, a treasure chest, and a wooden boat which were instrumented in order to detect some specific manipulation. In addition, the stuffed animal could be stroked, move its head and have a heartbeat as users manipulate the virtual squirrel (Fig. 2.24d).

As an alternative to simple vibrotactile feedback, Amemiya et al. [169] built a box with a mechanism which can asymmetrically translate a weight in order to change the perceived weight of the tangible prop (Fig. 2.24e). Meanwhile, Tanaka et al. [170] made a device able to provide torque feedback to the user. GyroCube, is a 2kg cube in which 3 flywheels rotate at high speed, and changing the speed of one of them induce a torque in the opposite direction (Fig. 2.24f).

Alternatively, some tangible objects are actuated in order to make them self-reconfigurable or mobile: Guinness et al. [171] used the Ollie robot to interact with the virtual environment, the robot is embedded with accelerometers but also sensors to measure the angle of rotating parts. In addition, the robot can also provide feedback as the wheels are actuated by motors (Fig. 2.25a). He et al. [54] proposed to use a cylindrical robot for the users to grasp or to put a real object onto the robot. The purpose of using a mobile robot is to alternatively render different virtual objects or a moving virtual object (Fig. 2.25b). Inoue et al. [172] made a tangible prop with several parts which can rotate with respect to one another. The device can be reconfigured by the users and adjust in a similar shape the corresponding virtual object or, the other way around, it can reconfigure itself physically

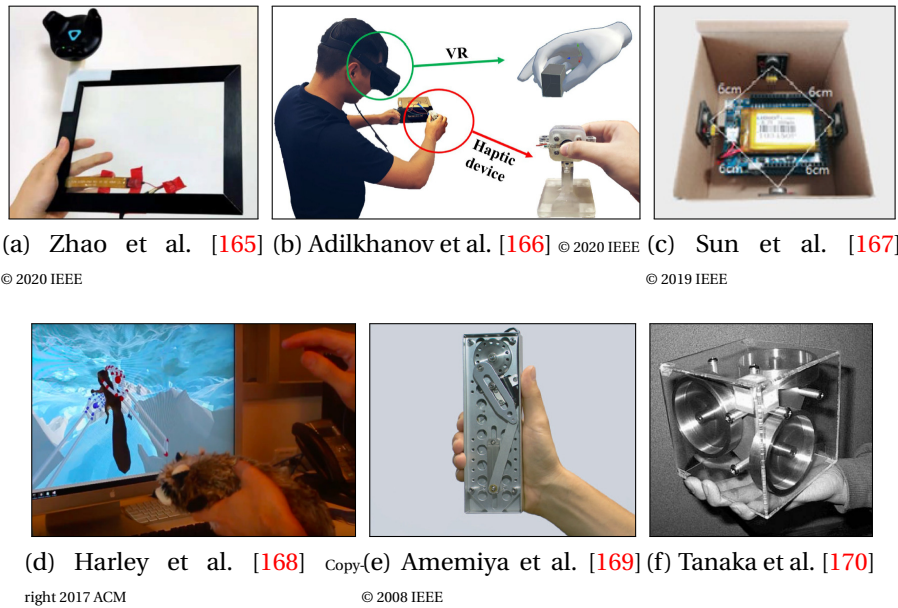


Figure 2.24: Actuated tangible objects, part 1. (a) Touch-based Interaction Using Electro-vibration Haptic Feedback [165], (b) VibeRo [166], (c) Smart Haproxy [167], (d) Diegetic Tangible Objects [168], (e) Asymmetric Oscillation Distorts the Perceived Heaviness [169], (f) GyroCube [170].

to assume the shape of the virtual environment (Fig. 2.25c).

Furthermore, toolkits were designed specifically for the users to reconfigure the tangible object depending on the VR interactions available: Arora et al. [173] designed a toolkit to make various shaped tangible props. VirtualBricks is composed of several bricks with dedicated usage: 1DoF rotation (or translation) sensors (or actuators), buttons, vibration motors or a lock mechanism to prevent separation of bricks. Each brick can communicate with the main system using Bluetooth modules (Fig. 2.25d). Similarly, Feick et al. [174] made another kit, TanGi, also based on tracked blocks which enable 4 interactions with feedback, two passive which are bending, and linear stretch, and two actives with 1 DoF respectively for translation and rotation (Fig. 2.25e).

Alternatively, Zhu et al. [175] proposed a toolkit made of strips the users can twist and assemble in order to make more complex and detailed rigid shapes. Instead of modules with dedicated mobility, they proposed more classic input (e.g., buttons, triggers) and output modules (e.g., vibrotactile modules) which can be attached anywhere on the object (Fig. 2.25f).

2.2.2 Tangible Surroundings

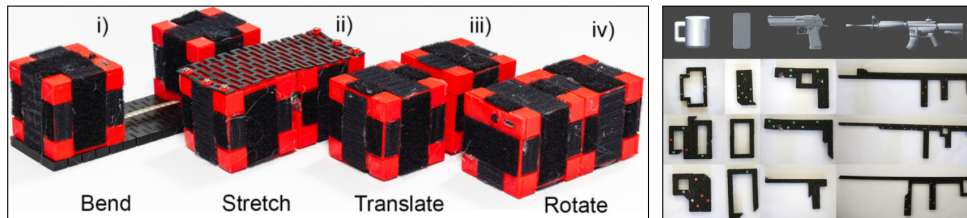
In this section, we describe *tangible surroundings* which give a physical shape to the whole virtual scene, and splitting them into 4 thematic subsections; Starting with tangible furniture, then various tangible surfaces. Finally, we will move toward floor elements, and structural elements like walls or poles.

2.2.2.1 Tangible Furniture

A real environment is almost never empty, there is always furniture with which one can interact: a chair to sit on, a table to lean on, etc. Thus, Simeone et al. [139] suggested in



(a) Guinness et al. [171] Copyright 2017 ACM (b) He et al. [54] Copyright 2017 ACM (c) Inoue et al. [172] Copyright 2019 ACM (d) Arora et al. [173] Copyright 2019 ACM



(e) Feick et al. [174] © 2020 IEEE (f) Zhu et al. [175] Copyright 2019 ACM

Figure 2.25: Actuated tangible objects, part 2. (a) GUI Robots [171], (b) Robotic Haptic Proxies [54], (c) Transformable Game Controller [172], (d) VirtualBricks [173], (e) TanGi [174], (f) HapTwist [175].

their Substitutional Reality to integrate the physical environment into the virtual one by substituting virtual furniture to similar real one (Fig. 2.26a).

As users are used to navigate through an environment filled with furniture, Simeone et al. [176] substituted virtual obstacles by actual furniture for the users to reach during a behavioral walking task (Fig. 2.26b). While, Wang et al. [177] made users walk along a redirected path across a virtual flat while they were actually moving in a smaller workspace, touching and avoiding some tangible furniture (Fig. 2.26c).

Cheng et al. [178] used two furnishing *tangibles* in a VR scenario, iTurk: a foldable prop made of 3 hinges panels which are tracked independently in order to render various virtual elements that the users will reconfigure during each step of the scenario, rendered alternatively as a suitcase, a fuse cabinet, a railing, and a seat. The second tangible is a pendulum made of a suspended ball which can render moving virtual objects such as flying droids attacking the user (Fig. 2.26d). Alternatively, Matsumoto et al. [179] altered the shape of a real squared table in order to display virtual tables with various numbers of sides (Fig. 2.26e).



(a) Simeone et al. [139] Copyright 2015 ACM (b) Simeone et al. [176] © 2017 IEEE (c) Wang et al. [177] © 2020 IEEE (d) Cheng et al. [178] Copyright 2018 ACM (e) Matsumoto et al. [179] Copyright 2017 ACM

Figure 2.26: Tangible furniture. (a) Substitutional Reality [139], (b) User Movement Behaviour [176], (c) A Constrained Path Redirection [177], (d) iTurk [178], (e) Magic Table [179].

2.2.2.2 Tangible Surfaces

The surroundings of an environment can occasionally contain various surfaces for the users to interact with and which often serve as anchor in space as the users are moving through the workspace: Insko et al. [3] used real counters to passively render a virtual environment in which participants would explore while being able to touch them with their hands as they walked (Fig. 2.27a). Similarly, Kholi et al. [180] used a single cylindrical tangible pedestal for the users to reach and lean on while they would explore the virtual environment within which several cylindrical pedestals were present. Each one would be alternatively re-registered with the real pedestal as the users were redirected while walking (Fig. 2.27b).

Otherwise, countertops can serve as stand-still interaction space: Follmer et al. [181] proposed a TUI concept, inFORM, to compose various kinds of interaction using a shape display which can actuated a grid of large pins as to dynamically change the shape of the surface. In addition, the system can be used to move around small round props while images can be projected on top of it (Fig. 2.27c). Similarly, Degraen et al. [182] made a Haptic Palette which can rotate and display various textures to the users while changing the texture or the color of virtual furniture (Fig. 2.27e). Diversely, Zenner et al. [183] developed an immersive tool which relies on tangible ramps onto which the users drop a ball and later retrieve it back while seeing a machine collecting the first ball as a message to process and generating a new virtual item afterwards (Fig. 2.27d).

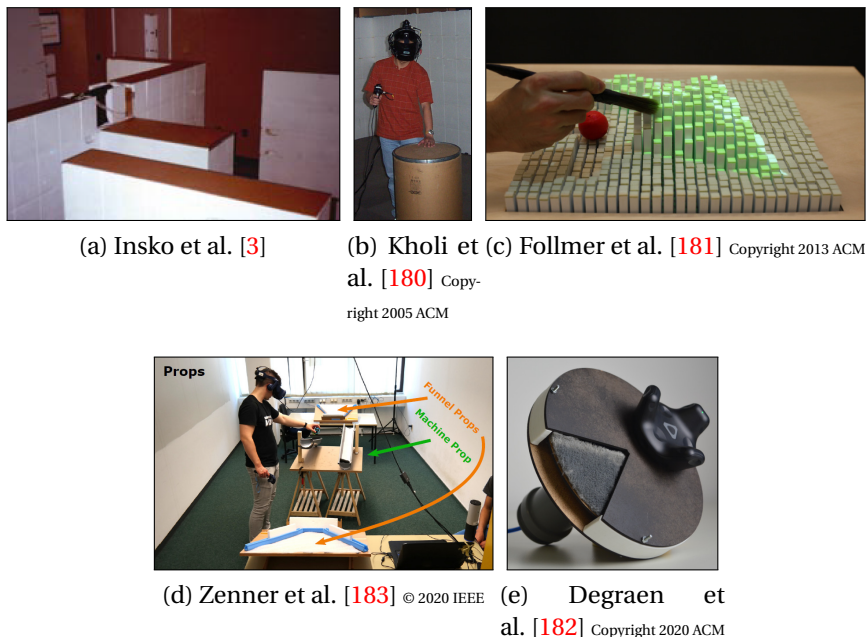


Figure 2.27: Tangible surfaces, part I. (a) Passive Haptics Significantly Enhances VE [3], (b) Passive Haptics With Redirect Walking [180], (c) inFORM [181], (d) Immersive Process Model Exploration [183], (e) Haptic Palette [182].

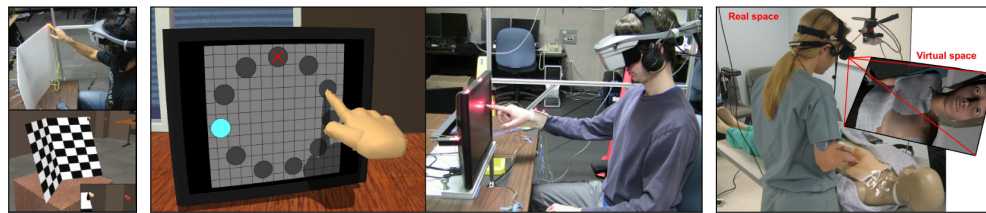
Surfaces often provide a hard or stiff feedback while being easy to use and easy to find. Any countertop, desk or pieces of furniture can serve such purpose: Matthews et al. [184] used a surface with two tangible buttons which users would press while pressing various virtual buttons in different configurations (Fig. 2.28a). While, Viaciana-Abad et al. [185] made participants press virtual buttons as they were touching a table either with the hand

or a stylus (Fig. 2.28b), and Zielasko et al. [186] used a desk and a vertical surface in order to support the interaction with a virtual menu (Fig. 2.28c). Similarly, Kholi et al. [187, 188, 189] used several furnishing *tangibles* which users could touch while seeing the virtual hand's motion altered in order to touch a virtual counterpart of different shapes or curvatures being touched. They first applied a virtual illusion to a table (Fig. 2.28d), then a retargeting touching technique to a foam board placed on a table (Fig. 2.28e) and finally simply on a flat surface to study how users would train and adapt to a warped virtual space (Fig. 2.28f).

Furthermore, tangible surfaces can be curved, Kotanza et al. [190] developed a VR clinical breast exam scenario where participants would have to palpate a tangible breast simulator placed on top of a dummy (Fig. 2.28g).



(a) Matthews et al. [184] (b) Viaciana-Abad et al. [185] (c) Zielasko et al. [186] © 2019 IEEE (d) Kholi et al. [187] © 2009 IEEE



(e) Kholi et al. [188] © 2010 IEEE

(f) Kholi et al. [189] © 2013 IEEE

(g) Kotanza et al. [190] © 2008 IEEE

Figure 2.28: Tangible surfaces, part II. (a) Remapped Physical-Virtual Interfaces [184], (b) Influence of Passive Haptic [185], (c) Menus on the Desk? [186], (d) Perceptual Illusions [187], (e) Redirected Touching: Warping Space [188], (f) Redirected Touching: Training and Adaptation [189], (g) Mixed Reality Human [190].

2.2.2.3 Floor Elements

Walking on tangible props can increase the feeling of actually being on a non-flat surrounding at various height: Hasanzadeh et al. [191] built a large prop which resemble a part of a tilted rooftop for the users to step on, while the virtual roof is displayed in the CAVE system (Fig. 2.29a). Similarly, Aoyagi et al. [192] used real training slack rails as tangible counterparts to a virtual slack between two buildings (Fig. 2.29b). Alternatively, Vasylevska et al. [193] made tangible bridges either flat or concave in order to render uneven virtual bridges which the users are crossing (Fig. 2.29c).

Many works focus on going up and down virtual stairs by make users walk on various tangible props: Kasarda et al. [194] used planks of various shapes to render virtual stairs on a flat floor: they used either large planks, large planks with bumps in the middle, or narrow planks (Fig. 2.29d). Whilst, Nagao et al. [195] used small sticks to render the corners of the virtual stairs (Fig. 2.29e). Later, Nagato et al. [196] used tilted props in order to ascend or descend stairs (Fig. 2.29f).



(a) Hasanzadeh et al. [191] © 2020 IEEE (b) Aoyagi et al. [192] © 2019 IEEE (c) Vasylevska et al. [193] © 2020 IEEE



(d) Kasarda et al. [194] © 2020 IEEE (e) Nagao et al. [195] Copy-right 2017 ACM (f) Nagato et al. [196] © 2018 IEEE

Figure 2.29: Floor elements. (a) A Study in Safety Interventions [191], (b) VR Bridges [193], (c) Tightrope Walking [192], (d) Virtual Stairs Travel Techniques [194], (e) Infinite Stairs [195], (f) Ascending and Descending [196].

2.2.2.4 Structural Elements

Structural elements such as walls and poles can also be used to support virtual interaction: Matsumoto et al. [197, 198] used a curved wall to guide the users along a straight path in the virtual environment (Fig. 2.30a), and a circular handrail to make users walk along an unlimited corridor (Fig. 2.30b). While, Batmaz et al. [199] also used a wall in order to perform an eye-hand coordination task in AR and VR (Fig. 2.30c). Alternatively, Eckstein et al. [200] made participants open and close a tangible window to reach for a virtual sphere outside of a virtual window (Fig. 2.30d). Tiator et al. [201] even made a low height wooden climbing tower for the users to climb onto while climbing a virtual mountain (Fig. 2.30e). And, Ahmed et al. [202] used several static shapes attached to the wall to evaluate several factor of the perception of distance within VR (Fig. 2.30f).

In some experiments, more complex structural elements were used: Chardonnet et al. [203] used a real harness and a metallic ladder for the users to climb in order to perform a virtual task on a power line (Fig. 2.30g). While, Cheng et al. [204] proposed a concept of immutable *tangibles*, TurkDeck, which are reconfigured and actuated by people to compose the tangible surrounding as users go through the virtual environment. The props are made of chipboard panels with hinges and magnets to hold the configuration. Metal pipes with various attachments are used to provide additional tangible contact and study supports (Fig. 2.30h).

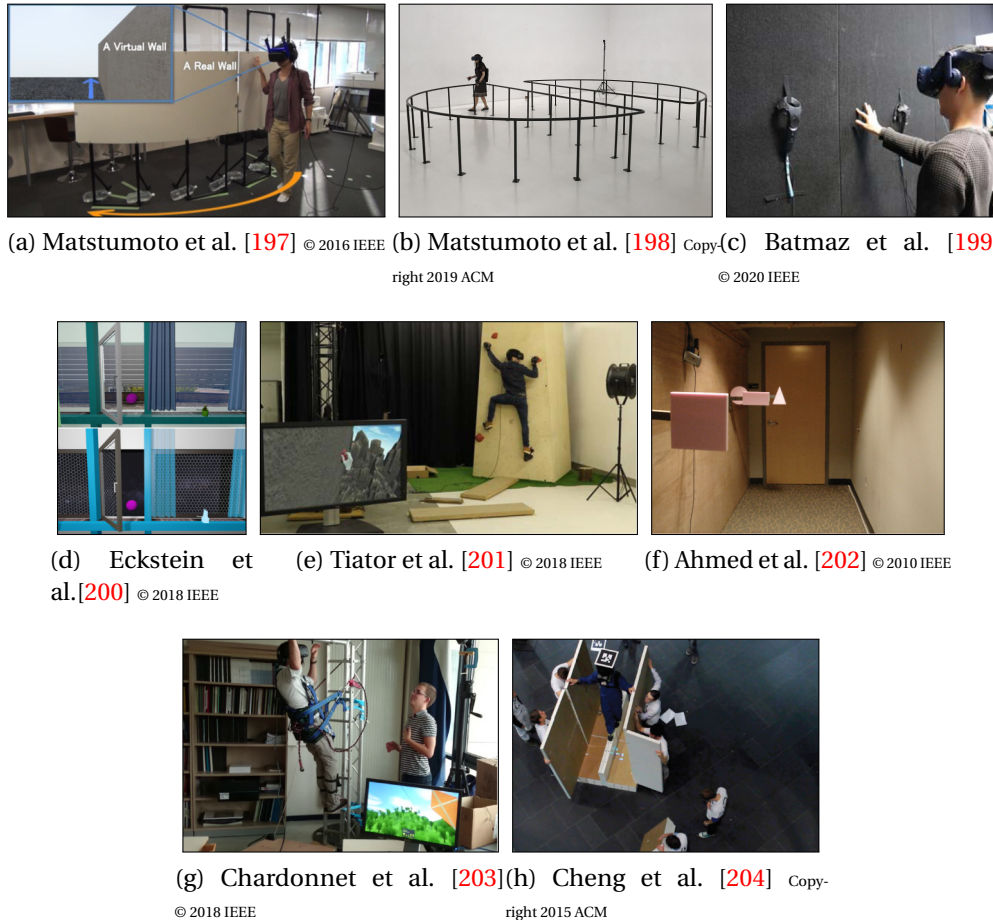


Figure 2.30: Structural elements. (a) Curvature Manipulation Techniques [197], (b) Unlimited Corridor [198], (c) Touch the Wall [199], (d) Smart Substitutional Reality [200], (e) Cliffhanger-VR [201], (f) Egocentric Distance Perception [202], (g) Simulator to Detect Acrophobia [203], (h) TurkDeck [204].

2.3 Application of Tangibles in Virtual Environment

In this section, we will focus on the applications, framework and research paradigm around the use of *tangibles* in virtual environments. Starting from the passive-haptics technique as described by Insko [3], research gradually pushed further, uncovering new prospects and applications which go beyond the simple passive-haptic technique. This section simply provides an objective overview of the applications for VR. We will analyze these works, their limitations and constraints compared to the contributions of exposed in this manuscript only in the last section of this chapter.

2.3.1 Passive Haptics

Tangibles were initially used as tangible props superimposed to virtual counterparts by Hoffman [2] who called them tactile augmentation as it provides the compelling sensations of real objects to the hand through their shape, weight and textures. By opposition to actuated haptic devices for which rendering such properties altogether is difficult and requires both physics simulation and haptic rendering algorithm in order to generate a realistic feedback, passive physical objects can render a virtual environment with no

simulation cost while being inexpensive and increasing the overall realism of the virtual environment. Later, Insko [3] defined the technique of using real passive objects to "physically simulate" virtual objects, passive haptics, and showed that it can also increase the sensation of presence.

Since then several studies focused on understanding the impact of passive haptics in virtual environments. Vician-Abad [185] performed an experiment where participants had to press buttons following a sequence they previously remembered, with the hand or a stylus, against a tangible surface or mid-air. Their results showed that adding a real surface increased both the sense of presence and the task performance of the users with no significant difference between the direct touch or the tool mediated touch. Whereas in absence of passive feedback, interacting with the stylus provides worst results than with the hand. Their findings also pointed out the benefit of providing a real contact to the user. Similarly, Zielasko et al. [186] studied the impact surface touch against mid-air interaction, either horizontal or vertical, for a menu selection. Participants had to specify on the menu the parameters of the single different object in a cloud of objects. However, they observed no significant difference between the conditions, which can only suggest that adding passive haptic feedback does not lead to negative effects. However, they observed a preference for the passive haptic feedback conditions. As contact is critical, Bovet et al. [205] argued that self-contact is also a strong source of passive haptic feedback and plays a role in the embodiment and thus in presence. In their experiment, they induced movement amplification and positioning offsets to decrease the sense of agency. Then, by enabling self-contact, they could mitigate the negative impact and observe a strong sense of agency despite moderate movement distortion.

In short, tangible props are regularly used in virtual environments as they often allow a natural interaction and a good immersion for a lower cost. In the following couples of paragraphs, we will highlight different applications cases and contexts where the passive haptics technique naturally fits together with Virtual Reality.

2.3.1.1 Recreational Virtual Scenario

Tangible can mediate virtual interaction in a simple way. For example, Oshima et al. [132] developed an AR air hockey game using tangible mallets with which users can hit a virtual puck (Fig. 2.31a). Similarly, in the AquaGuantlet game [206], users shoot computer-generated creatures superimposed onto a real scene. Users hold vibrotactile fake guns that turn into bigger rifles in the virtual world and vibrate whenever the users pull the trigger (Fig. 2.31b).

There can also be several *tangibles* over a large area to carry on a more complex virtual game. In that regard Cheok et al. [207] developed a mixed-reality game where players walk around a large room-size area and pick up real objects, as if they were playing a traditional non-virtual game. However, these real objects are augmented with superimposed virtual objects and figures, e.g., a real box is opened and inside it is found a virtual treasure. As the scenario progresses, the game transitions from AR to VR to change the environment accordingly. Villegas et al. [154] also developed an escape game where participants interact with several *tangibles* to solve enigma in VR (Fig. 2.31d).

Tangibles are good mediums to interact with the progress of a virtual scenario, especially by performing natural manipulation based on everyday life experiences. Billinghurst et al. [135] present an AR tangible book with enabling users to turn its pages, look at the pictures, and read the text as in a normal book. However, as they are wearing an AR HMD, they can also see 3-dimensional virtual models popping out of the pages and

acting the narrative (Fig. 2.31c). Alike, Song et al. [145] developed an AR storytelling environment which allows users to either create or play virtual stories by manipulating a tangible origami (Fig. 2.31e).

Similarly, Harley et al. [168] present a system for diegetic storytelling with tangible objects in VR. They developed four tangible objects prototypes, including a cube, a stuffed animal, a treasure chest, and a wooden boat which are instrumented in order to detect some specific manipulation. For example, the stuffed animal is a furry squirrel toy with a skeletal cage to give structural integrity to its body with a moving head and a heartbeat which can be either calm or accelerated as users stroke its back (Fig. 2.31f).



(a) Oshima et al. [132] © 1998 IEEE

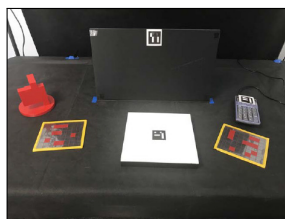


(b) Tamura et al. [206]



(c) Billinghurst et al. [135] © 2001 IEEE

© 2018 IEEE



(d) Villegas et al. [154]

© 2020 IEEE



(e) Song et al. [145] © 2019 IEEE



(f) Harley et al. [168] Copy-

right 2017 ACM

Figure 2.31: Recreational virtual scenario. (a) AR2Hockey [132], (b) AquaGuantlet [206], (c) Magic-Book [135], (d) Virtual Escape Game [154], (e) Storytelling Environments [145], (f) Tangible VR [168]

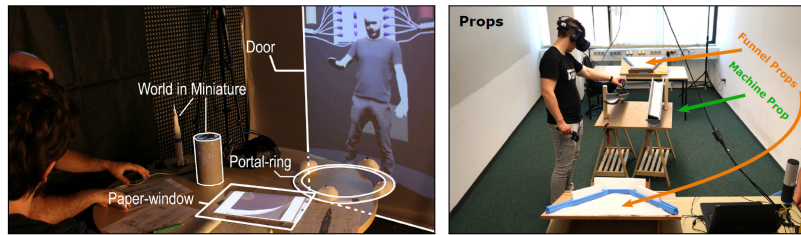
2.3.1.2 Virtual Working

Tangibles are also used for more serious activities. Kato et al. [136] proposed an interaction technique for city planning: by moving a cup around, users can pick up and move virtual elements in the AR environment (Fig. 2.32a). Then as well, Muender et al. [153] studied the impact of the shape fidelity of the tangible props in a virtual mock-up for scenic visualization in professional domains like cinematography, drama or architecture (Fig. 2.32b). Alternatively, Clergeaud et al. [148] proposed to use props combined with an HMD for asymmetric collaboration: users in a meeting room can put on an HMD and use props for a better communication and assistance from their remote location to a user immersed in the main VR environment (Fig. 2.32c).

Zenner et al. [183] developed an immersive tool which allows to generate a virtual environment with multi-sensory feedback based on tangible props. Instead of the 2D graph visualization used in professional domains, they proposed a 3D immersive exploration of event-driven process chains where participants can explore and learn about the targeted process simply by walking around, picking and dropping a tangible sphere on a specific slop area (Fig. 2.32d).



(a) Kato et al. [136] © 2003 IEEE (b) Muender et al. [153] Copyright 2019 ACM



(c) Clergeaud et al. [148] Copyright 2017 ACM (d) Zenner et al. [183] © 2020 IEEE

Figure 2.32: Virtual working, part II. (a) MagicCup [136], (b) Does It Feel Real? [153], (c) Asymmetric Collaboration [148], (d) Immersive Process Model [183]

2.3.1.3 Virtual Training Scenario

VR is especially efficient in order to develop training scenarios:

Kotanza et al. [190] developed a VR clinical breast exam scenario for medical education with a Mixed Reality Human (MRH), "a virtual human embodied by a tangible interface that shares the same registered space". The physician-assistant students performed a clinical exam by palpating a tangible breast simulator and speaking to the virtual MRH patient. Their initial studies showed that participants displayed a stronger social engagement over the RMH than previous studies as the interpersonal touch was close to a human-human interaction (Fig. 2.33a).

In the area of public safety, Gainer et al. [150] addressed a need for firefighters to have a VR simulation for the detection of hazardous material. They built a 3D-printed tangible prop similar to an actual air monitoring device with sensors embedded to enable interaction and manipulation of the virtual tool. According to Gainer et al. using custom props should enable the participants to learn better how to use the real device, but also decrease the cognitive load and increase the training transfer and achieve faster response to critical incidents compared to simulation relying on classic interaction with VR controllers (Fig. 2.33b). Similarly, Dong et al. [149] 3D-printed tangible props in order to provide feedback and compelling sensation in a training scenario, CryoVR: Biological scientists can learn to prepare bio-sample for Cryo-Electron Microscopy by following step by step the operations to carry on the expensive and fragile device, simply by manipulating the props in the virtual scenario (Fig. 2.33c).

Alternatively, augmenting real equipment in AR can also be used in order for teaching. Lowe et al. [142] proposed a framework around the idea of enhancing in real time physics experimental tool with AR as to provide additional information and visual display to help students understand physical phenomenon, e.g., displaying forces on a pendulum, displaying magnetic field lines of a magnet, highlighting the area of interest on a system, etc (Fig. 2.33e). Similarly, Yang et al. [141] provided a method and an application case to

use real chemistry equipment in VR as to allow students to perform potentially dangerous chemical reactions (Fig. 2.33d).

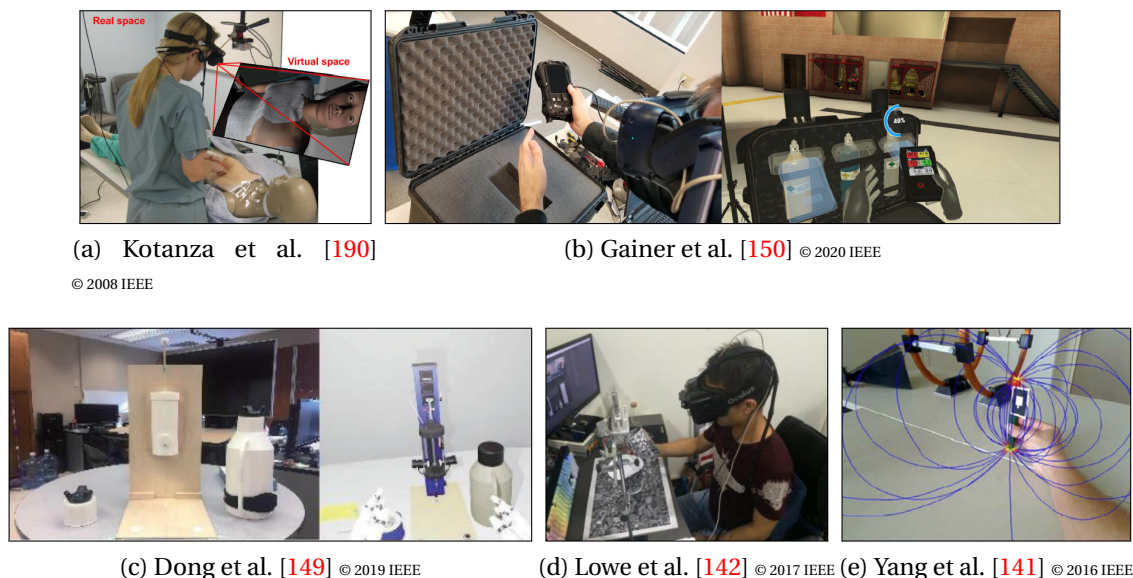


Figure 2.33: Virtual working, part II. (a) Mixed Reality Human breast exam [190], (b) Detection of Hazardous Materials [150], (c) CryoVR [149], (d) Augmenting Laboratories [141], (e) Perceptual Issues of Passive Haptics [142]

2.3.1.4 Risk Minimization Virtual Environments

VR also allows to immerse users in virtual environments which would be dangerous in the real environment. By adding passive haptic feedback, their experience can be very compelling while avoiding the risk of the real situation.

In that regard, Aoyagi et al. [192] developed a VR tightrope simulator where participants walk on a real slack rails laying on the floor while seeing themselves on a tightrope between two skyscrapers (Fig. 2.34a). Equivalently, Tiator et al. [201] proposed a high cliff climbing simulation in VR for the users to train themselves in a stressful situation while actually climbing on a safe and low high climbing tower (Fig. 2.34b). Alternatively, Hoffman et al. [208] proposed to use VR and passive haptic as to treat spider phobia. In their study, two groups of participants had to touch the virtual spider with their avatar's hand, one without any feedback and one with passive haptic feedback which could feel a furry body. Participants from the second group were later able to get closer to a real spider than the first one (Fig. 2.34c).

More recently, studies also used VR simulation with passive haptics in order to detect risky behavior. Hasanzadeh et al. [191] developed a simulation for roof intervention where participants were asked to perform action on a tangible slope in a CAVE system. participants had a tangible interaction with the roof while the surrounding area was displayed with the CAVE. By monitoring their behavior against different level of safety, they could trigger behavioral changes in order to detect risk-taking behaviors and identify at-risky workers (Fig. 2.34d). Similarly, Chardonnet et al. [203] developed a VR scenario where participants need to harness themselves to poll from a platform and then climb a little to catch a virtual kite stuck in power lines at 10 meters high, while in reality they are

actually harnessing themselves to a real metallic ladder. This scenario could be used to detect cases of acrophobia (Fig. 2.34e).

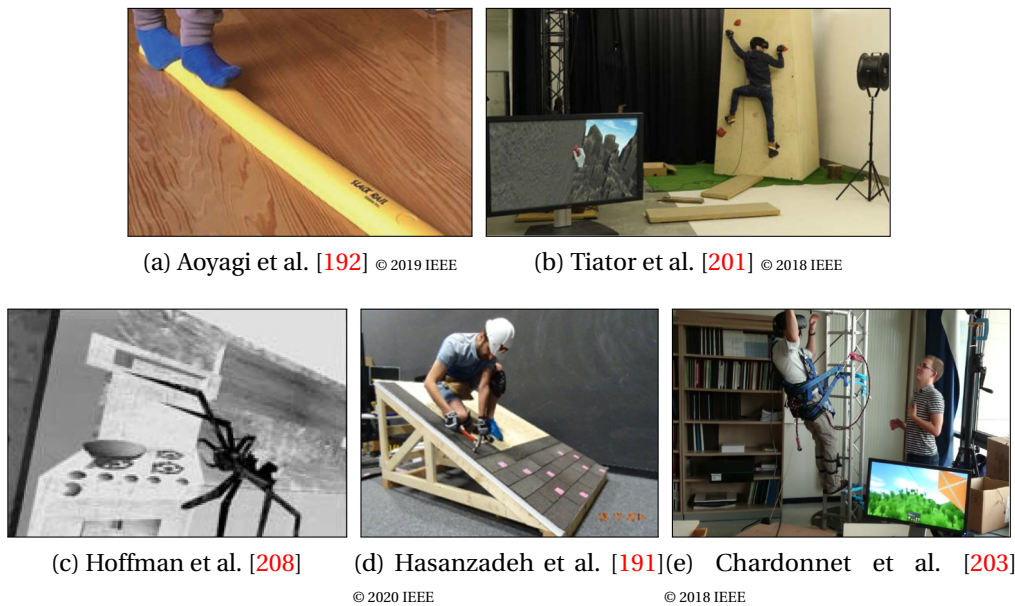


Figure 2.34: Risk minimization virtual environments. (a) Tightrope walking [192], (b) Cliffhanger-VR [201], (c) Treating Spider Phobia [208], (d) Risk-Tacking Behavior [191], (e) Simulator to Detect Acrophobia [203].

2.3.1.5 Data Manipulation

Using a tangible prop can also mediate the manipulation of data in a natural and easy way. Hinckley et al. [131] used a doll head embedded with sensors for surgeons to manipulate and visualize a virtual brain. They could also select cutting planes on the virtual brain by performing a natural two hand manipulation: simply moving a tool around the doll head (Fig. 2.35a). Similarly, Kruszynski et al. [146] developed an interface to visualize a virtual model of coral, by holding a 3D-printed one and touching it with a tracked stylus. The users can then select an area and obtain different measurements displayed on the screen in front of them.

Similarly, Montano-Murillo et al. [62] brought the stylus/tablet interaction paradigm into VR by fixing an actual stylus and tablet to VR controllers with 3D-printed supports. They can then perform touch interaction in VR while being able to move a volume attached to the virtual tablet in order to select points in the point cloud data (Fig. 2.35b).

Alternatively, Panchaphongsaphak et al. [162] developed a 3D touch sensitive interface which is shaped as a brain and attached to a 6-DoF force/torque sensor. They developed an algorithm able to reconstruct the interaction point on the prop by measuring the resulting force and torque on the base. Users are then able to select an area or define a cross section on the virtual model simply by touching it with their finger (Fig. 2.35c).

2.3.2 Beyond Passive Haptics

However, using just passive *tangibles* to register it to a virtual replica in order to provide feedback to the users is constraining. If the virtual scene contains several virtual elements



Figure 2.35: Data manipulation. (a) Doll Head [131], (b) Slicing-Volume [62], (c) Brain model [162]

which each needs to be register to a *tangible*, multiple tangibles have to be tracked at the same time or to be carefully calibrated at fixed locations. Moreover, making exact replicates is not necessarily possible and highly reduce the reusability of the tangible, whilst the human perception admits some range of error. Furthermore, with the current technologies, it becomes easily feasible to embed sensors and actuators into any *tangible*, i.e., to use actuated *tangibles*.

In the following Sections, we present works using *tangibles* which go beyond the sole passive haptics technique: Starting from re-registration in real-time of virtual elements on a single tangible, then reconfiguration of the real environment in real-time. After that, we will discuss works analyzing and using similitude and discrepancy between *tangibles* and virtual elements and works around the idea of enhancing the perceived haptic properties of *tangibles*. Lastly, we will discuss applications using ETHD, generic enhanced haptic controllers, and some new life-like paradigms.

2.3.2.1 Re-registration to Multiple Virtual Elements

A first idea to increase the re-usability of a tangible prop is to find ways to register it with various virtual elements in real-time. This can be achieved directly through successive registration in sequential tasks in the virtual scenario, registering a new virtual object to the tangible once a part of the task is done. For example, in Sun et al. [167] experiment, participants had to put the tangible prop down and wait for the next piece of the puzzle to appear on the prop before grasping it (Fig. 2.36a). Similarly, a new registration can be done as the users move toward a new location in the virtual environment, while bringing him back to the same place in the real workspace where they can find a new virtual object register to the same tangible prop: Kholi et al. [180] studied a redirecting technique which could always bring the users to the same tangible cylindrical pedestal while they reach a new pedestal in the virtual environment (Fig. 2.36b). Sait et al. [127] did something similar with the additional constraints of reorienting the virtual scene to correctly align the virtual element to interact with (lever or doorknob, etc.) with the tangible prop laying on a table (Fig. 2.36c). Cheng et al. [178] pushed the idea further by making the users reconfigure and adjust the position of the tangible prop to complete the task and also prepare the next virtual task they would reach later on. For example, in a room the users would need to open a fuse-box to switch a button which would become a 2-segments railing with buttons on it in the next virtual room (Fig. 2.36d).

In case users are standing still in the same virtual area, another method is to retarget the motion of the virtual hand in order to reach a new virtual element while reaching the same tangible one: Azmandian et al. [129] would make participants reach for a new cube and stack it on the previous one while actually always reaching the same tangible

cube and putting it elsewhere on the table (Fig. 2.36e). Han et al. [128] evaluated two methods to achieve a one to many approach also relying on physical reach mapping and showed that constant shifting between various positions would perform better than dynamic interpolation (Fig. 2.36f). Similarly, Kholi et al. [189] studied how users can adapt themselves to a warped environment where the registration configuration of tangible and virtual spots to touch on the surface would change at run time (Fig. 2.36g). On the contrary, Matthews et al. [184] studied the difference between retargeting the hand toward the tangible button or the tangible button toward the hand, as well as a bimanual retargeting where users would hold the tangible surface with one hand and touch the button on it with the other (Fig. 2.36h).

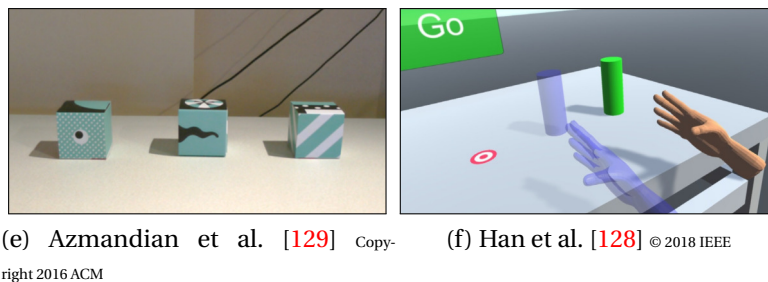


Figure 2.36: Re-registration. (a) Smart Haproxy [167], (b) Passive Haptics With Redirect Walking [180], (c) Physical Hand Interaction [127], (d) iTurk [178], (e) Haptic Retargeting [129], (f) Remapped Physical Reach [128], (g) Redirected Touching: Training and Adaptation [189], (h) Remapped Physical-Virtual Interfaces [184].

2.3.2.2 Reconfiguration of the Physical Environment

The tangible prop proposed by Cheng et al. [178] which users manipulate in different virtual locations is also reconfigurable as it is made of several hinged panels, making it possible to render an operable suitcase or fuse box. To avoid further issues, the tangible props are registered to virtual elements of similar shapes. However, by making them

reconfigurable, it becomes possible to register the same tangible props to virtual elements of different shapes.

In that regard, McClelland et al. [156] made a device in 4 hinged parts which can be bent in order to take various shapes whilst sensors detected the current configuration (Fig. 2.37a). Inoue et al. [172] connected several triangular parts with pivot joints with sensors and actuators in order to allow the users to reconfigure the device or make the device reconfigure itself (Fig. 2.37b). However, even if the device is reconfigurable, it does not necessarily assume the shape of the virtual element. Aguerreche et al. [155] made a device out of tripods links and hinges in order to provide a reconfigurable handle to grasp virtual objects (Fig. 2.37c). Reconfigurability can also apply to bigger elements such as surrounding props as Cheng et al. [204] showed when they made a whole tangible surrounding by moving a complete set of props as the users progressed through the virtual environment in their TurkDeck experiment. All props were positioned on the fly by a coordinated group of human workers (Fig. 2.37e).

Alternatively, to their man-actuated props, *tangibles* can be actuated in order to create the necessary tangible shape. Zhao et al. [157] proposed to use small cubicle mobile robots to automatically create an approximation of the targeted virtual object (Fig. 2.37d). Follmer et al. [181] proposed a TUI concept, inFORM, which can approximate a surface by changing the height of every pin of a 2D array (Fig. 2.37f), while Siu et al. [56] made a smaller array embedded on a mobile robot which can also change the orientation of the rendered shape (Fig. 2.37g).

As already explained in a previous section, hand-held devices can be reconfigurable in order to change their mass distribution [65, 66, 68, 69]. While providing a different visual, the change of inertia enforces the idea that the hold object is different. Shifty [65] with a single DoF of actuation can render virtual object of various length and thickness (Fig. 2.37h), while Transcalibur [66] with its two 2-DoF actuated weights can render virtual objects of asymmetrical shape (Fig. 2.37i). Alternatively, in addition to the weight translation, ShapeSense [68] can provide air resistance by actuating 3 different surfaces in order to adjust the amount of air resistance (Fig. 2.37j), and Drag:on [69] also provide air resistance but by automatically opening and closing fans (Fig. 2.37k).

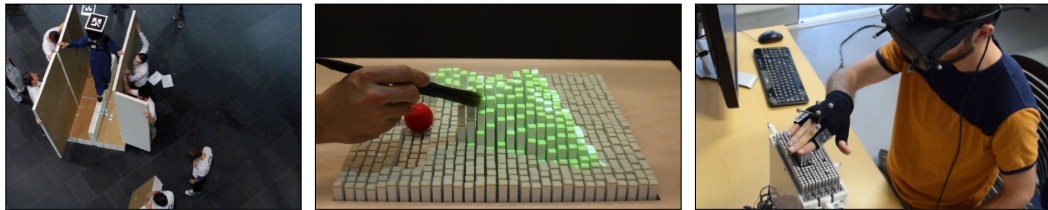
2.3.2.3 Similitude and Discrepancy between Tangibles and Virtuals

Having an exact replica between *tangibles* and their virtual counterparts is not necessarily mandatory as long as tangible objects presents similar affordances in parts most likely to be interacted with by users [139]. Moreover, some discrepancies like additional or missing parts are more critical when trying to substitute a tangible object of everyday live to a virtual one, as the users will feel something they are not seeing or see something they cannot feel. But, they pushed their concept further by proposing the Substitutional Reality framework, where the whole tangible workspace is brought into the virtual environment as each one would substitute a virtual element of similar shape, from small objects to the biggest furniture (Fig. 2.38a). Eckstein et al. [200] even suggested bringing smart home elements into the virtual environment. In the same line of work, Hettiarachchi and Wigdor [140] developed a system able to scan the surroundings to find objects of everyday life and compute their closest primitive shape in order to register them to the various virtual objects through a primitive shape matching process (Fig. 2.38b).

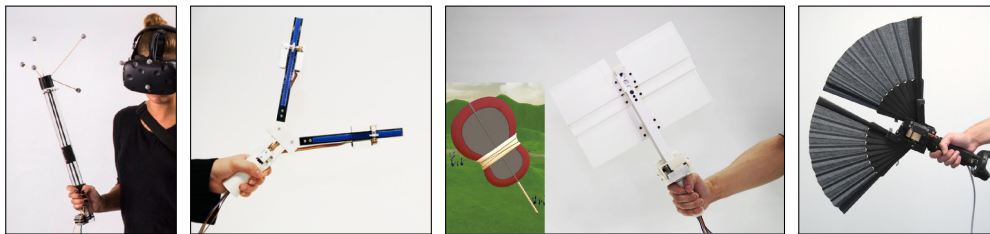
Muender et al. [153] also studied the impact of the shape fidelity of the tangible props in a virtual mock-up for scenic visualization. They made participants manipulate the virtual elements by grasping *tangibles* with 3 different levels of fidelity: simple wooden cylinders,



(a) McClelland et al. [156] Copy-right 2017 ACM (b) Inoue et al. [172] © 2019 IEEE (c) Aguerreche et al. [155] right 2010 ACM (d) Zhao et al. [157] Copyright 2017 ACM



(e) Cheng et al. [204] right 2015 ACM (f) Follmer et al. [181] Copyright 2013 ACM (g) Siu et al. [56] Copyright 2017 ACM



(h) Zenner et al. [65] © 2017 IEEE (i) Shigeyama et al. [66] Copyright 2018 ACM (j) Liu et al. [68] Copyright 2019 ACM (k) Zenner et al. [69] Copyright 2020 ACM

Figure 2.37: Reconfiguration of the physical environment. (a) HaptoBend [156], (b) Transformable Game Controller [172], (c) Reconfigurable Tangible Devices [155], (d) Robotic Assembly [157], (e) TurkDeck [204], (f) inFORM [181], (g) shapeShift [56], (h) Shifty [65], (i) Transcalibur [66], (j) ShapeSense [68], (k) Drag:on [69].

reconfigurable Lego toys and 3D printed exact replicas. Although, using replicas was more effective, approximated shapes made of Lego blocks would provide a more versatile and faster solution with sufficient fidelity (Fig. 2.38c). Knowing the users would hold the hand-held tangible by the hilt, Fujinawa et al. [61] developed a method to compute a weight distribution of the tangible which would provide compatible inertia perception to the virtual object the users would see. Both virtual and tangible would have similar handles and inertia while being altogether different. Their Haptic Shape Illusion is meant to design hand-held devices for tangible substitution or as a base design for further development of hand-held devices (Fig. 2.38d).

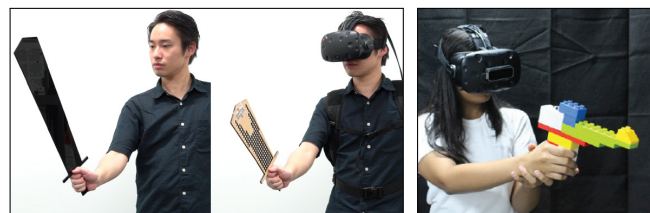
This idea of building the needed tangible to later use it within the virtual environment was a lead motivation in the design of toolkits made of blocks with dedicated purpose. VirtualBricks of Arora et al. [173] are toys like bricks which can interlock with each other while having single basic functions: one embedded IR tracking sensors; two can provide a rotating joint an actuated one and a passive with rotary encoder; similarly, two others have a single axis translation joint, an active and a passive; another one has a lock mechanism to prevent block from being separated; one can vibrate whilst the last one embedded a button. Linking such blocks with passive one, is possible to build a tangible with a dedicated purpose and an affordable shape, such as a gun, a fishing rod, or even a mixer for DJ. The

tangible can then be controlled in real time as Bluetooth module are embedded in each dedicated brick (Fig. 2.38e). Feick et al. [174] also designed a toolkit with main cubic blocks with Velcro on every side to connect them together. One block can be attached to a Vive tracker to track the tangible as a whole, while the dedicated blocks are a bit different and enable 4 interactions: two passive for bending and linear stretching, and two active to enable a single axis for rotation and translation. In addition to this blocks, they also designed ending blocks of various shapes like half spheres of several sizes, triangular parts or cubicle parts of various sizes and thickness, as to allow a high variability of shapes (Fig. 2.38f).

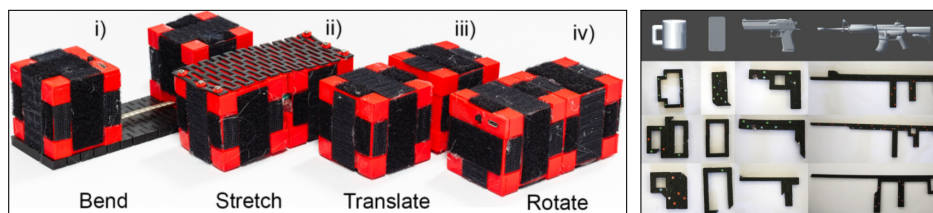
An alternative to block based toolkits, the HapTwist developed by Zhu et al. [175] is composed of Rubik's Twists, strips which are aggregates of small prism which can rotate with respect to one another, i.e., they can be twisted in order to take various shapes. By combining several strips with connection slots more complex shapes can be generated. Similarly, various input (button, or trigger) and output modules (vibrators, fan, thermo-electric) can be added at any location on the strips in order to enable further functionality (Fig. 2.38g).



(a) Simeone et al. [139] Copyright 2015 ACM (b) Hettiarachchi et al. [140] right 2016 ACM (c) Muender et al. [153] Copy-right 2019 ACM



(d) Fujinawa et al. [61] Copyright 2017 ACM (e) Arora et al. [173] Copy-right 2019 ACM



(f) Feick et al. [174] © 2020 IEEE

(g) Zhu et al. [175] Copy-right 2019 ACM

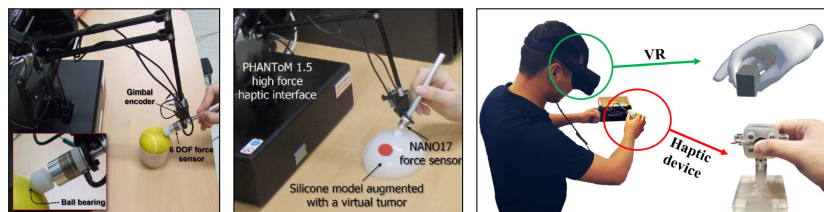
Figure 2.38: Similitude and discrepancy between tangibles and virtual elements. (a) Substitutional Reality [139], (b) Annexing Reality [140], (c) Does It Feel Real? [153], (d) Haptic Shape Illusion [61], (e) VirtualBricks [173], (f) TanGi [174], (g) HapTwist [175].

2.3.2.4 Enhanced Haptics Property of Tangibles

However, using reconfigurable close-in-shape props is not necessarily the only alternative to increase the reusability of *tangibles*. Since the human perception is not perfect but also

able to link different stimuli together, it is possible to influence it and change a perceived property of the *tangibles*.

With a soft tangible providing a base stiffness, there are several solutions to alter the stiffness. Jeon et al. [209] used a PHANToM force feedback interface to apply an additional force to the stylus held by the users which is proportional to the displacement of the object surface (Fig. 2.39a). Later, they [210] even simulated a virtual tumor during a breast palpation by increasing the stiffness of a Silicone model only at a specific location (Fig. 2.39b). Instead of actually modifying the force feedback of the user, it is possible to increase (resp. decrease) the perceived stiffness by decreasing (resp. increase) the amplitude of the virtual deformation. This pseudo-haptic approach has been used in several studies, for pinching either by using a deformable tangible [166, 63] (Fig. 2.39c, and Fig. 2.39d) or an actuated controller [90] (Fig. 2.39e), or even for a full hand grasp with a passive hand exerciser [64] (Fig. 2.39f). However, for such an approach, it is mandatory to have an estimation of the actual deformation of the tangible or the force applied by the user.



(a) Jeon et al. [209] (b) Jeon et al. [210] (c) Adilkhanov et al. [166] © 2020 IEEE
© 2010 IEEE © 2012 IEEE



(d) Matsumoto et al. [63] © 2017 IEEE (e) Lee et al. [90] Copyright 2019 ACM (f) Achibet et al. [64] © 2014 IEEE

Figure 2.39: Enhanced stiffness of tangibles: (a) Stiffness Modulation [209], (b) Virtual Tumors in Real Tissue [210], (c) VibeRo [166], (d) Passive Nonlinear Spring [63], (e) TORC [90], (f) Virtual Mitten [64].

Altering the perceived weight is also possible with a similar pseudo-haptic approach: Dominjon et al. [211] showed that when users are weighting up an object by making up and down movements, increasing or decreasing the amplitude of the virtual motion can also alter the perceived weight (Fig. 2.40a). Making the object vibrate with an asymmetrical weight translation can also induce a feeling of increasing or decreasing weight depending on the side of the maximal acceleration [169] (Fig. 2.40b). Alternatively, Minamizawa et al. [95] showed that inducing lateral skin stretch can also alter the perceived weight of the pinched object. They achieve this with a wearable device that can translate a belt against the fingers' skin (Fig. 2.40c).

It is also possible to alter the perceived texture of a tangible surface. Asano et al. [212] increased or decreased the roughness of a surface during a direct exploration of the finger by adding a vibrotactile stimulation with a wearable device (Fig. 2.41a). While Culberson



Figure 2.40: Enhanced weight of tangibles: (a) Influence of Control/Display Ratio [211], (b) Asymmetric Oscillation Distorts the Perceived Heaviness [169], (c) Gravity Grabber [95].

et al. [81] mediated the interaction with a stylus which could alter the perceived friction and roughness by synchronizing the feedback of voice coil actuators in the handle and the breaking force of the rolling ball at the fingertip (Fig. 2.41b). However, Lu et al. [75] used an alternative approach. They did not use any haptic feedback, but simply generated an auditory feedback in synchronization to the stylus' movement. Using different sounds of contact against virtual texture was enough to make the users feel they were exploring various textures (Fig. 2.41c).

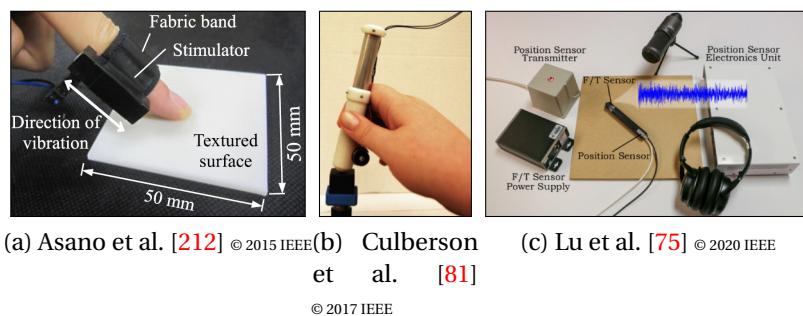


Figure 2.41: Enhanced textures of tangibles: (a) Vibrotactile Stimulation [212], (b) Displaying Roughness and Friction [81], (c) Rendering Sounds [75].

Lastly, the perceived shape of a tangible can be altered through pseudo-haptic, i.e., by altering the motion of the virtual hand by mapping the shape of the virtual object onto the tangible. As the users will explore the tangible object they will see the virtual hand exploring the virtual one without noticing the difference in motion: Ban et al. [124] retargeted the virtual hand in a way that the users would explore a cylinder with their fingertip as they would see their virtual hand sliding along a curved virtual vase (Fig. 2.42a). Similarly, Kholi et al. [187] remapped a virtual table of variable height onto a flat table (Fig. 2.42b) and Matsumoto et al. [179] even changed the number of sides the virtual table had (Fig. 2.42c). Spillman et al. [130] developed a method to adjust the warping on the fly as the users remove some part of the virtual knee while the tangible stays the same (Fig. 2.42d).

One could also make the users perceive added parts to the tangible: Borst et al. [213] used a flat surface combined with an exoskeleton haptic. The surface would provide the base contact while the pistons would apply forces to the users' fingers and would



Figure 2.42: Enhanced shape of tangibles: (a) MagicPot360 [124, 125], (b) Perceptual Illusions [187], (c) Magic Table [179], (d) Arthroscopy Surgical Simulator [130].

render virtual switches and buttons. Hence, adding new virtual elements onto the tangible (Fig. 2.43a). However, one could also remove virtual parts with pseudo-haptics: Strandholt et al. [138] made users plant a nail, screw a screw or saw a plank, even though there were no tangible nail or screw and the real plank remained uncut (Fig. 2.43b).

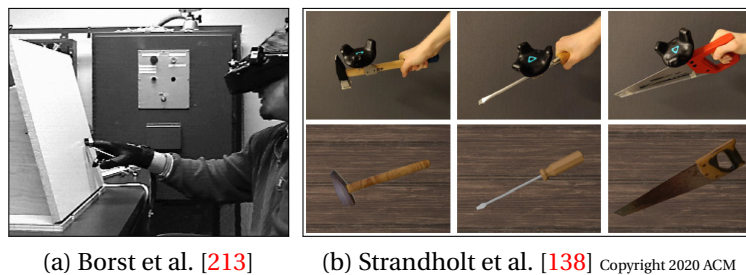


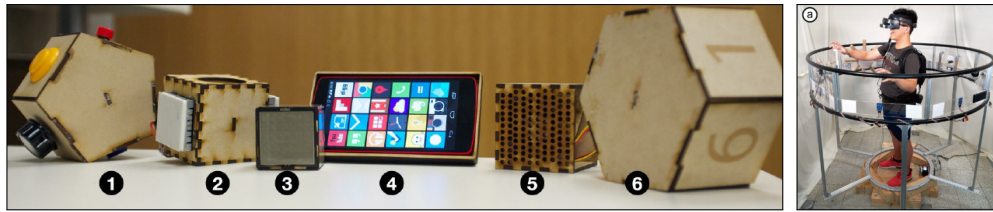
Figure 2.43: Enhanced tangible props by adding or subtracting parts. (a) Mixed Reality Virtual Control Panel [213], (b) Knock on Wood [138].

2.3.2.5 Encounter-Type Haptic Devices

An interesting paradigm for tangible interaction is the use of ETHDs (detailed in section 2.1.2.1) as they can address several previously mentioned points. They intrinsically re-register tangible and virtual elements by reconfiguring the tangible content in accordance to the users' movements while being compatible with prior works. In it indeed possible to combine them with techniques trying to make use of discrepancy between tangible and virtual, or those instrumenting the tangible props with sensors and actuators, as the end-effectors can be instrumented as well as Araujo et al. [45] did with their Snake Charmer (Fig. 2.44a).

Moreover, many technical solutions can be used as the base of the ETHD depending on the needs and constraints: they can be robotic arms [47, 42, 45, 46, 48] (Fig. 2.1, and Fig. 2.2) which come in various sizes and complexity, with great accuracy and speed but a restricted workspace. Or, as mobile grounded robots [54, 55, 56, 57, 58] (Fig. 2.4) which are constrained to a surface but are more affordable with great versatility. Or even as drones [49, 50, 51, 52, 53] (Fig. 2.3) which are nimble and can move freely in space. Huang et al. [59] even developed an encasing structure which can rotate around the users and provide many spots from which tangibles can be picked up or put down (Fig. 2.44b).

However, whichever solution is used, ETHD needs to be safe and have efficient path planning in order to not collide with the users as they are unable to actually see them while wearing a VR HMD.



(a) Araujo et al. [45] Copyright 2016 ACM

(b) Huang et al. [59]

Copyright 2020 ACM

Figure 2.44: Encounter-type haptic devices. (a) Snake Charmer [45], (b) Haptic-Go-Round [59].

2.3.2.6 Generic Enhanced Controllers

An alternative to tangible props and ETHD is the use of VR controllers. They are a good compromise between tangible props, bulky haptics, while providing a generic tangible shape to grasp for the user, they are unbound and allow users to evolve in a larger workspace. Additionally, as it is easier to track a rigid handle, it avoids the need to track the users' hand and are often used as a proxy to render either a virtual hand or a virtual tool in order for the users to interact with the virtual environment. Moreover, controllers are input devices with buttons and joysticks which are often mapped in order to enable various virtual interactions upon triggering, e.g., clench the virtual hand, fire a tool, or use the trackpad of classic haptic controllers in order to type text as proposed by Jiang et al. [214] (Fig. 2.45a).

Thus, controllers enable a large variety of usage as input for VR. However, Sinclair et al. [215] stated that they are also "unable to render a range of feedback required for a variety of envisioned VA/AR scenarios" since common haptic controllers only possess vibrotactile feedback. Recently, a new enhanced controllers paradigm emerged with additional feedback: Sinclair et al. [215] stated the need to provide "force feedback akin to the corresponding tool when used in the real world", while keeping inputs like buttons, joysticks or trackpad for generic interaction.

While Haptic Links [73] allows to have a stiff link between classic VR controllers and can render bimanual force feedback (Fig. 2.45b), some device aim at increased pinching interaction by providing force feedback simply on the index like Claw [86] (Fig. 2.45c), CapstanCrunch [87] (Fig. 2.45d), or the hybrid active/passive actuation device of Drills et al. [88] (Fig. 2.45e). These devices can then be used to either pinch any virtual objects, or press with the index on virtual elements such as buttons. Similarly, Lee et al. [90] targeted the tripod grasp, a three-finger pinching with which humans can naturally rotate small objects within their grasp. TORC can render this rotation interaction by having a 2D touch surface below the thumb. In addition, this device also enables a natural pinching interaction in order to grasp virtual objects and feel their stiffness (Fig. 2.45f).

In short, this new enhanced controller paradigm is targeting common and natural interaction in the real world to mediate a large set of virtual ones while keeping the pros of classical controllers.

2.3.2.7 Toward New Life-Like Paradigms

Recently, several works focus into embedding real life experiences into VR which, in the case of *Tangibles*, manifests by making use of the experience people have in order to provide a natural interaction:

Kato et al. [82, 83] work into importing common tools to VR by developing a very specific hand-held device, an actuated chopstick which can make the users believe they actually grasp a virtual object (Fig. 2.46a). Similarly, Lin et al. [216] made users type on a real keyboard while displaying a view of their hand and keyboard in the virtual environment in order to enable text entry in VR (Fig. 2.46b). Later, Otte et al. [164] added capacitive sensing to every key on a keyboard in order to enable a more natural text entry in VR where users could see which key they were touching before pressing it (Fig. 2.46c).

Alternatively, He et al. [55, 54] suggested using mobile robots in order to mediate social interaction with other people in a distant workspace. In their study, the robot moves on the table according to the action of their collaborator with a visible virtual counterpart or to take position before the users grasps it. Hence, they try out 4 collaborative scenarios: passing a mug, clinking drinks, playing tic-tac-toe or a city-builder (Fig. 2.46d).

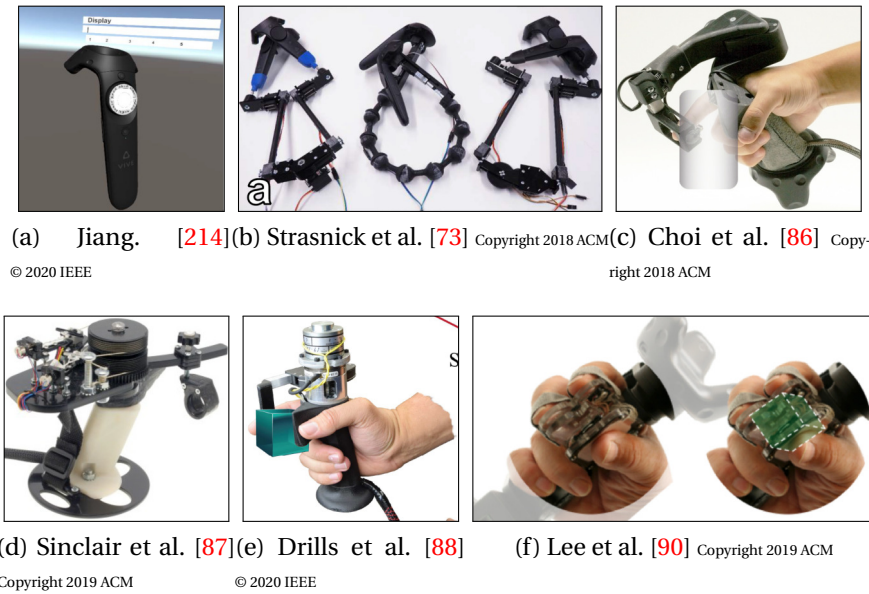


Figure 2.45: Generic enhanced controllers. (a) HiPad [214], (b) Haptic Link [73], (c) Claw [86], (d) CapstanCrunch [87], (e) Hybrid Active-Passive Actuation [88], (f) TORC [90].

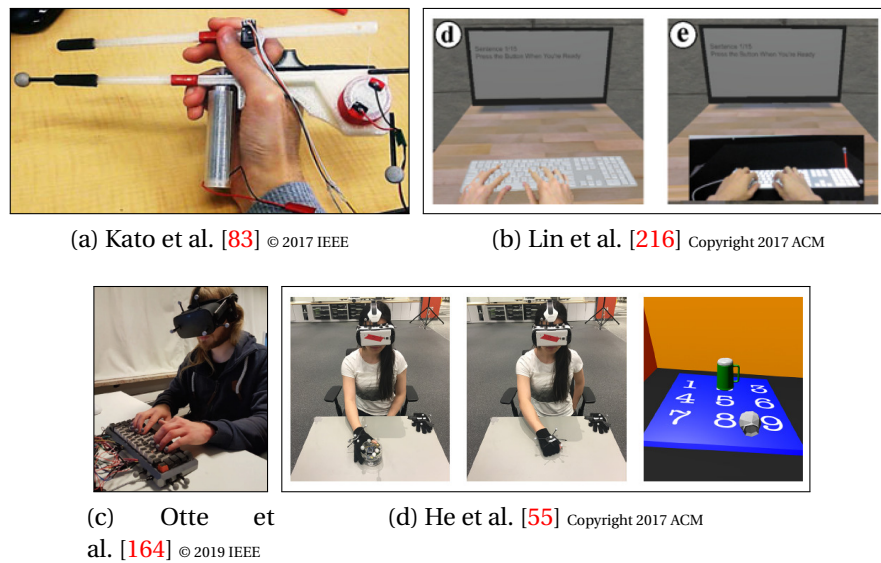


Figure 2.46: Toward new life-like paradigms. (a) HapSticks [83], (b) Visualizing the Keyboard [216], (c) Touch-sensitive Physical Keyboard [164], (d) PhyShare [55].

2.4 Discussion on the Role of Tangibles in VR Interaction

Classic usage of *tangibles* is to recreate the virtual environment with tangible replicas in order to provide a physical supporting structure matching what the users see in VR. Such 1:1 tangible replicas provide a high degree of immersion for the users [2, 3], especially as they can manipulate the various objects freely while seeing hands movements using virtual hands with accurate tracking, or their own hands with see-through technologies. In that regard, Hasanzadeh et al. [191] built a tangible surrounding which is a replicate of a rooftop onto which the users perform real building tasks. The tangible slop is placed in a CAVE

system in order to render working at high height to evaluate if workers have any risk-taking behaviors while working on roofing. Similarly, Dong et al. [149] 3D-printed several parts of a highly expensive device for Cryo-Electron Microscopy in order to make a VR simulator for teaching how to use the device without risking breaking it.

However, 1:1 tangible setups, although highly efficient, are often bulky and complex setups which justify their single usage and the amount of time needed to build them up, by the fact that they will be used over and over, for example, as a training purpose. The reusability of such setup is very limited, and the virtual scenario is often short and limited to a single scene, the one registered to the dedicated tangible setup. However, many studies have focus on solutions which can increase the reusability of tangibles by decreasing their dedication.

1. Having 1:1 replica is not mandatory because human perception can be altered as detailed in section 2.3.2.4: various kinds of haptic properties can be perceived differently (e.g., shape [213, 124, 187, 130], stiffness [209, 210, 166, 63, 90, 64], weight [211, 169, 95], texture [212, 81, 75], etc.) by employing various kinds of haptic illusions, such as pseudo-haptic approach where the motion is altered [166, 63, 90, 64, 211, 124, 187, 130], additional stimuli which serve as additional cues for the somatosensory system [20], additional force feedback [209, 210, 169, 213] or tactile feedback, by means of skin stretch [95], vibrotactile stimulation [212, 81] or possibly auditory to perform a cross-modal perceptual illusion [75].

These kinds of approaches are efficient to render several entirely different virtual objects with the same tangible, but also to dynamically modify properties of the same virtual object, either as a whole (e.g., increase of weight [95]), or partially (e.g., local increase of stiffness to simulate a tumor [210]).

Similarly to Asano et al. [212], in Chapter 3, we will start by *combining tangibles* and a *wearable haptic* in order to provide an additional, timely synchronized, tactile pressure which will *alter the perceived stiffness* the users have *of tangibles*.

2. As human perception intrinsically has imprecision (see. Section 2.1.1), this leaves small gaps for us to take advantage of. As mentioned in Section 2.3.2.3, it is possible to use a tangible to render a virtual object even if there are discrepancies between the two.

Either, because the difference is below the users' level of subconscious perception. In that case, users are not able to notice that the tangible is different from the virtual as both display compatible haptic and visual cues. This can be considered in the building process of tangibles: Fujinawa et al. [61] have proposed a method to generate the weight distribution of tangible hand-held devices compatible with the virtual element. It is also possible to make use of it when controlling self-reconfigurable tangibles [65, 66, 68, 69].

Otherwise, as Simeone et al. [139] have highlighted that there can be discrepancies as long as tangible objects present similar affordance to the virtual one, especially around parts most likely to be interacted with by users. Thus, many approaches focus on using tangibles while matching the global shapes [139, 200, 140, 153], as they can be reconfigured on the fly by users [156, 155, 204] or automatically [157, 56], and even derived toward the elaboration of toolkits. These enable users to build a tangible similar to the virtual object they will manipulate in the virtual environment while having sensors and actuators to enable interactions [173, 174, 175]. In that case, the users can perceive that tangible and virtual objects are different, but as

long as they have same affordances, same contextual functions and that there is no critical discrepancy, their immersion is maintained [139].

In Chapter 4, we will focus on the first case, where the users cannot consciously perceive the difference, as we will *induce discrepancies* between tangible and virtual objects *on three local properties* (width, local orientation and curvature). We will aim at finding the threshold starting which users can actually perceive a difference between what they feel of the tangible object and what they see of the virtual object whilst pinching them.

3. Having a single mapping of the virtual environment to the tangible setup where each virtual object is registered to a single tangible is constraining. Many methods were developed in order to enable multi-registration of several virtual objects to a same tangible as detailed in Section 2.3.2.1. The re-registration can either happen openly, for example, by simply registering a new virtual once the task is complete with the previous one. [167]. Or, it can be hidden from users, in a matter of increasing their immersion. The latest often rely on redirecting techniques where users are redirected to the same physical spot where the tangibles are while walking toward new virtual locations [180, 127, 178], or, whilst standing at the same physical spot, their real hands are redirected toward the same tangible as their virtual hands are reaching for another virtual object [129, 128, 189, 184].

Alternatively, the tangible can be embedded on an actuated device, e.g., a robotic arm, a grounded mobile robot or a drone as explained in Section 2.3.2.5. Due to their mobility, ETHD can automatically re-register a tangible to virtual elements by repositioning the end-effector as the users are about to interact with another virtual element. For example, Yafune et al. [44] rendered a whole virtual control panel by repositioning and reorientating a tangible cube which faces embedded various kinds of buttons and switches.

Another wide spread solution for multi-registration is the use of controllers, eventually enhanced one as described in Section 2.3.2.6. The users place the tangible on a virtual object and enable the registration through specific interaction with the controller (pressing a button, touching sensitive pad, or actuating an end-effector for more complex ones [86, 87, 88]).

In Chapter 5, we will enable multi-registration between virtual objects and tangibles following a similar approach to the ETHD: we will register together similar parts of the tangible and virtual objects and positioned them accordingly while making sure that their respective haptic properties are consistent with each other, i.e., we will use the gap mentioned in the previous point and minimize the local discrepancy between tangible and virtual objects. In short, we will suggest the users a pinching pose on the virtual object while making them grasp a tangible object with compatible haptic features (e.g., size, local shape, mass, local curvature).

Hence, there are many complementary methods to use *tangibles* to render virtual object in VR. However, several limitations and constraints have to be taken into account when registering virtual elements to *tangibles*:

- *Tangibles* are invisible to the users in the considered paradigm.
- There should be a "good" virtual representation of the hand/object interaction.
- *Tangibles* do not float.

1. Each tangible present in the real work space needs to have a virtual object registered to. As the users are blind to the real environment, they eventually can hit a tangible if no visual clue is provided, which will greatly flaw their immersion. The tangible might not be represented if it is in an area out of users' reach within the virtual scenario, e.g., hidden by another virtual element (door, wall, etc.), or the action of the users is re-targeted specifically away from the invisible tangible. Although, this issue is more something to be wary of than an actual limitation which need to be actively researched on.
2. The virtual representation of the interaction between the hand and the object should be carefully represented in the virtual environment, for the users to carry on naturally their actions with the objects, or at least without trouble. The common approach is to track both the tangible object and the users' hands accurately to render both the virtual hands and the virtual object accordingly, hence, mimicking the real interaction in the virtual environment. However, such method is heavily affected by the tracking system's inaccuracy:

Gainer et al. [150] used a Leap Motion in order to reconstruct a virtual hand and interact with their 3D-printed replica of an hazardous material device which was tracked using the HTC Vive tracking solution. However, as the Leap Motion is not meant to track hands whilst interacting with *tangible*, they snapped the virtual hand to the virtual object as soon as the users' hands was close enough to it, i.e., certainly grasping it. Alternatively, Zhou et al. [143] used an optical tracking system in order to track markers' positions and reconstruct both the users' hand and the *tangible*. Even if the tracking solution is cutting edge, when they tried to turn the surface of the various tangibles into touch surfaces to enable further touch interaction, they had to "slightly inflate the estimated surface by 10% so that the interacting finger can reach the estimated surface, and not be blocked by the physical object". In other words, the virtual contact was still impeded by the inaccuracy of the system when registering the virtual elements to the real ones. However, several alternative methods already solve this issue.

A first one is to remove the need to reproduce virtually the hand/object interaction. Villegas et al. [154] used a camera recording the users' field of view, segmented the users' real hands and tangible objects, then displayed the real representation in the virtual space. Alternatively, tool mediated interactions also solve this issue, either using *tangible props* [137, 138, 130], or hand-held device [82, 79]. Users' attention is shift away from the hand, which is just holding the tool and refocused the users' attention on the interaction between the tool and the environment. Whenever rough manipulation is needed, the inaccuracy of the virtual representation becomes less relevant [168, 152, 147].

A second one, which happens to be the most common, is to solve the high complexity of the hand manipulation by constraining the virtual interaction in order to provide an easier to render but credible under-actuated interaction with the virtual object. Users can be using *tangibles* which can deform along a single axis of motion, thus, easier to track and to render, e.g. a 1-DoF translation [166, 63, 64], or rotation [159, 171], or targeting a single kind of interaction like pinching [86, 87, 88]. Lee et al. [90] even mapped the motion of the thumb on a 2D tracking pad to several constrained DoF in order to allow a fine within-hand rotation of the virtual object.

Lastly, it is possible to directly address the inaccuracy of the registration due to the

tracking system, by using an additional sensor in order to track the actual state of contact between users' hands and tangibles. For example, by using a tactile surface embedded on the *tangible* [165] for the users to touch, or similarly to track object/object interaction [158, 62].

In Chapter. 6, we will address the registration issue directly by using an additional sensor in order to track the proximity between users' hands and *tangible*, then correct the relative positioning until tangible and virtual contacts are synchronized. Moreover, we will apply this approach to two different kinds of tracking solutions to show its versatility.

3. Lastly, even if virtual objects can be place anywhere in the work space, *tangibles* are bound by gravity, and they need a supporting structure whenever users are not carrying them, i.e., if the tangibles are not hand-held devices. When registering them altogether, the position of the virtual objects is constrained by the *tangibles'* position. They are often on tables, both in real and virtual spaces. However, some redirecting techniques allows users to grasp virtual object in a wider horizontal span [128] or vertical span [129]. In short, while always reaching for a tangible constrained to a tangible surface, users can be redirected toward a virtual element positioned anywhere in a 3D volume around the tangible surface [189, 184]. These techniques work especially well as human proprioception is inaccurate to estimate the position of the hand in mid-air movement [217]. Similarly, users can also walk toward several different virtual area while being redirected toward the same supporting structure which can hold many tangibles [180, 127]. Hence, reducing the amount of supporting structures needed. More recently, Zenner et al. [183] even proposed a setup which can relocate the tangible from one side to the other: as users drop the tangible in a virtual hole on one side, it is actually collected by a tangible ramp which brings it to a lower surface on the other side where a new virtual element appear for the users to grasp. Despite all these methods to expend the range of positioning of virtual objects, they are still bound to be in the vicinity of tangible surfaces.

An alternative to passive supporting structures is to use actuation to move *tangibles* around: the ETHDs 2.3.2.5 which can bring *tangibles* anywhere in a wider workspace as to register it to a virtual element, especially those using drones. Recently, Huang et al. [59] developed a novel kind of ETHD which encases the users and provides them many supports at several height all around them, from which users can pick and dock *tangibles*. The structure can even rotate in order to re-register some elements.

In Chapter 7, we will design an ETHD which is attached at the back of users' hand and which is able to engage and disengage a tangible from their grasp. This device takes advantage of the inaccuracy of the human proprioception, as the tangible is positioned relatively to the hand, even if the virtual hand is not exactly registered to the real one. Moreover, the whole workspace is available for interaction as the tangible can be engaged as soon as a virtual object is within grasp range.

Interestingly, many of these works tend to support Berger et al. [16] idea that providing the right amount of feedback is sufficient to give a compelling feedback even when using tangibles. Moreover, several works proposed alternative crafty solutions and workarounds to common issues, highlighting very interesting paradigm and perspectives. As a conclusion, the use of *tangibles* in VR is not limited to the long lasting passive haptic technique [3] but goes beyond that: the Substitutional Reality framework proposed by Simeone et al. [139], the generic enhanced controller, the encounter-type haptics, but also the idea

of increasing the reusability of tangible either across various virtual environment and/or within a single scenario through one-to-many registrations, either by embedding sensors and actuator into tangibles, by combining them with wearable devices or pseudo-haptic, or by developing toolkits to build the tangible with the required affordance and actuation functions. Although, we categorized the current state-of-the-art on the *tangible* in VR, we believe that is it too soon to draw the theoretical outlines of this framework as research on this topic is increasing over the recent years, and new ideas and approaches will emerge soon.

Part I

Improving the Rendering of Virtual Objects using Tangibles

Chapter 3

Enhancing the Stiffness Perception of Tangible Objects in Mixed Reality Using Wearable Haptics

Sommaire

3.1 Proof of concept: augmenting tangible objects stiffness using a finger wearable tactile device	73
3.1.1 Motivation and Concept	73
3.1.2 2-DoF Wearable Haptic Device	74
3.1.3 Demonstrator: Increasing the Stiffness of a Foam as It Is Pressed	75
3.2 Perceptual evaluation	75
3.2.1 Experimental Apparatus and Participants	76
3.2.2 Procedure	76
3.2.3 Conditions and Plan	77
3.2.4 Collected Data	78
3.2.5 Results	78
3.3 Use cases	81
3.3.1 Setup	82
3.3.2 Use Cases Descriptions	82
3.4 Discussion	84
3.5 Conclusion	86

In this Chapter, we are interested in improving haptic displays in virtual environments by taking the best of two simple haptic solutions: tangible objects and wearable haptics.

In order to provide feedback to the user, two wide spread solutions can be employed, each comes with advantages and drawbacks: Tangibles are known to be very effective at providing global and distributed shape sensations, but are often passive or unable to simulate several varying mechanical properties. Wearable haptic devices are portable, lightweight, inexpensive, and unobtrusive interfaces able to generate varying tactile sensations. However, these wearable devices can usually only provide ungrounded tactile stimuli (e.g., local shape, texture) and most kinesthetic sensations (e.g., weight, general shape) are missed [91]. Moreover, wearable devices can only provide stimuli to a reduced number of contact points (e.g., the fingertips), and increasing the number of these points directly affects the wearability and comfort of the system [36].

In this Chapter, we focus on *altering the perception* the user has *of the tangible* without actually modifying it: we propose to improve haptic displays in virtual environments by taking the best of two simple haptic solutions by combining tangibles and wearable haptics. The tangible provides convincing stiff contacts and distributed shape sensations through its shape, while the wearable, the hRing, can generate a varying tactile sensation which will serve as local cue and dynamically change the perceived mechanical properties of the object. In this work, the focus will be on altering the sensation of stiffness/elasticity of virtual/tangible objects, as it is a prominent tactile feature and it is relevant for many applications. Moreover, through this combination, the haptic interaction is not mediated by any external tool and the user's fingertip can directly contact the tangible surface, as illustrated in Fig. 3.1.

The main contributions of this work can be summarized as follows:

- we proposed a novel approach for enhancing the stiffness perception of tangible objects through wearable haptics;
- we designed a proof-of-concept system meant to render various sensations of stiffness for tangible objects in AR or VR, relying on a 2-DoF wearable tactile display for the finger;
- we conducted a user study assessing the possibility to alter the perceived stiffness of real objects using wearable haptic stimulation, as well as studying the importance of the locus of this stimulation;
- we designed several use cases in virtual and/or augmented reality, in order to illustrate the potential of this approach in different contexts, e.g., medical palpation, industrial training, entertainment.

In the remainder of this Chapter, we firstly expose the motivation and a proof-of-concept of this hybrid approach mixing tangible objects and wearable haptics for stiffness rendering. Then, we describe the protocol and results of the user study, assessing the possibility to alter the perceived stiffness of tangible objects through wearable haptic stimulation, as well as studying the importance of the locus of stimulation. Finally, we present various tangible settings and use-cases of the approach in VR and AR scenarios. Finally, the results and outcomes of the method are discussed.

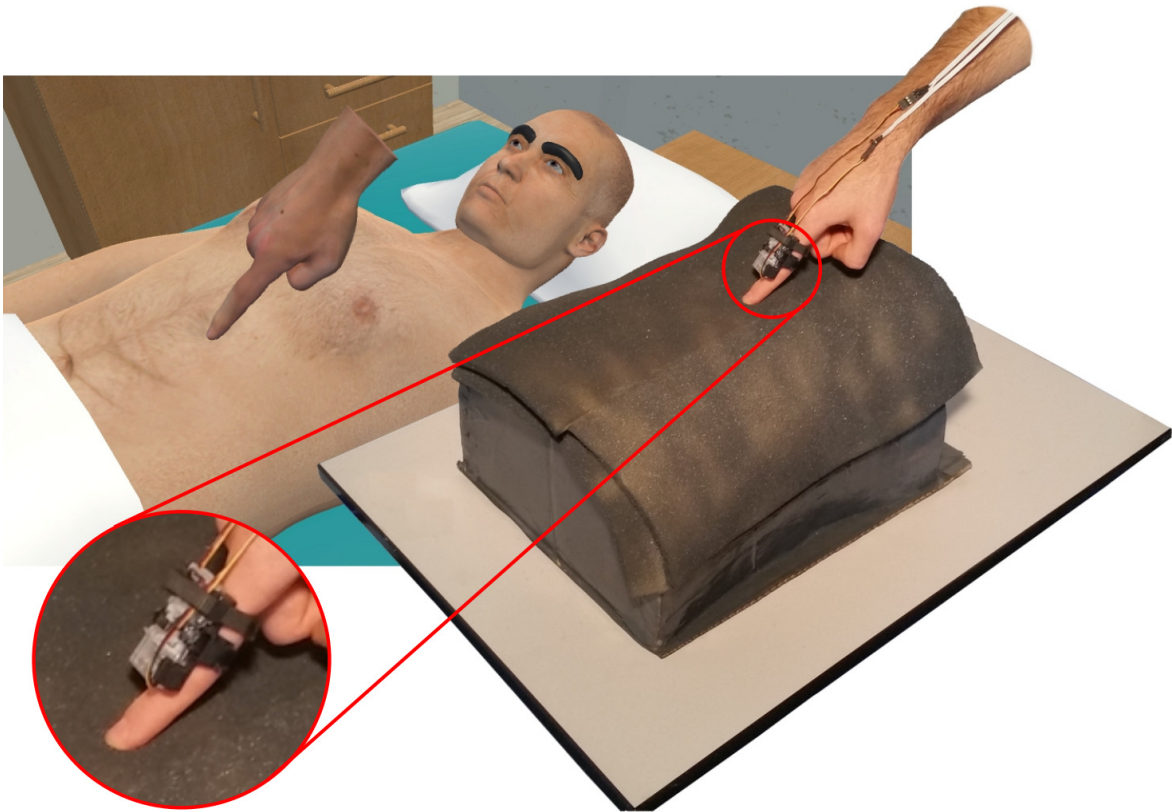


Figure 3.1: The approach implemented in a VR medical palpation simulator. We propose an innovative approach for improving haptic sensations in VR/AR applications, capable of dynamically changing the perceived stiffness of tangible objects by providing timely tactile stimuli through wearable haptic devices. Passive tangible objects (a tangible chest here) provide haptic information about the global shape/percept of the virtual objects, while wearable haptic devices provide haptic information about dynamically changing mechanical properties (local elasticity here).

3.1 Proof of concept: augmenting tangible objects stiffness using a finger wearable tactile device

3.1.1 Motivation and Concept

To improve the range and effectiveness of haptic sensations in virtual environments, we study the effect of combining tangibles (for simulating the global and distributed shape/percept of the virtual object) together with wearable haptics (for dynamically changing the mechanical properties of the object), in order to alter the perceived stiffness of the tangible (Fig. 3.1). When assessing the stiffness of an object, two phenomenon occurs simultaneously [26]: the skin of the fingertip is displaced as the amount of force applied increases, and the area of contact on the skin grows as the skin is deformed on the object's surface. Since controlling the growth of the contact area is difficult and not possible with our wearable, we mainly rely on the contribution of the relationship between the applied force and the finger displacement in the perception of stiffness. Thus, we increase the perceived stiffness of tangible objects by providing additional timely pressure stimuli on the finger's skin. To provide such stimuli, we used a 2-DoF wearable tactile device for the finger, similar to [96, 95].

3.1.2 2-DoF Wearable Haptic Device

We built a custom 2-DoF wearable haptic device able of providing pressure and skin stretch stimuli at the skin, shown in Fig. 3.2. Its actuation principle has been inspired by the device presented by Minamizawa et al. [95], while its design has been inspired by the “hRing” device presented by Prattichizzo’s group at the University of Siena [96]. It is composed of a static structure, housing two servo motors, and a fabric belt, that applies the requested stimuli to the skin. A Velcro strap band is used to secure the device on the finger. When the two servo motors rotate in opposite directions, the belt is pulled up or down, providing a varying force normal to the finger. On the other hand, when motors spin in the same direction, the belt applies a shear force to the finger. To adjust the device for different finger sizes, we built eight finger-device adapters, enabling us to adapt the size of the device in less than 15 seconds. The device weights 17 g for $42 \times 22 \times 33$ mm, and it can be worn at the fingertip as well as at the middle or proximal phalanges.

Since the servomotors are position controlled, it is only possible to command them with a desired angle. The relationship between the commanded angle and belt displacement for each motor is $\Delta b_i = r \Delta \theta_i$, $i = 1, 2$, where $r = 5$ mm is the radius of the servo motor pulley, Δb_i the commanded belt displacement due to the motion of motor i , and $\Delta \theta_i$ the i -th motor commanded angle expressed in radians. In our case, the two motors always rotate of the same angle, i.e., $|\Delta \theta_1| = |\Delta \theta_2|$ and $|\Delta b_1| = |\Delta b_2|$. Moreover, we only consider stiffness sensations and, therefore, we will always move the motors in opposite directions (as in Fig. 3.2b). Nonetheless, this 2-DoF design will enable us to quickly move toward testing, in the near future, the effectiveness of the approach for other types of tactile sensations. Finally, we can also relate the total vertical belt displacement $\Delta b_s = \text{sgn}(\Delta \theta_2) \Delta b_2$ to the normal force applied by the belt on the finger skin, $f_{tact} = k_{skin} \Delta b_s$, where k_{skin} is the finger stiffness value. In this work, the maximum displacement range of the device was 6 mm and we considered an isotropic elastic behavior with $k_{skin} = 0.5$ N/mm [96, 103].

Since this device cannot provide the sensation of making/breaking contact with the virtual environment (i.e., the belt always contact the skin), the contact area between the end-effector and the finger skip is constant. For this reason, in this work we do not consider the effect of the temporal change of contact area in the perception of stiffness (see also Section 3.4).

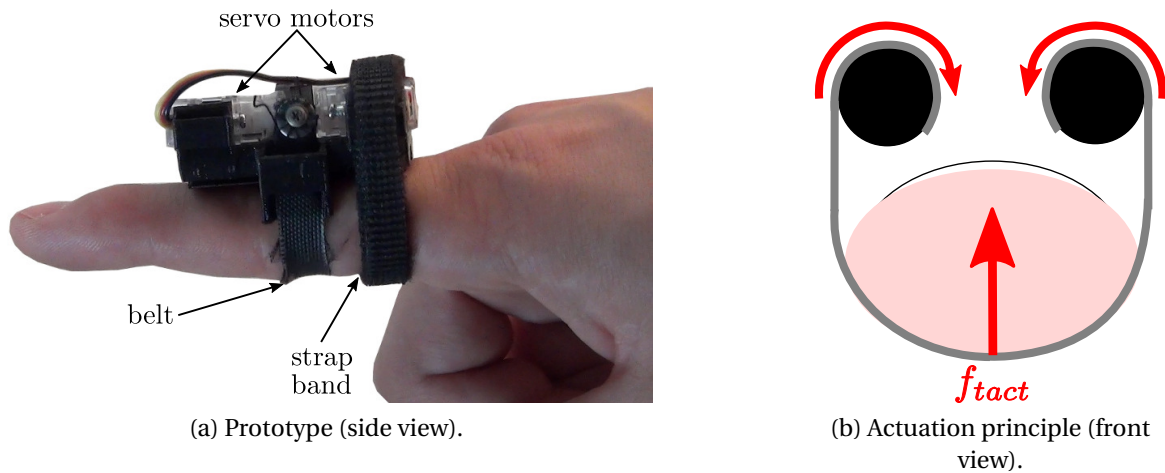


Figure 3.2: 2-DoF wearable haptic device used in the proof-of-concept [96]. When the motors rotate in opposite directions, the belt provides a varying pressure stimuli to the finger; when motors spin in the same direction, the belt applies a shear force to the finger.

3.1.3 Demonstrator: Increasing the Stiffness of a Foam as It Is Pressed

We now introduce the approach through a preliminary but representative prototype demonstrator. Section 3.2 will then carry out a human-subject study, to understand and quantitatively measure how to alter the perceived stiffness of tangible objects using wearable haptic stimulation, as well as addressing the importance of the locus of stimulation (e.g., fingertip vs. middle phalanx vs. proximal phalanx).

The setup is shown in Fig. 3.3. The user wears one wearable tactile device on the right index finger. We chose to place the wearable device on the proximal finger phalanx, in order to leave the fingertip free to interact with the tangible environment. The implications of wearing the device on the proximal phalanx instead of the fingertip are the focus of Section 3.2. In front of the user, on top of a table, we placed a small board with a foam of stiffness $k_{r,f} = 1.5 \text{ N/mm}$ (see Fig. 3.3a). This value was empirically derived modeling the foam as a spring system. Users can then repeatedly press the foam with the finger wearing the device. When compressed, the foam provides the user with a force $f_f = -k_{r,f}(z_f - z_{f,0})$, where z_f is the height of the foam when compressed and $z_{f,0}$ is its height when no load is applied (see Fig. 3.3b).

Our hypothesis is that, by providing timely tactile sensations through our wearable device, we can increase the perceived stiffness of the foam as the user presses it, making it feel stiffer and stiffer every time it is pressed. Specifically, we speculate that we can increase the perceived stiffness of the foam of 0.1 N/mm every time it is pressed. This concept is sketched in Fig. 3.3b: every time the user touches the foam, the wearable device provided a timely additional tactile force, aimed at increasing the foam perceived stiffness. This additional tactile force f_t considers again a spring model, $f_t = -k_{t,f}(z_f - z_{f,0})$, where $k_{t,f}$ is the *additional* stiffness we want the user to perceive. In our case, $k_{t,f} = 0 \text{ N/mm}$ the first time the user touches the foam and it increases of 0.1 N/mm every time the foam is pressed.

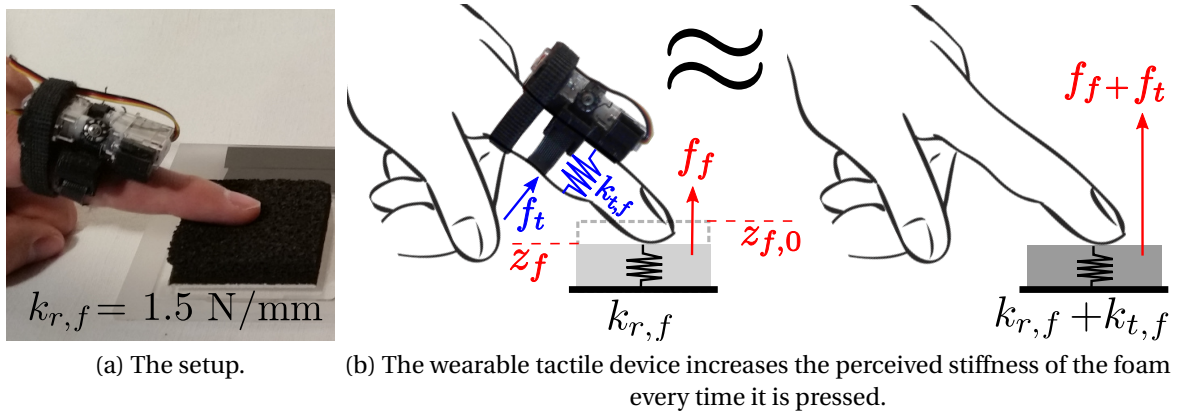


Figure 3.3: Proof-of-concept demonstrator. Users wear the wearable device on their index finger and interact with the foams. By providing timely tactile sensations through our wearable device, we want to increase the perceived stiffness of the foam as the user presses it.

3.2 Perceptual evaluation

We performed a perceptual evaluation that aims at assessing the capability of our wearable device to increase the perceived stiffness of real objects. We also wanted to evaluate the ef-

fect of moving the haptic stimuli away from the point of contact with the real environment. Our hypotheses are:

- H1. providing timely tactile stimuli through our wearable device makes the users perceive a real object stiffer than it actually is;
- H2. H1 is still valid even when providing these tactile stimuli far away from where the contact with the real object happens (i.e., the fingertip).

3.2.1 Experimental Apparatus and Participants

To study how the perception of stiffness of a real object is influenced by the wearable device, we conducted an experiment in which participants could interact with a piston-like tangible object representing our 1D stiffness. The setup is shown in Fig. 3.4. Subjects were asked to wear the wearable tactile device on their finger at different positions and look at a 52-cm-diagonal LCD screen showing the virtual scene. A 3-DoF grounded Falcon haptic interface (Novint Technologies, USA) was placed next to them, with its end-effector facing upwards and a tangible piston-like object fixed at the top. To avoid sliding, the tangible object was covered by a thin layer of rubber. Participant could feel different stiffness rendered by the Falcon when pressing on the tangible object with their *right index fingertip*. At the same time, additional tactile stimuli could be generated by the wearable device or not. Since the tangible piston-like was not too compliant, the induced temporal change of the contact area, when pressing pistons of variable stiffness, was almost constant. As the end-effector of Novint Falcon acted as a real piston, the position of the piston's head provided by the Falcon was used in order to elaborate the various feedback: to render a virtual piston with a similar displacement within the virtual environment on the screen, to render a force proportional to the displacement with the Falcon, and, to render a displacement of the belt proportional to the displacement of the piston's head with the wearable device.

To avoid any crossmodal effect, participants were isolated from external noise through a pair of headphones playing white noise.

Sixteen participants (13 males, 3 females, $M = 25.44$, $SD = 5.08$) took part to the experiment, all of whom were right-handed. Three of them had previous experience with haptic interfaces.

3.2.2 Procedure

As shown in Fig. 3.4a, the virtual scene is composed of a piston, whose position is linked to the position of the Falcon's end-effector.

Participants had to compare two pistons with different rendered stiffness, modeled by a 1D spring law: $f = -k\Delta z$ if $\Delta z > 0$ mm, 0 N otherwise, where Δz is the difference between the position of the Falcon's end-effector and the resting position of the piston (see Fig. 3.4b). Subjects were asked to interact with a first piston for 2 s after the first press, and then to move their fingertip away from the end-effector to enable its release. After that, they were asked to interact in a similar way with a second piston. After this second interaction, participants were finally asked to judge *which* of the two pistons felt *stiffer*. One piston served as a reference, displaying a reference stiffness k_{ref} provided only by the Falcon, while the other piston displayed a variable stiffness $k_{test,F} + k_{test,T}$ provided using both the Falcon and the wearable tactile device, respectively. The test stiffness $k_{test,T}$

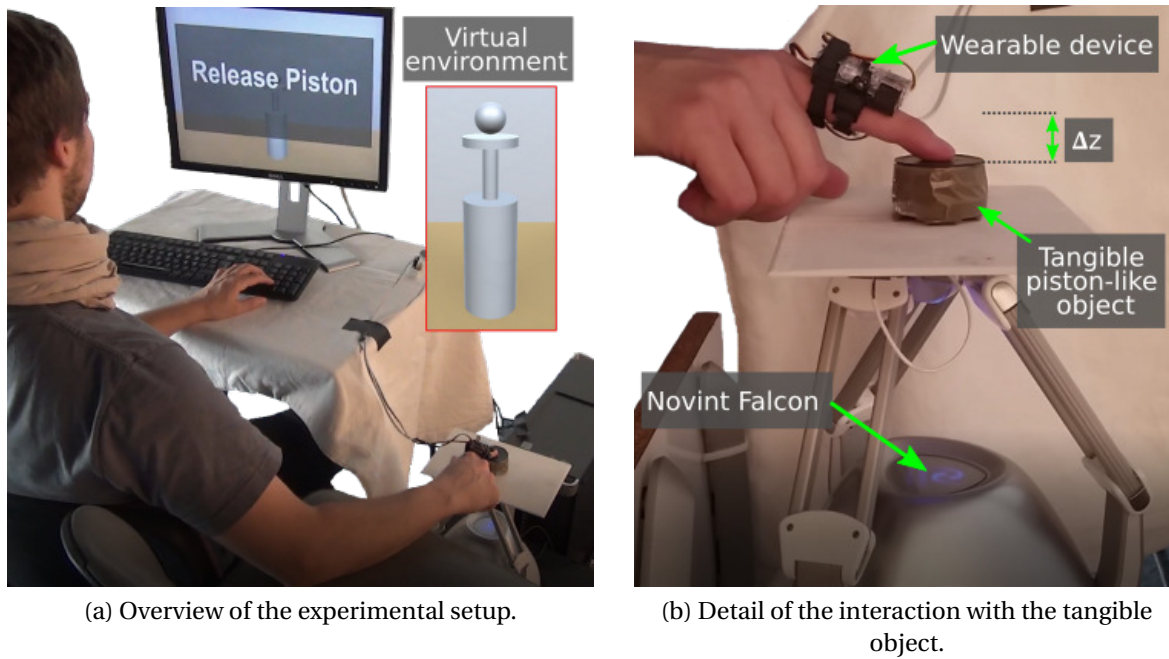


Figure 3.4: Perceptual evaluation. The Falcon haptic interface simulates the interaction with a tangible 1-DoF piston with variable stiffness. Whenever the user presses on the Falcon interface, the virtual piston moves accordingly.

provided by the wearable device was constant in all the conditions, while the test stiffness $k_{test,F}$ provided by the Falcon changed, as detailed below.

After preliminary testing, we considered 7 values of stiffness $k_{test,F}$ to be compared with the stiffness of the reference piston $k_{ref} = 0.1$ N/mm. The seven values of the test piston were: -30% , -15% , -7.5% , 0% , $+7.5\%$, $+15\%$ and $+30\%$ of the reference stiffness. In these seven conditions, the wearable device always rendered the same additional stiffness $k_{test,T}$.

The experimenter explained the procedures and spent about 2 minutes adjusting the setup to be comfortable before the subject began the experiment. The experiment lasted 50 minutes in total.

3.2.3 Conditions and Plan

Three conditions are considered in the experimental design:

- **C1** is the difference of stiffness between the reference piston and the test piston, $|k_{ref} - k_{test}|$. As mentioned before, three differences were possible: 0.0300 N/mm, 0.0150 N/mm and 0.0075 N/mm, corresponding to the absolute values of the difference of the six possible stiffness of the test piston with the stiffness of the reference piston.
- **C2** corresponds to a binary variable, which is true if the piston perceived as the stiffest is the one manipulated when the wearable device is active.
- **C3** is the position of the wearable device on the participant finger. Four possible positions were chosen: three on the finger pushing on the cardboard (Proximal, Middle and Fingertip of the right hand), and one on the index fingertip of the left hand of the participant.

The order of presentation of the two pistons and the order of the finger positions were counterbalanced to avoid any order effect: every couple of pistons was therefore presented in all orders. Thus, participants were presented with 140 trials, divided in 4 blocks (C3) of 35 trials in a different randomized order for each block. Each block of 35 trials presented a set of couples of pistons made of the 6 differences of stiffness values (C1), and the case of equality with 5 trials for each.

3.2.4 Collected Data

For each couple of piston, we collected as an objective measure the **participant's answer**. This answer corresponds to the piston (first or second) which was reported by the participant as the stiffest. The measure was then collected as a true discovery rate, i.e., if the answer corresponds to the stiffest value rendered.

Participants also completed a subjective questionnaire at the end of the experiment in order to not bias them but its content. In addition, the technical terms were defined in the questionnaire. Each question was answered using a 7-item Likert scale:

- Q1: It felt like pressing a **real piston**.
- Q2: The **haptic device** on your finger contributed to the **perception** of stiffness.
- Q3: The **combination** of both cutaneous and kinesthetic sensations contributed to the **perception** of stiffness.
- Q4: The **tactile device** provides a **higher contribution** to the perception of stiffness.
- Q5: **Practicing improves** the **association** of both cutaneous and kinesthetic sensations.
- Q6: The **locations** of the tactile feedback **did not influence** my perception of stiffness.
- Q7: After the experiment, I felt **tired**.

3.2.5 Results

Recognition rate of the stiffest piston. To study the recognition rate of the stiffness in function of the three conditions, we used a logistic regression model on the collected data to model the probability of recognition of the stiffest piston with respect to the three independent variables **C1**, **C2** and **C3** defined in the experimental design. The participants are considered as a random effect in the model.

We performed an analysis of deviance of the logistic regression model and we found a significant marginal effect for both **C1** ($p < 0.001$) and **C2** ($p < 0.001$), as well as an interaction effect between **C2** and **C3** ($p = 0.016$).

We performed a post-hoc analysis on the condition **C1** using a Tukey test adapted to the logistic generalized regression model. We found that all the differences of stiffness between the reference and test pistons were significant ($Z = 4.19$, $Z = 9.14$, $Z = 5.27$ for the differences between 0.015 and 0.0075, 0.03 and 0.0075, and 0.03 and 0.015 respectively, and $p < 0.001$ for the three differences).

Concerning the interaction effect between the **C2** and **C3**, we performed a pairwise comparison on all the pairs based on least squares means estimates. Figure 3.5 shows, for each of the four different positions on the fingers, the probability of finding the stiffest piston in function of the differences of stiffness (**C1**). The plot distinguished whether

the piston with the activated wearable device was considered as the stiffest or not (**C2**). Both the data and the model built from the analysis are shown. The probability of finding the stiffest piston differs when the wearable device is activated or not, in function of the wearable device position on the finger. There is a significant difference between the left fingertip position and the others ($Z = 2.82$ and $p = 0.028$ for the right fingertip, $Z = 2.31$ and $p = 0.042$ for the middle position, and $Z = 2.55$ and $p = 0.033$ for the proximal position). As shown in Figure 3.5, the difference between the probability of finding the stiffest piston when the stiffest piston is the one with the wearable device and when the stiffest piston is the reference is smaller for the left fingertip position (blue curve) than for the other positions.

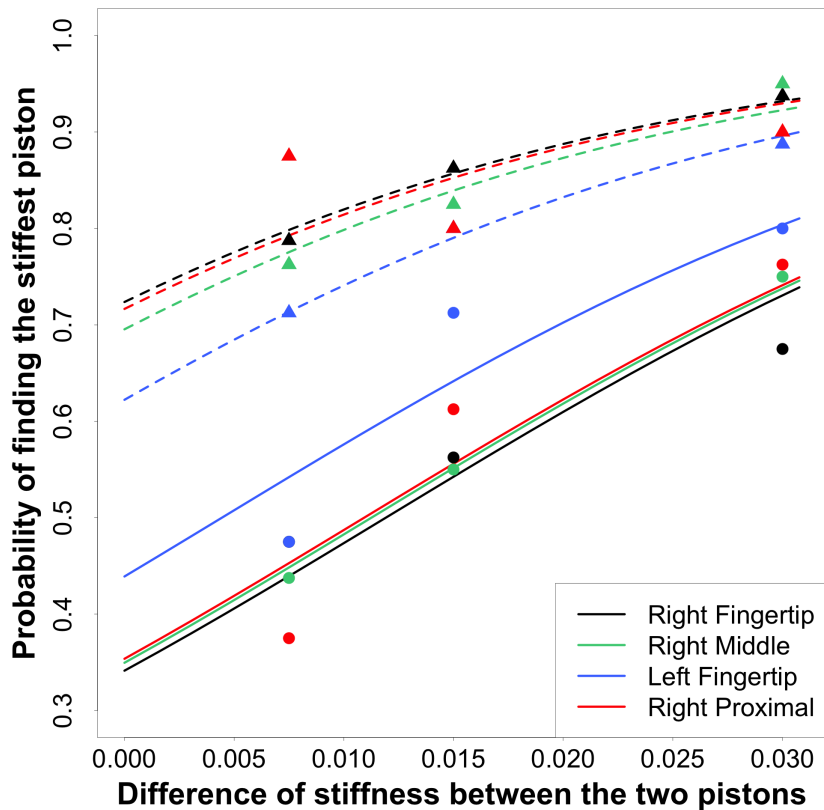


Figure 3.5: True discovery rate in function of the difference of stiffness between two pistons for the four different finger positions. Data are plot as points: triangle when the wearable device was considered as stiffer than the reference, circle otherwise. The plain/dashed lines represent the fitted curves to the data for each case.

We also analyzed the probability of finding the stiffest piston when there was no difference between the stiffness of the reference and the test pistons. We used a logistic regression model on the collected data to model the probability that the stiffest perceived piston was the one with the wearable device. We performed an analysis of deviance of the logistic regression model and we found a significant marginal effect for **C3** ($p < 0.001$). We performed a post-hoc analysis on the condition **C3** using a Tukey test adapted to the logistic generalized regression model. We found a difference between the middle and the right fingertip positions ($Z = -4.46$, $p < 0.001$), as well as the left and right fingertip positions ($Z = -2.90$, $p = 0.019$).

Psychometric curves. The four psychometric curves corresponding to the different stimulation locations (device positions) are shown on Figure 3.6. As can be observed, there

is a clear offset: all these curves are shifted to the left of the point (0,0.5). This means that the presence of the additional cutaneous stimulus has well increased the stiffness sensation. We could compute the Point of Subjective Equality (PSE) and the Just Noticeable Difference (JND) values for each curve. The results are: for the right fingertip (JND: 18.3%, PSE: -13.7%), right intermediate phalanx (JND: 17.9%, PSE: -10.8%), right proximal phalanx (JND: 17.7%, PSE: -11.9%), and left fingertip (JND: 17.5%, PSE: -6.5%). These JND values are similar to the magnitudes generally reported in previous psychophysical studies on stiffness perception [26], suggesting that the discrimination capability did not change drastically in the study. Then, the four PSEs are all negative, which still tends to validate our hypotheses H1 and H2 (and the increase in stiffness sensation due to the tactile cue). Moreover, the PSE and the perceived stiffness sensation seems to be lower in the case of the remote (left hand) finger condition compare to all the other (right hand) conditions. The experiment had not been specifically designed to compute psychometric curves, we did not produce the reference psychometric curve where the wearable device would never be activated. The PSE and JND values provided here should be taken cautiously. A dedicated user study with advanced statistical analysis should be conducted to confirm these preliminary results.

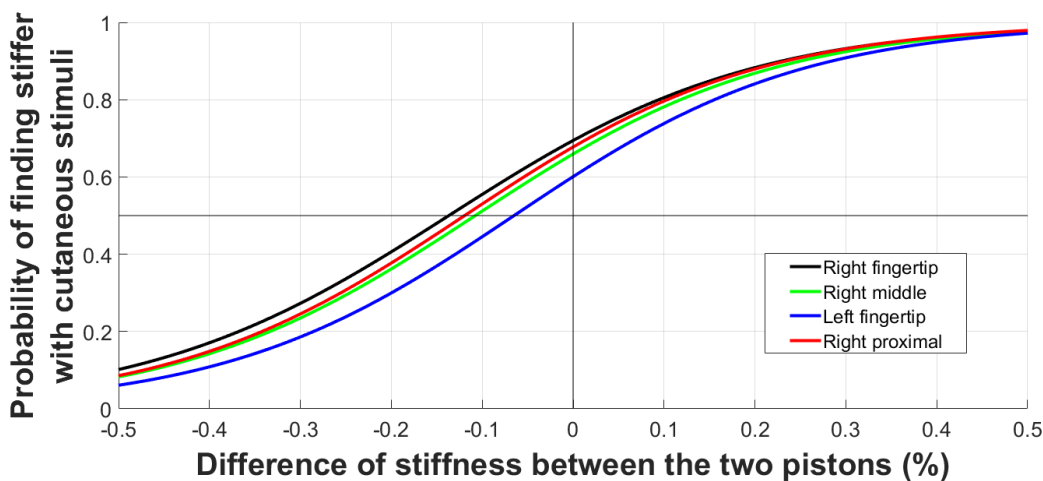


Figure 3.6: Psychometric curves for each location of the wearable device.

Subjective questionnaire. Figure 3.7 presents the answers collected through a subjective questionnaire (7-point Likert scale). Regarding the perception of the piston, participants reported that the piston barely seemed real (Q1, $M = 4.75$; $SD = 1.64$). Regarding the contribution of the haptic device to the perception of stiffness, most of the participants agreed to this assumption (Q2, $M = 5.63$; $SD = 1.36$). The combination of both devices seems to contribute to this perception of stiffness (Q3, $M = 5.56$; $SD = 1.58$). 5 participants gave the maximal rank. The participants did not particularly feel that the wearable device provided a higher contribution to the perception of stiffness (Q4, $M = 4.34$; $SD = 1.80$).

Regarding the experiment, practicing was not also considered as considerably improving the association of both cutaneous and kinesthetic sensations (Q5, $M = 5.06$; $SD = 1.34$). Participants felt that the locations of the wearable device were highly influencing their perception of stiffness (Q6, $M = 2.81$; $SD = 1.59$). Nine participants gave almost the minimal rank to the question 6 concerning the non-influence of the device locations. Finally, most of the participants reported overall medium levels of fatigue (Q7, $M = 2.93$; $SD = 1.56$).

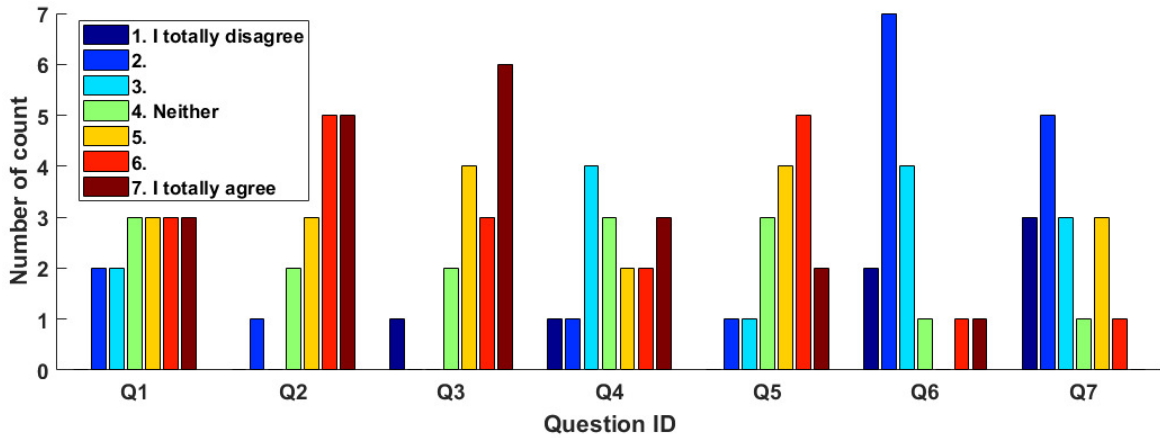


Figure 3.7: Bar-graph of the answers for each question. Q1: **pressing real piston**, Q2: **haptic device to perception**, Q3: **combination to perception**, Q4: **tactile device’s higher contribution**, Q5: **Practicing improves association**, Q6: **locations did not influence perception**, Q7: **Fatigue**.

Intrinsic perception of increased stiffness. As mentioned above, we asked subjects to recognize which piston felt “stiffer”. The stiffness of the two pistons was rendered either by the Falcon interface alone or by the Falcon interface plus the wearable haptic device (see Section 3.2.2). Therefore, the wearable device was activated only during the interaction with one of the two pistons. This situation may inadvertently induce subjects to link the presence of tactile stimuli to an increased stiffness level. Would subjects still find the haptically-augmented piston stiffer if we did not ask “which piston feels stiffer”?

In order to see if people would naturally tend speak about stiffness, we enrolled 28 additional naïve subjects, and we asked them to carry out a single repetition of the perceptual experiment of Section 3.2, i.e., interact with two pistons, one haptically-augmented through the wearable device and one rendered solely by the Falcon interface. We did not provide any information prior to this test, nor did we ask anything about stiffness, at the end of this interaction; instead, we simply asked “How did you perceive the second piston with respect to the first one?” 18 out of 28 subjects found the piston augmented with the wearable device to be “stiffer,” or “resisting more to my pressing,” or “providing more force when pressed.” This result hints toward the idea that providing wearable tactile stimuli when touching a tangible object directly and intrinsically elicits an increased stiffness sensation. This simple test does not prove that there is an effect, but might provide an interesting prospect for a future experiment.

Summary. The results of the perceptual evaluation show a significant effect of the stiffness perception when the wearable device was active. Both the objective measure and the subjective questionnaire confirm the increase of the stiffness perception when the haptic device and the wearable device are combined. Concerning the device positions on the fingers, there was no significant difference in the objective measure, but participants reported differences of stimuli in their answers to the questionnaire. The stimuli on the contralateral fingertip was however found less strong in the post-hoc analysis.

3.3 Use cases

After the preliminary prototype of Section 3.1.3 and the quantitative evaluation of Section 3.2, we apply the approach to five use cases. Several passive and inexpensive tangible

objects provide haptic information about the global shape/percept of the virtual objects, while the wearable haptic device provides haptic information about the dynamically changing mechanical property: the stiffness. A video showing these scenes can be found at <https://youtu.be/qA4xr81V4WA>.

3.3.1 Setup

Considering the results of Section 3.2, the wearable tactile device is worn on the user's index proximal phalanx. This configuration enables us to dynamically increase the perceived stiffness of the tangible objects, as detailed in Section 3.2.5, and, at the same time, it also enables the users to directly and naturally interact with the real environment using their fingertips.

The considered use cases in VR are shown in Table 3.1, and each tangible object is associated to a virtual one of similar shape. In these scenes, users wear either one or two wearable tactile devices on their proximal finger phalanges as well as a HTC Vive head-mounted display, which shows the virtual scene. Users sit or stand in front of a table on which tangible objects are laid down, and they are free to move their hand around. The motion of the user's hand is tracked using a Gametrak device, which registers the position of the volar side of the hand, and an inertial measurement unit (IMU), which registers its orientation (see also the bottom right picture of Table 3.1). These two pieces of information combined together enable us to reach a reasonably accurate tracking on the position and orientation of the user's hand. Similarly to [218], since we track the volar side of the hand, the user should not move the index finger with respect to the palm (i.e., IP and MCP joints should be fixed). A hand avatar mimics the motion of the human hand in the virtual environment. The position of the hand avatar in the scene with respect to the virtual objects is carefully adjusted to match the position of the human hand with respect to the tangible objects. In this way, whenever the user touches one of the tangible objects in the real environment, the hand avatar touches the correspondent virtual object in the scene. The activation of the wearable device is then computed in real time, knowing the penetration depth in the virtual (and real) object as well as the given stiffness property. The virtual scene has been built using Unity 5.6, which renders the virtual scene and computes the contact interactions between the hand avatar and the virtual foams.

We also considered two AR use cases, shown in Table 3.2. The setup is the same as the one described above. However, this time, users are asked to wear a Microsoft HoloLens instead of the HTC Vive head-set, which projects a virtual scene onto the real environment. Users can therefore look directly at the real environment and at their own hand while the HoloLens superimposes the virtual objects onto the tangible ones.

3.3.2 Use Cases Descriptions

Use case #1 in VR: inflating a balloon. The VR scene is composed of one rounded pump, a pressure indicator, and a balloon (see the first column of Table 3.1). The user is able to interact with the virtual pump which is superimposed to a *deformable* tangible object. Each time the pump is pressed, the displayed level of pressure rises, the balloon is inflated and, thus, the stiffness of the pump increases. These dynamic changes in the pump stiffness are provided through the wearable tactile device, by altering the perceived stiffness of the tangible pump, which does not change during the experience.

Use case #2 in VR: launching two rockets. This use case is a follow-up of the previous one: the pressure system is the same, however the balloon is replaced by a set of rockets with launch buttons (see the second column of Table 3.1). The propulsion power of the rocket depends on the amount of pressure inserted into the system prior to launch. The second tangible object is a pushbutton. It acts as a spring with a *hard and non-deformable* head whose perceived stiffness is also enhanced depending on the pressure. As before, these dynamic changes in pressure when interacting with the pumps and buttons are provided through the wearable tactile device.

Use case #3 in VR: petting a rabbit. The VR scene is composed of a basket, a scale, and a rabbit (see the third column of Table 3.1). The users can move the rabbit from the basket to the scale and pet it by holding the tangible object, a simple cylinder made of foam, which coarsely resembles the rabbit. The rabbit breathing activity is simulated by inflating and deflating its abdomen, and it speeds up whenever the rabbit is lifted or moved too fast. As the rabbit breathes, its overall shape and stiffness vary. The user is able to feel these variations through two wearable tactile devices, worn on the right index proximal finger phalanx and on the right thumb proximal finger phalanx.

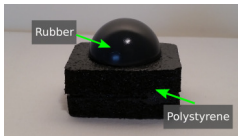
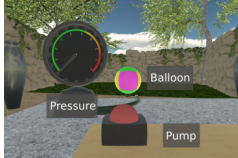
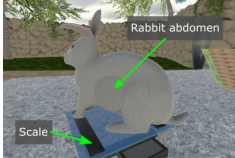
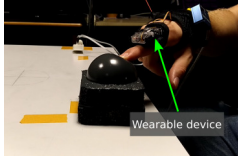
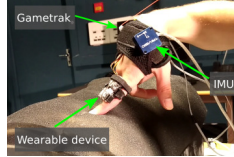
	Inflating a balloon	Launching rockets	Petting a rabbit	Abdomen palpation
Tangible objects				
VR scene				
Mixed interaction				

Table 3.1: Virtual Reality (VR) scenes. Each column refers to one VR use case. The first row shows the tangible objects employed, which are all passive and inexpensive. The second row shows the VR scene presented to the user through a HMD. The third row shows the user, wearing one or two wearable tactile devices, interacting with the tangible environment. The wearable devices are in charge of dynamically changing the perceived stiffness of the tangible objects according to what happens in the VR scene.

Use case #4 in VR and AR: abdomen palpation. This use case, in VR, is shown in the fourth column of Table 3.1. The scene is composed of a patient laying on a table inside a medical examination room. In front of the human user, we place a large parallelepiped made of foam, which coarsely resembles the abdomen of the patient and has constant stiffness. The user has to palpate the abdomen and locate a virtual cyst, simulated by a stiff sphere with a diameter of 3 cm [219]. When the fingertip avatar touches the simulated

cyst-like sphere, the wearable tactile device is activated, rendering the increased stiffness of the area.

This palpation user case was also carried out in AR (see the first column of Table 3.2). The same VR scene described above is now superimposed to the real environment. The position of the superimposed virtual scene is carefully adjusted to match the position of the foam abdomen. Whenever the user touches the foam in the real environment, the user sees his hand touching the virtual abdomen and eventually feels an increase of stiffness.

Use case #5 in AR: forearm palpation. The setup is shown in the second column of Table 3.2. In this case, the tangible object is a real human forearm, placed on a table in front of the human user. The virtual scene is composed of two disks, superimposed to the human forearm, one near the wrist and one near the elbow. As before, the user wears one wearable tactile device on the right index proximal finger phalanx. Users are asked to palpate the real forearm and touch the two highlighted regions. As users palpate the forearm, their fingertip is directly in contact with the forearm skin. Whenever the fingertip touches one of the two highlighted regions, the wearable tactile device is activated, making the area feel stiffer.

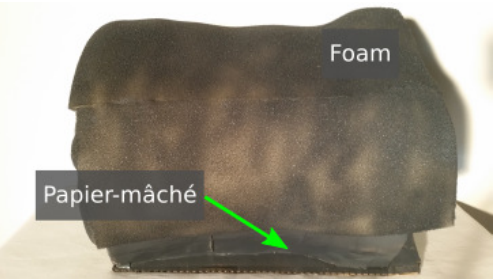
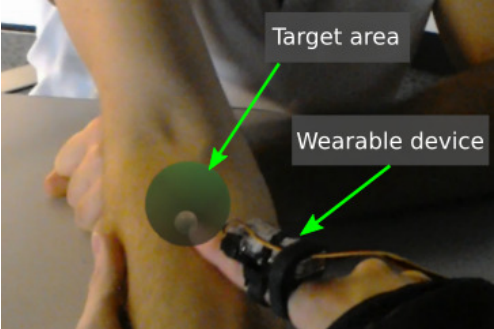
	Abdomen palpation	Forearm palpation
Tangible objects		
Mixed interaction		

Table 3.2: Augmented Reality (AR) scenes. Each column refers to one AR use case. The first row shows the tangible objects employed. The second row shows the mixed-reality view, provided to the user through the Microsoft Hololens. The wearable device is in charge of dynamically changing the perceived stiffness of the tangible objects according to what happens in the AR scene.

3.4 Discussion

In the study, results showed a strong effect when wearing the active device, regardless of the locus of stimulation, i.e., the wearable haptic device did indeed increase the piston

perceived stiffness. It is also interesting to note that users had the feeling that the position of the device holds importance. Some of them would prefer to have it on the fingertip, while others would rather have it away from it. Despite this result, we found no significant difference between the considered loci of stimulation: fingertip, middle phalanx, proximal phalanx, or fingertip of the contralateral hand. However, the stiffness augmentation effect when providing tactile stimuli on the contralateral fingertip was found less strong than when providing stimuli on the finger interacting with the tangible object.

These results are quite promising. Indeed, retaining the stiffness alteration effect even when moving the tactile stimulus away from the contact point with the tangible object (i.e., the fingertip) opens up several interesting opportunities. For example, moving the wearable device toward the proximal finger phalanx leaves the fingertip free to directly interact with the tangible objects, providing a more natural haptic sensation. Touching tangible objects while wearing wearable devices on the fingertips has been in fact already proven to significantly reduce the effectiveness of AR systems [105]. Moreover, leaving the fingertip free can also improve the performance of model-based trackers [96].

In this work, we developed several use cases with stiff objects, always passive, whose stiffness was dynamically enhanced either globally or locally while pressing on them, holding them, or exploring them. Although the proposed approach is quite effective and promising, there are still several questions to be answered. For example, how to prevent the users from paying attention only to the device activation, instead of the perceived overall stiffness for a task similar to the palpation. In our experiment we only used a single level of additional stiffness with the wearable, it could be interesting to compare various levels of activations, as keeping the wearable activated at all time with various levels would seem to be a good idea for a searching task.

we can only *increase* the perceived stiffness of tangible objects, while it does not seem trivial to make them feel less stiff than they actually are. In this respect, an idea could be to start the interaction with the wearable device applying an initial force to the finger skin, and then partially release the belt when coming in contact with the tangible object. Since it is known that pressure mechanoreceptors tend to adapt to constant pressure stimuli [220], a timely decrease of pressure at the finger when touching the tangible object may decrease its perceived stiffness. Another interesting open question is how much can we increase the perceived stiffness of tangible objects via wearable haptics. Finally, even if the belt could be extended away from the finger surface, the system has no mean to know if the contact is actually broken. Thus, the wearable device is not able to effectively break contact with the finger skin, and we were unable to take advantage of the effect of the temporal change of contact area, which is known to help stiffness perception [221, 222].

Lately, the proof of concept was extended to other types of haptic sensation [223], as the 2-DoF wearable device can also provide skin stretch stimuli. In this work, the effect of combining simple passive tangible objects and wearable haptics for improving the display of varying stiffness, friction, and shape sensations was studied. Again, by providing timely cutaneous stimuli with the same wearable finger device, we can make an object feel softer or more slippery than it actually is, and induce the illusion of encountering bumps and holes. These proposed approaches were finally evaluated in three user studies [223] which will not be further exposed in this manuscript.

3.5 Conclusion

We introduced an innovative approach for VR and AR immersive environments, capable of dynamically altering the perceived stiffness of tangible objects by providing timely tactile stimuli through wearable haptic devices. This approach combines the haptic capabilities of both tangible objects and wearable haptics, delivering them through unobtrusive and inexpensive systems. Passive and uncomplicated tangible objects provide haptic information about the global shape/percept of the virtual objects, while wearable haptic devices provide haptic information about dynamically changing mechanical properties. We believe that these two pieces of haptic information combined together could significantly improve the effectiveness and immersion of haptic-enabled VR and AR experiences. We considered a representative proof-of-concept scenario, in which we used a 2-DoF wearable tactile device at the fingers. Whenever the user interacts with a tangible object during VR or AR experiences, the wearable device dynamically modifies its stiffness perception, making the tangible object feel more or less stiff depending on what is happening in the virtual scene. We used a wearable haptic device at the level of the proximal finger phalanx, and we could leave the user's fingertip free to directly interact with the tangible environment. A user study and five use cases showed the potential and viability of the approach. Taken together results pave the way for novel haptic systems in VR/AR applications better exploiting the multiple ways of providing simple and low-cost haptic displays.

Chapter 4

How Different Tangible and Virtual Objects Can Be While Still Feeling the Same?

Sommaire

4.1 Methods	88
4.1.1 Experimental setup	89
4.1.2 Experimental task and procedure	89
4.2 User study #1: Width	90
4.2.1 Procedure Description	90
4.2.2 Experimental Design and Participants	91
4.2.3 Results	91
4.3 User study #2: Local Orientation	92
4.3.1 Procedure Description	92
4.3.2 Experimental Design and Participants	92
4.3.3 Results	93
4.4 User study #3: Local Curvature	94
4.4.1 Procedure Description	94
4.4.2 Experimental Design and Participants	94
4.4.3 Results	94
4.5 Subjective Questionnaire	95
4.6 Discussion	96
4.7 Conclusions	97

Tangible objects are used in Virtual and Augmented Reality to convey the haptic sensation of touching virtual objects. Yet, for the illusion to work, the haptic characteristics of the tangible objects should match as much as possible those of the corresponding virtual ones in terms of, e.g., size, local shape, texture, mass. In other words, there should be a *good* correspondence between what users see in the virtual environment and what they touch in the real world. However, human perception is not perfect and any estimation of a tangible property comes with error. As a consequence, some amount of discrepancy between the tangible and its virtual representation should be indiscernible for the user.

Hence, in this Chapter, we will *intentionally induce unnoticeable discrepancies* between the two in order to understand how different a virtual object can be from its tangible counterpart without the user noticing (see Fig. 4.1). This question is important for all those working in the field of immersive environment, and its answer can open interesting avenues for the use of few tangible objects in the rendering of multiple virtual ones. Of course, the visuohaptic perception of objects encompasses several different dimensions, including the object's size, shape, mass, texture, and temperature.

The main contributions of our work address three representative haptic features - width, local orientation and curvature, - which are particularly relevant for grasping. We carried out three human subject experiments, one for each criterion, that we will describe in the next section. A video summarizing our work is available at the following link <https://youtu.be/xREuZbh6tLc>.

In the remainder of this Chapter, we first expose the method used for the three different user studies which will be detailed one by one afterward. Finally, the results and outcomes of the experiment are discussed.

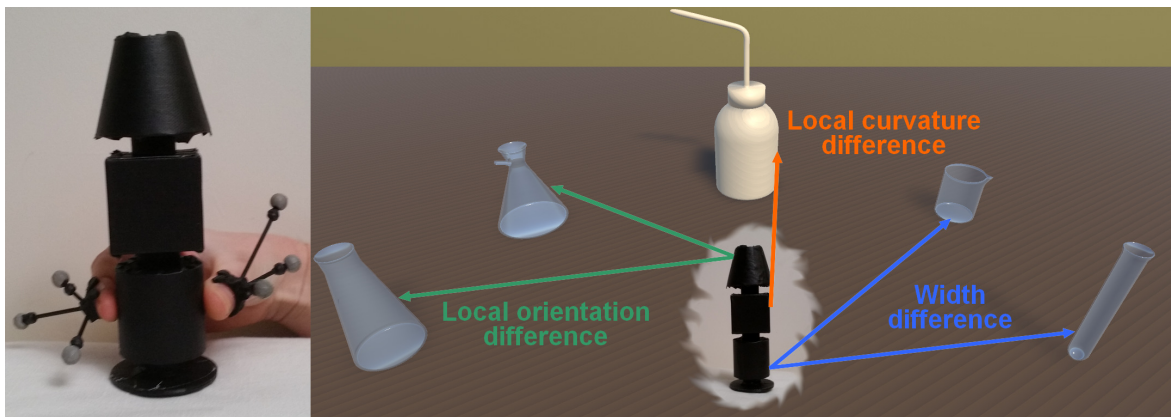


Figure 4.1: Objective of our study: understanding how different a tangible object (left) can be from virtual objects (right) without the user noticing the mismatch. We focused our study on three specific criteria: width, local orientation, and curvature.

4.1 Methods

The goal of our user studies is to measure the Just-Noticeable Difference (JND) of the discrepancy between a couple of tangible and virtual objects during 2-finger grasping, in terms of the three above-mentioned haptic dimensions: width, local orientation, and curvature.

4.1.1 Experimental setup

Fig. 4.2 shows the setup. Participants wear a HTC Vive headset displaying the virtual scene. A Bonita Vicon system tracks the subjects' thumb and index fingertips using markers placed on the dorsal side of their fingers (avoiding the nails). Doing so, the subjects' finger pads are always left free to interact with the tangible object (TO).

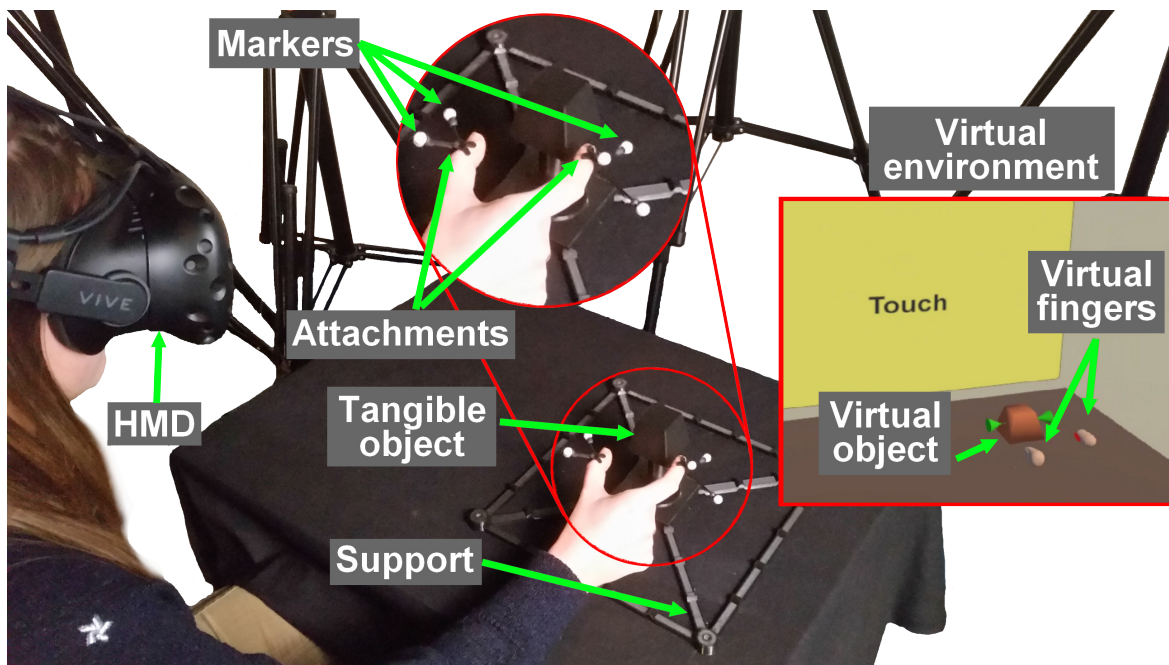


Figure 4.2: Setup for the three experiments. Inset shows the virtual environment during the task.

Two virtual fingertips mimic the motion of the subjects' fingertips in the virtual environment. This simple representation of the user's hand [224] has been chosen to avoid occluding the virtual object from the user's point of view (see inset of Fig. 4.2). The virtual scene is composed of an instruction panel and a table, supporting the considered virtual object (VO). The position of the VO in the virtual scene matches the position of the TO in the real environment. In other words, whenever users grasp the TO, they also grasp the VO. We ensure a good matching between the positions of the TO and VO by securing the TO on a 3D-printed structure, which is placed on a table in front of the user. Moreover, at the beginning of each experiment, we calibrate the system to also ensure a good matching between the subjects' fingertips and their virtual avatar. More details on the tracking solution can be found in Appendix B.

4.1.2 Experimental task and procedure

Participants are asked to grasp the TO at a designated pinch location, highlighted by two green cursors, while seeing the VO through the headset (see Fig. 4.2). At every new grasping trial, the system induces a discrepancy between the TO and VO by altering the considered criterion, i.e., it creates a mismatch of width, local orientation, or curvature where the subject grasped. We use only one tangible object per experiment, while several different virtual objects are shown to the participants (see Fig. 4.3). Whenever participants arrive at the highlighted pinch location, the object turns red and a "hold" message is displayed for 2 s on the virtual panel in front of the user. After that, the object turns green, and the panel asks the user to "release" the object. Right after releasing the object, a question appears on

the panel, asking the participants to compare their perception of the considered criteria between the TO and the VO. Finally, the experimenter fakes the changing of the TO, to prevent participants from understanding that only one TO was used throughout the whole experiment. This procedure can be seen in the previously mentioned video.

Before the beginning of an experiment, we explain the procedure to the participants and we spend about three minutes adjusting the setup to be comfortable. Then, the participants spend about two minutes practicing the interaction with two couples of TO and VO. They performed practice trials on 3 different VO/TO pairs but with another reference shape than those used for the actual experiments: a cylinder for the width, a cone for the tilting angle and a cylinder for the curvature. The experimenter could thus verify that the participant had well-understood the question.

The three experiment took around half an hour for 9 practice trials and 175 trials.



Figure 4.3: The tangible objects used for the three user studies: a cube, a trapezoid prism, and an ellipsoid. Participants are asked to grasp at the center of each shape, which is 8 cm from the table (dotted line).

4.2 User study #1: Width

4.2.1 Procedure Description

The objective of this first user study is to investigate how much the *width* of a virtual object can differ from the one of a tangible one without the user noticing. We use a cube as the reference shape (left object of Fig. 4.3), as it is a well-known shape which is easy to recognize from any point of view. Participants are asked to grasp the virtual object and its tangible counterpart, comparing their width and answering the question: “Is the tangible object larger than the virtual one?”

As mentioned in Sec. 4.1.1, we ensure that whenever the users touch the TO, they also touch the VO. To achieve this result, when the width of the VO and TO differs, we employ a simple virtual warping effect to (slightly) redirect the virtual fingers [189]. To do so, we applied an offset on the two fingers’ positions in order to match the virtual width of the pinch.

The needed offsets between the 2 fingers was applied gradually to each finger from 10 cm away up to the contact point to make it less noticeable with a maximum offset of

2 mm for each finger. However, in the end, the question users had to answer was once the contact was made with the object as they had to assess the actual grasp width.

4.2.2 Experimental Design and Participants

We consider the cube width as the independent variable, with a reference value for the tangible cube of $w_{ref} = 4.0$ cm (left object of Fig. 4.3) and 9 comparison widths for the virtual cubes 2.4, 3.2, 3.6, 3.8, 4.0, 4.2, 4.4, 4.8, 5.6 cm (see Fig. 4.4). We compute the comparison widths $w_{ref}(1+\Delta)$ with $\Delta \in \{0\%, \pm 5\%, \pm 10\%, \pm 20\%, \pm 40\%\}$. We chose this range of comparison widths so that the covered range contains JND values already registered in the literature [20]. For each trial, participants had to determine which object (tangible vs. virtual) had the larger width. Each pair was repeated 7 times, resulting in 63 comparisons for each participant. The experiment lasted 10 minutes in total. Before the experiment, participants also performed three practice trials with cylinders, the diameter of the tangible one was 4cm while the virtual one had a width difference of $\pm 25\%$. We chose to have 2 excessive differences and an exact one to make sure participant understand that they had to compare what they feel to what they see and also that they have to choose an answer even if it difficult to tell.

We enrolled 17 participants (9 males, 8 females, $M = 21.59$, $SD = 1.58$), all of whom were right-handed.

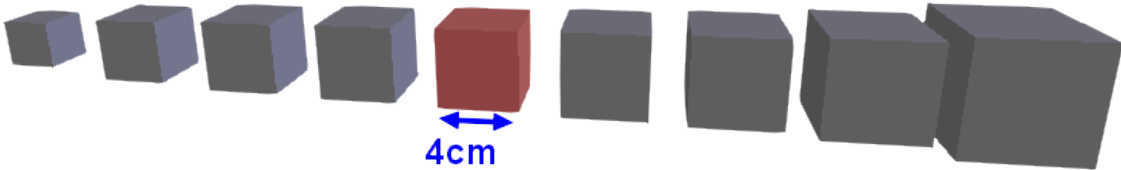


Figure 4.4: User study #1: width. The virtual cubes having variable widths $w_{ref}(1+\Delta)$, $\Delta = \{0\%, \pm 5\%, \pm 10\%, \pm 20\%, \pm 40\%\}$ are compared with the reference cube ($w_{ref} = 4.0$ cm), shown in red. In the real environment, participants always grasped the tangible cube shown on the left of Fig. 4.3.

4.2.3 Results

First, we compute the percentage of answers in which the tangible object felt *larger* than the virtual object. As expected, as the width of the VO increases, the less often the participants feel the TO larger. Then, using Weber's law, we compute the Weber Fraction as $k = \Delta I/I$, where ΔI refers to the JND threshold and I is the reference width. The JND threshold can be determined as the value of the stimuli in which the recognition ratio is 75%. To compute this value, we fit the psychometric curve $f(x) = (1 + e^{(\alpha x + \beta)})^{-1}$ to the data (with $\alpha = 1.12$ and $\beta = -0.4546$), as shown in Fig. 4.5. The 75% JND is -0.23 cm, or 5.75% of the reference width. The corresponding Weber fraction is $k = \Delta I/I = 0.0575$. Furthermore, the Point of Subjective Equality (PSE) is 0.16 cm.

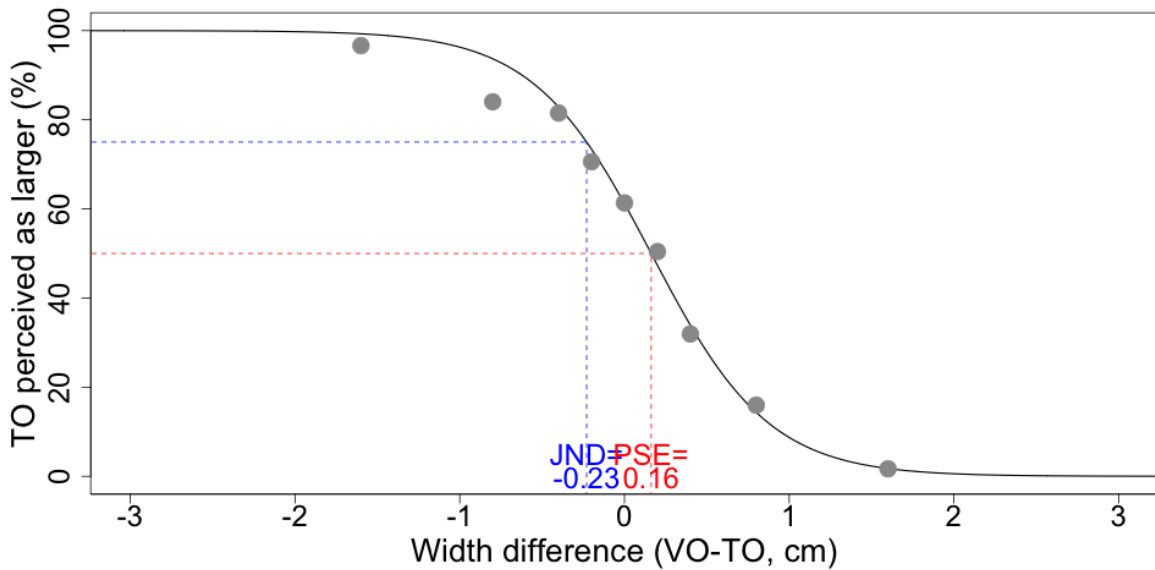


Figure 4.5: User study #1: width. Psychometric curve fitting the average percentage of answers (grey points) in which participants considered the tangible object as larger than the virtual one. The 75% JND is represented in blue while the PSE is in red.

4.3 User study #2: Local Orientation

4.3.1 Procedure Description

The objective of this second user study is to investigate how much the *local orientation* of a virtual object’s face can differ from the one of a tangible object without the user noticing. We use a trapezoid prism as the reference shape (middle object in Fig. 4.3). Participants are again asked to grasp the virtual object and its tangible counterpart. Then, they are asked to compare the local orientation at the grasping point, answering to the question: “Are the faces of the tangible object more tilted than those of the virtual one?”

For this experiment, users had to grasp pyramids of several apex angle. From a reference one, we would symmetrically tilt more or less each side of the pyramid. However, we also truncated them so that they would have the same height (Fig. 4.6). At the pinch location, all of them had a width of 4cm. Each face is titled from the vertical by a given angle, but we will consider here the total tilt angle by adding both of them since one is sensible to this total tilt when pinching an object.

4.3.2 Experimental Design and Participants

We consider the local orientation of the prism faces as the independent variable, with a reference angle for the tangible prism of $a_{ref} = 10^\circ$ (middle object of Fig. 4.3) and 7 comparison angles for the virtual prism $2^\circ, 6^\circ, 8^\circ, 10^\circ, 12^\circ, 16^\circ, 18^\circ$ (see Fig. 4.6). We avoid having a cube or inverted angles since it might lead to additional perceptual effect which could prevent us from obtaining the JND. We compute the comparison angles $a_{ref}(1 + \Delta)$ with $\Delta \in \{0\%, \pm 20\%, \pm 40\%, \pm 80\%\}$. At the pinch location, all virtual prisms have a width of 4 cm. Participants compared each couple of objects 7 times, yielding to $7 \times 7 = 49$ comparisons for each participant. The experiment lasted around 10 minutes. Before the experiment, participants also performed three practice trials with with cones of $0^\circ, 30^\circ$ and 60° apex angles while the tangible one was 30° .

We enrolled 17 participants (10 males, 7 females, $M = 21.59$, $SD = 1.58$), all of whom were right-handed.

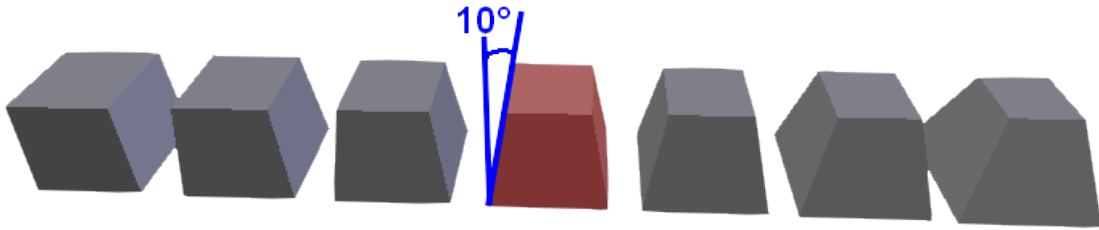


Figure 4.6: User study #2: local orientation. The virtual prisms having variable faces orientations $a_{ref}(1 + \Delta)$, $\Delta = \{0\%, \pm 20\%, \pm 40\%, \pm 80\%\}$ are compared with the reference prism ($a_{ref} = 10^\circ$), shown in red. In the real environment, subjects always grasp the tangible prism shown at the middle of Fig. 4.3.

4.3.3 Results

First, we compute the percentage of answers in which the tangible object felt *more tilted* than the virtual object. As before, as the tilting angle of the VO increases, the less often the participants feel the TO as more tilted. Then, we compute the Weber Fraction using the 75% JND. To compute the latter, we again fit the psychometric curve $f(x) = (1 + e^{(\alpha x + \beta)})$ to the data (with $\alpha = 0.26$ and $\beta = -0.022$), as shown in Fig. 4.7. The 75% JND is -4.38° , or 43.8% of the reference orientation angle. The corresponding Weber fraction is $k = 0.438$. Furthermore, the PSE is 0.09° .

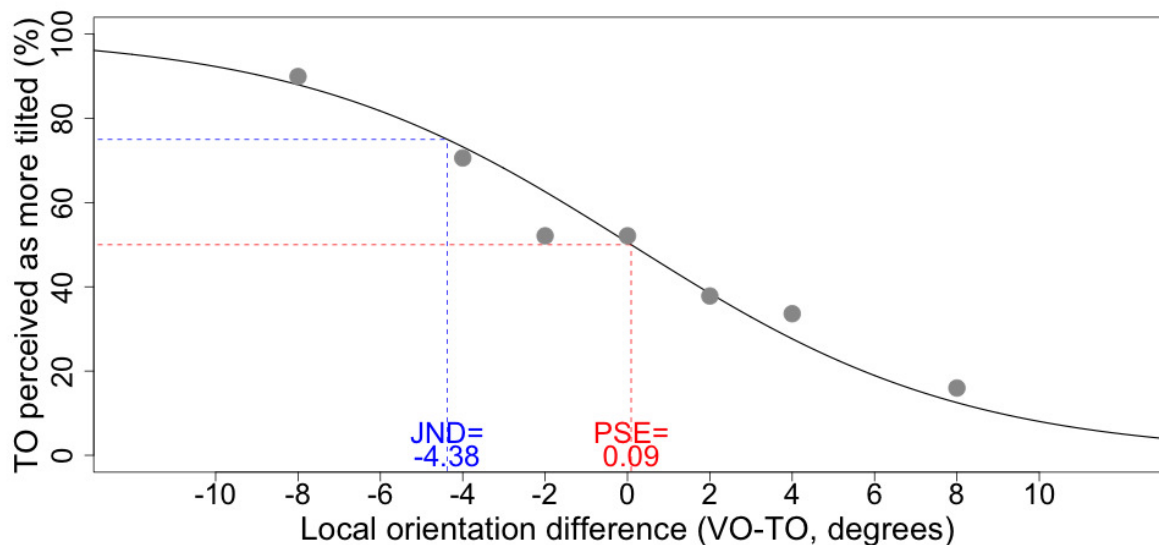


Figure 4.7: User study #2: local orientation. Psychometric curve fitting the average percentage of answers (grey points) in which participants considered the tangible object as more tilted than the virtual one. The 75% JND is represented in blue while the PSE is in red.

4.4 User study #3: Local Curvature

4.4.1 Procedure Description

The objective of this third and last user study is to investigate how much the *local curvature* of a virtual object's faces can differ from the one of a tangible object without the user noticing. We use an ellipsoid as our reference shape (right object of Fig. 4.3). Participants are again asked to grasp the virtual object and its tangible counterpart. Then, they are asked to compare the curvature at the grasping point, answering to the question: "Are the faces of the tangible object more curved than those of the virtual one?"

4.4.2 Experimental Design and Participants

The size of the tangible ellipsoid is $4 \times 4 \times 5$ cm, with an estimated curvature at the grasping point of 52 m^{-1} in the horizontal plan and 33 m^{-1} in the vertical plan.

This parameter is more difficult to grasp and assess. Thus, we did not change the curvature at the pinch location with curvature steps, but rather applied some deformation (dilatation and compression) to the reference ellipsoid. Starting from an ellipsoid of $4 \times 4 \times 5 \text{ cm}$, which serves as a reference to 3D-print the tangible, the estimated curvature at the contact areas were 52 m^{-1} in the horizontal plan and 33 m^{-1} in the vertical plan. Then, we deform the ellipsoids by changing the height and keeping the width at 4 cm , and thus modify the curvature in the vertical plan only. The applied deformations were centered around a 5 cm height: 0%, $\pm 8\%$, $\pm 16\%$, 32%, 64% (Fig. 4.8).

Thus, we consider the curvature of the ellipsoid in the vertical plan as the independent variable, with a reference curvature for the tangible ellipsoid of $c_{ref} = 33 \text{ m}^{-1}$ (right object of Fig. 4.3) and 9 comparison curvatures for the virtual ellipsoid 12, 19, 24, 28, 33, 39, 47, 72, 269 m^{-1} (see Fig. 4.8). We compute the comparison curvatures as $c_{ref}(1 + \Delta)$ with $\Delta \in \{-63.6\%, -42.4\%, -27.3\%, -15.2\%, 0\%, +18.2\%, +42.4\%, +118.2\%, +715.2\%\}$. At the pinch location, all virtual ellipsoids have a width of 4 cm. Participants compared each couple of objects 7 times, yielding to $7 \times 9 = 63$ comparisons for each participant. The experiment lasted around 10 minutes.

We enrolled 15 participants (7 males, 8 females, $M = 21.4$, $SD = 1.40$), all of whom were right-handed.

At the beginning of the experiment, participants would perform 3 practice trials with deformed cylinder, one which would show extremely curved areas at the pinch location, one which would show flattened areas and a perfect cylinder in the middle. We took extra care to be sure that the users fully understood the question and answered it with the right relation order in mind since some participant in a pre-experiment answered the exact opposite.

4.4.3 Results

First, we compute the percentage of answers in which the tangible object felt *more curved* than the virtual object. Then, we compute the Weber Fraction using the 75% JND. To compute the latter, we fit the psychometric curve $f(x) = (1 + e^{(\alpha x + \beta)})^{-1}$ to the data (with $\alpha = 0.061$ and $\beta = -1.77$), as shown in Fig. 4.9. The 75% JND is 22 m^{-1} , or 66.6% of the reference tilting angle. The corresponding Weber fraction is $k = 0.666$. Furthermore, the PSE is 29.04 m^{-1} .

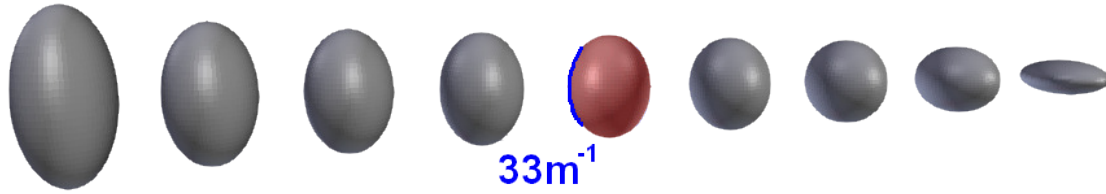


Figure 4.8: User study #3: curvature. The virtual ellipsoids having variable faces curvatures $c_{ref}(1 + \Delta)$, $\Delta = \{-63.6\%, -42.4\%, -27.3\%, -15.2\%, 0\%, +18.2\%, +42.4\%, +118.2\%, +715.2\%\}$ are compared with the reference ellipsoid ($c_{ref} = 33 \text{ m}^{-1}$), shown in red. In the real environment, participants always grasp the tangible ellipsoid shown in the right of Fig. 4.3.

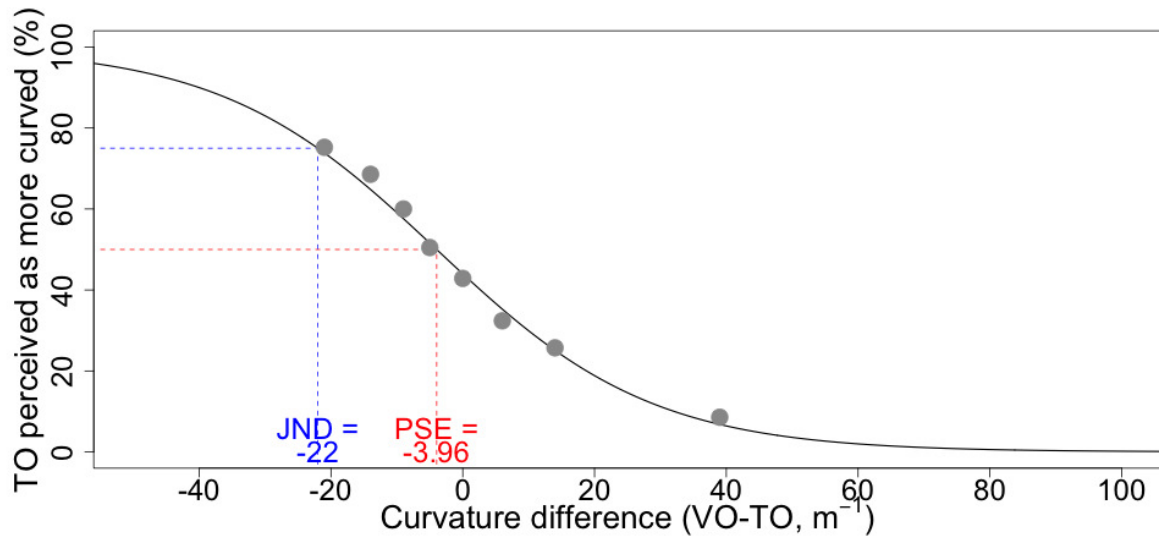


Figure 4.9: User study #3: curvature. Psychometric curve fitting the average percentage of answers (grey points) in which participants considered the tangible object as more curved than the virtual one. The 75% JND is represented in blue while the PSE is in red. For clarity, the $\Delta = 715.2\%$ value is not represented.

4.5 Subjective Questionnaire

In addition to the three user studies, the participants also fill a subjective questionnaire using a 7-point Likert scale. We asked the following questions: (Q1) “Was it easy to feel the difference of width between the tangible and virtual cubes?”; (Q2) “Was it easy to feel the difference of tilting between the tangible and virtual prisms?”; (Q3) “Was it easy to feel the difference of curvature between the tangible and virtual ellipsoids?”; (Q4) “Did it feel like you were seeing your own fingertips?”; (Q5) “Did you feel tired at the end of the experiment?”.

Results show that feeling the difference in width and local orientation was quite easy (Q1: $M = 4$, $SD = 1.57$; Q2: $M = 3.63$, $SD = 1.21$). However, it was quite difficult to feel the difference in local curvature (Q3: $M = 2.84$, $SD = 1.46$). The corresponding barplots are reported in Fig. 4.10. The matching between the virtual and the real fingertips appears to be well perceived (Q4: $M = 5.11$, $SD = 1.52$). At the end of the experiment, participants felt a bit tired (Q5: $M = 4.05$, $SD = 1.68$).

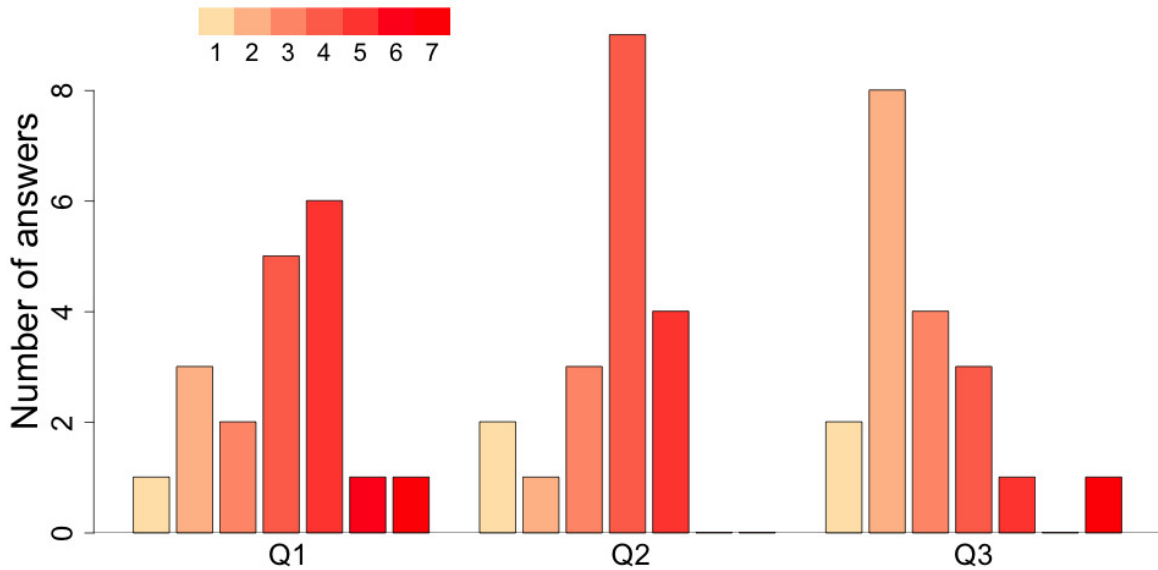


Figure 4.10: Barplots (7-point Likert scale) representing the participants answers to the questions on the easiness of perception of the difference between TO and VO for the three criteria: Q1 (width), Q2 (local orientation), Q3 (curvature).

4.6 Discussion

The objective of this Chapter is to measure how different virtual and tangible objects can be without the user noticing. Toward this objective, we carried out three human subject experiments considering the perception of size, local orientation, and curvature during grasping. Results showed a 75% JND of 5.75%, 43.80%, and 66.66% for the perception of width, local orientation, and local curvature during grasping, respectively around references values of 4 cm, 10° , and 33 m^{-1} . Those values were selected as central values in the range of realistic values for pinch grasping.

Although no one directly addressed this question for VR, these results are consistent to similar perceptual results in the literature. Ernst and Banks [20] found an 84% JND of 0.04 times the average ridge height (55 mm) when providing both visual stimuli. On the other hand, the haptic-only JND was 0.085 times the average height. In our case, the 84% JND is 10.75% of the cube size (40mm). This difference might be explained by the fact that our participants could see the cube in 3D. Moreover, in this Chapter, we are studying a discrepancy-related JND, which poses a different questions w.r.t. the one considered in [20]. Subjects in Ban et al. [125] were asked to explore a tangible vertical surface with their index finger while seeing a slanted virtual surface on the screen (70°). The ratings of a questionnaire suggest that the two objects (tangible and virtual) felt almost the same. Simeone et al. [225, 139] found that affordance and function are the most important tracts when rendering virtual objects through tangible props. For this reason, they suggest to focus on maximizing the shape similarity around areas the user is likely to interact with (e.g., a handle). Unfortunately, they did not report any quantitative data on how to do this. Finally, subjects in Kwon et al. [144] took 65% more time to grasp a tangible object when its virtual representation significantly differed. In our experiments, we used the tangible object as reference. It would also be interesting to use the virtual object as reference and change the properties of tangible ones, to observe whether there are any biases. However, as we simulate the change of the tangible object for each repetition of the experiment, we believe that the bias was minimum. Moreover, size and distance in VR tends to be

underestimated. It is consistent in our work as the PSE we obtained for the width is positive (and negative for the curvature). However, we cannot isolate this effect with our user study as it was not designed for it. The above-mentioned design could provide additional insights on the question. However, our results were obtained in VR and as many other VR-related factors are involved, they should only be considered from a VR perspective. Our results open new interesting avenues for the use of tangible objects different from their virtual counterpart. The psychometric curves reported in Secs. 4.2, 4.3, and 4.4 enable researchers to understand when it is acceptable for a tangible object to approximate the haptic features of virtual ones. Doing so, one tangible object can be used to render multiple virtual ones without the user noticing.

From these initial results, we could analyze the haptic features of a virtual environment and then, knowing that it is possible to have some discrepancy, automatically generate one or more tangible objects, able to provide the best possible sensations in the rendering of the virtual scene. Alternatively, one could also change the virtual scene to improve the expected visuohaptic matching and, therefore, the illusion of presence (e.g., remove certain types of surfaces which are difficult to render with the available tangible objects). It may also enable to predict the illusion of presence and take action if deemed insufficient (e.g., by increasing the number of tangible objects in use).

Although these results are interesting, they are just the beginning of a long line of research. The haptic perception of an object does not only comprise size, local orientation, and curvature. It is therefore important to extend this study to other important haptic features, such as texture, mass, and temperature. More reference values would also be needed to better determine the Weber's fraction, and it would be interesting to do so for each feature as well as for different grasping poses. We also did not take into account that humans have fingertips of different size and elasticity, which can significantly affect how they perceive a surface. Another limitation is that we only considered 2-fingers grasping. We may find different results for other types of interaction. This work also does not directly address any possible confusion due to inherent tracking issue such as occlusions or calibration residual offsets. This issue may be solved by considering different tracking techniques [103] or additional tracking error compensation methods as well as more complex haptic proxy approaches to compensate such case. Finally, we also found that some participants had serious difficulties in recognizing even very large discrepancies. We plan to study this phenomenon in depth, to ensure a minimum guaranteed level of performance for all subjects, even the less perceptive ones.

4.7 Conclusions

Tangible objects are often used in VR and AR to provide distributed haptic sensations of touching virtual objects. However, it is often not possible to create tangible replicas of all the virtual objects in the scene and one would want to re-use some of those as much as possible, nor is it always possible to create an exact replicate. Thus, it is to be expected that there would be some discrepancy between the tangible objects and the virtual ones. This Chapter wants to directly address this issue, by measuring how different a virtual object can be from its tangible counterpart without the user noticing. Therefore, we tried to quantify this noticeable perceptual difference between virtual objects and their tangible counterpart during a 2 fingers pinching, by considering the perception of width, local orientation, and local curvature. Although some papers have addressed this problem from a qualitative point of view, to the best of our knowledge, this Chapter represents the first effort to quantify this noticeable perceptual difference between virtual and tangible objects in virtual reality.

Our experiments show that, while pinching, it was possible to induce discrepancy between what the user feel of the tangible object and what he sees from the virtual one by 5.75%, 43.8%, and 66.66% respectively for the width, local orientation and local curvature. Those results suggest that it is indeed possible, to a certain extent, to match different virtual and tangible objects without the user noticing. This aspect will be further studied in the next Chapter 5.

Chapter 5

Toward Universal Tangible Objects: Optimizing Haptic Pinching Sensations in 3D Interaction

Sommaire

5.1 Description of the Algorithm	102
5.1.1 Object description: a set of pinch poses	103
5.1.2 Cost Function: rating the association	106
5.1.2.1 First criterion: Pinch width	106
5.1.2.2 Second criterion: Projected distance to mass center	107
5.1.2.3 Third criterion: Pinch tilting	109
5.1.2.4 Fourth criterion: Patch Orientation	109
5.1.2.5 Fifth criterion: Patch curvature	110
5.1.3 Algorithm Implementation	113
5.1.3.1 Step #1: Computation of General Mesh Properties	113
5.1.3.2 Step #2: Patch Generation	114
5.1.3.3 Step #3: Pinch Generation.	115
5.1.3.4 Step #4: Pinch Comparison.	115
5.1.3.5 Step #5: Best Match Extraction.	116
5.2 User Study	116
5.2.1 Experiment Description	117
5.2.1.1 Participants	117
5.2.1.2 Experimental Apparatus	117
5.2.1.3 Procedure	118
5.2.1.4 Design	119
5.2.2 Conditions	119
5.2.3 Collected Data	120
5.2.4 Results	121
5.2.4.1 Static Task	121
5.2.4.2 Dynamic Task	121

5.2.4.3 Questionnaire	123
5.3 Discussion	124
5.4 Conclusion	125

When using tangible objects to provide haptic sensations of virtual elements, users naturally interact with these objects by relying on their visuohaptic perception, i.e., a combination of what they see of the virtual elements and what they feel of the tangibles. Chapter 4 previously highlighted that, while pinching, there could be some discrepancies over geometrical properties that the users could not perceive. However, users are only aware of the characteristics of a tangible object at the part they touch, while the remainder is unknown to them when they cannot see the tangible object. It is only important that the tangible object matches *locally* its virtual counterpart. Indeed, multiple parts of the same tangible object can be used to render multiple virtual objects, as long as they resemble each other wherever the user interacts with them.

Thus, in this Chapter, we will study further the possibility to have discrepancies between tangible and virtual in order to *pair a single tangible to multiple elements of the virtual environment*. However, for the illusion to work, the haptic features of the tangibles should match those of the corresponding virtual objects, i.e., there should be a good correspondence between the, e.g., size, local shape, texture, mass of the tangible object with respect to its virtual counterpart. Toward this objective, we present an algorithm that analyzes different tangibles and virtual objects to find the grasping strategy which best matches the resulting haptic pinching sensation. Starting from the meshes of the considered objects, the algorithm guides users toward the grasping pose which best matches what they see in the virtual scene with what they feel when touching the tangible object. By selecting different grasping positions according to the virtual object to render, it is possible to use few tangible objects to render multiple virtual ones (see this idea in Fig. 5.1).

The main contributions of our work can be summarized as follows:

- a novel algorithmic approach for using few tangibles to render multiple virtual objects, maximizing haptic fidelity;
- a preliminary user study assessing the effectiveness of the proposed approach for a set of representative objects.

In the remainder of this Chapter we first detail the pinch matching algorithm, then, we evaluate the approach in a "grasp and lift" user study. Finally, the results and outcomes of the experiment are discussed.

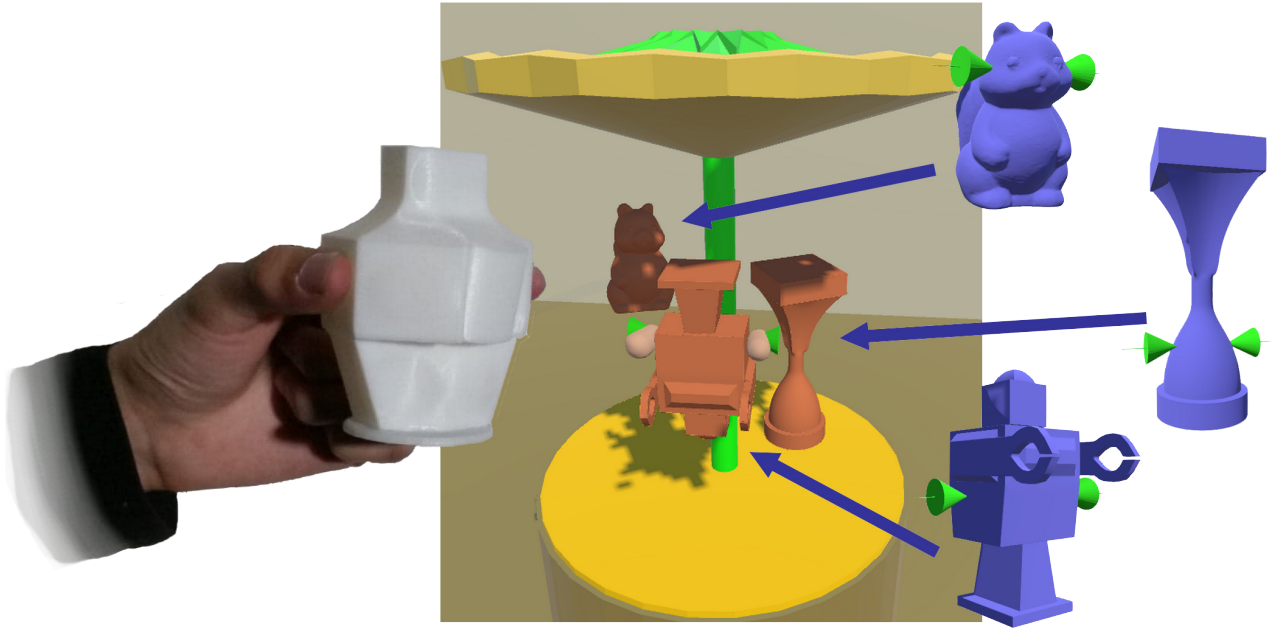


Figure 5.1: Illustration of the approach through a carousel of virtual objects that can be grasped using a single “universal” tangible object. The user is able to turn the virtual carousel and manipulate the three virtual objects using the suggested pinch poses (in green). These poses are proposed by our algorithm to best match the corresponding haptic pinching sensations with the tangible object.

5.1 Description of the Algorithm

The objective of this algorithm is to provide users with coherent sensations, matching what they see on the display with what they touch in the real environment. Given a set of virtual and tangible objects’ meshes, the algorithm identifies two grasping/pinching poses: one on the virtual object and one on the tangible object, maximizing their similarity in terms of haptic perception. The computation is performed during the preprocessing phase, and the generated grasping matches are used to provide guidance to the user in VR. Starting from the meshes of all considered objects, our algorithm behaves in the following way. First, it identifies feasible 2-fingers pinching poses on the considered tangible and virtual objects. Then, for each pose and for each object, the algorithm evaluates a series of haptically-salient characteristics: distance between the two fingertips, distance of the pinch from the center of mass, relative orientation between the two fingertips, local surface orientation and curvature. We have identified these features as a representative - yet non exhaustive - set of important grasping information. Next, the algorithm identifies the two most similar pinching poses, one on the tangible and one on the virtual object, evaluated in terms of the above metrics. Finally, the chosen pinching pose is highlighted in the virtual scene for the user to grasp. It guarantees the best match between what the users see on the display and what they feel when grasping the tangible object. The perceptual result highly depends on the intrinsic characteristics of the available tangible and virtual objects. The algorithm is only able to find the best solution given the available objects in the scene, which is not guaranteed to lead to a good/credible interaction. As expected, if a tangible replica of every virtual object is available, the algorithm will make the users grasp the virtual and tangible objects in almost the same place.

As one can notice, the haptically-salient characteristics are mostly local geometrical properties, except for the distance to the center of mass. This property depends on the global shape of the objects and conveys the idea that, when handling an object (grasp it, lift

it, move it around), humans will often have some expectations over its inertia. To avoid extreme mismatches regarding the inertia, we chose to restrict our work to any object which has a distinct principal component which will act as the main axis of inertia. Moreover, we will have the virtual object and tangible object's principal component parallel at all time, when registering them together for manipulation.

In light of those considerations, we make several assumptions on the interaction technique and the nature of the tangible and virtual objects for our method:

- User will only have a 2-fingers pinching interaction with the objects.
- User will only interact with a designed contact area where the perceived properties will match. There is no guarantee that the objects have any similarity elsewhere.
- Other properties related to texture, material and temperature and the underlying discrepancies will not be considered in this work.
- The objects will have a prismatic shape, i.e., will have a distinct principal component, which will act as the main axis of inertia.

In the remaining parts of this section we will describe the parametrization of the objects in terms of local haptic characteristics, then we will detail the cost function rating the similarity between two pinch poses, and finally we will describe how the algorithm works.

5.1.1 Object description: a set of pinch poses

“A grasp is every static hand posture with which an object can be held securely with one hand” [226]. In this work, as a starting point, we only consider thumb-index fingers precision grasps, as defined by Cutkosky [227]. As only two fingers are involved, we refer to this type of grasp as a “pinch,” and we then refer to the pose of the two fingertips during the grasp as a “pinching pose.”

As the user grasps an object with two fingers, there are two contact areas which can be circumscribed by circular patches on the mesh. Each patch is then defined as a vicinity of points around a certain distance of the patch's center P , i.e., the larger radius of a fingerprint, r_p . Fig. 5.2 shows an example of a virtual object covered with patches and pinches.

Two patches can define a pinch pose, i.e., a grasping pose between the thumb and the index. We will arbitrarily order those patches with the index 1 and 2, thus referring to their respective centers with P_i , with $i \in \{1, 2\}$. We also define $\vec{v} = \overrightarrow{P_2P_1}$ as the vector representing the direction of the axis of the orientated pinch, and $C = \frac{P_1+P_2}{2}$, the center of the pinch. Since the purpose of the approach is to associate a pinch pose (2 ordered patches) on a tangible object to a pinch pose (2 other ordered patches) on a virtual one. In addition to the subscript $i \in \{1, 2\}$ to differentiate two patch of the same pinch, we use the subscripts t for tangible and v for virtual. Thus, we can compare the patch 1 of the tangible object t_1 with the patch 1 of the virtual one v_1 and (respectively t_2 with v_2). The object has a principal component by hypotheses which is arbitrarily oriented and noted \vec{u} along which is the virtual mass center M . As shown on Fig. 5.3, we can organize the pinch poses PP_i with $i \in [0; n - 1]$ along the principal component by projecting their centers onto this axis. Thus, we describe the objects as a set of pinch poses along their linear representation.

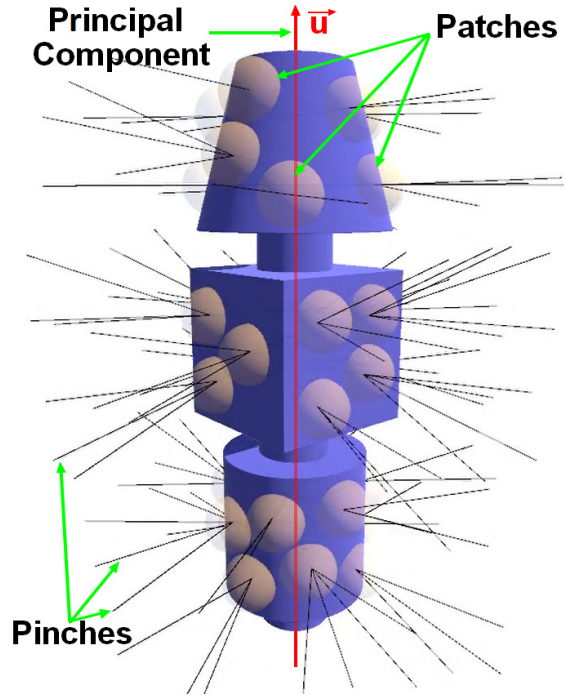


Figure 5.2: Example of Virtual Object with patches (pink spheres) and pinches (black lines).

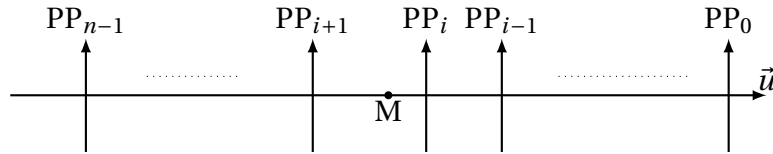


Figure 5.3: 1D representation of an object, with several numerated pinch poses

Each pinch pose describes locally the object through the various properties which are either related to the pinch itself, through the position of the patches, or related to the two patches defining it. These properties are used to compare pinch poses (PP) between Tangible Objects (TO) and Virtual Objects (VO). The geometric values of interest which describe a pinch pose are represented on Fig. 5.4:

- Signed distance between the mass center M of the object and C_p the projection of the pinch pose's center C on \vec{u} : d_i with $i \in \{v; r\}$, or in other words: the coordinate on the 1D representation.
- Pinch width: w_i with $i \in \{v; r\}$, distance between both patches: $w_i = \|\vec{v}_i\|$
- Pinch tilting: ϕ_i with $i \in \{v; r\}$, the signed angle between \vec{v}_i and \vec{v}_{i_p} , its projection onto the orthogonal plan to \vec{u} . A pinch pose is not tilted ($\phi_i = 0$), if it is orthogonal to \vec{u} .
- Eccentricity: e_i with $i \in \{v; r\}$, the distance between the pinch center and its projection onto \vec{u} .

The geometric values of interest which describe the curvature of a patch are represented on Fig. 5.5:

- Principal curvatures directions: \vec{d}' , \vec{d}'' .
- Principal curvatures: k' , k'' along those directions.
- Patch normal \vec{n} .

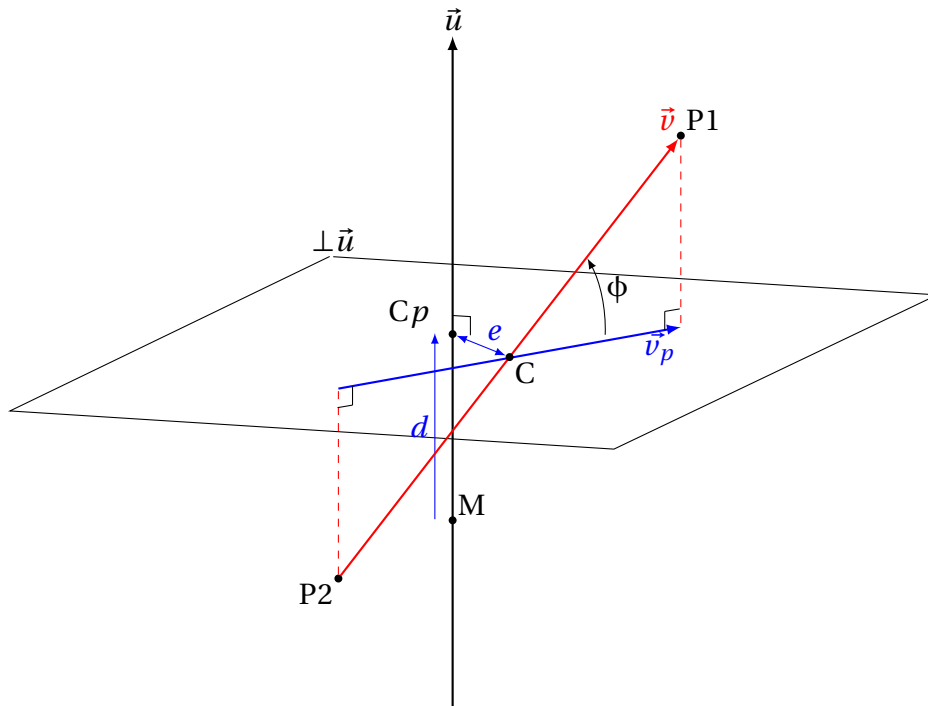


Figure 5.4: Description of the geometric values of interest on a pinch pose.

The two principal curvatures k' and k'' (with $k'' < k'$) are described in the Monge basis $\{\vec{n}, \vec{d}', \vec{d}''\}$ obtained through a second order fitting of the patch's points and can represent several kind of paraboloid (elliptic, hyperbolic, cylinder, etc.) [228].

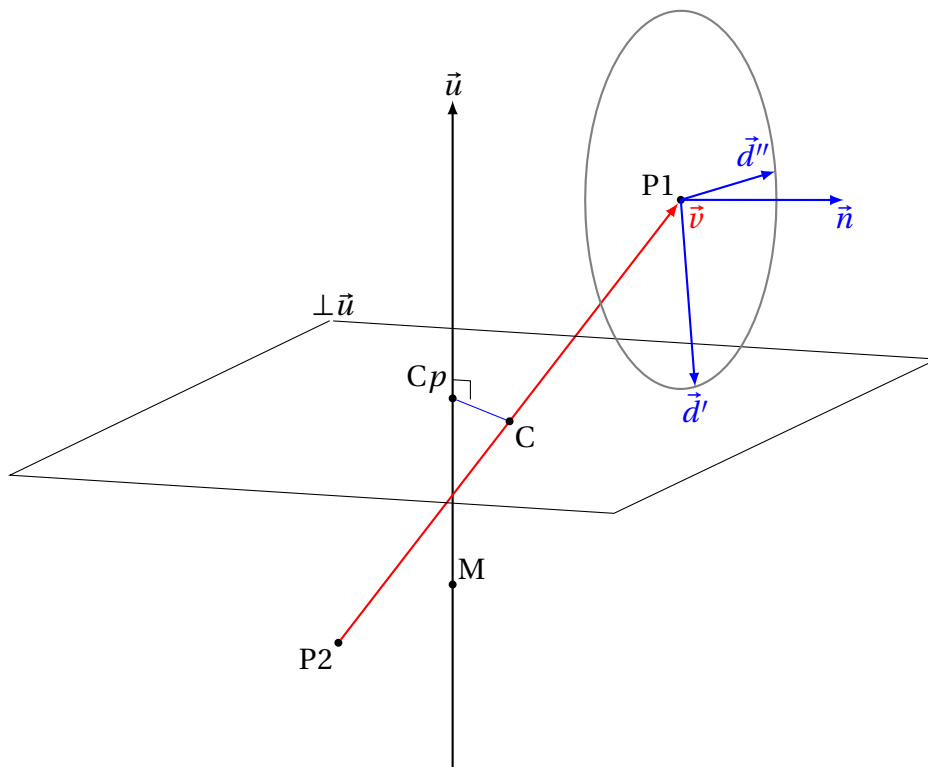


Figure 5.5: Description of the geometric values of interest on the first patch of a pinch pose.

This approach considers the global shape of an object (\vec{u}, M) as well as its local sub-shapes (d, w, ϕ) and surface properties ($\vec{d}', \vec{d}'', \vec{n}, k', k''$). Even if we introduced it for

clarity, we will neglect the effect of the pinch eccentricity: Although some pinches could have some eccentricity, i.e., the pinch axis will not intersect the principal component, we made the hypothesis that the objects are prismatic and that the effect of the eccentricity on the perceived inertial will be negligible compared to the distance to the mass center along the principal component. Moreover, we believe that users would unconsciously tend to grasp an object with a low eccentricity as to avoid it from slipping between their fingers.

5.1.2 Cost Function: rating the association

In order to evaluate the similarity of two pinch poses on virtual objects (VOs) and tangible objects (TOs), we propose a cost function which can rate the similarity between two pinches based on the following criteria:

- Pinch width
- Projected distance to mass centers
- Pinch tilting
- Patches orientation
- Patches curvatures

The cost function P_{global} rates the association between a tangible and a virtual PP within $[0, 1]$. Two identical pinches will score 1. However, if even a single one of these criteria shows an important difference between a tangible and virtual PP, this association will be fully rejected, i.e., having a score close to 0. We build the function for each one of the previous criteria so that they individually range in $[0, 1]$ and multiply them. If any criterion rates low, it prunes the global score:

$$P_{global} = P_{distCent} \times P_{width} \times P_{pinchTilt} \times P_{patchTilt} \times P_{curv} \times P_{ecc}$$

Each cost function of the various criteria will be a Gaussian of the difference between the two PP over one criteria, with a given variance σ^2 and no normalization factor. We will set σ at the just valid difference. Thus, if the difference is lower than σ , the score is higher than 0.61. If it is between σ and 3σ , the association is borderline on this criterion and is likely to be rejected if other criteria are also borderline. If it is higher than 3σ , then the association will be rejected as the resulting score is lower than 0.012. The table 5.1 summarizes of all criteria which are displayed in the remaining part of this section. In this first approach, each cost function is equally important and could be considered as having the same weight. However, due to the exponential properties, decreasing the weight of one property is equivalent as decreasing the associated variance.

5.1.2.1 First criterion: Pinch width

Hershberger and Misceo [229] discovered that, between vision and haptic information, neither modality inherently dominates the perceived size of an object. Discordant haptic information biases visual size estimates by as much as discordant visual information biases haptic size estimates. Since neither modality captures the other one completely, a discordant stimulus will be perceived as discordant. Flanagan and Mandomir [230] also found that the width of the grasp affects the object's perceived weight. Therefore, it is important to adequately match the size of the tangible object with respect to its virtual counterpart.

Table 5.1: Examples of how criteria are evaluated. The rows show a representative example of how each criterion is used to find a pinch match between two different shapes, i.e., one tangible and one virtual objects. Each column shows one criterion and how the matching pinch would be chosen if considering only that criterion. For each object, the blue triangles indicate the two pinching positions p_1, p_2 , the blue line the vector $\overrightarrow{P_1P_2}$ connecting them, the red line the object's first principal component, the red dot its center of mass, and the green line a perpendicular to the principal component.

	width	dist2cent	pinchTilt	curvature	patchTilt	All
Tangible Object						
Virtual Object						

To address this important point, we consider the perceived size of the object as our first criterion. We compare the width of the pinch on the TO, w_t , and the one of the VO, w_v , by simply computing the width difference: $\Delta w = w_t - w_v$ relative to the width of the tangible object:

$$\Delta w_n = \frac{w_t - w_v}{w_t}$$

σ_w is defined as the variance of the relative width difference which simply acts as a scale measure (ex: 25%). The cost function is then modeled as a Gaussian:

$$P_{width} = \exp\left(-\frac{\Delta w_n^2}{2\sigma_w^2}\right)$$

5.1.2.2 Second criterion: Projected distance to mass center

Although an object's weight can be already estimated when it rests on a stationary hand [21], its perceived weight and size when wielded is determined by its resistance to rotational forces of the user's limbs. When moving a grasped object around, users would be aware of the global inertia of the object and could tell if they are holding the object on the middle or on an edge. they would have some expectations on the object's mass distribution in their hands. Thus, users would feel that something is wrong if they *see* that they are holding the object at the lower part while feeling that they are actually *holding* the object by the upper part.

To take this property into account with our simplified model, this criterion focuses on the relative projected distance of the associated pinch to their respective object's mass center d_i . The mass center of both objects should be on the same side of the pinch pose, which means that d_v and d_t have the same sign. Otherwise the association has to be penalized and the cost brought to zero. As shown in Fig. 5.6, the first case should be avoided in favor of the second.

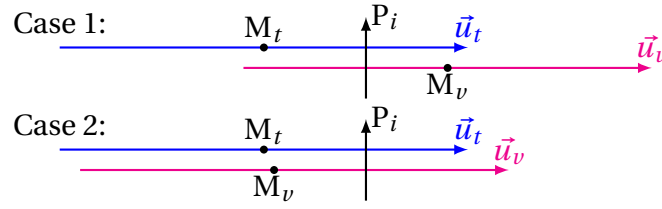


Figure 5.6: First case, mass centers are on both side of the superposed pinch poses. Second case, mass centers are on the same side of the superposed pinch poses.

This seems especially important if the pinch is far away from the mass center. However, when the pinch poses are close to the mass center of the tangible object, we can expect that the side of the mass center of the virtual object holds less importance. Since humans cannot visually determine the exact location of the mass center of an object, it will be less conflicting for the users when they are actually grasping the object close to the mass center. This case corresponds to the pinch on the tangible object being within a given radius from the mass center, $|d_t| < r_p$, with r_p the radius of the patches. Thus, the cost is computed differently if the user is grasping the object close to the center of mass ($|d_t| \leq r_p$), or not ($|d_t| > r_p$)

If $|d_t| \leq r_p$, the cost has two contributions as shown on Fig. 5.7, a large one (in blue) to discriminate pinches between close and far from the center of mass, and a smaller contribution (in red) on a smaller scale which discriminates between pinches close to the center of mass which one are the closest to d_t . The large one is constant within $]-r_p; r_p[$ and decrease with a Gaussian outside weighted by 0.95. The smaller contribution is weighted by 0.05, and is a Gaussian centered on d_t .

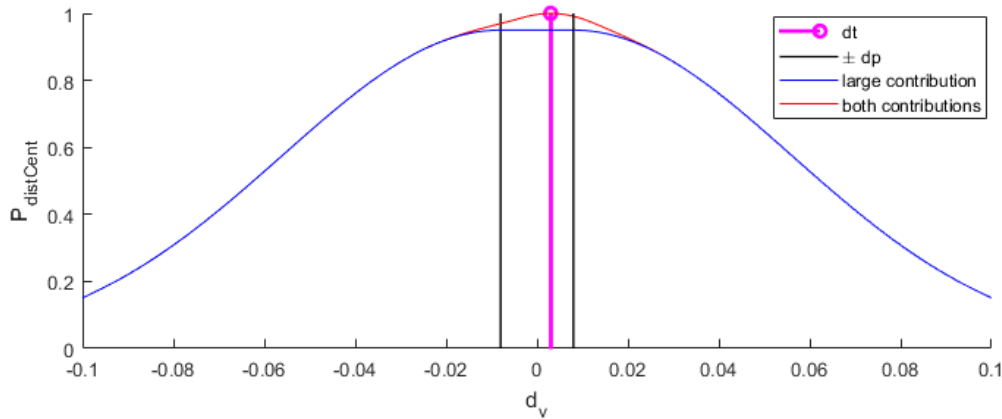


Figure 5.7: Cost Function: projected distance to mass center, close to mass center. The blue curve is the large contribution, flat in the middle, the red one is the sum of both contributions with a maximum of 1 if $d_v = d_t$ and d_t within the range $]-r_p; r_p[$.

If $|d_t| > r_p$, both contributions are centered on d_t and are Gaussian of different variance. However, we penalize the case were $d_v \times d_t < 0$ and $|d_v| > r_p$, i.e. both pinch poses are on different sides of mass centers as illustrated in Fig. 5.8.

Sum up of the criterion There are 2 contributions in the function, a small one with a small variance σ_s (ex: r_p), and a large one with a larger variance σ_L (ex: $6r_p$). The cost

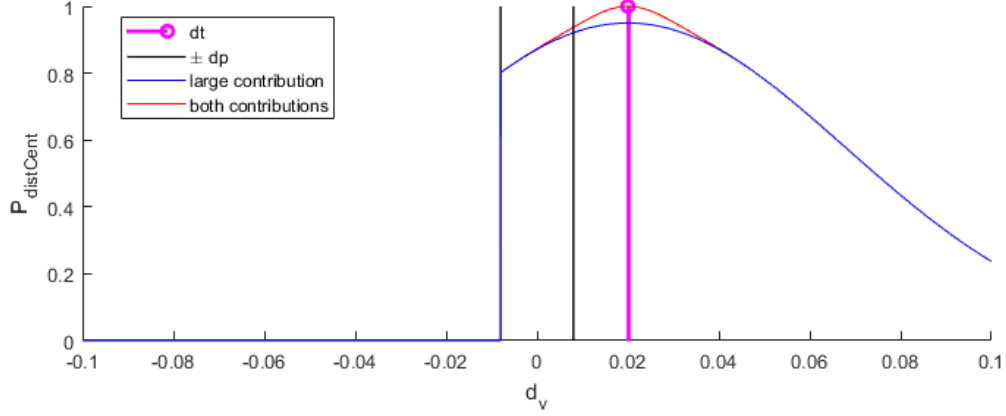


Figure 5.8: Cost function: projected distance to mass center, away from mass center. Cost function of d_v when $d_t > r_p$, the cost is brought to zero if d_v is on the other side of the central area. If $d_t < -r_p$, the function would be mirrored

function is then:

if $|d_t| \leq r_p$

$$P_{distCent} = 0.05 \exp\left(-\frac{(d_v - d_t)^2}{2\sigma_s^2}\right) + \begin{cases} 0.95 & \text{if } |d_v| < r_p \\ 0.95 * \exp\left(-\frac{(d_v - \text{sign}(d_t)r_p)^2}{2\sigma_L^2}\right) & \text{otherwise} \end{cases}$$

else ($|d_t| > r_p$)

$$P_{distCent} = \begin{cases} 0.05 \exp\left(-\frac{(d_v - d_t)^2}{2\sigma_s^2}\right) + 0.95 * \exp\left(-\frac{(d_v - d_t)^2}{2\sigma_L^2}\right) & \text{if } d_p + \text{sign}(d_t)d_v > 0 \\ 0 & \text{otherwise} \end{cases}$$

5.1.2.3 Third criterion: Pinch tilting

This criterion is a complement of the previous one, if the pinching is tilted with respect to the principal component, the inertia will be perceived differently when handled and moved around. Thus, we compare the inclination angle of the pinch on the TO, ϕ_t , and the one of the VO, ϕ_v , by simply computing the difference: $\Delta\phi = \phi_t - \phi_v$, which is scaled by the associated variance σ_ϕ (ex: 13 deg). The cost function is modeled as a Gaussian:

$$P_{pinchTilt} = \exp\left(-\frac{\Delta\phi^2}{2\sigma_\phi^2}\right)$$

5.1.2.4 Fourth criterion: Patch Orientation

This criterion is the first patch-related criterion. Each patch has its own inclination to the pinch pose's axis and each pair of patches is compared to be sure that they have similar inclinations: patch 1 (resp. 2) from the virtual pinch with patch 1 from the tangible one (resp. 2), using the patches' normals: $\vec{n}_{v1}, \vec{n}_{v2}, \vec{n}_{t1}, \vec{n}_{t2}$.

The cost is based on the angle between both normal of the associated patches (with respect to the orientation of the association): ψ_1 for the first pair of patches (P_{v_1}, P_{t_1}) and ψ_2 for the second (P_{v_2}, P_{t_2}). The relative orientation between the one of the two pair of patches is represented on Fig. 5.9. If both pairs of normal are aligned, the angle should be null and the cost should be high. If one of the 2 angles is high, the association should be penalized.

However, each normal is expressed in a local basis similar for both pinch (virtual and tangible). In that regard, a new basis is made with the pinch pose's axis v , the principal component u projected in the orthogonal plan of v , u_p , and the third vector to complete the basis $v \times u_p$. We then have:

$$\psi_1 = \arccos(\vec{n}_{v_1} \cdot \vec{n}_{t_1}) \text{ and } \psi_2 = \arccos(\vec{n}_{v_2} \cdot \vec{n}_{t_2})$$

To compute the cost of this criterion, we use σ_ψ^2 as the variance of the patch parallelism. The cost function is then:

$$P_{patchTilt} = \exp\left(-\frac{\psi_1^2 + \psi_2^2}{2\sigma_\psi^2}\right)$$

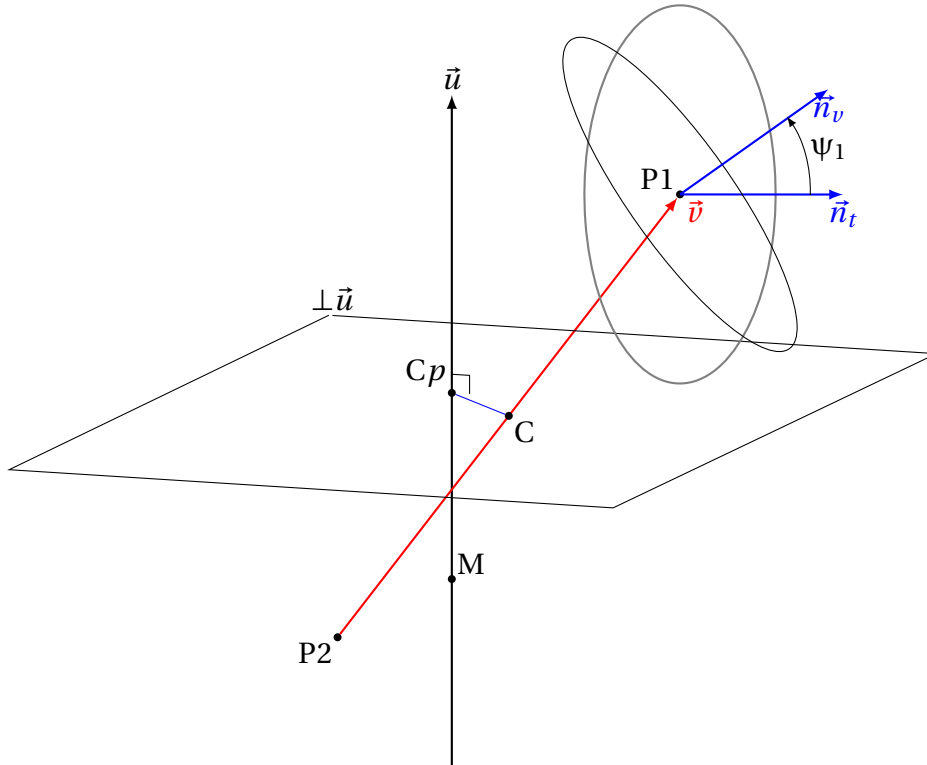


Figure 5.9: Difference of orientation between two patch registered in the same local basis.

5.1.2.5 Fifth criterion: Patch curvature

This criterion is also a patch-related criterion. When associating two pinch poses, both pair of patches should have similar curvatures on the two principal directions of curvature. Moreover, the orientation difference between each Monge basis [228] should be low enough so the direction of curvature will be almost aligned after registration. First, we compare both curvatures of each pair: k_{v_i}' with k_{t_i}' through $\Delta k_i' = k_{v_i}' - k_{t_i}'$, k_{v_i}'' with k_{t_i}'' through

$\Delta k_i'' = k_{v_i}'' - k_{t_i}''$ (with $i \in \{1, 2\}$). These 4 differences provide us the first 4 terms of the cost function for this criterion:

$$P_{\Delta k_i'} = \exp\left(-\frac{\Delta k_i'^2}{2\sigma_k^2}\right) \text{ with } i \in \{1, 2\}$$

$$P_{\Delta k_i''} = \exp\left(-\frac{\Delta k_i''^2}{2\sigma_k^2}\right) \text{ with } i \in \{1, 2\}$$

Furthermore, the difference of orientation between the principal directions of curvature of the two patches can be obtained by computing the angle α_i between \vec{d}_{v_i}' and \vec{d}_{t_i}' , leading to:

$$P_{\Delta\alpha_i} = \exp\left(\frac{\alpha_i^2}{2\sigma_\alpha^2}\right) \text{ with } i \in \{1; 2\}$$

Similarly to the patch orientation, these angles hold meaning only if both vectors are projected on the local basis linked to the pinch axis.

However, within a given patch i , if k_i' and k_i'' have close values, the described paraboloid is almost of revolution (be it a bump or a hole), meaning that the direction of the principal curvature \vec{d}_i' holds little importance as the user will not be able to perceive any direction of curvature.

The same goes if both curvatures have low values. In that case the patch is almost flat, be it a hyperbolic, elliptical or cylinder paraboloid. The orientation of the curvature will not be perceived either by the user. In that case, an error of orientation of a pair should not worsen the score of the cost function. We propose to weigh this angular difference according to the curvature value: if the curvatures of a patch are almost similar or null, then the weight w_{patch_i} should go down to zero as the orientation holds little importance. If either one of two patches (real and virtual) have a non-relevant curvature orientation, it should not impact the second one, so we add their contributions:

$$\frac{\alpha_i^2}{2\sigma_\alpha^2} \times \frac{w_{patch_t} + w_{patch_v}}{2} = \frac{\alpha_i^2}{2\sigma_\alpha^2} \times \frac{g(k_{t_i}', k_{t_i}'') + g(k_{v_i}', k_{v_i}'')}{2}$$

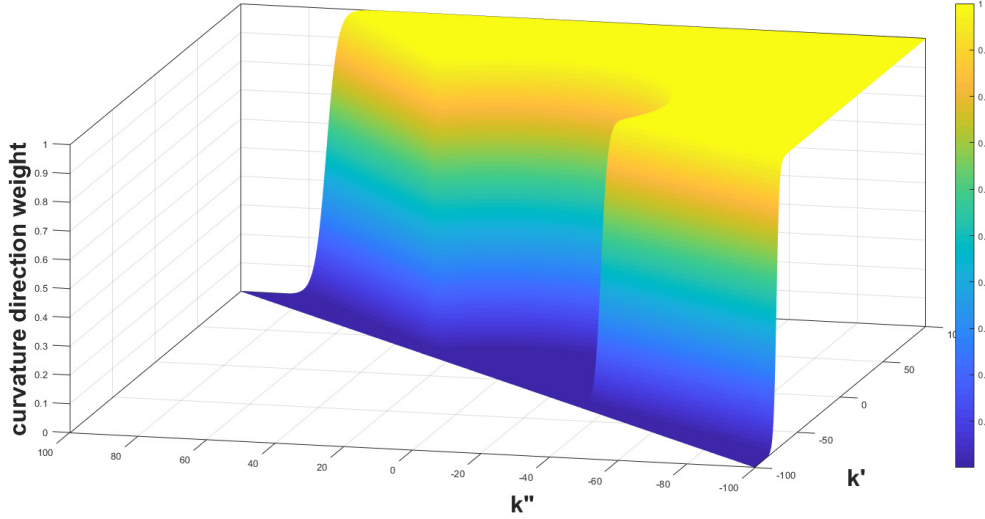
The function $g(\cdot)$ should weigh 1 whenever the orientation hold importance, and 0 otherwise. As already said, there are 2 cases where the weight needs to be pulled down to zero. First, when the paraboloid is of revolution (the 2 blue stripes in Fig. 5.10), which will be considered in a subfunction $g_1(\cdot)$. Second, when the paraboloid is almost flat (the circular blue part in the center in Fig. 5.10), which will be considered in a subfunction $g_2(\cdot)$. $g(\cdot)$ is then the product of these two factors:

$$g(k_{t_i}', k_{t_i}'') = g_1(k_{t_i}', k_{t_i}'') \times g_2(k_{t_i}', k_{t_i}'') \text{ resp. for } k_v$$

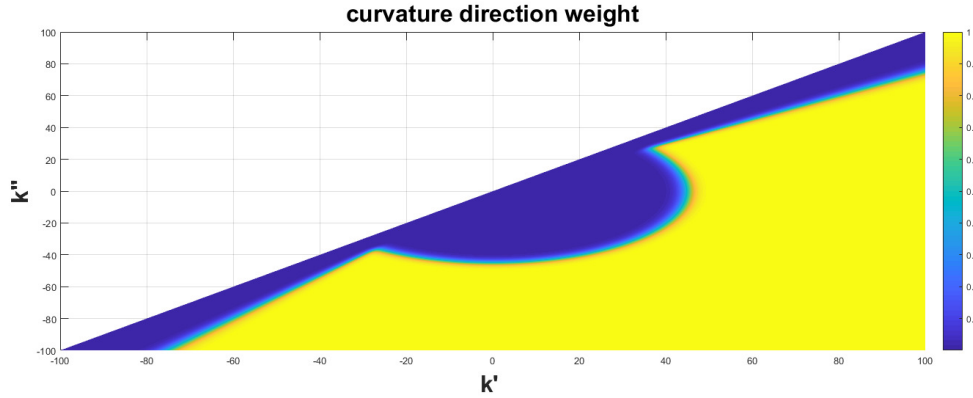
Revolution paraboloid: $g_1(\cdot)$ If $k_{t_i}' \geq k_{t_i}'' > 0$, $\frac{k_{t_i}''}{k_{t_i}'} \in]0, 1]$: both curvatures are similar when $\frac{k_{t_i}''}{k_{t_i}'}$ is close to 1 (resp. for k_v).

Similarly, if $0 > k_{t_i}' \geq k_{t_i}''$, $\frac{k_{t_i}'}{k_{t_i}''} \in]0, 1]$: both curvatures are similar, when $\frac{k_{t_i}'}{k_{t_i}''}$ is close to 1 (resp. for k_v).

In these two cases, as it is a paraboloid of revolution the weighting is close to 0. Otherwise, both curvatures have different sign and the paraboloid is a saddle. Thus,



(a) 3D view.



(b) Top view.

Figure 5.10: Function $g(\cdot)$: weight orientation of patch curvatures. Blue area, the direction of the main curvatures do not matter, the weight is zero. However, the weight is 1 on the yellow area since user can feel the direction. Since $k' > k''$ by definition, half of the space is not defined.

the corresponding weighting is close to 1 to take the relative orientation into account. As each ratio variate between 0 and 1, the weight should be going from 1 to 0. Thus, to ensure a continuous transition, $g_1(\cdot)$ is computed as follow:

$$g_1(k_{t_i}', k_{t_i}'') = \begin{cases} \frac{1}{1 + \exp\left(c_1 \left(\frac{k_{t_i}''}{k_{t_i}'} - c_0\right)\right)} & \text{if } k_{t_i}' \geq k_{t_i}'' > 0 \\ \frac{1}{1 + \exp\left(c_1 \left(\frac{k_{t_i}'}{k_{t_i}''} - c_0\right)\right)} & \text{if } 0 > k_{t_i}' \geq k_{t_i}'' \text{ resp. for } k_v \\ 1 & \text{otherwise} \end{cases}$$

c_0 and c_1 can be chosen to adjust the range of variation and the slope (e.g. 0.75 and 60).

Flat paraboloid: $g_2(\cdot)$ If $|k_{t_i}'|$ and $|k_{t_i}''|$ are close to zero (resp. for k_v), the patch is almost flat. Thus, the weighting should be close to 0 with:

$$g_2(k_{t_i}', k_{t_i}'') = \frac{1}{1 + \exp\left(-c_2(k_{t_i}''^2 + k_{t_i}'^2 - k_{t_{th}}^2)\right)} \text{ resp. for } k_v$$

k_{th} can set the radius into which we want to have a low gain while c_2 enables to control the variation rate of this weight (ex: 45 and 0.01). The resulting weight function $g(k_{t_i}', k_{t_i}'') = g_1(k_{t_i}', k_{t_i}'') \times g_2(k_{t_i}', k_{t_i}'')$ is visible on Fig. 5.10. The resulting cost for the angles is then:

$$P_{\Delta\alpha_i} = \exp\left(\frac{\alpha_i^2}{2\sigma_\alpha^2} \times \frac{g(k_{t_i}', k_{t_i}'') + g(k_{v_i}', k_{v_i}'')}{2}\right)$$

Finally, we obtain the following cost function for this criterion:

$$\begin{aligned} P_{curvature} &= P_{\Delta k_1'} \times P_{\Delta k_2'} \times P_{\Delta k_1''} \times P_{\Delta k_2''} \times P_{\Delta\alpha_1} \times P_{\Delta\alpha_2} \\ &= \exp\left(-\frac{\Delta k_1'^2 + \Delta k_2'^2 + \Delta k_1''^2 + \Delta k_2''^2}{2\sigma_k^2}\right) \\ &\quad - \sum_{i=1}^2 \frac{\alpha_i^2}{2\sigma_\alpha^2} \times \frac{(g(k_{t_i}', k_{t_i}'') + g(k_{v_i}', k_{v_i}''))}{2} \end{aligned}$$

5.1.3 Algorithm Implementation

The algorithm should generate possible registration between TOs and VOs, which mean, find pinch poses on the objects and rank the association between them using the cost function described above. Assuming we only have the mesh of the tangible and virtual objects at the beginning, the method follow 5 successive steps:

- Computing the global properties of the objects.
- Generating patches and compute their properties.
- Generating pinch poses and compute their properties.
- Computing the cost for each pinch poses pairs between a VO and a TO.
- Extracting the registration with highest score.

All the mesh processing was done using the CGAL library. A suggested generation of pinch poses is presented in Fig. 5.11.

5.1.3.1 Step #1: Computation of General Mesh Properties

The first step of the algorithm is to compute the general mesh properties for every object which will be needed later to get all the patches and pinches' properties:

- The principal component, which will serves as the main axis along which the pinches will be organized. It is computed under the assumption that the volume of the object has an uniform density.
- The normal to the mesh for each vertex oriented toward the outside of the mesh.
- The local curvature around each vertex, which will provide the two mains curvature components along their orthogonal directions, as described in Section 5.1.1.
- The ridges of the mesh, which can be defined as a curve along which one of the principal curvatures has an extremum along its curvature line [231]. The first inset of Fig. 5.11 shows an example of computed ridges.

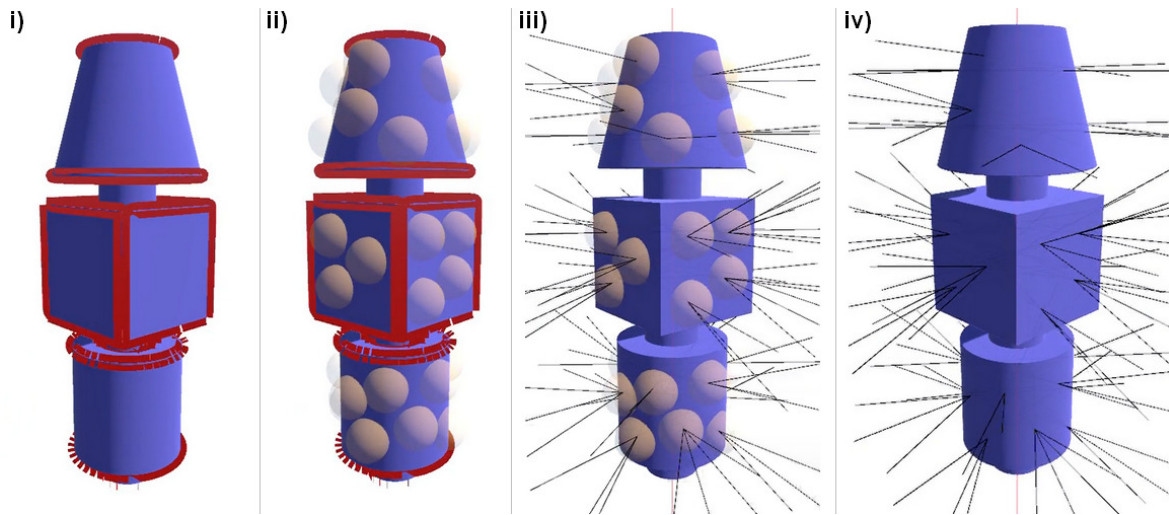


Figure 5.11: Suggested generation on valid pinch poses. i) computing ridges in red, ii) randomly generating non overlapping patches represented by transparent spheres, iii) connecting two patches generates a pinch represented by a black line, iv) keeping only the valid pinches in black in the end.

5.1.3.2 Step #2: Patch Generation

The second step is to find suitable contact locations on the object which could be used to create pinch poses. Any ridges or edges should be avoided as they provide complex tactile information which can easily break the association (Fig. 5.11-ii).

The idea is to randomly select a point, then gather its vicinity to create a potential patch. By checking several criteria, invalid patches should be removed gradually from the pool of all potential patches which is equal to the number of vertices in the mesh. To avoid endless drawn, we set a maximum number of patches. If the object is too small to reach the maximum number of patches, we also set a maximum number of discarded patches.

For each valid patch, we get its mean normal and its curvature, i.e., the local Monge basis $(\{\vec{n}, \vec{d}', \vec{d}''\})$ and the two main curvature values (k' and k'').

In order to discriminate invalid patches, we apply successively the following criteria:

- **Proximity to ridges:** If a patch is crossed by a ridge, then it is rejected. However, this solution rely on a good detection of ridges and these can be found all around the mesh. If computed with a high enough order [231], each ridge would have a strength and a sharpness value. The sharpness represents how thin the ridge is and how high the difference of both curvatures is. While the strength comes from an integration along the ridge and represents how "long and flat" it is. Only the ridge with higher value of strength and sharpness correspond to the borders and critical area of the mesh, while the lower value could be detected on almost any flat surface. Unfortunately, this detection is highly dependent on the mesh (vertex density, smoothness, etc.) and the thresholds of strength and sharpness are set manually.
- **High curvature value and high estimation error:** Patches with too high curvature values can also be rejected as it could be a small artifact, a corner or a ridge. Moreover, the estimation of the curvature provides the overall error which reflects the quality of the estimation. High errors can be caused by sharp edge, or rough surface. However, a high error can also occur if the patch is around a sharp edge or because the surface has lots of asperities.

- **Non-overlapping patches:** we can prevent patches from overlapping each other simply by rejecting one when it is within range of already existing valid patches. It is possible to allow some partial overlap, however, too much overlap might leave some part of an object without any patch if the maximum number of patches has already been reached.

It is also possible to set the patches manually instead of relying on a random generation. Because of the experimental design of the experiment which will be described in the next section, the patches of all objects were set manually.

5.1.3.3 Step #3: Pinch Generation.

Once the patch and their properties have been obtained, we can use them to create possible pinch poses by pairing them (Fig. 5.11-iii). However some pairs should be discarded, in order to reduce the amount of pinches and to keep only realistic grasps (Fig. 5.11-iv). Thus, we discard potential pinches if they do not fit several criteria, each criterion diminishing the pull of valid pinch poses:

- **Pinch maximum width:** Pinch poses which are too wide to be grasped naturally should be rejected, for example if the pinch width exceeds 6.5cm.
- **Non-slippery contacts:** When holding something with 2 fingers, contact forces have to be within the friction cone for both fingers to avoid any slipping. With only two contact forces, their direction is along the line between both application points. Thus, we can compute both angles between the pinch pose's axis and both patches' normal. If any of the two angles exceeds the apex of the friction cone (e.g., $25^\circ - 30^\circ$), it might slip and the pinch pose is rejected. This criterion also avoids unrealistic grasping where the two patches are on the same side of the object. The real value of the friction coefficient is not necessarily known as it will depend on the surface properties of both the object and the users' skin. However an underestimation of this value will guarantee that they will never slip.
- Pinch which are too tilted from the principal component can also be discarded as we hypothesize that the objects have a prismatic shape.

Having acceptable pinch poses around the object, all of their properties can be computed: the signed distance to the center of mass d , the pinch width w , the pinch tilting ϕ .

5.1.3.4 Step #4: Pinch Comparison.

Having all the needed properties, we can compare them to pair similar pinch poses from the VOs to those from the TOs. When registering them, the TO is fixed in space as it is put on a table, and the VO is positioned in order to superimpose both pinch poses. Both principal components are parallel at all time, as it was an assumption for the pinch parameterization. Hence, two rotations are locked for the VO. Then, we superimposed both projected centers of the two pinch poses, which locks the 3 translations. And finally, both projected pinch axes carried by \vec{v}_{p_v} and \vec{v}_{p_t} are aligned which locks the last rotation around the principal components.

However, there are still 4 different ways to associate 2 pinch poses: the objects can be registered so that:

- u_v and u_t have the same or opposed direction
- v_v and v_t have the same or opposed direction

In other words, the principal component and/or the pinch pose of one object (always virtual for example, since the tangible is fixed in space) can be flipped. The following table highlights the 4 different associations which are coded in a single variable called *association mode*.

mode	\vec{u}	$-\vec{u}$
\vec{v}_p	0	2
$-\vec{v}_p$	1	3

Depending on the mode, some orientations might change, which would then also bring some change to the properties of the pinch pose of the VO which are compared to those of the TO. The changes are shown in the following table:

Mode	0	1	2	3
Distance to M	d_v	d_v	$-d_v$	$-d_v$
Pinch Width	w_v	w_v	w_v	w_v
Pinch tilting	ϕ_v	$-\phi_v$	$-\phi_v$	ϕ_v

As for the patch properties, they do not change with the orientation, but the local basis to compare the various angles need to be computed according to the inversion of one principal component. However, when comparing two pinches, we also compare the patches in pairs. In mode 0 or 1, we compare t_1 with v_1 and respectively t_2 with v_2 (see notation introduced in section 5.1.1). However, when flipping the virtual pinch pose we swap the pairs then compare t_1 with v_2 and respectively t_2 with v_1 . Thus, all the available pinch poses are compared by computing the cost function detailed in Section 5.1.2, in order to evaluate the possible registration.

5.1.3.5 Step #5: Best Match Extraction.

At the end of the previous step we then have the results of the comparison of all possible pinch poses. Keeping the pair with the highest score should provide a correct matching between the tangible and the virtual.

However, we are not limited to choose the best matching pose only to have a one-to-one mapping between tangible and virtual objects. The proposed algorithm is quite flexible and can be applied to a larger number of objects. There can be a one-to-many registration, alternatively registering various virtual object to the same tangible. Considering an experimental setup composed of n tangible objects and m virtual ones, with $m \gg n$. Our algorithm can analyze all the scene at once and find the best pinch for each virtual object using the available set of tangible ones.

5.2 User Study

We conducted a preliminary user study to evaluate the users' perception when they are manipulating a tangible object (TO) and visualizing virtual objects (VO) that do not always match the manipulated tangible object. The participants were able to manipulate three basic tangible shapes: a cone, a cube and a cylinder (see Table 5.2). The virtual objects were designed as a combination of these three different shapes. The participants were asked to rate the similarity between the tangible manipulated object and the virtual seen object.

The suggested grasping positions of our approach were compared to grasping positions suggested by a global registration of the tangible and the virtual objects.

The main hypotheses of our user experiment are:

- H1: when the tangible object and the virtual object are the same, the user perceives the objects as similar.
- H2: when the tangible object and the virtual object are different, the pinching positions suggested by our approach improves the perceived similarity between the two objects.
- H3: whether the user is just touching the tangible object or lifting it, the perceived similarity remains identical.

5.2.1 Experiment Description

5.2.1.1 Participants

Twelve participants (10 males, 2 females, $M = 26.67$, $SD = 5.31$) took part in the experiment, all of whom were right-handed.

5.2.1.2 Experimental Apparatus

The setup is shown in Fig. 5.12. Users wore an HTC Vive headset which displays the virtual scene with the virtual objects superimposed with the tangible one. A Bonita Vicon system combined with the Blade software was used to track their thumb and index fingers, at the back of which we positioned 3D-printed attachments holding a constellation of markers. We made sure that the pad of each finger remained free from the attachments, and to ensure that these did not move we secured them with wig tape. Using this tracking system, participants were able to control index and thumb avatars of their fingers in the virtual environment. This minimalist hand representation [224] has been chosen to avoid occluding the virtual object from the user's point of view (see inset of Fig. 5.12). The virtual scene is composed of an instruction panel and a pedestal onto which one VO is standing.

We chose not to track the tangible object not to affect its weight distribution by adding a constellation of markers which would need to be far enough from the top of the object as it could create occlusion with the markers of the fingers. To know its position, we built a 3D-printed support, fixed to the table, which kept the tangible object at a known location. To make sure that the TO was correctly replaced at the beginning of each trial, the support and the TO base had complementary shapes and magnets. This support also served as a reference point in the real environment. The virtual scene was then centered on this point using a Vive Tracker. Since Blade had also its own reference frame, we calibrated it using a third constellation. Therefore, the position of the TO was always known, standing on the calibrated support, while the VO was generated onto the TO at the beginning of the interaction. The virtual fingers were calibrated through the tracked constellations by touching a tangible prop at a specific known location. This allowed us to know where the contact between the fingers and the TO was with respect to the reference. In this way, we ensured that, whenever users were touching the TO, they were also touching the VO accordingly. This also resulted in the VO always moving together with the TO. This tracking solution is further detailed in Appendix B.

Visual feedback was used to guide users toward the target grasping pinches. Two virtual green cones indicated where the user was supposed to grasp the virtual (and tangible)

objects. This pose was generated following the algorithm presented in Section 5.1. Visual feedback was also used to let participants know when they arrived close enough to the targeted pinch: whenever the users' fingers were closer than 5 mm to their target pinch location and their orientation error w.r.t. the pinch main axis was lower than 14° , the grasping was considered successful and the VO turned red [232]. Holding this position for 1 s validated the pinch. This visual feedback was needed as the system did not have access to the state of the tangible contact: once the user was close enough and not moving anymore, it assessed that the tangible was actually hold and would notify the users that they can start lifting it. Although users had to adjust themselves to the system in order to begin the trials, they also had to assess the objects once they were grasped and independently to the grasping procedure. A better solution to this issue is tackled in Chapter 6.



Figure 5.12: Setup of the experiment. Insets show the virtual environment during the task.

5.2.1.3 Procedure

During the experiment, participants were asked to perform two tasks: a static task, where they simply grasped the objects; and a dynamic task, where they grasped and lifted the objects.

First, participants were asked to grasp the objects as indicated on the screen, matching their two virtual fingers with the pose suggested by the algorithm via the green virtual cones (see first inset of Fig. 5.12). When the pinch is validated, the object either turns green to confirm the end of the task (static task), or it turns blue to instruct the user to lift it (dynamic task). In this latter case, participants were asked to lift the tangible object up 10 cm and tilt it on each side. After that, participants were asked to put the object down and the task was considered completed. Thanks to the magnets on the support, it was easy to put back the tangible object on its original location. At the end of each trial, participants were asked to answer the following question: “How much does the tangible

object correspond to the virtual one?" (see second inset of Fig. 5.12) using a 7-item Likert scale.

The experiment started with an explanation of the procedure and the signature of the consent form. Then, a calibration of the virtual fingers was performed for each participant. Participants went first through all the trials of the static task, and then through the ones of the dynamic task. Before each task, 3 random practice trials were performed to ensure that the user had understood the interaction, the task, and that the calibration was done properly. For each task, participants went through all the pinch pose registrations of the TO with the 6 VOs, either with or without our algorithm, in a random order. Since the algorithm allows a translation along the principal component axis, some of the computed registrations brought the VOs to be partially below or above the TO. The height of the pedestal was modified accordingly. The experimenter also faked the change of the tangible object between each trial.

5.2.1.4 Design

We chose a unique TO composed of three basic shapes: a cone, a cube, and a cylinder (see the representation in Table 5.2). The three shapes have the same height and the same width in the middle. The VOs correspond to a combination of these three different shapes. As a result, we ended up with 6 VOs (see Table 5.2).

In this experiment, we only considered three possible pinch poses on the TO, located at the middle of each shape (see Table 5.2, for their localization). Then, we used our algorithm to compute the best match between these poses and one potential pinch pose for each VO. We decided to take a set of 17 potential valid pinch poses per VO among the initial set of infinite pinch poses. The matching positions provided by our algorithm are shown in Table 5.2.

To better evaluate the influence of Criterion #2 (distance to the center of mass) on the suggested pinches, we divided the experiment in two identical parts: a first one where the participant had just to pinch the object (static task), not manipulating the tangible object and thus feeling any inertia, and a second one where the participant had to lift the object (dynamic condition). This order was not counterbalanced since the dynamic task could bring some additional cues about the properties of the tangible object.

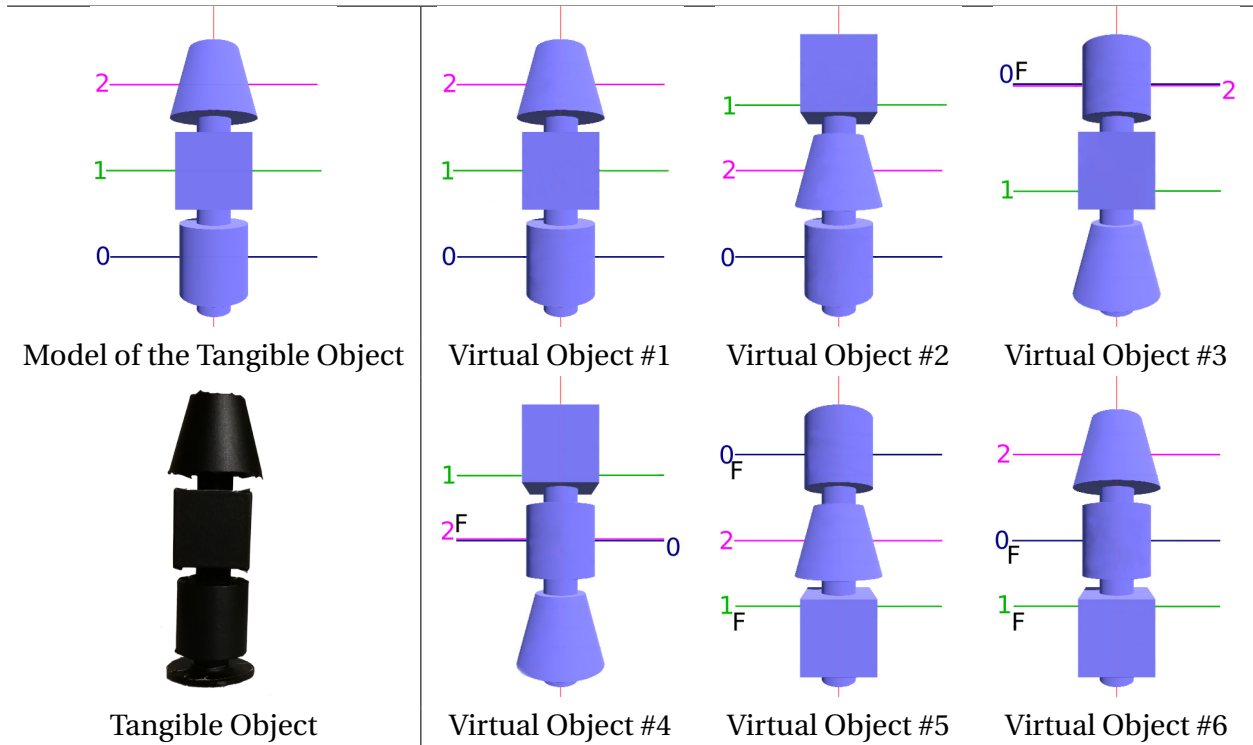
In order to assess the performances of our approach, we chose to compare the registration provided by our algorithm with a reference corresponding to a simple global superimposition of the VO with the TO, i.e., we superimpose the object based on their overall dimension similarity: usually they are aligned based on their height: either aligning the bottom, the top or the middle part of the object. However, as objects are put on tables, it is more common to align their bottom faces.

For each task (static/dynamic), the participants had to evaluate the registration between the three pinch poses on the TO (cone, cube, cylinder) and three pinch poses on the VO (middle of the object for the *Ref* algorithm, generated following the description in Table 5.2 for our algorithm). Thus, for 6 different VOs, we obtained a block of 18 pinch poses \times 2 algorithms = 36 trials. The different poses were presented in a randomized order within a block. The participant had to do each block three times, for a total of 108 trials for a task, and therefore 216 trials in total for the whole experiment, which lasted 1.5 hours.

5.2.2 Conditions

Three conditions are considered in our experimental design:

Table 5.2: Tangible object (left) and the 6 virtual objects (right). All pinch poses are in the frontal plan. The three pinch poses of the TO are: 0 in blue at the middle of the cylinder, 1 in green at the middle of the cube and 2 in magenta at the middle of the cone. The associated pinch poses computed by our algorithm on each virtual object are displayed with the same color code. The "F" means that the registration was performed by flipping the VO upside down.



- **C1** is the registration algorithm between the TO and the VO: the algorithm of reference *Ref* corresponds to a superimposition of both objects, without using any information on the object properties; our algorithm is using the cost function described in Section 5.1 for finding the matching pose on the VO, given a pose on the TO.
- **C2** is the shape manipulated on the TO: cone, cube or cylinder (see Table 5.2).
- **C3** corresponds to the virtual object. The 6 VOs are represented in Table 5.2.

5.2.3 Collected Data

For each trial, we collected the participant's answers on the correspondence between the VO and the TO using a 7-item Likert scale. Participants also completed a subjective questionnaire at the end of the experiment, following a 7-item Likert scale:

- Q1: It felt like **grabbing** a real object.
- Q2: It felt like **lifting** a real object.
- Q3: It was **hard to grab** the object at the right location.
- Q4: It felt like I was **seeing my own fingertips**.
- Q5: The **shape** allows me to tell if both objects correspond to each other.
- Q6: The **curvature** allows me to tell if both objects correspond to each other.

- Q7: The **width** allows me to tell if both objects correspond to each other.
- Q8: The **perceived inertia** allows me to tell if both objects correspond to each other.
- Q9: I felt **tired** at the end.
- Q10: It felt as if the displayed objects were not all positioned at the **same height**.

We also asked them the following question at the end of the questionnaire “How many different tangible objects did you interact with in the experiment?”.

5.2.4 Results

5.2.4.1 Static Task

The answers of the participants concerning their perceived correspondence between the TO and the VOs are summarized in Table 5.3.

To study the perceived correspondence between the TO and the VO when they are identical, we first analyzed the ratings for the answers concerning VO #1 only (first column of the table). We combined answers from both algorithms since the pinch poses are identical for VO #1. We found a significant effect of the shape using a linear mixed model on the ratings ($F(2,202) = 10.02, p < 0.001$). We performed a post-hoc analysis on the condition **C2** using a Tukey test. Bonferroni correction was used for all post-hoc analysis. We found that the correspondence between the cones of the TO and the VO was less perceived than for the cube ($Z = 4.4, p < 0.001$) and for the cylinder ($Z = 2.93, p = 0.009$). We did not find any significant effect between the cube and the cylinder for VO #1.

To study the perceived correspondence in the general case, we used a linear mixed model on the collected data to model the probability of perceived correspondence with respect to the three independent variables **C1**, **C2** and **C3** defined in the experimental design. The participants are considered as a random effect in the model. We performed an analysis of variance of the model and we found a significant effect for all conditions **C1** ($F = (1, 1274) = 466.48, p < 0.001$), **C2** ($F = (2, 1274) = 30.39, p < 0.001$), and **C3** ($F = (5, 1274) = 51.62, p < 0.001$) as well as an interaction between **C1** and **C2** ($F = (2, 1274) = 17.83, p < 0.001$).

We performed a post-hoc analysis on **C1** using a pairwise comparison and we found that the participants rated higher the correspondence between TO and VO for the poses proposed by our algorithm compared to the reference algorithm ($Z = 21.6, p < 0.001$), whatever the object ($p < 0.001$ for all with $Z = -8.06$ for the cone, $Z = -16.47$ for the cube and $Z = -12.88$ for the cylinder). We performed also a post-hoc analysis on **C2** knowing **C1** using a pairwise comparison. For the reference algorithm, we found that the correspondence between the cylinder of the TO and the corresponding VO was rated higher than the cone ($Z = 2.87, p = 0.01$) and the cube ($Z = 3.08, p = 0.005$). For our algorithm, the participants rated lower the correspondence between the cone of the TO and the corresponding pose on the VO compared to the cube ($Z = -8.21, p < 0.001$) and the cylinder ($Z = -7.70, p < 0.001$). Finally, we performed also a post-hoc analysis on **C3** and we found that VO #1 was rated higher than the other VOs ($p < 0.001$ for each VO) and then VO #4 was rated lower than the other VOs ($p < 0.001$ for each VO, except with VO #5 with $p = 0.007$). We found also that VO #2 was rated higher than VO #5 ($p = 0.04$).

5.2.4.2 Dynamic Task

The answers of the participants concerning their perceived correspondence between the TO and the VOs are summarized in Table 5.4.

Table 5.3: Ratings (Means and SD) for the static task using a 7-item Likert scale on the correspondence between the TO (first column, three shapes: cone, cube and cylinder) and the six different VOs, for the two compared algorithms (Reference and our approach). Ratings are in bold when TO shape and VO shape were identical.

	VO #1	VO #2	VO #3	VO #4	VO #5	VO #6
Cone <i>Ref</i>	6.06 (1.09)	2.19 (1.28)	3.47 (1.48)	2.11 (1.33)	3.08 (1.73)	5.97 (1.00)
Cone <i>Ours</i>	6.02 (1.03)	5.86 (1.13)	3.22 (1.61)	3.17 (1.52)	6.03 (1.16)	6.06 (1.22)
Cube <i>Ref</i>	6.58 (0.55)	2.44 (1.78)	6.53 (0.69)	2.47 (1.90)	2.28 (1.63)	2.39 (1.91)
Cube <i>Ours</i>	6.50 (0.56)	6.28 (0.91)	6.39 (0.93)	6.28 (0.81)	6.19 (0.86)	6.33 (0.76)
Cyl. <i>Ref</i>	6.31 (0.89)	6.39 (0.69)	3.50 (1.28)	3.81 (1.55)	2.78 (1.82)	2.78 (1.85)
Cyl. <i>Ours</i>	6.44 (0.84)	6.47 (0.84)	6.44 (0.69)	5.89 (1.06)	6.56 (0.56)	5.69 (1.37)

To study the perceived correspondence between the TO and the VO when they are identical, we first analyzed the ratings for the answers concerning VO #1 only. We combined answers from both algorithms since the pinch poses are identical for VO #1. We found a significant effect of the shape using a linear mixed model on the ratings ($F(2, 202) = 5.18$, $p = 0.006$). We performed a post-hoc analysis on the condition **C2** using a Tukey test and we found that the correspondence between the cones of the TO and the VO was less perceived than for the cylinder ($Z = 3.15$, $p = 0.004$). We did not find any significant effect between the cube and the cylinder as well as between the cube and the cone for VO #1.

As for the static task, we used a linear mixed model on the collected data to model the probability of perceived correspondence with respect to the three independent variables **C1**, **C2** and **C3** defined in the experimental design for the general case. We performed an analysis of variance of the model and we found also a significant effect for all conditions **C1** ($F = (1, 1274) = 422.07$, $p < 0.001$), **C2** ($F = (2, 1274) = 48.76$, $p < 0.001$), and **C3** ($F = (5, 1274) = 61.09$, $p < 0.001$) as well as an interaction between **C1** and **C2** ($F = (2, 1274) = 29.68$, $p < 0.001$). We performed a post-hoc analysis on **C1** using a pairwise comparison and we found that the participants rated higher the correspondence between TO and VO for the poses proposed by our algorithm compared to the reference algorithm ($Z = 20.54$, $p < 0.001$), whatever the object ($p < 0.001$ for all with $Z = 5.70$ for the cone, $Z = 16.03$ for the cube and $Z = 13.85$ for the cylinder). We performed also a post-hoc analysis on **C2** knowing **C1** using a pairwise comparison. For the reference algorithm, we found that the correspondence between the cylinder of the TO and the corresponding VO was rated higher than the cone ($Z = 2.43$, $p = 0.04$). For our algorithm, the participants rated lower the correspondence between the cone of the TO and the corresponding pose on the VO compared to the cube ($Z = -10.62$, $p < 0.001$) and the cylinder ($Z = -10.59$, $p < 0.001$). Finally, we performed also a post-hoc analysis on **C3** and we found that VO #1 was rated higher than the other VOs ($p < 0.001$ for each VO) and then VO #4 was rated lower than the other VOs ($p < 0.001$ for each VO).

Table 5.4: Ratings (Means and SD) for the dynamic task using a 7-item Likert scale on the correspondence between the TO (first column, three shapes: cone, cube and cylinder) and the six different VOs, for the two compared algorithms (Reference and our approach). Ratings are in bold when TO shape and VO shape were identical.

	VO #1	VO #2	VO #3	VO #4	VO #5	VO #6
Cone <i>Ref</i>	5.97 (1.30)	2.22 (1.48)	3.11 (1.41)	2.28 (1.37)	2.89 (1.51)	6.19 (0.95)
Cone <i>Ours</i>	5.92 (1.18)	5.03 (1.32)	3.06 (1.47)	2.42 (1.20)	5.42 (1.23)	5.92 (1.30)
Cube <i>Ref</i>	6.28 (1.03)	2.42 (1.50)	6.61 (0.60)	2.50 (1.50)	2.44 (1.48)	2.67 (1.79)
Cube <i>Ours</i>	6.25 (0.91)	6.33 (0.83)	6.44 (0.77)	6.08 (0.81)	6.14 (0.99)	5.97 (1.00)
Cyl. <i>Ref</i>	6.25 (0.84)	6.17 (0.97)	3.42 (1.38)	3.28 (1.49)	2.89 (1.56)	2.83 (1.40)
Cyl. <i>Ours</i>	6.58 (0.55)	6.47 (0.81)	6.28 (1.00)	5.69 (1.31)	6.39 (0.80)	5.78 (1.42)

5.2.4.3 Questionnaire

Regarding Q1 and Q2, most of the participants felt like grabbing ($M = 5.67, SD = 0.75$) or lifting ($M = 5.58 ; SD = 0.86$) the real object during the experiment. Regarding the difficulty to grab the object (Q3), the feeling is split between the participants ($M = 4.00, SD = 1.35$) with rates from 2 (2 participants) to 6 (2 participants). Participants mostly felt that they were seeing their own fingertips (Q4, $M = 5.17, SD = 1.77$). Fig. 5.13 shows the answers to our subjective questionnaire for the questions regarding the properties of the object (Q5 to Q8). Among the different properties proposed for rating to the participants, they mostly felt that the shape allowed them to tell if both objects correspond to each other (Q5, $M = 5.92, SD = 1.03$) as well as the curvature (Q6, $M = 5.42, SD = 1.44$). The answers were more mitigated for width (Q7, $M = 3.83, SD = 1.77$) and inertia (Q8, $M = 4.75, SD = 1.88$). Finally, most of the participants reported overall medium levels of fatigue (Q9, $M = 5.33; SD = 1.37$). Most of the them also reported the difference of height between the displayed objects (Q10, $M = 5.33, SD = 1.80$). The answer to the question regarding the number of different tangible objects they were interacting with was between 2 to 20 ($M = 7.5, SD = 5.34$).

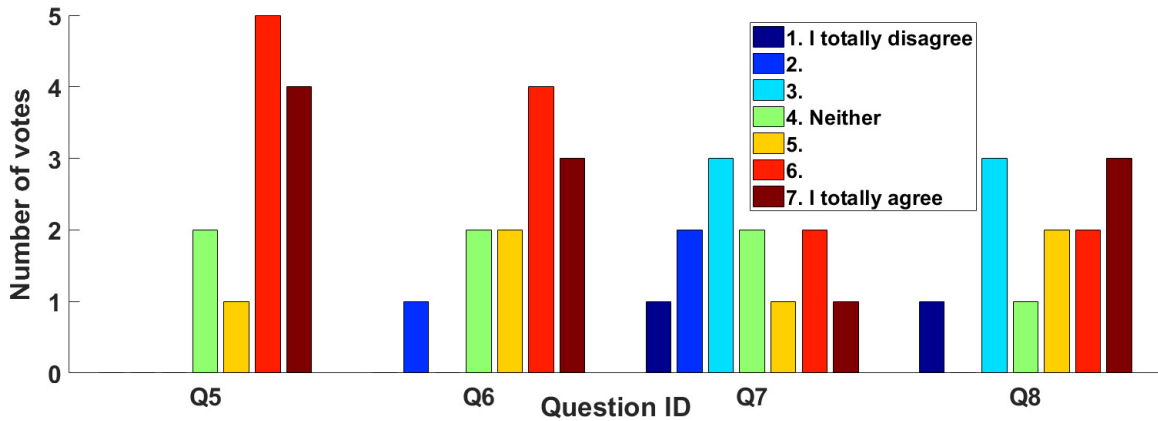


Figure 5.13: Bar-graph of the answers for questions 5 to 8 concerning the properties of the object that helped the participants to find a correspondence between the TO and the VO. Q5: shape, Q6: curvature, Q7: width, Q8: perceived inertia.

5.3 Discussion

In this Chapter, we propose to use few tangible objects to enable 3D interactions with multiple virtual ones. To do so, we devised an algorithm which performs an exhaustive search on all the feasible pinching poses on the available objects, to find the best match in terms of haptic sensations. The algorithm is designed to provide the best available match between what the user sees in the virtual environment and what he feels when grasping the tangible object.

To evaluate the effectiveness of our approach, we carried out a user study. Twelve participants were asked to grasp objects of different shapes in virtual reality, all rendered by the same tangible, and evaluate how much the former corresponds to the latter. We made three hypotheses, described at the beginning of Section 5.2. First, we wanted to understand if participants are actually able to recognize when they are touching the same object in the real and virtual environments (H1). Results show that, indeed, they can. Values in bold in Tables 5.3 and 5.4 show users' ratings when provided with the same tangible and virtual shape. As expected, in both conditions (our algorithm and simple superimposition) ratings are very high. The second question we raised is whether, when tangible and virtual objects are different, using our approach improves the perceived grasping sensations with respect to using a standard superimposition (H2). Ratings show that our algorithm was able to well combine the considered haptic features and find convincing pinches between the given tangible and virtual objects. We registered improvements in ratings of 48.8% and 45.1% with respect to a standard superimposition matching technique in the case of static and dynamic grasping tasks, respectively. From Tables 5.3 and 5.4 we can see that ratings when using our algorithm are significantly closer to the ground-truth than when using simple superimposition. We also hypothesized (H3) that the above results hold when grasping an object with no subsequent motion (static task) as well as when lifting it up (dynamic task). Results show indeed little difference between the two tasks. At the end of the experiment, participants were also asked to guess how many tangible objects were used during the trials. Answers spanned from 2 to 20, with an average of 7.5 objects, and no one guessed that only one tangible object was used!

Thus, our algorithm showed promising perspectives to associate two compatible pinches on two different objects. Although the cost function considers each of the component criteria as equally important some of these criteria are likely to have greater perceptual significance than others. It would be interesting to study which one should be prioritized

in order to give it a higher weight in the cost function. However, as already said, weighting is mathematically equivalent to adjusting the variance of each criteria. Giving a higher priority to a criterion is the same as giving it a small variance in order to reduce the allowed discrepancy.

A drawback of our experiment is that we did not assess the full capability of the algorithm. With our experimental design, we needed to control the grasping location as to avoid bias. Hence, we did not assess the capability of the algorithm to automatically generate grasping poses. It would be interesting to do so in a future experiment. However, to avoid bias due to the random generation, we would need to have a large enough pool of participants doing a larger number of trials. Similarly, we used basic shape to compose prismatic objects and it would be interesting to evaluate the algorithm against non-trivial shapes. As long as the objects are compatible with the pinch description we used (see section 5.1), the algorithm should still be able to perform correctly: it will find patches, create possible pinches and then extract their properties to compare them and provide a score. However, to evaluate the algorithm against non-trivial shapes, we would need to find a suitable and representative pool of objects which would present interesting properties and provide results without bias due to the object set itself.

Although we used a state-of-the-art tracking system, it is not easy to consistently and robustly track the fingertips at all time, and any discrepancy between the motion of the user's fingers and the virtual avatar will degrade the experience. However, when the same shapes were registered between the TO and VO, the experiment still gave the best scoring, highlighting the fact that the tracking issues did not hinder the perception of the users.

5.4 Conclusion

We presented an innovative haptic approach which enables the use of a reduced number of tangible objects for interacting with multiple different virtual ones, by *pairing different parts of the same tangible to different virtual elements*. The need for such an approach stems from two conflicting requirements. To achieve a compelling illusion, there should be a good correspondence between what users see in the virtual environment and what they touch in the real world. In other words, the haptic features of the tangible and virtual objects should match. However, this calls for the creation of tangible replicas of all the virtual objects in the scene – which is often not possible. Therefore, it is important to devise approaches maximizing tangible/virtual objects matching, even when these are different. The proposed algorithm addresses this problem. It analyzes the provided tangible and virtual objects to find the best pinch in terms of matching haptic sensations. It starts by identifying several suitable pinching poses on all objects. Then, for each pose, it evaluates a series of haptically-salient characteristics. Next, it identifies the two most similar pinching poses, one on a tangible and one on a virtual object. Finally, it highlights the chosen pose, which provides the best matching sensation between what users see and touch.

We tested our approach in a user study. Twelve participants were asked to grasp different virtual objects, all rendered by the same tangible one. For every virtual object, our algorithm found the best pinching match on the tangible one, and guided the participant toward that grasp. Results show that our algorithm was able to well combine several haptically-salient object features to find corresponding pinches between the given tangible and virtual objects. At the end of the experiment, participants were also asked to guess how many tangible objects were used during the experiment. No one guessed that we used only one, proof of a convincing experience.

This work then opens several interesting prospects: we could scan the real environment

to exploit the real physical surroundings of the user. Our technique would then enable to provide precise pinching sensations. However, of course, this raises the challenge of real-time tracking algorithms. Moreover, using our algorithm, we could analyze the haptic properties of a given virtual scene, and we could try to automatically generate and 3D print, one (or more), *universal* tangible objects able to provide the best possible match in terms of haptic sensations.

Finally, although the results of our user study are promising and statistically significant, we believe that more experiments could be conducted, considering more objects, different tasks, different contexts.

Part II

Improving the Registration between Tangibles and Virtual Objects

Chapter 6

Capacitive Sensing for Improving Contact Rendering with Tangible Objects in VR

Sommaire

6.1 Capacitive Sensing for Tangibles in Virtual Reality	130
6.1.1 Context of Application	130
6.1.2 Prior Capacitive Sensing Applications	131
6.1.3 Motivation: Embedding Tangibles with Proximity Capacitive Sensing	132
6.2 Method	134
6.2.1 Capacitive Sensitivity to Human Hand	134
6.2.2 Apparatus	135
6.2.3 Capacitive Sensing	135
6.2.3.1 Measurement Principle	136
6.2.3.2 Technical aspects	139
6.2.4 Signal Characterization	141
6.2.5 Visuohaptic Retargeting	141
6.3 User Study	144
6.3.1 Experimental Methods	144
6.3.1.1 Participants	144
6.3.1.2 Experimental setup	144
6.3.1.3 Experimental procedure	145
6.3.1.4 Experimental Design	145
6.3.1.5 Experimental variables	147
6.3.1.6 Collected Data	147
6.3.2 Experimental Results	147
6.4 Discussion	149
6.5 Conclusion	151

As already highlighted in the previous chapters, using tangibles can provide rich and compelling feedback. However, registering a tangible and a virtual object together often leads to misplacements and mismatches: being tracked or placed at a calibrated position, the tangible might not be correctly registered to the virtual object due to tracking inaccuracy. Moreover, the tracking and reconstruction of the virtual hand can also induce errors between the user's hand and the virtual hand's relative configuration. Furthermore, there can be morphological discrepancies between user's hand and the virtual representation, as well as, deliberately introduced discrepancies between the tangible and the virtual object as we did in Chapter 4. All of these possible sources of error can aggregate themselves into a resulting error which can hinder the user's immersion as he is touching an object: the user can end-up feeling a tangible contact without touching the virtual object or, inversely, seeing the virtual object being touch without actual feedback.

In this Chapter, we will compensate this small-scale *resulting positioning error* in order to achieve a better *visuohaptic synchronization upon contact* and preserve immersion during contact interaction in VR. We employ one tangible object to provide haptic sensations, which is equipped with capacitive sensors to estimate the general proximity of the user's fingertips to the surface. This information is then used to retarget, *prior to contact*, the finger position obtained from the external optical tracking system, toward the tangible object's surface.

The main contributions of our work can be summarized as follows:

- we propose an innovative approach for enhancing contact rendering in VR when using tangible objects, instrumenting the latter with capacitive sensors;
- we design and showcase a sensor and a visuohaptic interaction technique enabling high contact synchronization between what users see and feel;
- we conduct a user study showing the capability of our combined approach vs. two stand-alone state-of-the-art tracking systems (Vicon and HTC Vive) in improving the VR experience.

In the remainder of this Chapter, we first present the context and motivation of using capacitive sensing coupled with tangibles in VR. Then, we present the method we developed and which is then evaluated in a user study. Finally, the results and outcomes of the technique are discussed.

6.1 Capacitive Sensing for Tangibles in Virtual Reality

6.1.1 Context of Application

Immersive Virtual Reality (VR) must actively engage one's senses, so as to make the user feel truly there in the virtual world [4]. One important facet to achieve this objective remains the *synchronization* of motion and sensory feedback between the human users and their virtual avatars. Whenever one user moves a limb, the same motion should be replicated by the avatar; similarly, whenever the avatar touches a virtual object, the user should feel the same haptic experience. Di Luca et al. [233] recently studied the range of tolerable visuohaptic asynchronies when touching an object. Participants could not reliably detect the asynchrony if haptic feedback was presented less than 50 ms after the view of the contact. The asynchrony tolerated for presenting haptic feedback before the visual one was instead only 15 ms. These results suggest rather stringent requirements for

haptic-enabled VR systems. Achieving this visuohaptic synchronization is also important for the perception of the object's properties. For example, Di Luca et al. [234] showed that a delay in presenting visual and force information introduces a bias in the perception of compliance. Knorlein et al. [235] proved that a similar effect holds also when interacting with virtual objects: delays of haptic feedback resulted in decreased perceived stiffness, while visual delays caused an increase in perceived stiffness. This synchronization has been deemed important also in collaborative and distributed virtual environments [236].

To ensure a good match between the motion of the users with respect to their avatars, commercial VR systems already provide vision-based solutions able to track the headset or a dedicated active prop (e.g., the HTC Vive tracker). Other more advanced approaches consist in tracking a set of markers constellations worn directly by the user (e.g., Vicon and Optitrack systems). However, they require a clear line of sight and their performance significantly degrades in the presence of disruptions, e.g., occlusions, calibration errors, suboptimal light conditions or positioning of the markers.

Ensuring a good match between the haptic stimuli experienced by the virtual avatar and the user is also very challenging. In this respect, a popular approach consists in using tangibles to provide distributed haptic sensations when grasping virtual objects. However, tangible props exacerbate the issues of the above-mentioned commercial tracking systems, making their co-existence rather difficult. Indeed, these limitations will add up with miscalibration, partial tracking and modeling discrepancies of virtual objects (or hand avatar) with their tangible counterparts (or user's hand), leading to a resulting error in the relative positioning between the virtual hand and the virtual object, i.e., a remaining virtual gap or interpenetration upon tangible contact. Thus, breaking the synchronicity of the virtual and tangible contact.

Hence, we developed an approach to track and render contacts with tangible objects in VR, to compensate such relative positioning error, to achieve a better visuohaptic synchronization upon contact and to preserve immersion during contact interaction in VR. Toward this objective, we proposed to instrument a tangible object with capacitive sensors thank to their interesting properties; First, they are sensitive to the human hands, as it has natural capacitive properties, and enable natural hand interaction without intermediary component; Second, covering the surface of the tangible with simple conductive materials, such as thin copper band or conductive paint, is sufficient to turn them into capacitive sensitive electrodes. Lastly, when conditioned properly, capacitive sensors are proximity sensors which can provide an estimation of the general proximity of the user's fingertips to the surface. Thus, we will use the sensor's output to retarget, *prior contact*, the motion obtained from the standard vision tracking system, toward the virtual object's surface.

6.1.2 Prior Capacitive Sensing Applications

Capacitive sensing has been widely use in Human-Computer Interaction as the human body naturally behaves like a capacity [237].

Capacitive sensing can be used to detect whenever a contact occurs with a human part [238, 239]. For example, Hinkely et al. [238] used the simple contact detection to improve mouse and trackball and develop several interaction techniques which only required to know whether or not the user was touching the device. While Sato et al. [239] went further, and developed a method which could characterized the nature of the contact by applying an excitation of varying frequency instead of a fixed one, the Swept Frequency Capacitive Sensing. As each body part will affect the envelope frequency in a different way, they were able to discriminate different body gestures during contact. Honigman et

al. [240], simplified the Swept Frequency Capacitive Sensing method by providing an open source library for Arduino with simplified electronics.

However, capacitive sensing can also provide proximity information by measuring small variation of capacitance [241, 242]. Lü et al. [242] developed a method to measure variation of capacitance from $0pF$ to $700pF$ with high accuracy and resolution. Using a grid of capacitive electrodes makes possible to track a user's finger on a plane, which is nowadays how we interact with most tactile/touch screens [243]. Yu et al. [244] proposed a similar approach to track tangible objects on a capacitive screen, and using active modulation circuits embedded in the tangible objects to encode additional IDs information and to reduce the contact area of the spatial tags.

Lastly, some technical solutions provide combined information: absolute contact information, proximity detection, and a 2D tracking with a grid of electrodes [245, 246, 247]. Rekimoto et al. [245] developed a sensor architecture for making interactive surfaces sensitive to hand and finger gestures. It was constructed by laying a mesh of transmitter/receiver capacitive electrodes on the surface. Similarly, Lee et al. [247] developed a grid of 16×16 electrodes. Each can provide proximity and pressure information, as the layer is flexible and deforms upon contact. In addition, several grids can be assembled together and compose a sensitive skin for robot applications like grasping objects with a robot hands manipulators or avoid obstacles as Novak et al. [246] previously did.

In short, this work came within the scope of the capacitive sensing technologies for human-computer interaction. Similarly to Sato et al. [239], we proposed to instrument our tangible objects with a single electrode. However, we used a fixed frequency excitation instead of a varying frequency, focusing mostly on sensing proximity information. Compared to the work of Rekimoto et al. [245] on graspable interface which could detect the position of a tangible object grasped by a user, we worked on the proximity of the user from such tangible object.

6.1.3 Motivation: Embedding Tangibles with Proximity Capacitive Sensing

As mentioned in Section 6.1.1, it is important to achieve a good temporal matching between what users see in the VR and what they feel in the real environment. For example, when using tangible objects, it is of paramount importance to synchronize the moment the virtual hand touches the virtual object with the moment the user's hand touches the tangible prop. Any discrepancy, such as a gap or an interpenetration as shown in Fig. 6.1, will be promptly recognized by the users, breaking their immersion. Tracking issues, calibration errors, and modeling mismatches between tangible and virtual objects can severely affect this synchronization, as position and orientation errors tend to add up.



Figure 6.1: Exaggerated examples of discrepancies upon tangible contact: as the user is touching the tangible object (middle), there can be a virtual gap (left) or virtual interpenetration (right) between the virtual finger and the virtual object's surface.

In usual approach, the position of the user's hand and the tangible objects are only tracked. Thus, as the simulation only have access to the position of the various elements, any virtual interaction is positioned based, e.g., the virtual elements need to be close enough to enable the virtual interaction, usually as a virtual collision is triggered. However, in case of positioning errors some issues can arise: this virtual collision might not occur at all if the user encounters the tangible too early and is then unable to reach the virtual one. As the virtual event is not triggered, the virtual interaction cannot carry on (e.g., a virtual button is not pressed, a virtual object is not considered as grasped, etc.). Alternatively, if the virtual event triggers too early, the user might end up engaging the virtual interaction without actual haptic feedback. The simulation does not have any information about the actual status of the real contact, only the position of the various elements which is not necessarily accurate. Using a sensor such as pressure sensors would provide some additional information about the status of the real contact which can be used to trigger the virtual event correctly. However, contact sensors only inform about the real contact when it occurs, leaving no time to smoothly adjust the position of the avatar with respect to the virtual object.

To solve these issues, we propose to instrument the tangible object with a capacitive sensor which is able to provide an image of the proximity of the user's hand prior contact, i.e, to have a continuous estimation of the general distance of the user to the surface. Additionally, with appropriate thresholding, it also gives absolute contact information, i.e., whether or not the user is touching the surface. Therefore, as information are provided well before the contact happens, it is possible to perform a smooth correction of the errors and an effective combination with external trackers.

In this work, as a proof of concept, we instrumented a tangible cube with three capacitive sensors placed on three different faces (see section 6.2.2). We combined the information coming from these sensors with the tracking information coming from a tracking system to adjust the rendering displayed to the user with an HMD. We especially worked on enhancing the visuohaptic feedback when using tangible objects: to smoothly adjust the synchronicity between tangible and virtual contacts. By correcting the local position of the virtual finger toward the virtual object with respect to the local position of user's real finger toward the real object, we can make sure that the event on each side, virtual and real environments, are brought close enough for the user not to perceive any difference.

We expect to significantly improve the performance of contact rendering in VR when using tangible objects by correcting the normal distance to the surface, hence compensating various error sources which can flaw the user's experience:

- **Tracking Issues:** the reconstructed position (or orientation) can be ill-conditioned leading to wrong position and orientation in some area, the tracking system used can also be insufficient to reconstruct the hand position with enough accuracy, which is critical around the part of the hand which will actually touch the tangible, the contact area.
- **Calibration Errors:** when registering tangible and virtual elements, it is common to have remaining positioning or orientation offsets between them.
- **Modeling Mismatches:** there can be mismatches between the mesh of the virtual element and the actual tangible one, be it between the tangible and virtual object, or the hand avatar and the user's hand. Those mismatches can be modeling errors in some case or even voluntary introduced through a rendering technique (see Chapter 5).

When choosing a tracking solution to reconstruct objects and human part's motion, all those possible sources of error can add up together and result in discrepancies during the interaction. Since most systems are unable to tell at the same time if a tangible contact does occur and with which part of the user's hand (e.g. not being able to discriminate between the pad, the tip or even the side of a finger), the interaction is not robust and can fail. In our case, we will see that we can discriminate whenever a contact occurs and provide a credible visual representation of the contact without actually knowing which part of the finger is actually touching.

6.2 Method

As the user approaches and then touches the tangible object, the virtual environment should render as closely as possible the approach and contact of the avatar's hand with the corresponding virtual object. As to compensate for the virtual resulting positioning errors, and achieve contact synchronicity, we propose to target the motion of the virtual hand along the normal of the object's surface, by combining the local estimation of the signed distance along this direction from the capacitive sensor with the global tracking information coming from commercially-available optical trackers. In the following section, distance will always refer to the projected component along the normal direction to the targeted surface, i.e., the height in the surface local frame.

6.2.1 Capacitive Sensitivity to Human Hand

By adding a conductive layer on the surface of a tangible object and connecting it to a detection circuit, we can create an instrumented tangible object sensitive to any capacity change in its vicinity. As the human hand is a complex distribution of electrical charges and dielectric, each part of it will contribute to the total capacity C_p detected by the electrode (see Fig. 6.2).

Referring to the capacity equation, $C = \epsilon_r \epsilon_0 \frac{S}{e}$ where ϵ_0 , ϵ_r are the vacuum and relative permittivity values, S is the area of overlap of the two plates of the capacitor (e.g., the hand and our electrode), e the distance between the two plates. Therefore, the closer the hand is to the tangible object, the higher the capacity is. For example, as shown in Fig. 6.2, when nothing is in the detection range, $C_p = 0$; if the user's hand moves in range of the instrumented object, each part of it will contribute to the capacity detected, $C_p = \sum C_i$. However, if one part of the hand is significantly closer than the rest, it will provide a significant contribution compared to the others. For example, in the right-hand side of Fig. 6.2, the fingertip contributes significantly more than the rest of the hand, $C_1 \gg C_2 \approx C_3$, and therefore and we will have $C_p \approx C_1$.

As the electrode is covered by a thin layer of tape, e decreases drastically, without being null once the user touches the surface, leading to an important increase of C_p . When pressing on the surface, the fingertip will deform and spread on the surface, increasing the contact area S , hence, C_p increases even further.

To sum up, it is possible to instrument any tangible object by adding a conductive layer. The surface being flat or curved, the overall capacity C_p will increase whenever the hand is getting close to the surface. The closest part of the hand will provide the main contribution to C_p and as it gets closer to the electrode, the contribution of the other parts of the hand become negligible, i.e., the hand posture holds little importance the closer it gets to the electrode. Then, using a circuitry which is sensitive to this variation of capacity, we are able to obtain an image of the distance to the electrode, i.e., to track the state of the real contact

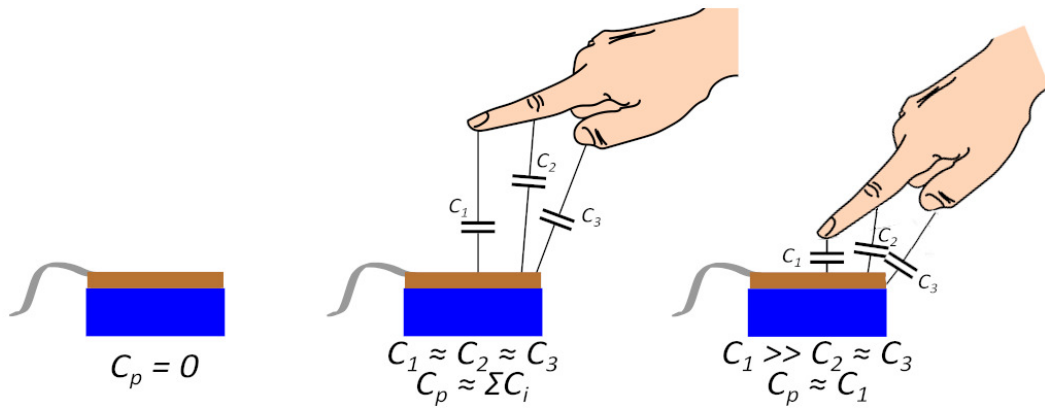


Figure 6.2: Capacitive sensitivity to user's hand. Each part of the hand contributes to the total capacity. The closer a part is to the surface, the higher the capacity. Once one part is about to touch the surface, it provides an important contribution to the total capacity, rendering the other parts' contributions negligible.

between the user's hand and the targeted surface. In the follow-up we will only consider flat electrodes.

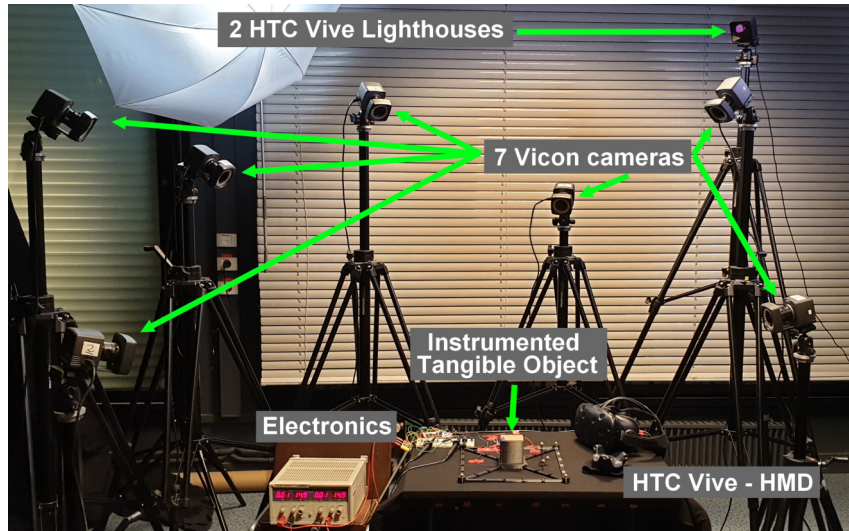
6.2.2 Apparatus

The experimental setup illustrating the principle of our approach is shown in Fig. 6.3b. It is composed of a tangible cube, instrumented on three of its faces with 2-cm-wide copper electrodes, acting as our proximity sensors. The cube is fixed on a rigid structure placed on a table in front of the human user, which position is calibrated and known by the system, so as to guarantee precise and reproducible settings. Hence, the location of each electrode is known in the calibrated support's frame. The user wears an HTC Vive head-mounted display (HMD) on the head, an attachment with three reflective markers on the back of intermediate phalanx of the right index finger, and a Vive Tracker on the back of the hand. As a first tracking system, the user's right index is tracked using 7 Vicon cameras combined with Blade software. Markers are placed on the back of the fingertip to leave the finger pad free to interact with the tangible object. This tracking solution is detailed in Appendix B. As a second tracking system, we secured an HTC Vive tracker to the back of the user's palm. The two optical tracking systems are never used at the same time and can either be used alone or in combination with the capacitive sensing system (see Section 6.3). The fingertip is always left free to interact with the tangible object. Both tracking will be alternatively used to control the motion of a virtual hand avatar rendered in the virtual environment using Unity3D. The whole setup is visible in Fig. 6.3b.

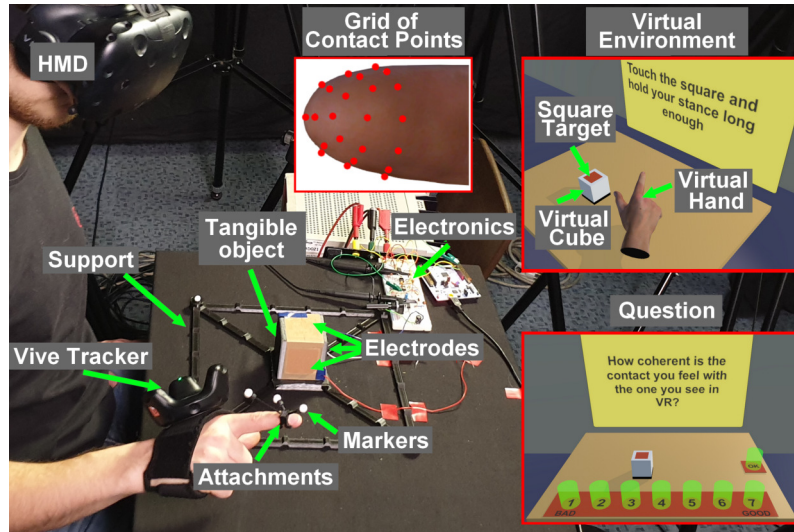
In order to calibrate both systems, users are asked to touch a virtual cube placed on a table displayed in front of them. The virtual object is represented in the real world by our instrumented tangible cube, which is also placed on a table in front of the user. The cube is connected to a support whose position is calibrated.

6.2.3 Capacitive Sensing

As said in Section 6.1.3, a tangible cube is instrumented with capacitive sensor made of copper layers on three of its faces. Since the hand/electrode capacity C_p increases as the user's hand gets close to the tangible surface, measuring the variation of C_p provides an



(a) Global Setup



(b) Hand Tracking

Figure 6.3: Experimental setup.

image of the distance between the finger and the electrode and even discriminates the two state of contact between the user's hand and the targeted surface.

6.2.3.1 Measurement Principle

The detection circuit is composed of an RLC oscillator with an additional copper electrode connected between L and C_0 , thus acting as a second capacitor C_p (see Fig. 6.4a). The oscillator will phase shift and attenuate the excitation signal $A_0 \sin(\omega t)$, providing the output signal $A_1 \sin(\omega t + \varphi)$. The fig.6.4b shows in dark blue the general behavior of the amplitude A_1 and the phase shift φ due to the excitation.

The resonance frequency of this oscillator being $f = 1/(2\pi\sqrt{L(C_0 + C_p)})$, the excitation frequency will always be f_0 , set as the resting resonance frequency, i.e., the resonance frequency at which the user is infinitely far from the electrode. There are still parasitic capacitance $C_{parasites}$ coming from the surrounding and the circuit itself which would contribute to C_p giving $f_0 = \frac{1}{2\pi\sqrt{L(C_0 + C_{parasitic})}}$, but to ease the notation we will consider that $C_p = 0$ when the user is not engaging the electrode. As the circuitry is also grounded

through the power supply, the parasitic capacitance is stable.

Therefore, when the user's hand is getting closer to the electrode, C_p increase which decrease the resonance frequency f . As illustrated in Fig.6.4b both the phase and amplitude curve shift to the left as the resonance frequency f get further away from the resting resonance frequency f_0 .

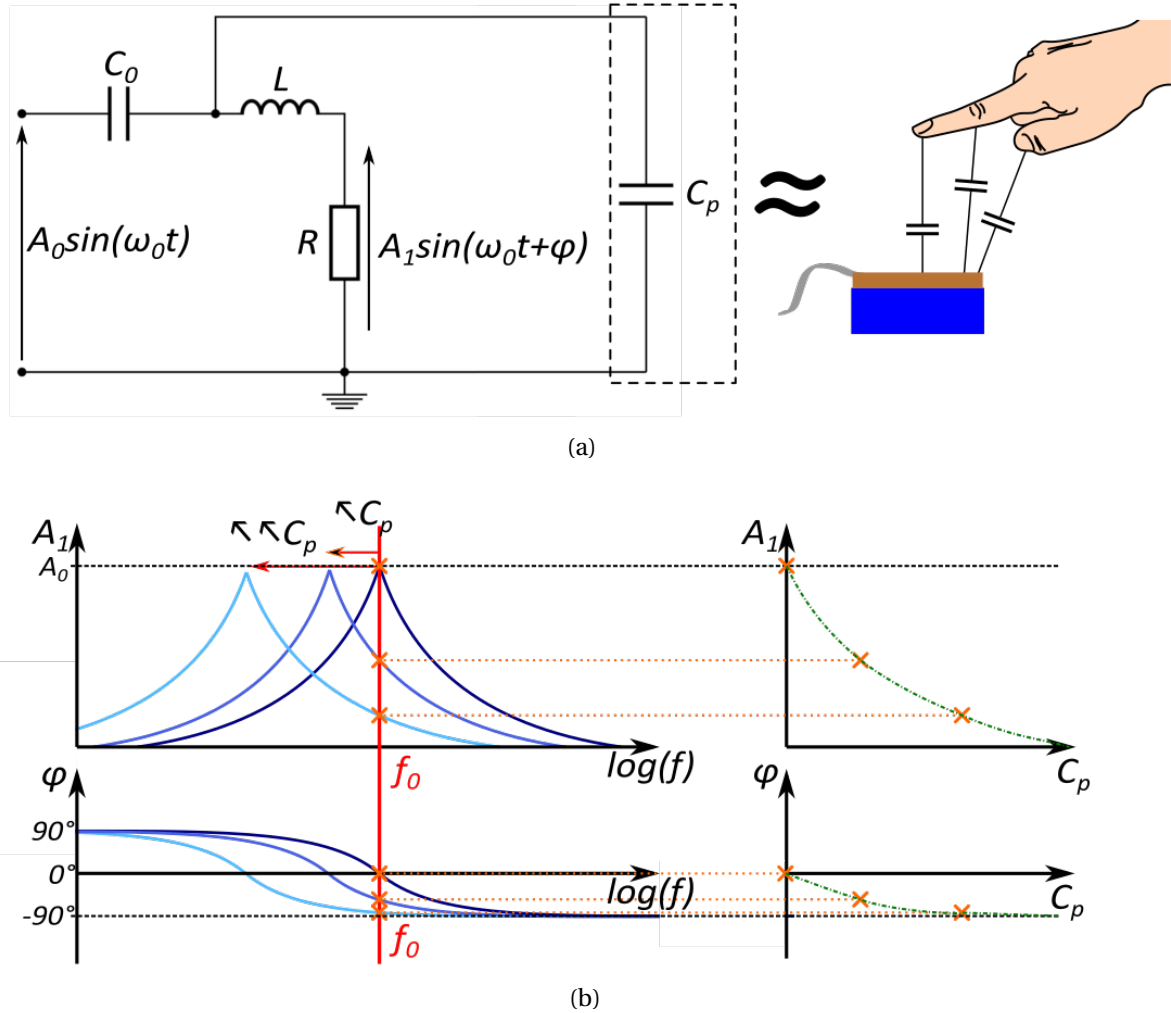


Figure 6.4: a) RLC Oscillator sensitive to the variation of the capacitor C_p . b) Capacitive sensing system. Amplitude and phase shift variation of frequency response due to variation of C_p .

In short, with an excitation signal at the resting resonance frequency f_0 , the amplitude A_1 will drop from the maximum value A_0 to 0 while the phase shift φ will go from 0° to -90° , with respect to the user proximity. Moreover, even if the slope of the oscillator's response also changes a bit with C_p , A_1 and φ , variations are strictly decreasing with the distance. Thus, the variation of those two values is an indication of the proximity without actual measurement of C_p .

In order to measure their variation, we propose to multiply the input and output signal with an analog multiplier. Hence, we obtain as output of the multiplier:

$$V_{out} = \frac{A_0 A_1 \cos(\varphi)}{2} - \frac{A_0 A_1}{2} \cos(2\omega_0 t)$$

As a result, there is a continuous component $\frac{A_0 A_1 \cos(\varphi)}{2}$ carrying the salient information A_1 and φ , and a higher frequency component which can easily be eliminated through filtering.

The whole conditioning process of the sensing unit is shown on Fig. 6.5. The DAC (Digital Analog Converter) of our processing board (NUCLEO-F446RE, with Arm Cortex M4) generates the reference input voltage $A_0 \sin(\omega_0 t)$, which enters the RLC circuit shown in Fig. 6.4a. The output voltage $A_1 \sin(\omega_0 t + \varphi)$ holds the information on the user's proximity, which we multiply with the reference input so as to bring the salient information to the DC component of the signal. We then filter the signal to select and amplify the DC component.

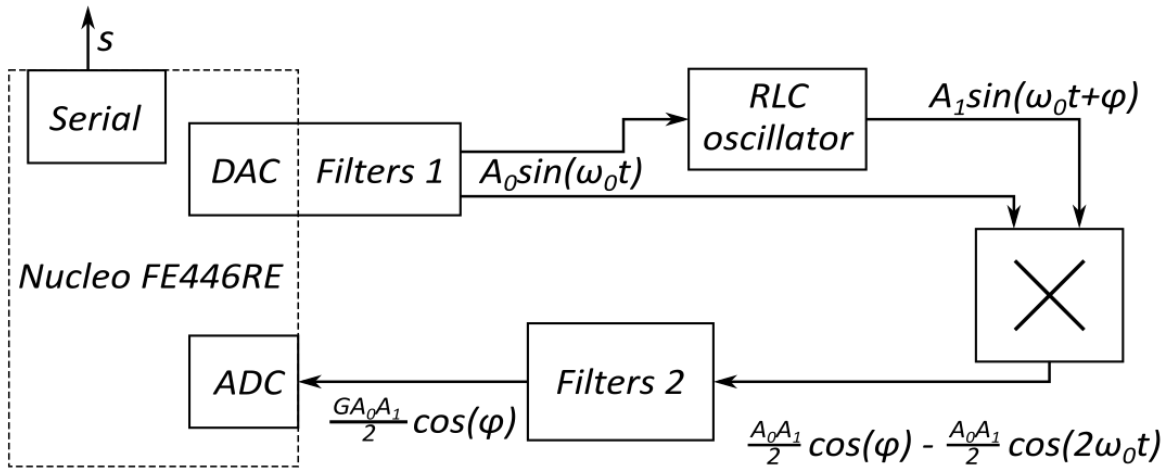


Figure 6.5: Conditioning of the RLC oscillator to generate the sensing signal s .

Finally, by normalizing the continuous component, we acquire and generate a signal $s \propto A_1 \cos(\varphi)$ ranging from 1 to 0 with respect to the user's proximity, from the edge of the range of detection (1) to the contact (0) as illustrated on Fig. 6.6.

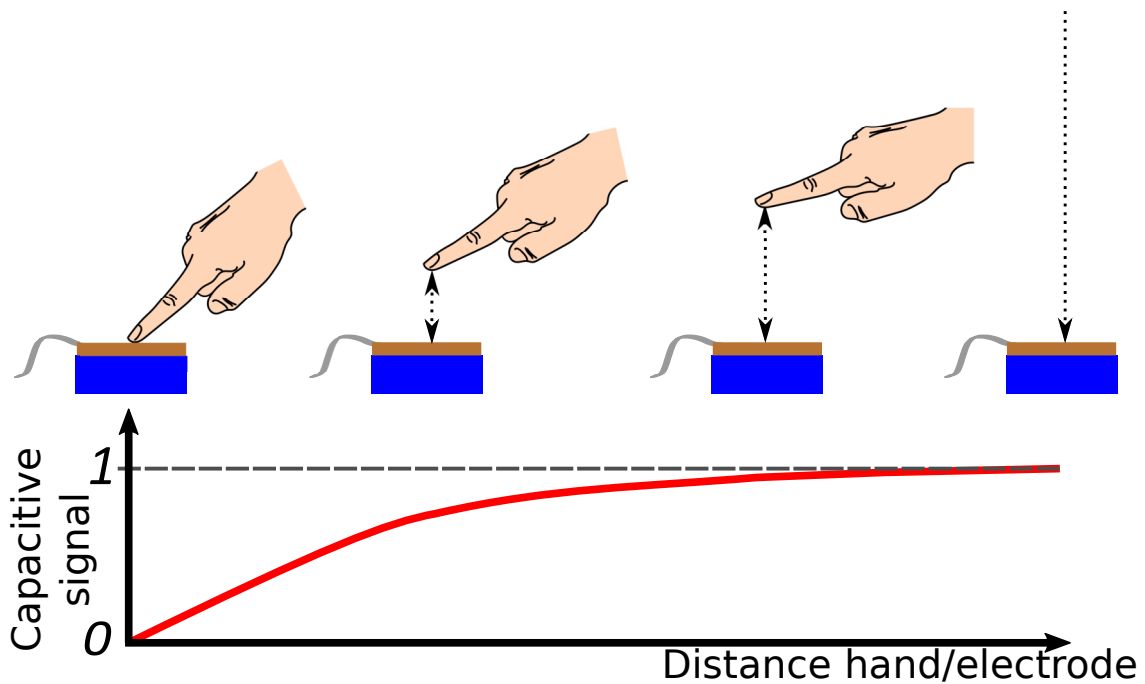


Figure 6.6: The conditioned signal s , providing an estimation of the proximity of the user.

6.2.3.2 Technical aspects

In order to use this sensor correctly, excitation signal has to be at the resting resonance frequency f_0 of the oscillator. However, this frequency is dependent of the electronic components of the oscillator, as well as the parasitic capacity $C_{parasitic}$ due to the geometrical shape of the electrode and its surroundings (conductors, dielectric, etc.).

We used a Nucleo F446RE microcontroller in order to control and adjust the frequency of the excitation signal with enough precision, as well as acquire the conditioned signal, and transmit the signal s to the virtual environment made with Unity3D. It possesses two DMA (Direct Access Memory) allowing to quickly transfer data between memory and hardware components without going through the CPU, which make it possible to use an ADC and DAC at a higher rate than without DMA: either by reading pre-computed array to generate a sin wave, or by filling an array of acquired values which will be averaged later by the CPU. The electrical sensor is composed of several parts, shown in Fig. 6.5: first, generation of the excitation signal at the resting resonance frequency; Second, modulation of the oscillator with the user's proximity, then, conditioning of the signal with a multiplier and filters; Finally, acquisition of the continuous component which reflect the proximity of the user.

Generation of the sinusoidal excitation. The Direct Digital Synthesizer (DDS) method, [248], was used to generate a sinusoidal wave of variable frequency $f = \frac{n}{2^R} f_s$, where f_s is the sampling rate, 2^R the size of the accumulator which will sample the phase of a sinusoidal waveform, and n the step increment used to read value within the accumulator. Basically, the frequency resolution is $\frac{f_s}{2^R}$ and it is possible to change f by simple modification of the step n up to $n = 2^{R-1}$, meaning the frequency could go up to almost $\frac{f_s}{2}$. In order to have a small enough step frequency, we need an accumulator as large as possible and a frequency sufficient to generate the needed range of frequency but not too large to avoid decreasing the step frequency. We used $f_s = 4\text{MHz}$ and $R = 13$, which means that the step frequency was about 500Hz, while the average value of f_0 was around 500kHz.

Obtaining such high sampling rate required that we use the DMA (Direct Access Memory) component of the Nucleo board, which allows to quickly transfer data between memory and hardware components, i.e., to copy the content of an array to the DAC (Digital Analog Converter) without any processing from the CPU and at a higher rate. The array which will be read by the DMA is actually the previously mentioned accumulator which is filled with the amplitude value of the sinusoidal wave obtained from the incremental step of the phase accumulator over 2^R values.

In addition, this method also allows to control the amplitude of the excitation signal by scaling up and down the value extracted from the tabular.

As shown in Fig. 6.5, the method is coupled with a first layer of filters as the DDS method is not sufficient to generate a real sinusoidal wave. The obtained signal has a fundamental at f_0 but also many harmonics of higher orders which can be eliminated with a low-pass filter with a cutoff frequency higher than 500kHz. Furthermore, the signal is not centered as the DAC is not symmetrical and cannot generate negative voltage, but a high-pass filter with a low enough cutout frequency can remove the continuous component. Thus, a first filtering layer is needed to filter the higher harmonic and keep the fundamental, to filter the continuous component and to add some gain to avoid having a too small signal.

Conditioning of the proximity signal. The obtain sinusoidal signal, $A_0 \sin(\omega_0 t)$, is used as the excitation of the RLC oscillator which phase shifts and attenuates the input as the resonance frequency shift away from the resting state at the resonance frequency, with respect to the user proximity, providing the output signal $A_1 \sin(\omega_0 t + \varphi)$. We will then multiply both signal to obtain the needed continuous component $\frac{A_0 A_1 \cos(\varphi)}{2}$. However, the multiplier also divides the output by 10 and gives a second component at $2f_0$. Moreover, the ADC can only convert voltage between 0V and $V_{max} = 3.3V$. Taking everything into account, it is necessary to filter the higher frequency components with a low pass filter and to amplify the signal with an amplifier to bring the resting state signal close to the maximum voltage of the ADC. Since the operational amplifier has a fix gain-bandwidth product, the amplifier filter also acts as an additional low-pass filter, attenuating even more the parasites at higher frequency. Furthermore, since the amplification is significant, it was mandatory to stabilize the output offset of the operational amplifiers. and ensure that, we obtain a true 0V when the input of the circuit is connected to the ground. We thus obtain the signal $\frac{GA_0 A_1 \cos(\varphi)}{2}$ which variate from V_{max} at the resting state to 0V at contact.

Acquisition of the proximity signal. The signal can then be acquired and pre-processed by the Nucleo board. To ensure a high acquisition rate, a second DMA is set in order to store the data from the ADC to an array. Whenever the array is half filled, an interruption is triggered and the CPU computes the average value over this half array generating the signal s and sending it to Unity3D through serial link at 60Hz. The size of the array and the acquisition rate of the DAC are chosen to send the sensed value at slightly more than 60Hz¹.

Calibration of the sensing unit. Lastly, an initial calibration is done in order to set the amplitude A_0 and the resting resonance frequency f_0 , whenever a new electrode is plugged or something with capacitive properties is moved and change the parasitic capacity of the electrode (e.g. the leg of the user bellow the table, a metallic object on the table, etc.). As the participants took place on the chair, they themselves added a contribution to the overall parasitic capacity, especially as the table had metallic parts. This contribution would not be negligible compared to the absence of the users. However, any change in the body position would have negligible effect on the overall parasitic capacity: users could lean forward or move their legs below the desk without affecting the base calibration. We simply asked them to sit and remove their arms from the table for the duration of the calibration, in order to be sure that they would not put their hands in the working detection range of the sensor.

Because of the discrete frequency synthesized with the DDS method, it is not possible to get precisely the exact value of f_0 . If the frequency is slightly lower than the resonance frequency, when a user is getting closer to the electrode, the signal will first start to increase as the curve shifts to the right (see Fig. 6.4a). Thus, there is a need to be slightly above the resonance frequency. In order to find the just above frequency, we simply search for the maximum mean value of two successive frequencies. Once this maximum found, the frequency at the higher is used. Additionally, as DDS method enables scaling the amplitude of the excitation we will adjust numerically the amplitude of the excitation signal to make sure that the output, close to the resonance frequency, at the resting state is close and below V_{max} . This two steps calibration are performed automatically by a simple searching

¹Handler on Unity3D's side would just drop the extra value whenever two come in on the same frame.

script.

Contact detection. Before each set of trials with a new electrode, we had to fix a threshold in order to discriminate when the tangible contact occurred: below the threshold we would consider having a tangible contact between the user and the electrode. As users get closer to the electrode, the sensed capacity increases with an increasing rate. Thus, between near contact and contact, the variation is so high that the signal would just saturated once the contact was made. Thus, it was easy to set an acceptable threshold by adding to the saturation value a small offset (e.g. 1% of the signal's variation range). To get the value, we asked participant to touch the electrode for a few seconds and fixed the threshold accordingly.

In addition, we also used two slightly different thresholds for making and breaking contact in order to avoid the false detection of two successive contacts as the user is encountering the tangible a single time. The breaking contact threshold was slightly higher than the making contact threshold so the noise would not untrigger the contact.

6.2.4 Signal Characterization

The relationship between the signal acquired by our capacitive sensing unit and the proximity of the user is not straightforward to estimate, as it is also dependent on the size of the hand, its dryness, and how the user approaches the electrode. Even if it is expected that the signal is not totally consistent nor accurate, a mean behavior is targeted, as it would later serve as a reference for the visuohaptic retargeting. We estimated this relationship by enrolling five participants which were asked to close their right hand in a fist with the index finger pointing out (as in Fig. 6.4a) and then move steadily along a straight line, along the normal to the electrodes, displayed to them in the HMD. They carried out six back and forth movements of 40 cm. The position of the hand was tracked using the Vicon. Using these data, we fitted a mean curve between the signal coming from the capacity sensor vs. the Vicon-measured distance from the electrode registered using the Vicon Bonita system. We used the `nlinfit` MATLAB tool to fit this curve. Fig. 6.7 shows the registered points as well as the fitted curve.

As expected, there is a common behavior between each participants with variation around the mean fitted curve. As it is clear from the figure, the capacitive sensing system shows a good sensitivity close to the electrode, but it quickly degrades as the user moves away. One lookup table was created for each electrode, as they do not have the exact same mean behavior. Later, they will be used to have an estimation of the proximity given the signal value. The procedure was repeated for each one of the three electrodes, so as to evaluate a mean behavior for each one of them and fill lookup tables which will be used to obtain a distance estimation from the capacitive signal s (see Section 6.2.3).

6.2.5 Visuohaptic Retargeting

Now that we know how to relate the data gathered from the capacitive sensing with the user's proximity to the tangible object, we aim at combining it with the optical tracking system, by performing an interpolation between the two along the surface's normal.

One can already notice that, even if the behavior is close, some participant will be above the fitted curve while others will be below it. Moreover, the hand pose and orientation might also add more discrepancies, especially in the bend area. Furthermore, at a high distance the curve is almost flat, meaning that small variation of the signal will end-up

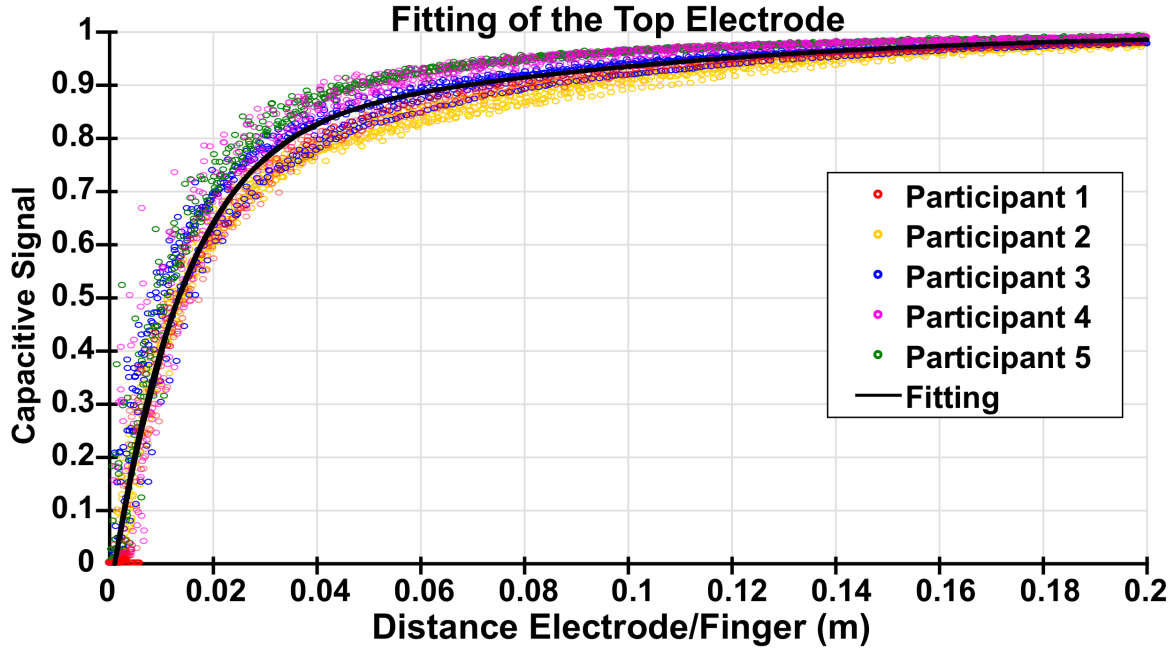


Figure 6.7: Acquired signal vs. Vicon-measured distance from the electrode for the top electrode data. The best fit is plotted as a solid black line.

with large variation of the distance. Thus, as the signal is noisy, relying on this part of the curve will lead to high jitter. However, the errors between individuals decrease and become smaller as the signal is getting close to zero. Thus, the idea is to use the real tracking height when the user is far, and to use the capacitive sensing height estimation when the user is really close.

Let us call z_{capa} the distance between the user and the tangible object as estimated by the capacitive system (see Section 6.2.4) and α its normalized value, i.e., $z_{capa} = \alpha z_M$ with z_M being the maximum detection range (e.g., $z_M=40$ cm for our top electrode). Similarly, let us call z_{trac} the distance between the user and the tangible object as estimated by the optical tracking system. The interpolation between z_{capa} and z_{trac} can be controlled using α . However, as seen on Fig. 6.8a, when the user is far from the electrode, α (and z_{capa}) is too noisy to be sufficiently reliable. Thus, it is required to rely only on the external tracking system at far distance. Furthermore, when the user is close to the electrode, the tracking system is erroneous, while the capacitive estimation is more precise and reach 0 upon tangible contact. Similarly, we rely only on the capacitive sensing at close distance. For this reason, we define a transformed version of α , which spans between 0 and 1 in the range $[\alpha_m, \alpha_M]$, i.e.,

$$\alpha_{th} = \begin{cases} 0 & \text{if } \alpha \leq \alpha_m \\ \frac{\alpha - \alpha_m}{\alpha_M - \alpha_m} & \text{if } \alpha_m < \alpha < \alpha_M, \\ 1 & \text{if } \alpha \geq \alpha_M \end{cases} \quad (6.1)$$

Fig. 6.8a shows α and α_{th} for one representative user during six back-and-forth movements. Finally, we can proceed with retargeting the position of the user's finger according to both tracking information, i.e.,

$$z_{fin} = \alpha_{th} z_{trac} + (1 - \alpha_{th}) z_{capa}. \quad (6.2)$$

Whenever the user is farther than α_M from the electrode, we only consider information coming from the optical tracking system, disregarding the capacitive sensing data. When

the user is between α_M and α_m , we consider a combination of the two, starting to smoothly include capacitive data at α_M and weighting it more and more while we approach α_m . When the user is closer than α_m to the tangible object, we only consider information coming from the capacitive sensing system, disregarding the optical tracking data. In our case, $\alpha_m = 0.1$ as to avoid any transition between z_{capa} and z_{trac} when the user's hand is below 5 cm height, and $\alpha_M = 0.5$ as the capacitive height estimation is too noisy above 30 cm.

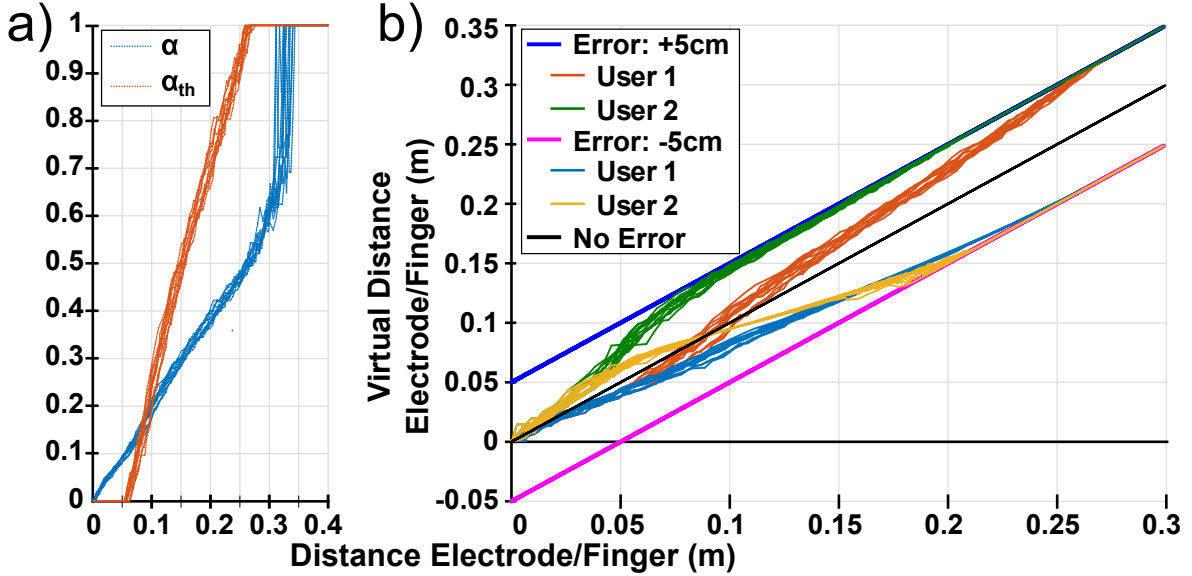


Figure 6.8: Visuohaptic retargeting. First inset: α and α_{th} processed from a participant's data. Second inset: behavior of the interpolation for two participants against constant simulated offsets.

Fig. 6.8b shows four representative examples of this approach. We consider two situations where the optical tracking system measures the distance between the user and the tangible object with an error of either +5 cm (blue solid line) or -5 cm (pink solid line), while the capacitive sensing system works correctly (no estimation error). The retargeting was computed by adding those simulated errors to the trajectory acquired for two of the participants during the signal characterization of Section 6.2.4. If no capacitive sensing is employed, users either touch the tangible object before the contact in the virtual environment occurs or touch the virtual object before the contact with the tangible object occurs. Either way, this is expected to impair the resulting interaction. Combining the proximity capacitive data with the global optical one enables us to address this mismatch. The green and red lines of Fig. 6.8b show how the combined estimated position z_{fin} is corrected as the distance between the user and the tangible object diminishes, leading to an increased visuohaptic synchronization and higher immersion at the contact. We can notice that z_{fin} converge toward the error free trajectory (black line) either from above or from below, as the capacitive sensor either over or under estimate the distance to the electrode around the bent of the fitting.

It is important to highlight that capacitive sensing only provides information regarding the proximity of the user's finger to the electrode, conveying no information on the orientation of the finger itself. This information can only come from the global tracking system. For this reason, while the position of the virtual avatar is adjusted according to the visuohaptic retargeting mechanism described above, its orientation with respect to the tangible object is not. We consider the finger to be oriented as estimated by the

global optical tracking system and the distance detected by the capacitive sensor to be that between the tangible object and the closest point on the finger. Thus, we apply the retargeting to the closest point of the virtual finger to the virtual object's surface as to make the virtual contact plausible. As to be able to run this adjustment at runtime, we consider a grid of 23 points spread around the virtual fingertip (see Fig. 6.9). These points are placed below the virtual skin surface, from 1 mm for the pad to 0.5 mm for the sides, to allow interpenetration as if some deformation of the virtual finger would occur upon contact and avoid having an unnatural tangential virtual contact.

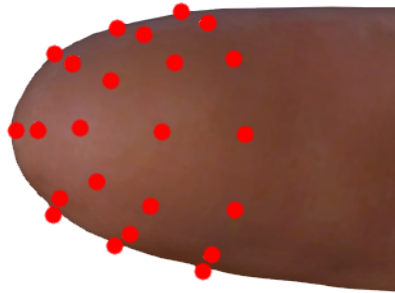


Figure 6.9: Grid of contact points represented with red sphere dots.

6.3 User Study

We carried out a user study to assess the performance and viability of our combined capacitive-optical approach vs. standard optical-only tracking techniques when interacting with tangible objects in VR. The three hypotheses of our study are:

- H1: Using our capacitive sensing system together with an optical tracking system improves the perceived coherency and synchronicity of the contact;
- H2: H1 is valid both for brief contacts (e.g., tapping on the tangible object) and sustained contacts (e.g., apply a constant pressure on the tangible objects);
- H3: Seeing the virtual distance between the fingertip and the object (lateral point of view) increases the perception of any existing discrepancy vs. having an occlusion between the fingertip and the object (contact with back or top faces of the cube, see Fig. 6.3b).

6.3.1 Experimental Methods

6.3.1.1 Participants

18 participants (12 males, 6 females, $M = 28.5$, $SD = 0.88$) took part in the experiment, all of them were right-handed.

6.3.1.2 Experimental setup

We used the setup described in Section 6.2.2 and shown in Fig. 6.3b, equipping the participant with both a Vive Tracker and reflective markers for the Vicon. The tangible object was instrumented with three electrodes, on the top, right side, and back faces of the cube. As the Vive Tracker was placed on the back of the hand, we assumed that participants always

kept their hand closed with the index finger pointing out (as in Fig. 6.3b). Participants were asked to keep their hand in a natural way as to avoid being tense and without being constrained. Additionally, to help the participant assess the contact, the shadow of the virtual finger was rendered onto the cube's faces. The virtual environment was composed of a virtual version of the tangible cube, which position was carefully aligned. The face the participant had to interact with was colored in red. To help participants assess their distance from the tangible object, we cast the shadow of the virtual finger onto the object.

6.3.1.3 Experimental procedure

Participants performed two interaction tasks: a "touching" task, where they had to approach the target object's face and touch it for 3 seconds without breaking contact; and a "tapping" task, where they had to approach the target's face and tap on it 10 times. Participants were asked to contact the object naturally, as they would intent to do with a real object. For the "touching" task, they were asked to first touch the virtual red square. As soon as the contact with the tangible electrode was validated, they were asked to maintain the contact for a long enough span of time without moving the index. They were suggested to hold the pose for 3 seconds, to make a clear distinction between a maintained touch and a bouncy tap. As for the "Tapping" task, they were asked to tap 10 times, regularly, on the surface. But also to slightly tilt their hand in several directions to tap each time with a different area of their fingertip. At the end of each repetition of the task, participants answered the question "How coherent is the contact you felt with the one you saw in VR?" (see lower inset of Fig. 6.3b) using a 7-item Likert-like scale.

The experiment started with a written explanation of the procedure and the signature of a consent form. Then, participants watched a short video demonstrating the two tasks mentioned above and were reminded to: touch the displayed red square at the center with their index, keep their hand in the same pose as the virtual one for the whole experiment, reach for the object in a natural way while sitting straight on the chair with the table in front of them. They were also reminded to focus on answering the question despite possible unwanted tracking behavior such as flipping hand, jitter, lag, or tracking loss, any which could lead to unnatural motion of the virtual hand.

Then, an initial calibration of the virtual hand was done for each tracking system separately, by placing the participant's real finger on the upper face constrained in position and orientation with a 3D-printed prop (Fig. 6.10). As the real and virtual finger were placed at the same pose, the needed position and orientation offset were computed with respect to each tracking system specifics in order to provide an acceptable registration of the virtual and user's hand.

Participants then went through a set of trials for the "touching" task, then the "tapping task", for each one of the three electrodes, for each tracking system. At the beginning of the 6 sets, a fast calibration of the targeted electrode was performed to find f_0 (see Section 6.2.3). Before each task of the first set, 3 random practice trials were performed to ensure that the participant had understood the instructions, the tasks, and that the calibration were done properly. For each task, participants went through repetitions of the interaction with and without the capacitive sensing. At the end of the experiment, participants filled the final subjective questionnaire.

6.3.1.4 Experimental Design

We used two different tracking systems. The Vicon tracking is known to be precise and reliable and was considered as the reference or state-of-the-art tracking system. The HTC

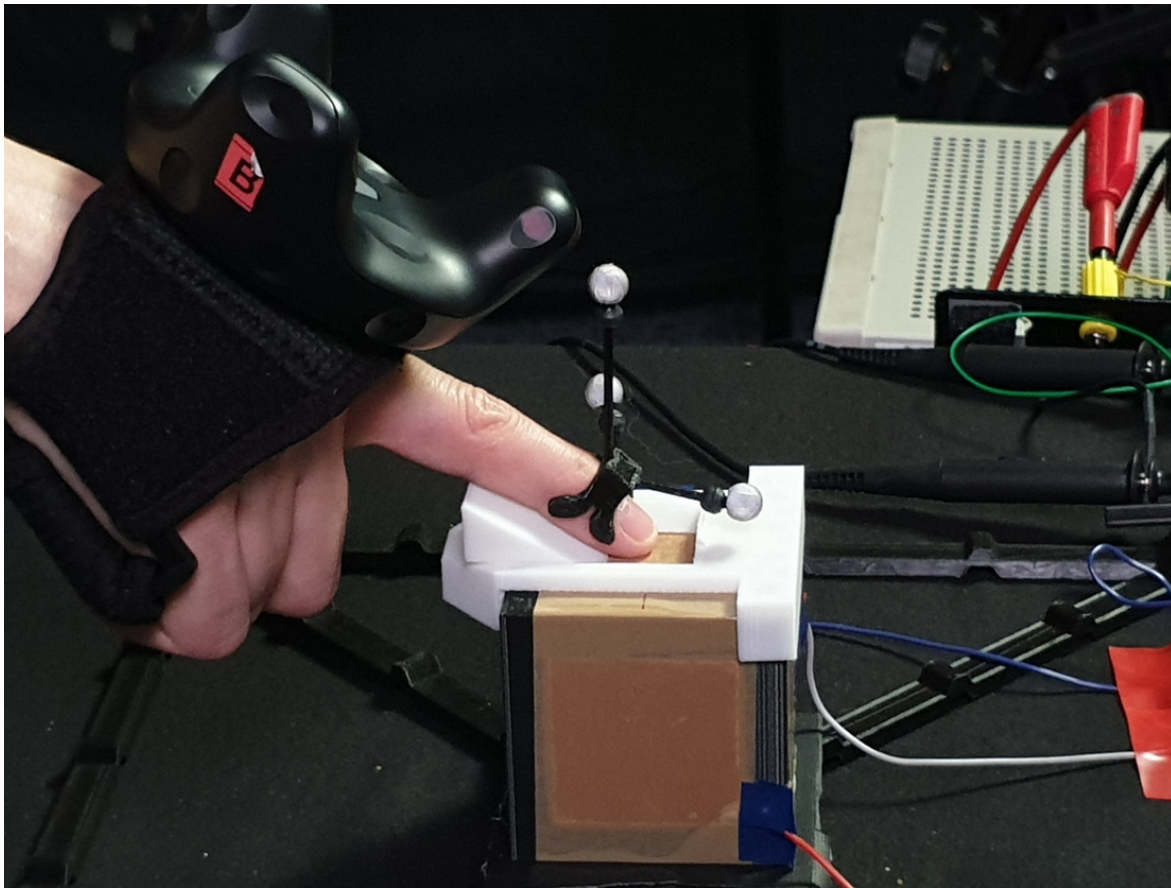


Figure 6.10: 3D-printed calibration prop.

Vive tracker is one of the most affordable VR solution but its usage comes with more drawbacks: more jitters, tends to drift, higher position and orientation errors. Moreover, as the Vive Tracker is more cumbersome, it can only be placed around the palm. Since it was meant to track the fingertip of the index, additional errors were coming from any change of the hand-pose, especially if the participant bent his index instead of keeping it straight. With time, one can expect some participants to release their index without noticing. Additionally, the calibration which superimposes the fingertips of the real and the virtual hands could lead to mismatches between the virtual model and the real hand. These cumulative errors could apply for both tracking systems. It is this kind of error that our approach should mitigate.

To sum up, in order to assess if our approach can compensate different kind of errors, we will apply our visuohaptic interaction first to a robust distal phalanx tracking system with small but constant orientation and positioning errors, and second to a palm tracking system with larger and varying orientation and positioning errors.

The two tasks were performed on three different faces of the cube: when the finger of the participant is hiding the contact area on the object, on the top of the cube; when the object is hiding the contact area on the participant's finger, at the back of the cube; when the contact area is visible from the side, neither the object or the finger being hidden, on the lateral side of the cube. The cube is positioned slightly on the left of the table so the participants can see the right face from the side, and close to them enough so they can touch the back face of the cube easily.

Participants were wearing both tracking parts for the whole experiment, first to ensure that the initial calibration for both systems were valid for the whole experiment, second

to avoid suggesting a clear distinction between the two tracking systems. Therefore, the experiment was split in 6 blocks to have all combinations between the two tracking systems, and the three faces of the cube. The ordering of the three faces was counterbalanced following a Latin square. Participants performed two blocks in a row with the two tracking systems for each cube face. The order between the two tracking systems was counterbalanced for each cube face, meaning there would be $3 \times 2 = 6$ different block ordering. In each block, the participants always performed the "touching" task then the "tapping" task. And for each task, there were 6 repetitions, with and without capacitive sensing correction for a total of 12 trials per task presented in a randomized order. Thus, each participant did 72 trials per task, for a total number of 144 trials for the whole experiment, which lasted an hour.

6.3.1.5 Experimental variables

We considered four experimental conditions:

- C1:** Optical tracking (T: Vive Tracker, V: Vicon Bonita)
- C2:** Capacitive sensing (E: Enabled, D: Disabled)
- C3:** Cube face (Tf: Top, Sf: Side, Bf: Back)
- C4:** Task (To: Touching, Ta: Tapping)

6.3.1.6 Collected Data

For each trial, we collected the participants' answers regarding the coherence of the contacts on a 7-item Likert scale, as well as, for each frame, the external tracking data, the corrected position, the virtual distance from the virtual hand to the targeted face projected onto the face's normal, the sensing output and the absolute contact boolean state. Then, we computed the mean error at contact for each trial, i.e., the mean of the previous distance whilst contact occurred, i.e., the mean visual gap or interpenetration distance displayed to the participant whenever the physical contact occurred. Participants filled a subjective questionnaire using a 7-item Likert scale at the end of the experiment. The questions were the following: (Q1): It felt like tapping a real cube; (Q2): It felt like touching a real cube; (Q3): It felt like I was seeing my own hand; (Q4): I felt tired at the end.

6.3.2 Experimental Results

Contact coherency. In order to study the participants answers regarding the contact coherency, we used a linear mixed model on the collected data, with respect to the four conditions **C1**, **C2**, **C3** and **C4**. We performed a step-wise selection of the model variables. The participants were considered as a random effect in the model. Our analysis of variance on the selected model showed a significant effect of **C1**, **C2**, **C3** ($F(1, 2560) = 792.55$, $F(1, 2560) = 626.37$ and $F(2, 2560) = 106.42$ respectively, $p < 0.001$ for the three conditions). No significant effect was found for **C4**, the task condition ($p = 0.91$). The coherency ratings for both tasks were very similar ($M = 4.5$, $SD = 1.92$ for the static task, $M = 4.51$, $SD = 1.97$ for the dynamic task). Concerning **C1**, there was a significant difference in the ratings when the capacitive system was activated ($M = 5.28$, $SD = 1.44$) or not ($M = 3.72$, $SD = 2.06$). Concerning **C2**, there was a significant difference in the ratings between the two tracking systems ($M = 5.2$, $SD = 1.63$ for the Vicon system, $M = 3.81$, $SD = 1.98$ for

the HTC Vive system). Finally, there were significant differences between the three faces of the cube ($M = 4.89$, $SD = 1.84$ for the top face, $M = 3.95$, $SD = 1.99$ for the side face, $M = 4.67$, $SD = 1.86$ for the back face). Results are summarized in Table 6.1. An interaction effect was found between **C1** and **C2** ($p < 0.001$). A Chi^2 test showed that whatever the capacitive system was enabled or not, there was a significant difference between the two tracking systems ($p < 0.001$ for both tests). Similarly, whatever the tracking system used, there was a significant difference between the two states of activation of the capacitive sensing ($p < 0.001$ for both tests). An interaction effect was also found between **C1** and **C3** ($p < 0.001$). We also found a significant effect between **C2** and **C3** ($p < 0.001$), and between **C3** and **C4** ($p < 0.001$).

Table 6.1: Ratings on the Contact Coherency (CC) and on the Error at Contact (EC) in millimeters. Mean (and Standard deviation) for the two tracking systems in function of the three faces of the cube, depending on the state of the capacitive system (D: Disabled, E: Enabled).

		Top face	Side face	Back Face
CC	Vicon	D: 5.60 (1.32) E: 6.06 (0.93)	D: 2.75 (1.31) E: 5.61 (1.08)	D: 5.57 (1.24) E: 5.58 (1.25)
	Tracker	D: 2.87 (1.78) E: 5.05 (1.33)	D: 2.68 (1.97) E: 4.76 (1.64)	D: 2.89 (1.77) E: 4.63 (1.68)
EC	Vicon	D: 2.75 (1.92) E: 0.18 (0.20)	D: 7.94 (2.07) E: 0.15 (0.16)	D: 3.06 (2.59) E: 0.16 (0.17)
	Tracker	D: 14.9 (14.8) E: 0.17 (0.18)	D: -8.38 (17.5) E: 0.16 (0.17)	D: 27.8 (13.2) E: 0.15 (0.17)

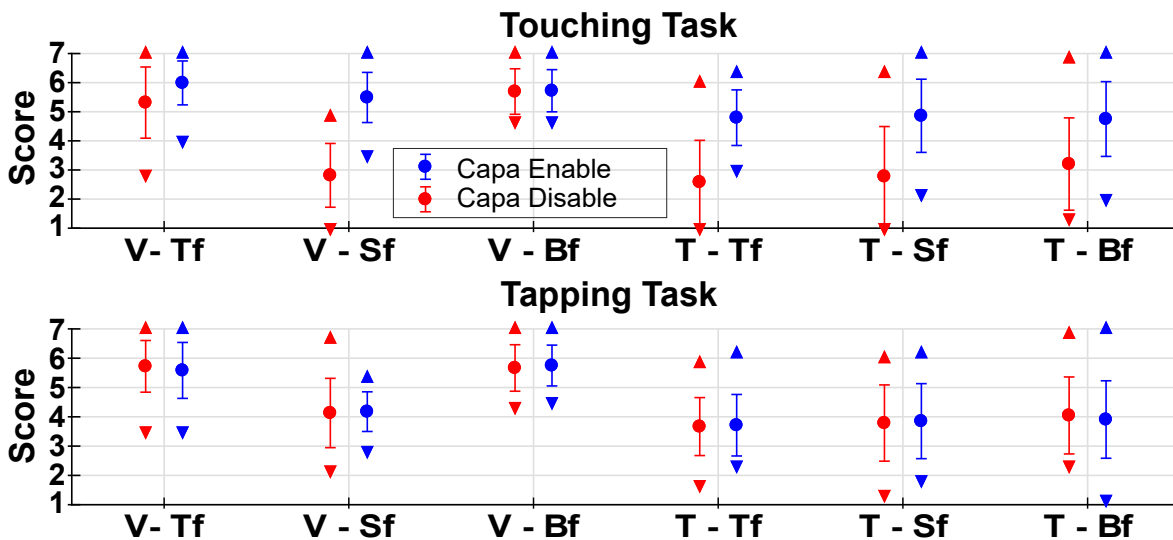


Figure 6.11: Mean score over all trials and participants for each condition, with or without capacitive correction and both task: the standard deviation is represented by a bar, min and max by triangles.

Error at Contact. In order to study the mean error at contact, we used a linear mixed model on the collected data, with respect to the four conditions **C1**, **C2**, **C3** and **C4**. We performed a step-wise selection of the model variables. The participants were considered as a random effect in the model. Our analysis of variance on the selected model showed a significant effect of **C1**, **C2** and **C3** ($F(1, 2547) = 485.61$, $F(1, 2547) = 160.75$ and $F(2, 2547) = 74.53$ respectively, $p < 0.001$ for all the conditions). An interaction effect was found between

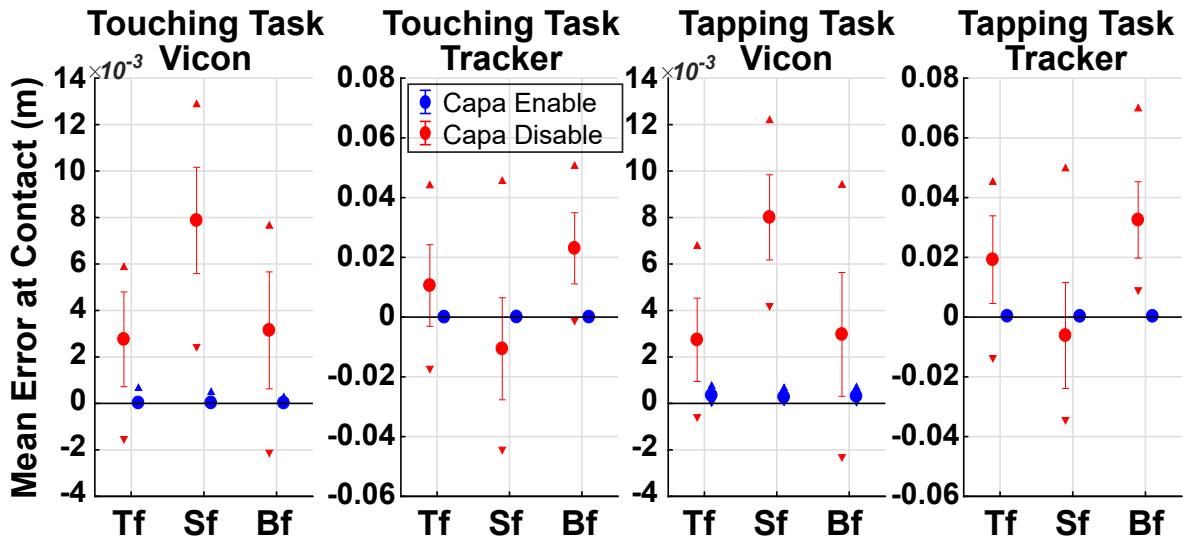


Figure 6.12: Mean Error at Contact over all trials and participants for each condition.

C2 and all the other conditions ($p < 0.001$). We also found an interaction effect between C1 and C3 ($p < 0.001$).

Subjective questionnaire The subjective questionnaire (Fig.6.13) shows that, overall, participants felt like tapping and touching a real object, bit slightly less for the first one. However, even if they would rather agree that the virtual hand was there own, the ownership of the hand is medium.

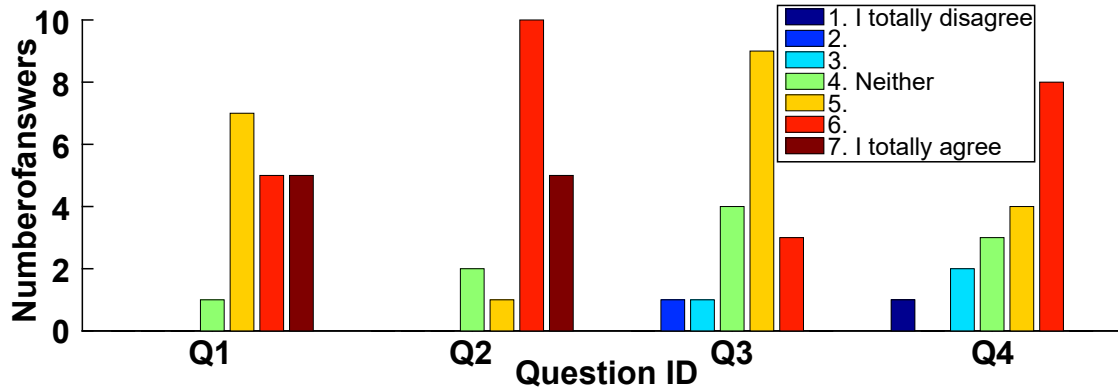


Figure 6.13: Bar-graph of answers for the general questions. Q1: tapping real cube (M: 5.78 SD: 0.94), Q2: touching real cube (M: 6 SD: 0.91), Q3: own hand (M: 4.67 SD: 1.03), Q4: tired at the end (M: 4.83 SD: 1.42).

6.4 Discussion

As the statistical analysis shows a significant effect on condition C2, and that the ratings are globally increased whenever the capacitive sensing is enabled (Fig. 6.11, Table. 6.1), we can conclude that our capacitive system does increase the overall contact coherency. Additionally, the interaction effect between C1 and C2 shows that for both tracking system independently, the difference is significant for the state of activation of the capacitive sensing. This significant difference is corresponding to an increase of the rating when capacitive sensing is enabled. Thus, H1 is validated.

However, H2 is not validated as no significant effect was found on C4. The mean increase of rating for the touching task is clearly visible in Fig. 6.11. However, for the tapping task, the ratings do not seem to change. It is unclear for us if participants were less sensitive to discrepancies for repetitive brief contacts, as long as the physical contact was consistent. At least, the capacitive sensing did not decrease the ratings which suggests that it can only improve the perceived coherency from brief to maintained contact.

The side face does change the behavior of the participants, as the statistical analysis showed a significant effect on C3. Naturally, one could say that as they were able to have a clear line of sight, they would be more critical on the perception of the contact coherency. This can be observed when the Vicon is used (Fig. 6.11), the ratings are lower than the other faces because of the remaining visible gap when the capacitive sensing is not used. As expected, adding the capacitive sensing increased the rating because of the reduction of the gap. But this behavior is not observed when using the Vive Tracker (Fig. 6.11). Thus, H3 is not validated.

We also used a metric to monitor the remaining error at contact (Table. 6.1). When adding the capacitive sensing, the error at contact is brought down below millimeter's level in all conditions, supporting hypotheses H1 and H2. This estimation still shows a remaining error up to 0.5 mm in some cases, as the sensor's threshold for breaking contact is higher than for making contact, thus leading to a slight overestimation of the distance at contact especially for the tapping task. Despite this simple threshold solution, the mean error at contact is drastically reduced. In addition, the grid of points is set to reach 0.5 to 1 mm of interpenetration, making the error at contact non-visible to the participant whenever the capacitive sensing is enabled. Furthermore, Fig. 6.12 also shows that the remaining error when using the Vicon is two times higher for side face than for the two others when capacitive is disabled. This is a consequence of the calibration of the setup as a whole: all orientation and positioning errors add up this way. The fact that the error is higher on this face when using the Vicon, might be an additional reason why the scoring is lower compared to the two other faces and thus might hinder the hypothesis H3. Moreover, as shown in Fig. 6.12 and Table. 6.1 using the Vicon ended up leaving a constant visible gap, while using the Vive Tracker brought much more variation with cases of interpenetration upon contact. This might have affected the participant's behavior in different ways and be an additional reason why H3 could not be validated.

Whenever the capacitive sensing was used, the error at contact was drastically reduced, i.e., calibration errors and mismatches were mitigated. It seems that it can smoothen the variations between all conditions. In light of these results, instrumenting a tangible object with capacitive sensing seems to improve indeed the contact coherency, even if the tracking system used is less accurate.

The evaluation of the mean and standard deviation of the error at contact (without capacitive correction in red on Fig. 6.12) does support that using a Vicon tracker on the distal phalanx is indeed more precise and accurate tracking solution than using a Vive Tracker on the palm. Indeed, the first one has a remaining errors in millimeters while the second one in centimeters. Moreover, even when the capacitive sensing is enabled, there is still a significant difference in ratings between the two tracking systems. However, we believe that using an affordable tracking system, such as a Vive Tracker coupled with capacitive sensing, could represent a reasonable compromise compared to an expensive optical solution alone such as the Vicon. Even if it does not perform as well as the Vicon without capacitive sensing in average, the addition of capacitive to the Vive Tracker gives a better coherency for the side face and provides a smoother behavior between faces, while the overall error at contact is smaller. Furthermore, this capacitive sensing also provides

absolute contact information, i.e., a direct information about the contact itself. Thus, it could be used as an event trigger, especially instead of an unreliable position-based estimation of the contact when using a tracking system alone. For example, grasping or releasing a virtual object whenever the tangible one is actually grasped or released.

Although we only instrumented the flat surface of a cube, it is possible to instrument surfaces of any curvature as only the overall proximity from the conductive electrode and the user's skin is influencing the capacity C_p . Using an arbitrary shape would just change the behavior of the fitted curve. Simply by adjusting the fitting and some parameters, the whole method would still work. Additionally, one can also change the sensitivity of the oscillator, i.e., the detection range by changing C_0 . The smaller C_0 is, the smaller variation of C_p can be detected, the further the detection range will be. In addition, the size of the electrode also impacts the range of the detection and the width of the detection area. Therefore the technical solution can be adjusted according to the application needs. Moreover, our approach is compatible and complementary with prior studies [129, 128, 173], which could lead toward generic tabletop VR setups using a small number of dedicated tangible objects and compatible with a wide variety of virtual scenarios.

6.5 Conclusion

We presented a new approach for using tangible objects in VR, so as to achieve high visuohaptic contact synchronicity between the tangible and virtual environments. By instrumenting a tangible object with capacitive sensing, we could estimate the proximity of the user to this object. Then, we proposed a visuohaptic retargeting technique to combine the capacitive sensing and standard tracking systems information. Seamlessly merging these two pieces of information enables to adjust the position of the user's virtual finger with respect to the tangible object along the normal at its surface, so as to account for remaining relative positioning errors. Hence, avoiding interpenetration or gap between the virtual object and hand avatar, when the real hand is in contact with the corresponding tangible object.

We tested our approach in a user study enrolling 18 participants. They were asked to interact with a tangible cube in immersive VR and assess the coherency of the virtual and tangible contacts, either by using only the optical tracking (standard approach), by or combining optical tracking with capacitive sensing (our approach). We considered two optical tracking systems (HTC Vive; Vicon Bonita) and two interaction tasks (tapping on the object; approaching and touching it), yielding a total of 144 interactions per participant. Results show that our approach significantly increased the perceived coherency and synchronicity of the VR experience, correcting common relative positioning errors inerrant to the use of optical tracking systems and tangible objects. The proposed approach is compatible with any type of external tracking system and can be easily extended to different types of virtual environments and tangible objects of arbitrary shapes. However, the correction introduces unnatural motion prior contact which can be perceived by the users and hinder their immersion. Despite this issue, we believe that there are room for improvements on the capacitive signal integration and that this work is complementary of prior works on tangible objects in VR.

Chapter 7

WeATaViX: WEearable Actuated TAngibles for Virtual reality eXperiences

Sommaire

7.1 The WeATaViX haptic interface	154
7.1.1 Motivation and Consideration	154
7.1.2 Design and description	155
7.1.3 Evaluation of the device performance	157
7.2 Interaction technique in VR	158
7.2.1 Command of the Servomotor	158
7.2.2 States of the Grasp Interaction	159
7.3 User study	160
7.3.1 Static task	161
7.3.2 Dynamic Task	161
7.3.3 Results and Discussion	162
7.4 Use case	163
7.5 Conclusion and perspectives	164

Registering tangibles to virtual element comes with various limitations and constraints. In Chapter 6, we addressed the common resulting errors of the setup which prevents the users from having a simultaneous tangible and virtual contact during interaction. However, additional constraints arise when using tangible, especially when they are grounded and passive. First, they need supporting structures to be put on and are spatially constrained by the layout of the various supporting structures in the real working space. Thus, virtual objects are also constrained in space. Second, it is difficult to change between several virtual objects registered to a same tangible as this one is fixed in space, as redirecting techniques are necessary and also have their own constraints (see sec. 2.3.2.1). Third, in the case that the real work space is crowded with tangibles, each one of them needs to be registered at all times to a virtual element in order to avoid any collision from the user.

In this Chapter, we developed a haptic device which can *provide a tangible* for the users *to grasp and release anywhere in the workspace*, enabling a one-to-many registration and without any need for extra tangibles of any kind, keeping the entire real space empty. This wearable haptic interface is designed to enable a natural manipulation of tangible objects in Virtual Reality with an interaction concept between encounter-type and tangible haptics.

It can bring a tangible object in and out of contact with users' palm, rendering making and breaking of contact with, and allowing grasping and manipulation of virtual objects.

The contributions of this Chapter can be summarized as follows:

- we designed and evaluated the base performance of a unusual type of wearable device for natural manipulation of tangible objects in VR,
- we conducted a user study to evaluate the device capability to render compelling grasp and release interactions with static and slowly moving virtual objects in various configuration, while using a minimalist interaction technique,
- we designed a use case scenario in order to illustrate the potential of the approach in a comprehensive context where virtual apples are to be grasped in various places and configurations.

In the next section, we first present the concept and design of the WeATaViX and its characteristics. Then, the interaction technique used to control the device is detailed, followed by the user evaluation which investigates the capability of the device to enable a grasp and release interaction. Finally, we propose a short use case in a virtual orchard.

7.1 The WeATaViX haptic interface

7.1.1 Motivation and Consideration

Manipulation of objects in virtual reality (VR) commonly suffers from the absence of haptic sensations. As such, it is often unclear whether contact between one's virtual hand and virtual objects has been made, whether an object is properly grasped or not, and what the physical properties of the hand-object contact are. Conventional haptic interfaces for VR, be they grounded [38], body-grounded [36], or handheld [82] address this issue by applying forces to the users through an end-effector (e.g., a stylus), which mimics sensations of making and breaking contact as well as effects of mass, inertia, and collisions with the environment. However, such interactions are always mediated by the interface's end-effector, degrading the experience as the users feel that they are grasping the interface's handle instead of the virtual object. It also prevents simultaneous manipulation and exploration of the virtual object as the users hold permanently the end-effector in their hand. Encounter-type haptic displays (ETHDs) solve the issue of rendering sensations of making and breaking contact, bringing their end-effector in contact with the users only when collisions with virtual objects occur [249]. Many types of grounded [43] and body-grounded ETHDs [250] exist. However, very few tackle the issue of grasping and manipulating objects. One work in this direction is that of [47], whose device allows grasping and throwing of the tangible end-effector. However, it is dedicated to juggling and users cannot perform other kinds of manipulation. Araujo et al. [45] however, used a robotic arm whose joints can be deactivated in order to allow free manipulation of the tangible attached to its end. But, its workspace is limited to the length of the arm. However, Flyables [52] solve some of these restriction by making a small drone graspable by the user, assuming a good tracking system and adapted control scheme of the drone. Passive haptics offers an alternative solution, superimposing virtual objects with similar tangible ones to create the illusion of truly manipulating virtual entities [2]. However, maintaining consistency between the virtual and physical environments in the context of passive haptics requires adequate prop placement, scene calibration and tracking which

can add further complexity. Meanwhile, the number of required props for passive haptics increases with the complexity of the scene, making this approach unmanageable in rich virtual environments. Ultimately, these issues quickly make tangible interaction complex even for seemingly simple virtual environments. Several different approaches aiming at rendering multiple virtual objects with few tangible ones exist to address this issue. They use reconfigurable or active tangible objects [55, 251], augment passive props via wearable haptics [95] and pseudo-haptic [211], or use techniques to re-register them [129, 128].

Our novel solution, “WeATaViX”, can solve most of the mentioned issue or at least provide a reasonable trade-off. At the interface between ETHDs and passive haptics, it takes the form of a wearable encounter-type device whose end-effector is a tangible object. It aims to provide physical presence for virtual objects while remaining as simple and unobtrusive as possible. The device is grounded on the back of the hand, secured to the skin via an ergonomic adhesive silicone layer. A servo motor moves a rigid link equipped with the tangible object towards and away from the users’ palm in order to engage and disengage the tangible from the users’ grasp. Hence, the users’ hand remains free all the time and a tangible is available as soon as they reach for a virtual object, which can be anywhere in the workspace as it is attached to the users’ hand. As the device is secured to the users’ hand, the relative placement between the tangible and users’ hand mimics that of their virtual counterparts, without a real need to separately track the hand and the object. If a virtual object is in the vicinity of the virtual hand, the tangible is engaged, otherwise, it is removed. The only requirement is to display the virtual hand close enough to the real one so as to not conflict with the user’s proprioception. Additionally, using a sensor on the tangible to discriminate when the users are grasping the tangible is sufficient to control a 2 states open/close animation of the hand. Thus, it is compatible with any standard tracking system able to provide a position and orientation of the real hand, even when the tracking system is not entirely accurate, since human proprioception tolerates some errors [217].

7.1.2 Design and description

A prototype of the device is shown in Fig. 7.1. It is composed of a 3D-printed structure to be placed on the back of the hand. Its profile is slightly curved to fit the shape of the hand. On the internal side, it is anchored in an adhesive silicone skin based on work by Chossat et al. [252], guaranteeing good adherence, comfort, and adaptability to different hand morphologies and skin properties. The silicone is a rectangular solid slightly bent made of two layers. The inner one is a 1.5 mm thick adhesive layer created by mixing together Smooth-on Ecoflex 00-30 (1 part A, 1 part B) and Smooth-on slacker (2 parts) to increase adhesiveness. The second one is a 3 mm thick flexible layer made of Smooth-on Ecoflex 00-10 poured around the adhesive layer in order to stabilize the structure and prevent tearing of the adhesive layer. The 3D-printed ABS parts are anchored into the second layer via small protruding feet placed into the silicone during the curing process. Having a 4.5 mm thick rectangular thick silicone layer allows to stick to various hand morphologies. It spreads the stress due to the hand deformation and avoids having locally high stresses which could the silicone to fall. Furthermore, the silicone layer is completely painless to remove, as it does not tear off skin or hair. And it leaves no adhesive residue on the skin.

A HTC Vive Tracker can be attached on the external side of the 3D-printed structure. The distal side houses a HiTec HS-5065MG servomotor which controls the rotation of the lever arm onto which the tangible object, a foam ball, is attached in such a way as to bring it towards or away from the user’s palm. The entire structure is adaptable to different hand sizes: The servo holder’s position can be adjusted up and down along the border

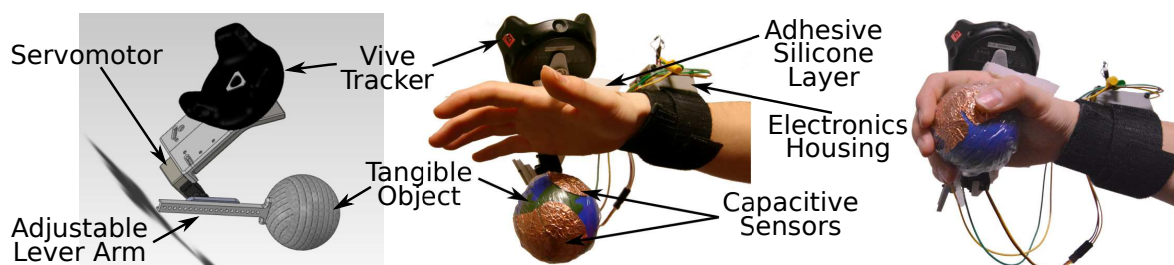


Figure 7.1: Haptic device composed of a 3D-printed part anchored to an adhesive silicone layer attached to the hand. Two capacitive sensors cover the tangible, respectively facing the palm and the fingers during grasp closure.

of the palm, while the lever arm is adjustable in length to accommodate varying hand morphology between users.

The tangible object is equipped with two capacitive sensors made of copper layers serving as electrodes and connected to an Arduino Nano which uses the CapacitiveSensor library in order to process and communicate the value of each sensor to Unity3D.

We use a pair of simple capacitive sensors (Fig. 7.1) to detect contact respectively between the user's palm and the tangible object and between the user's fingers and the tangible object. The sensors are created by wrapping a layer of copper foil around the tangible object, onto which wires are soldered and connected to inputs on a microcontroller through a simple circuit shown in Fig. 7.2. The sensor design is built around the Arduino CapacitiveSensor library running at $\approx 300\text{Hz}$ on an Arduino Nano board housed on the wrist of the user. By thresholding the computed values, it is possible to detect whenever the users are actually touching one of the two copper electrodes. A first electrode is placed on the side facing the palm to detect whenever the palm touches the tangible. It was only used for debugging and to evaluate the device performances. The other electrode is on the other side of the tangible sphere and is large enough to be sure that the fingertips touch it as the users are closing their hand to grasp the sphere. In addition, the tangible is wrapped in plastic film to hold the electrode in place and prevent the wire from moving and breaking the soldered joint. It also prevents the users from directly touching the electrode, which would just cause the sensor to collapse, but is thin enough to have large variation between contact and non-contact.

The servo motor is driven using a Pololu Micro Maestro 6-Channel USB Servo Controller housed on the wrist of the users alongside the Arduino board. A computer running the VR application at a framerate of approx. 90Hz, queries the Arduino at every frame, causing an interruption triggering the return of the current capacitive sensor values as a response. Unity application then calculates the commands to be sent to the servo motor based on the current state of the virtual environment and sends the corresponding command to the Pololu controller via USB.

The device was designed with minimal weight as a target, weighing 85 g without the Vive tracker (185 g with tracker). Fig. 7.3 shows the VR setup. The HTC Vive tracker enables hand position and orientation tracking and, together with the capacitive sensors, animation of the user's hand avatar in VR. A video of the device in action is available at <https://youtu.be/JtcEYlwogpA>.

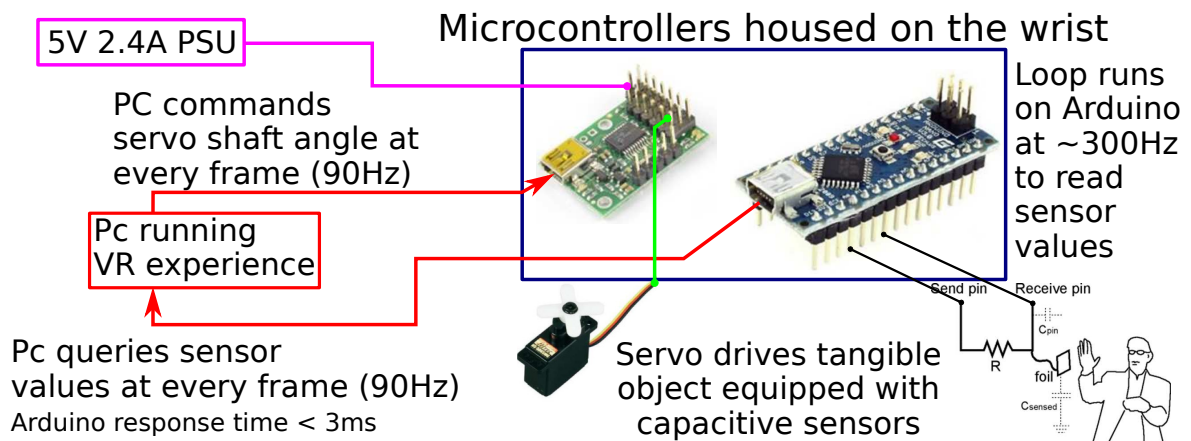


Figure 7.2: Schematic of the interconnected electronics structure for sensing and control. The capacitive sensing uses the Arduino CapacitiveSensor library.

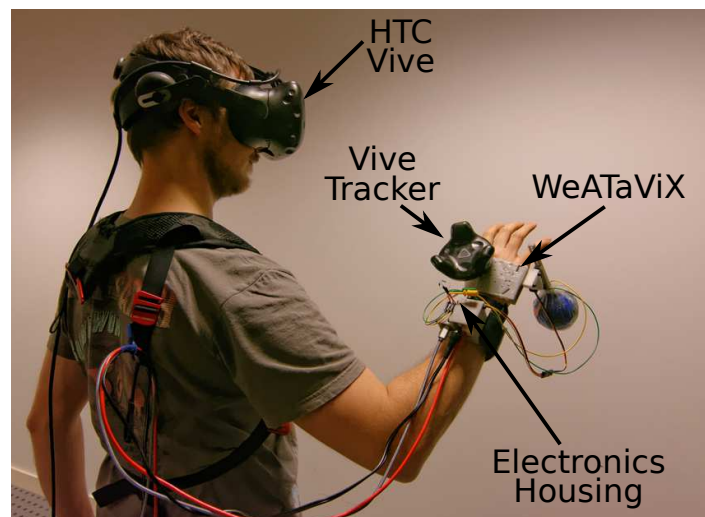


Figure 7.3: VR setup. A user is wearing an HTC Vive, the WeATaViX is attached to his hand with the silicone. The wires are attached to his shoulder as to avoid hindering his movement.

7.1.3 Evaluation of the device performance

Silicone Performance. The skin-safe silicone layer allows good adhesion of the structure to the skin even when the servomotor is active and during fast hand movements. We observed that the device continues to adhere well even after prolonged use (> 45 min) and throughout several attaching/detaching cycles (> 30 cycles).

Interaction delay. With the device mounted on a user's hand, we measured the delay between the command to engage the tangible and the contact detection on the palm, starting either far from the hand (servo shaft rotation of 80°), or very close (servo shaft rotation of 5°) to contact (0°). Over 100 trials, we measured a mean delay of 225 ms for the far position (SD 7.2 ms) and 49 ms for the near-grasp position (SD 8 ms). This leads us to estimate the fixed delay due to communication to be around 38ms and the servo shaft rotation speed to be around the nominal rotation speed of $210\text{ ms}/90^\circ$ despite the tangible object.

Influence of motor vibrations. The motor’s motion sometimes induced transient vibrations of the Vive tracker which propagated to the hand avatar. To quantify this effect, a user wore the device with the palm facing downward against a fixed supporting structure. We recorded the tracker position while applying step motions to the servo shaft using the full range of movement of the tangible to maximize such vibrations. Over the course of 20 trials, we obtained a mean stabilization time of 612 ms for the tracker, with induced positional errors up to 4.03 mm (SD 0.87 mm) and maximum angular errors of 2.76° (SD 0.43°).

7.2 Interaction technique in VR

We implemented the simplest functional interaction technique for our device, with the aim of evaluating what functionalities and limitations are thus incurred. The rendering of an interaction between the users’ hands and the tangible object uses a simple distance-based triggering paradigm: The tangible is brought toward the user’s palm as the virtual object gets closer to the reference position P_{ref} on the virtual hand. When the users close their grasp, the sensing triggers an animation of the virtual hand closing onto the virtual object at the reference position. When the users open their grasp, the virtual object is released and the tangible is driven away from the user’s palm.

7.2.1 Command of the Servomotor

Assuming there is a virtual object to grasp within range, the servomotor’s command is computed from the virtual distance between the position of the virtual object P_{obj} and the reference grasping location in the virtual hand, P_{ref} . The command of the servomotor is computed between 0 and 1, 0 being maximum engage angle for which the tangible is in contact with the user’s palm. This value is calibrated beforehand as it depends on the user. Conversely, 1 represents the maximum opening/disengaging angle.

However, we do not want the tangible to be engaged if the virtual object is behind the hand. Thus, P_{obj} is projected onto the axis orthogonal to the palm and gives the projected signed distance z between P_{obj} and P_{ref} . If $z > 0$ then the virtual object is in front of the palm and the command is computed from the distance, otherwise the object is behind the palm and the device is commanded to the open position. We will call x, y the transverse component of the projection. The command is then computed as follows:

$$c_{servo} = \begin{cases} \frac{\sqrt{IS(x^2+y^2)+nSz^2}}{d_{threshold}} & \text{if } z \geq 0 \\ \frac{\sqrt{IS(x^2+y^2)}}{d_{threshold}} & \text{if } 0 > z > d_{backThreshold} \\ 1 & \text{otherwise} \end{cases}$$

$d_{threshold}$ is the threshold distance at which the tangible starts to be engaged. In order to avoid having the tangible being engaged while the virtual object is on the edge of the palm, we introduced nS the normal scale and IS the lateral scale. Diminishing IS reduce the impact of the lateral translation on the command, i.e., the tangible is not engaged when the virtual object is near the palm but is supposed to be out of grasp reach.

$d_{backThreshold}$ is meant to avoid having discontinuity near P_{ref} : In the case where the virtual object penetrates the palm and the users do not close their hand fast enough, the tangible would disengage fully without this safeguard. In order to avoid any discontinuities, we locked the command on the normal axis for a few centimeters behind P_{ref} . In addition,

as discontinuities can still arise at $d_{backThreshold}$, a box collider was added behind the palm preventing the virtual object from crossing the discontinuity in any direction.

We set $d_{threshold}$ to 8 cm which is of the same order of magnitude as the range of motion of the tangible. nS is set to 1 by default and IS has an empirically determined value 0.08. Given human hand characteristics, we set $d_{backThreshold}$ to 4 cm which is slightly more than the average thickness of a hand.

The virtual object is subject to the simulation's physics, except when it is grasped, in which case it is rigidly attached to the virtual hand. This command is used in any state of the grasp interaction.

7.2.2 States of the Grasp Interaction

The grasp interaction is made of 3 different states: The free state when the users reach for possible tangible, the grasp state and the release states are connect as shown in Fig. 7.4. Initially, all interactible virtual objects are in a free state, and the servo shaft is kept in an open position (object out of hand).

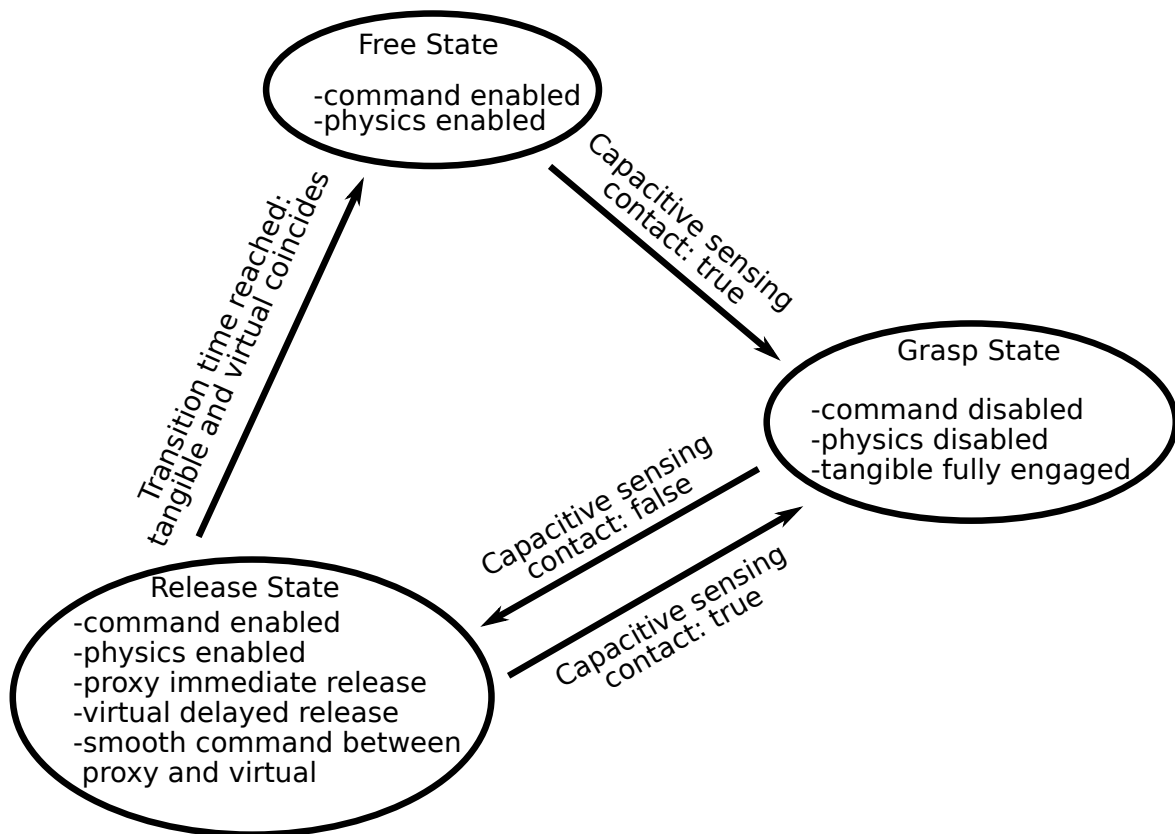


Figure 7.4: State machine of the grasp interaction.

Free State In this state, the users can open and close their hand without restriction as the tangible is disengaged until they reach for a virtual object which is subject to the simulation's physics. Whenever a virtual object comes close enough to the users' hand, the motor's shaft angle is driven as described in Section 7.2.1, moving the tangible object towards the user's palm. In the case where several virtual objects are within reach, the closest one is selected to compute the command, which allows to avoid any discontinuities.

Once the virtual object is close enough to the virtual hand, the tangible is already close to the users' palms. As soon as the users' fingers touch the capacitive sensors through grasp closure, the virtual object drifts to the predefined grasping location, fitting a natural power grasp while the hand avatar is animated to envelop the virtual object. The transition toward the grasp state is then complete.

Grasp State In the grasped state, the virtual object's physics are deactivated and the virtual object is attached to the closed virtual hand while the tangible is fully engaged and held by the users. As soon as the users release their grasp, the capacitive sensing trigger the transition toward the release state.

Release State Since the haptic device has some perceptible delay, we designed an interaction which releases the tangible a bit earlier than the virtual release. Instead of releasing the virtual object 38 ms later (mean delay of the device) which can produce discontinuities, we chose another approach to guarantee a smooth transition: Upon release of the physical grasp, an invisible virtual proxy is released with a position computed from the hand speed, and followed by the virtual object 10 ms later, re-enabling its physics. The tangible is immediately driven by smoothly interpolating the command position between that of the proxy and that of the virtual object over 100 ms (see Fig. 7.5). This solution masks the device response time when releasing an object, making releasing interactions more synchronous between haptics and vision by voluntarily introducing a controlled delay in the visual rendering.

In addition, the command of the servomotor is computed as usual, taking into account whether the users are moving their hand immediately away from the virtual object or not. If the users reach for the virtual object again and grasps it, it will trigger the system into the grasp state. Otherwise, the system switches back to the free state once the interpolation of command position catches up with the visible virtual object. Although simple, this interaction technique elicited positive feedback from users involved in our user study.

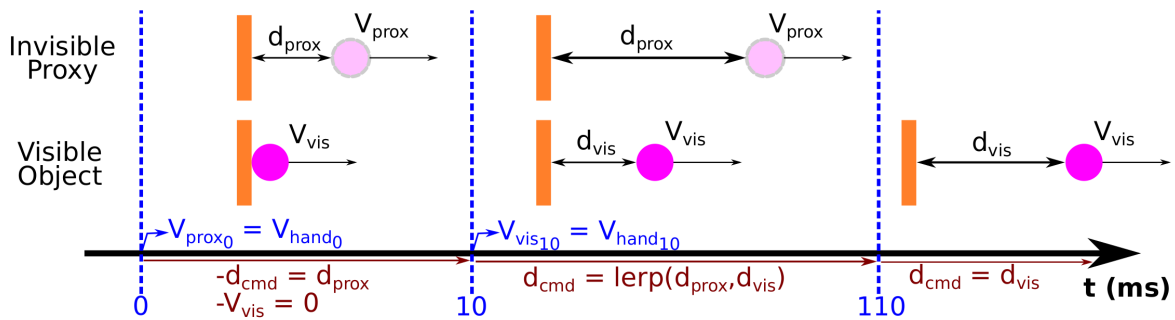


Figure 7.5: Invisible proxy and visible object are released at 0 ms and 10 ms with the current hand speed v_{hand} . Their positions relative to the predefined grasping location in the virtual hand (d_{prox} , d_{vis}) are used to compute a smooth command d_{cmd} .

7.3 User study

We conducted a user study to evaluate our device and interaction technique in VR. We designed tasks covering a wide range of grasp and release interactions with different object speeds and positions relative to the user in order to determine the range of interactions supported by our device. 14 right-handed subjects (10 males, 4 females; ages 22-58 ($M=29$))

participated in the study after providing written informed consent. Subjects wore the haptic device on their right hand, adjusted for their own power grasp. They viewed the virtual environment through a HTC Vive HMD, and held a Vive controller in their left hand to answer the experimental questions. We evaluated grasping and releasing in a static task where the virtual objects did not move, and in a dynamic task where the objects moved and had to be caught by the user. The virtual tasks lasted around 45 min per participant.

7.3.1 Static task

In the static task, we evaluated grasping and releasing behaviours of a spherical virtual object to be grasped and put back from different orientations. Our intent was to evaluate both interaction performance and believability for different picking and placing approaches.

Experimental task. Subjects stood facing a 10-cm-side cube (see Fig. 7.6-A) with the object appearing on one of its faces. Participant had to remove their hand outside of an 80cm-diameter interaction region centered on the cube, to unlock the start of the trial. The start was triggered by entering the interaction region. Then, they had to grasp and pick up the object using their dominant hand and bring it outside of the interaction region, after which they answered a first experimental question regarding synchronicity of the haptic and visual grasping interaction. They responded using a 5-point Likert scale ranging from “Not at all synchronous” (0) to “Totally synchronous” (5).

In the second part of the interaction, starting outside of the interaction region, they had to precisely place the object back onto a highlighted face of the cube. The object turned green when in the region where releasing it would be counted as successful and turned red if the object was intersecting the face of the cube, to signify a failure in case of release. Upon releasing the object, they answered another question regarding synchronicity of the haptic and visual release using the same 5-point Likert scale. If at any point during the trial the subjects accidentally caused the object to drop, the trial was considered a failure. Subjects were instructed to minimize failures and task execution times.

Experimental Procedure Participants began by performing 3 practice trials, then performed a total of 108 trials covering all combinations of grasping and releasing orientations with 3 repetitions each. After the trials, subjects filled out a subjective questionnaire evaluating realism and ease of the interaction, device wearability and obtrusiveness, and task difficulty on a 5-point Likert scale.

7.3.2 Dynamic Task

In the dynamic task, subjects were to catch virtual objects traveling at different speeds and arriving at different locations relative to their body.

Experimental task A cannon fired a single spherical object in a linear trajectory chosen amongst 7 options (see Fig. 7.6-B.2). The object travelled at one of three speeds: 1 m/s, 2 m/s or 3 m/s. Speeds and trajectories were chosen randomly such that an equal number of each speed was attempted for each trajectory and an equal number of attempts was made per trajectory. Subjects failed the trial if they failed to catch the sphere and immediately proceeded to the next. After each catch, they were asked to rate synchronicity between the physical and virtual interaction, responding using the same 5-point Likert scale as in the static task.

Experimental Procedure Subjects performed 3 practice trials, a total of 105 trials covering all combinations of object speeds and catching locations with 5 repetitions each, after which they filled out a similar subjective questionnaire to those from the static task.

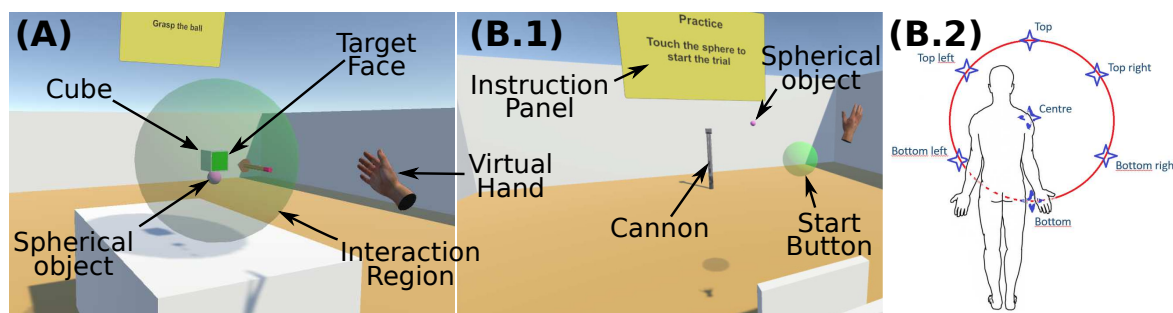


Figure 7.6: Static (A) and dynamic (B.1) task environments. (B.2) The 7 catching positions.

7.3.3 Results and Discussion

Static task. There was no visible effect of picking or placing position for all metrics, indicating that our device allowed similar task performances regardless of configuration, despite a single physical object approach and release direction. Task times were measured between the moment subjects entered the interaction region to the moment they respectively left it with the object in hand or completed the placing task. Picking task times were consistent within subjects, but variable between subjects ($M=2.51$ s, SD 1.98 s). Placing task times followed a similar pattern ($M=2.31$ s, SD 2.56 s). These task completion times indicate the device allows picking and placing interactions in reasonably short times.

We measured the time between user's grasp closure and the contact between the tangible sphere and the palm of the hand. While the measured values cannot provide any definitive conclusions, as subjects might prevent or delay the contact between the object and their palm by gripping it with the fingers, we can draw tentative conclusions based on the sign of this delay which informs us about whether subjects react or anticipate arrival of the tangible in their palm. About half the population grasped the tangible object with the fingers first, while the other half waited for the physical object to collide with their palm for closing their grasp, which is an important consideration for the design of interaction techniques intended for assisting subjects during grasping.

Subjects were consistently successful in both picking and placing tasks ($M=96.03\%$, SD 5.51% for picking; $M=86.24\%$, SD 9.04% for placing). Combined with the short task completion times, this is indicative of high adequacy of our device for grasping and releasing static virtual objects. We measured grasping positional error as the absolute distance separating the virtual object and the grasping position on the palm at the time of detected grasp closure. It appears all grasping orientations yielded similar errors ($M=2.6$ cm, SD 1.1cm). Subject's evaluation of picking synchronicity appears to positively correlate with grasping positional errors. Overall, subjects rated picking interactions as synchronous ($M=3.91$, SD 0.86) and placing interactions as even more synchronous ($M=4.17$, SD 0.92), but not significantly.

Grasped objects were perceived as realistic ($M=4.14$, SD 0.66), again reflecting adequacy of the device to manipulating static virtual objects. Users overall felt only moderately free in their movements ($M=3.71$, SD 0.82). They reported device weight, motor vibrations and wiring as sources of obtrusiveness, rating the device as only moderately unobtrusive ($M=2.71$, SD 0.73), indicating that the device was a bit heavy, that motor vibrations and

shifts in mass during movement were slightly disturbing, and that the wiring and wrist assembly as well as the tangible object holding rod could sometimes be felt. This highlights the need for compact, wireless and lightweight designs for such devices. Subjects reported high perceived virtual hand ownership ($M=4$, $SD\ 0.55$), indicating that even with very rudimentary animation of the virtual hand our system is capable of maintaining immersion. The task was reported as being moderately easy ($M=3.42$, $SD\ 0.94$) and did not cause excessive fatigue to subjects on average ($M=2.64$, $SD\ 1.15$), though this varied a lot from subject to subject. Subjects pointed out the disturbing device weight during prolonged use, making further weight reductions as a future design priority.

Regarding different picking orientations, subjects reported the Right, Top and Bottom faces as easiest ($M=4.29$, 4.36 and 4) while the Front, Rear and Left faces were reported as the hardest ($M=3.93$, 3.28 and 3). Interestingly, the bottom face was perceived as easy although grasping precision was the poorest on that face, and similarly the left face was perceived as hard although grasping precision was higher than average on that face. Subjective difficulty more or less reflects grasping precision for the other 4 faces. Regarding different placing orientations, the right and top faces were ranked easiest ($M=4.29$ and 4.14 resp.), the other 4 orientations are similarly easy going from Front to Bottom to Rear and Left ($M=3.57$, 3.29 , 3.14 and 3). Subjects did not report noticing the visual delay introduced by our interaction technique during object releases.

Dynamic task. Regarding grasp closure delay, in this task, almost all subjects tended to close their fingers ahead of the contact between the tangible object and the palm, indicating that subjects adapt their behavior to the task. These adaptations should be taken into account when designing interaction techniques supporting a wide range of tasks. Catching position did not seem to affect this metric. Caught objects were perceived as moderately unrealistic ($M=2.93$, $SD\ 1.07$), far below the perceived realism in the static task (means significantly different, $p < 0.001$, 2-sampled t-test). This is to be expected as the catching task amplified the perceptual effects of delays in our system. Subjects again felt moderately free in their movements ($M=3.43$, $SD\ 1.09$) and rated device obtrusiveness similarly to that in the static task ($M=2.57$, $SD\ 0.76$). Subjects reported a lower perceived virtual hand ownership than in the static condition ($M=3.07$, $SD\ 1$; means significantly different, $p < 0.01$, paired t-test). Device limitations in the dynamic task combined with task difficulty seem to negatively affect the capacity of the device to ensure immersion. This highlights the need for improving the interaction technique if dynamic tasks are to be executed. Subjects reported that even on failed tasks, when the ball hit the hand and bounced off, the tactile feedback felt realistic. However, they also reported perceived delays in the haptic feedback which complicated the task and led to low perceived realism. Finally, the device required users to adapt their catching strategy, leading them to perform unnatural movements. This highlights a limitation of the current device and interaction technique when interacting with fast moving virtual objects.

7.4 Use case

To showcase the adaptability of our device to multiple interactible virtual objects as well as the freedom of movement it provides, we designed a use case in which the users can freely roam about a virtual orchard, picking apples from trees, the ground, or tables, catching them as they fall, and even using them as ammunition in a game of "knock the cans" (see Fig. 7.7). A video summarizing our work, shows an extended exploration of the virtual

Orchard at the following link <https://youtu.be/JtcEYlwogpA>.



Figure 7.7: Use case: (A) Pick and throw an apple; (B) Catch an apple falling from a branch.

7.5 Conclusion and perspectives

We presented and evaluated a novel wearable haptic interface at the boundary between encounter-type displays and passive haptics. The device is grounded on the back of the hand thanks to an ergonomic adhesive silicone layer and uses a servomotor to bring a tangible object towards and away from a user's hand. We described a simple interaction technique for VR allowing users to naturally grasp, manipulate and release objects while receiving compelling haptic feedback.

Our device provides a simple and effective solution for tangible interaction with multiple virtual objects in large workspaces, with high adaptability to virtual environments. By grounding the device on the back of the user's hand, our system is unaffected by tracking issues influencing conventional passive haptics. Furthermore, by mixing aspects from tangible haptics and encountered-type displays, our work opens perspectives towards ETHDs that provide the possibility of manipulation and object exploration through grasp closure.

While our current solution only features a single fixed tangible, the ultimate goal will be to provide interactions with interchangeable or reconfigurable end-effectors in order to increase adaptability. Our device received positive feedback from users during its experimental validation, however several issues and limitations remain to be overcome. In the short term, it will be necessary to make our device at least partially wireless and more compact to increase portability and freedom of movement. Also, a reduction of the carried mass, introduction of mechanical damping elements between the servo and tracker, and improvements to the control law are avenues we wish to explore to overcome the issue of unwanted vibrations.

Chapter 8

Conclusion

In this manuscript, entitled "Haptic Rendering in Virtual Reality during Interaction with Tangibles", we focused on the use of *tangibles* to provide rich and compelling feedback with regards to the virtual objects to which they are registered, during interaction in a VR context while using HMD. We addressed several aspects which can influence the immersion of the user in two main axes of research. The first axis focused on *improving the rendering of virtual objects using discrepant tangibles*, while the second axis addressed *improving the registration between tangibles and virtual objects*.

In Part I of this manuscript, we worked toward the elaboration of various strategies to render a virtual element with a tangible while maintaining an acceptable level of immersion. We proposed three approaches: 1) *altering the perception* the user has of the tangible, 2) *intentionally inducing unnoticeable discrepancies* between the tangible and its virtual representation, and, 3) *pairing a single tangible to multiple elements of the virtual environment*.

Chapter 3 focused on *altering the perception* the user has of a tangible by combining it with a wearable haptic device in order to improve the display of stiffness sensations in virtual environments. The skin pressure provided by the hRing served as an additional cue which added to the tangible's stiffness and altered the overall perceived stiffness. A proof-of-concept was developed where the perceived stiffness of real/tangible objects was arbitrarily augmented by providing timely tactile stimuli at the fingers. Then, a user study showed that adding the tactile pressure does increase the perceived stiffness. In addition, it showed that it is not necessary to convey the tactile stimuli exactly where the interaction with the real object happens, e.g., at the fingertips. In fact, providing tactile stimuli at the middle and proximal finger phalanges or even on the other hand enables more direct and natural interaction with the real environment as the fingertip remains free, while there is little degradation of the haptics performance. Finally, we illustrated our approach both in VR and AR, within several use cases and different tangible settings, in order to dynamically increase stiffness globally or locally according to virtual events.

Chapter 4's focus was set on *intentionally inducing unnoticeable discrepancies* between a tangible and the virtual element registered to it, by altering the virtual element on three independent haptic properties when pinching between the thumb and index: width, local orientation, and curvature. In order to assess the threshold of induced discrepancy at which users can unconsciously perceive a difference during pinching, we designed user studies enabling us to determine the Just-Noticeable Difference. These results were consistent with similar perceptual results in the literature. In addition, they suggested that it is indeed possible to make use of imperfect human perception in order to come up with techniques

relying on tangibles which are globally different to the virtual elements.

Chapter 5 focused on *pairing a single tangible to multiple elements of the virtual environment* of matching properties. To do so, we proposed a grasp matching method which registers grasp poses of tangible and virtual objects together, without any regard for the overall shape of these objects. The developed algorithm is able to generate and compute haptic-salient properties of pinch poses on the different objects. Despite having different shapes, the objects can be registered as long as the haptic cues at the tangible pinch location are compatible with the virtual representation. Finally, a user study was conducted and showed that the algorithm could combine several haptically-salient objects' features to find corresponding pinches between the given tangible and virtual objects without significant difference between a simple grasp task and a grasp and lift task.

In Part II of this manuscript, we addressed the second axis around the common limitations and constraints occurring when registering *tangibles* and virtual objects together. We proposed addressing these registration issues on two different scales: 1) on a finer scale, by *compensating setup errors to achieve contact synchronization* between both real and virtual hand/object contacts, and, 2) on a wider scale, by *providing a tangible to grasp and release anywhere in the workspace*, without any spatial restriction.

Chapter 6 focused on the local aspect of hand/object interaction. We addressed the issue of the *remaining positioning error* which classically arises *when registering tangible and virtual elements together*. We first proposed an approach to *compensate* such error *upon contact between the user and the tangible object*. We instrumented a tangible with a custom capacitive sensor to assess the proximity of the user's hand in order to retarget the virtual hand toward the surface of the virtual object as the real hand gets closer to the tangible's surface, thus, synchronizing both virtual and tangible contacts despite the initial positioning error. Finally, a user study was carried out with two different hand tracking solutions, fingertip tracking and palm tracking. It showed that combining capacitive sensing with optical tracking improves the *visuohaptic synchronization of tangible and virtual contacts*.

Chapter 7's focus was devoted to whole workspace scale considerations of hand/object interaction. We designed a device that enables the user to *grasp a virtual object anywhere while providing an actual tangible* within his hand. It is an extremely simple and light weight device, at the intersection of wearable and encounter-types as it is attached to the back of the hand with adhesive silicone, leaving the inner part free and with a single servomotor is able to rotate a tangible toward or away from the user's palm. It enables natural grasp interaction as the tangible is brought within grasp reach whenever the user reaches for a virtual object. As the tangible is controlled to reproduce the object/hand proximity happening on the virtual side, there is no need to track the tangible independently. Furthermore, it is compatible with any standard tracking system able to provide a position and orientation of the real hand that does not conflict with the user's proprioception. Then, we used an interaction technique as simple as possible to assess the capability and limits of the device in a user study. Results showed that the device can render compelling grasp and release interactions anywhere in the workspace with static and slowly moving virtual objects.

Future Works

This section addresses the current limitations of the interaction techniques and interfaces that were presented in this manuscript and proposes possible solutions that could be

investigated as future work.

Enhancing the Stiffness Perception of Tangible Objects in Mixed Reality Using Wearable Haptics

- **Decrease Stiffness.** The current approach can increase stiffness by simply adding a synchronized tactile stimulus. However, it is not possible to decrease it. An idea would be to pre-pressure the fingertip and release the pressure as the user presses on the tangible object with an adequate pressure/displacement relation.
- **Increase the effect.** Adding visual and pseudo-haptic effect to our approach should allow us to further increase perceived stiffness. Either by amplifying or attenuating the virtual motion compared to the actual motion of the user's hand, similarly to Dominjon et al. [211]. Or, by introducing delays into the system, since Knorlein et al. [235] showed that delaying the haptic feedback resulted in decreased perceived stiffness, while visual delays caused an increase in perceived stiffness.
- **Testing our approach in concrete VR applications** We also suggest carrying out further user studies to evaluate our approach in concrete applications (medical, industrial, entertainment) similarly to our use cases.

How Different Tangible and Virtual Objects Can Be While Still Feeling the Same?

- **Determine Weber's Fraction.** Only one reference value was used for each experiment. However, more reference values would be needed to determine Weber's fraction for each feature.
- **Extend to Other Parameters.** Next steps could be to induce discrepancies onto other parameters, such as inertia, texture, roughness, etc. These would definitely open novel opportunities for using a reduced number of tangible objects to render multiple virtual ones in VR.
- **Extend to other Interactions.** Pinching is not the only way we commonly interact with objects. It could be interesting to extend the study to similar features for different grasping poses (Medium Warp, Writing Tripod, etc.), or interaction other than grasping, like index or full palm touch.
- **Change tangible.** As already stated, it could also be interesting to use the virtual object as a reference and change the properties of tangible ones, to observe whether there are any biases.

Toward Universal Tangible Objects: Optimizing Haptic Pinching Sensations in 3D Interaction

- **Additional Criteria.** Our algorithm does not consider that humans have fingertips of different sizes and compliance, which might affect how they perceive a surface. Moreover, we only considered a reduced number of criteria for our metric. For future work, it would be important to include other perceptually-relevant properties, such as the object's texture, the eccentricity of the pinch or even extend the inertia

related criteria to transverse components. It also does not consider the relative importance of our different criteria, which should be carefully weighted according to their perceptual relevance in grasping.

- **Relative Pinching Orientation.** Along the principle component, the pinch poses also have their own orientation. When already registering a TO and VO with a primary pinch, we could take the orientation of the other pinches into consideration in order to find secondary pinching. This would allow the user to grasp the pair at several poses with a single registration, enabling bimanual pinch interaction on the same tangible.
- **Interaction Technique.** The interaction techniques used to grasp the objects can be improved, to ensure that the user always grasps the objects at the right location and to remove the introduced delay. For example, adding touch-sensors onto the tangible.
- **Adding a New Shape.** It would be interesting to conduct a similar experiment while introducing a virtual shape which does not exist onto the tangible object, e.g. a pyramid, and see if the participants could tell if the primitive was ever actually grasped.

Capacitive Sensing for Improving Contact Rendering with Tangible Objects in VR

- **Unnatural Motion.** The correction introduced unnatural motion prior contact which can be perceived by the users and hinder their immersion. As the interpolation relies on a mean fitting over five participants, the capacitive sensing can over- or under-estimate the distance to the surface as the signal/distance relation for each participant can either be above or below this mean. As a result, the motion of the virtual hand can be accelerated or slowed down with respect to the real hand, breaking the 1:1 ratio between real and virtual hand movements. Participants reported perceiving such behavior.

As the signal is not used when the participant's hand is still far from the electrode, a solution could be to not fit the whole curve but only where it is almost linear, i.e., near contact. Then we can confront several models: global fitting, personal fitting, or even a simple linear model with various slopes. When participants are focused on an actual task, it is conceivable that a linear model with a slope chosen beforehand by the user might be sufficient.

Another solution could be to rely on a dynamic correction: for example by computing the offset between the tracking and the capacitive when the first contact occurs and then update this offset at each tangible contact, hence, minimizing the redirection.

A final solution could be to use a better data fusion algorithm such as a Kalman filtering, however a whole model has to be developed based on the chosen tracking solution and the features and needs of the VR application.

- **Electronics Calibration.** Another limitation is that a calibration is needed to determine the resting resonance frequency f_0 of the circuitry when a new electrode is plugged. Moreover, this frequency tends to shift with temperature or capacitive change in the environment. However, this could be solved with a script regularly checking for f_0 , whenever the user is outside of its detection range.

- **Toward a Wireless solution.** In order to allow the user to grasp and lift the tangible, it could be interesting to make the sensor wireless. However, making this capacitive sensing wireless might be challenging: The capacitive sensor needs to be grounded and the easiest way to do so is by grounding the power supply. Moreover, its calibration is dependent on the surrounding which might change whenever the tangible is moved elsewhere. However, it might be possible to get around this limitation by designing a docking system which would re-connect the electrode and enables back the sensing when the object is put down.

WeATaViX: WEearable Actuated TAngibles for Virtual reality eXperiences

- **New structural design.** In the short term, it will be necessary to make our device at least partially wireless and more compact to increase portability and freedom of movement. Our user study highlighted the issue of the device's mass still being too high for comfort. This is mainly due to the use of a Vive tracker and the fact that we did not fully optimize the design for minimum mass: lowering printed volume, plastic assembly screws and a lighter tracker could solve this issue. The current design is focused on VR environments containing no physical objects. But this is also somewhat a limitation regarding the footprint of the device around the hand, which limits potential interactions with tangible surfaces (e.g. walls, the floor, and other physical objects in the environment) as well as with the user's own body. The system is wired and thus does not fully profit from its mobile capabilities. Making it fully mobile would require a wireless solution, which entails battery power, lightweight batteries and electronics issues (grounding for the capacitive sensing to work). Lastly, making a thinner layer of silicone with non-adhesive protruding rings to secure the silicone around the fingers might help in reducing the total mass while spreading the load over the hand. However, we have to be careful on the design as thinner silicone tends to have a higher stress gradient (especially due to torsion) which can prevent it from adhering to the skin. Using a stickier silicone can also be considered to find an acceptable compromise.
 - **New actuation.** The current actuation solution, despite being cheap and easy to use, is not optimal. We observed unwanted vibrations of the tracker induced by the servomotor as well as delay in the actuation which hindered interaction with moving objects. A solution would be to use a small motor with an encoder in order to design a more robust close-loop with an adequate corrector.
 - **New interaction techniques.** There is currently only a single reference position for interacting perfectly and as the tangible object lags behind, the temporal window for the user to close his finger decreases. Hence, without assistance grasping moving virtual object requires some learning of optimal interaction strategies for the device. Developing new interaction techniques with visual aids, contact prediction, and possibly, re-targeting toward the grasp reference position, or, sticking the virtual ball to the virtual hand for a short laps of time might compensate these shortcomings.
- Additional capacitive sensors.** Currently, the device only allows a single physical grasp position. Additional capacitive sensors should allow a differentiation of grasps and thus a much wider range of object manipulations. Our interaction technique also only admits a single optimal virtual grasping location, so by providing the user with various forms of grasping assistance may improve usability.

New rendering techniques. Since the tangible is controlled in position, it should be possible to make it apply more or less pressure in the users' palm or fingers by moving it around the reference position so as to render various weight and inertia. We could go further in adaptability by changing the nature and shape of the end-effector or even by embedding tactile actuators onto the device to provide additional feedback such as vibration, or skin stretch.

Long term perspectives

Tangible Tabletop for VR

In this manuscript, we proposed several methods for rendering virtual objects using tangibles: either by adding tactile cues with a wearable haptic or by making use of acceptable levels of discrepancies between tangibles and virtual objects. These approaches are compatible with prior work using tangibles and focusing on the re-registration of the tangible 2.3.2.1, making them reconfigurable 2.3.2.1, altering their haptic properties 2.3.2.4 through various means, or simply repositioning them using ETHDs 2.3.2.5. Moreover, as we proposed a capacitive solution to ease the registration of tangibles and virtual objects, especially upon interaction but which requires electronic wiring, one could think of developing a table scaled version similar to Rekimoto's [245] but in compliance with specific VR needs. This tangible tabletop for VR could be a dedicated setup, just like containing various tangibles providing base tangible interactions, while the virtual objects could be rendered using the previously mentioned approaches to enable more complex interactions. In addition, complementary wearable devices could be designed to provide the just-necessary [16] additional feedback to dynamically modify the perceived properties of the tangibles. Lastly, a more complex version of such a setup could rely on encounter-type devices as Huang et al. [59] did by providing slots on a rotating rack onto which tangibles are placed.

Toward Universal Tangibles

In this manuscript, we proposed a method which matches grasping poses of similar properties between tangible and virtual objects to register them together in the virtual environment and suggest a grasping pose to the users that will prevent them from noticing the discrepancies between both objects. As the users are engaged in a task, and know that grasping it elsewhere would impede their immersion, they should be more disposed to grasp the virtual object at the design location.

However, we only consider pinching in our work; extending our approach to other types of grasping should be possible. Our approach can be generalized to any kind of grasping: generating the corresponding patches and poses, extracting their properties, computing a cost function to compare them, and extracting the best matches. For example, extending our method to precision grasps with 3 fingers would require extending the description of our poses to a third contact patches which would be geometrically contained with the other two and add new criterion. The whole Human Grasp Taxonomy [60] could be addressed in this way to provide a virtual scene to a larger pool of matching between tangibles and virtual objects.

Moreover, one could develop a whole Universal Tangibles framework where tangibles are tracked and analyzed in real time in a similar fashion to Hettiarachi [140], to suggest several possible valid grasping of different kinds and at different locations to the users.

Alternatively, it should be possible to generate a set of tangibles with various kinds of generic shapes which could be matched to plenty of different virtual objects through multiple hand grasps. Once we have various grasp poses and their characteristics, we can recreate the corresponding patches in a 3D frame and fill the holes between them to create a complete mesh, i.e., generate a new object. As for obtaining the necessary grasping poses, we could compare all virtual objects of a VR environment using our approach and keep the best matches across the largest number of virtual objects. This would result in fewer tangibles while each one has multiple possible registrations with virtual objects.

Appendix A

Author's publications

Journals

- **X. de Tinguy**, A. Lécuyer, C. Pacchierotti, M. Marchal. "Capacitive Sensing for Improving Contact Rendering with Tangible Objects in VR". In *IEEE Transactions on Visualization and Computer Graphics*, Vol.27, no. 4, pp. 2481-2487, 2021.
- D.S.V. Salazar, C. Pacchierotti, **X. de Tinguy**, A. Maciel, M. Marchal. "Altering the stiffness, friction, and shape perception of tangible objects in virtual reality using wearable haptics". In *IEEE Transactions on Haptics*, Vol.13, no. 1, pp. 167-174, 2020, **Honorable Mention**.

International Conferences

- **X. de Tinguy**, T. Howard, C. Pacchierotti, M. Marchal, A. Lécuyer. "WeATaViX: WEearable Actuated TAngibles for Virtual reality eXperiences". Two first authors. In *Proc. of Haptics: Science, Technology, Applications: 12th International Conference, EuroHaptics*, pp.262-270, 2020.
- **X. de Tinguy**, C. Pacchierotti, M. Emily, M. Chevalier, A. Guignardat, M. Guillaudeux, C. Six, A. Lécuyer, M. Marchal. "How Different Tangible and Virtual Objects Can Be While Still Feeling the Same?". In *Proc. of IEEE World Haptics Conference*, pp. 580-585, 2019.
- **X. de Tinguy**, C. Pacchlerotti, M. Marchal, A. Lécuyer. "Toward Universal Tangible Objects: Optimizing Haptic Pinching Sensations in 3D Interaction". In *Proc. of IEEE Conference on Virtual Reality and 3D User Interfaces*, pp. 321-330, 2019.
- **X. de Tinguy**, C. Pacchierotti, M. Marchal, A. Lécuyer. "Enhancing the Stiffness Perception of Tangible Objects in Mixed Reality using Wearable Haptics". In *Proc. of IEEE Conference on Virtual Reality and 3D User Interfaces*, pp. 81-90, 2018.

Demo & Contest

- **X. de Tinguy**, T. Howard, C. Pacchierotti, M. Marchal, A. Lécuyer. "WeATaViX: WEearable Actuated TAngibles for Virtual reality eXperiences". **Demo at EuroHaptics**, 2020, **Best Demo Award**.

- H. Brument, R. Fribourg, G. Gallagher, T. Howard, F. Lécuyer, T. Luong, V. Mercado, E. Peillard, **X. de Tinguy**, M. Marchal. "Pyramid Escape: Design of Novel Passive Haptics Interactions for an Immersive and Modular Scenario". *In Proc. of IEEE Conference on Virtual Reality and 3D User Interfaces, 3DUI User Interface Contest*, pp. 1409-1410, 2019, **Best 3DUI Demo Award**.

Appendix B

Tracking Solution

In Chapters 4, 5 and 6, we used a tracking system relying on 7 Vicon cameras combined with a Blade software in order to track the motion of the user's fingertips. This system is compatible with the HTC Lighthouses and rely on the reconstruction of the position of markers in space. Each marker is labeled and composed specific constellations which position and orientation can be reconstruct if at least 3 markers are available. We used one constellation for the thumb and one for the index, for a total of 6 markers tracked at the same time. In these Chapters, users had to interact with tangible objects by grasping, lifting or simply touching them. However, embedding a constellation of markers on these tangibles was not possible as there could have been occlusions between the 2 constellations of the fingers and the one on the tangible, preventing the system to correctly reconstruct the various positions and directly hindering the virtual representation of the interaction with the tangible. Moreover, 3D-printing a support for the markers on the tangible would have change its weight distribution and users could have possible hit it during the experiments. Thus, we came up with the idea of indirectly tracking the tangible by putting them on a support which position was fixed and calibrated beforehand.

In this Appendix, further detailed will be given on the system: First a general overview will expose the whole components of the apparatus. Second, we will detail how the tangibles are indirectly tracked. Then, we will explain how the thumb and index are tracked using 3D-printed attachments housing the constellations of markers, and how the virtual avatars are calibrated to superimposed correctly the real fingers.

General Overview

In order to enable manipulation of tangible objects in VR using a HTC Vive, we developed a tracking solution which rely on the use of 7 Vicon cameras with Blade which can tracked markers in space, coupled with a calibrated support onto which objects can be put (Fig. B.1). Tracking several markers forming a constellation allows us to reconstruct the position of the user's thumb and index. However, we avoid putting a constellation of markers on the object itself as it is small and occlusion could occurs if too many markers were present at the same time in a reduced space, i.e., when the users are grasping the tangible. However, we can make strong enough assumptions on the tangible object's position so that whenever the users are touching or pinching the virtual object using the virtual hand/fingers, they actually pinch or touch the corresponding tangible with their real hands/fingers. This can be achieved by positioning the tangible accurately with respect to the virtual elements, i.e., on a fixed tangible support whilst the tangible is put down, or between the users' fingers whilst it is lifted.

With this setup, there are 3 different frames which needs to be correctly aligned: the VR frame coming from the HTC Vive and SteamVR software, the Vicon and Blade software, and the tangibles (a table with tangible props on it).

It is essential to ensure that the relative positioning between the real hand/fingers and tangible objects are accurate, as the virtual hand has to touch the virtual object as the real one touches the tangible. However, the positioning of the virtual elements with respect to the user is not as essential since human proprioception is not as accurate [217]: the virtual hand can be imperfectly superimposed with the real one as long as the same mispositioning occurs between the tangible and the virtual object. Since, the VR frame tends to drift a little bit over time when using a first version of the HTC Vive, we reconstructed the relative positions of the virtual elements (hand/fingers and objects) and the virtual rendering of the touch/grasp in the Vicon’s frame, and only then, re-position everything in the VR frame.

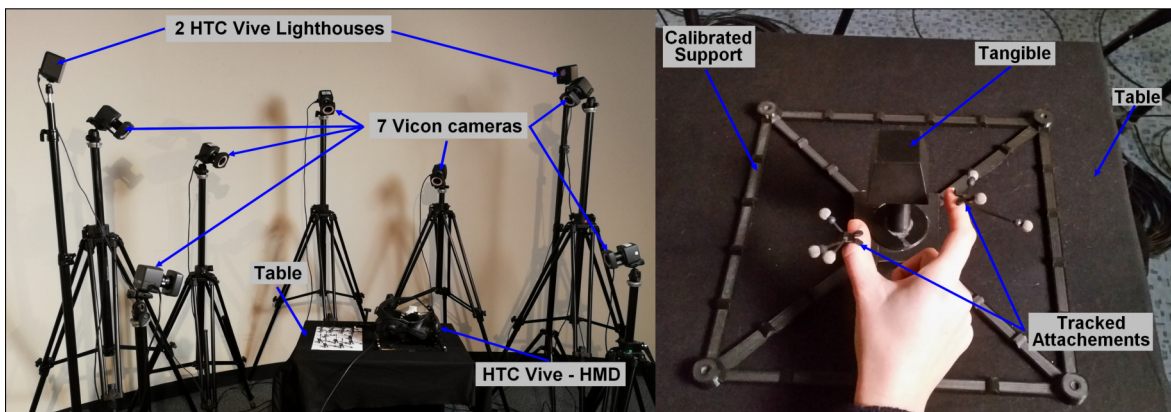


Figure B.1: Tracking Setup to enable tangible and finger tracking.

Tangibles indirect Tracking

In order to indirectly track the tangible, we come up with a solution where the position of the tangible is constrained: either the object is put at a specific spot on the table, or it is currently hold between the user’s thumb and index (which tracking will be discussed in the next section).

We designed a large support which is fixed to the table (see Fig. B.2). The support possesses marker holders at each corner. Using only 3 markers, we can reconstruct the position of the center of the support as well as its orientation in the Vicon’s frame. Once an object is placed on the support, it’s relative position to the support is known. Hence, we can deduce the position of any face of the tangible in space.

As long as the tangible is on the support, its position and orientation are known. Once the users lift it, we can assume that it is between the thumb and index. However, in order to still know the position of the tangible when the users put it down, we designed a tangible receiver part on the support which is made of a 3D smooth shape and containing 2 magnets (see Fig. B.3). Below the tangible is a complementary shape within which 2 other magnets are located. The combination of magnets and the flared smooth 3D shapes allows to guide the tangible toward the right location if is slightly misaligned as well as prevent it from falling on the side. When the tangible is fully connected to the support, air gaps remain between the ferrite magnets in order to reduce the amount of force users have to excrete to detach the tangible from the support, while still being strong enough to stabilize it.

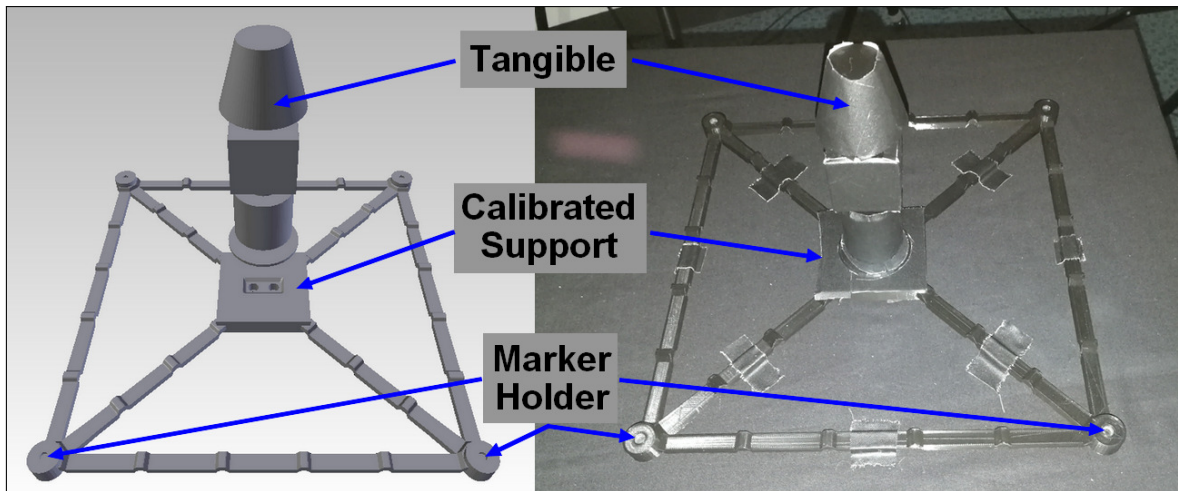


Figure B.2: Left: CAD model of the support. Right: 3D-printed support.

In short, the tangible can be picked up and put down easily by the user, without actually tracking it. However there are two limitation with this passive solution: the system cannot tell if the user actually grasped the object, nor can it tell if the object has slipped between the users' fingers and where did it fall. The design of the user studies of chapter 4 and chapter 5 took these limitations into consideration, while chapter 6 is actually solving the first limitation.

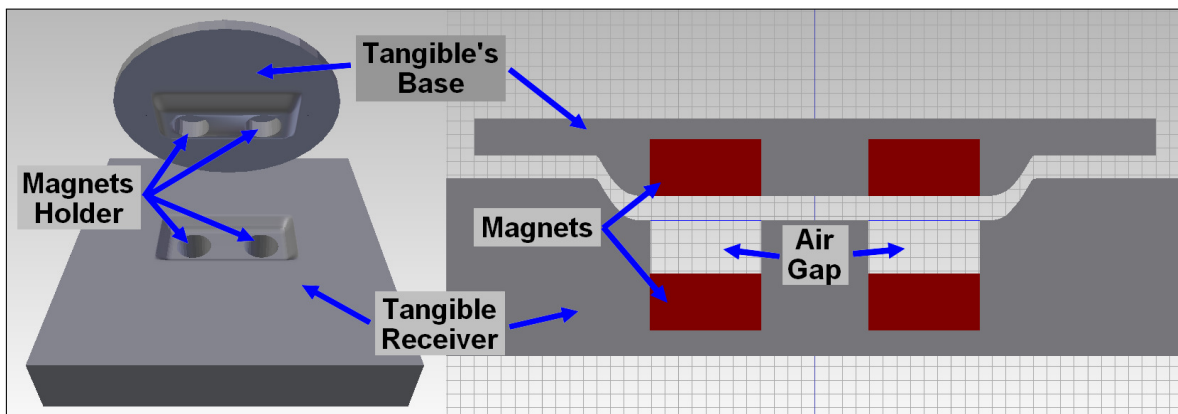


Figure B.3: Connection between the support and the tangible.

Thumb and Index Tracking

As we did need an accurate tracking of the fingertips, we directly tracked the distal phalanx as if it was a rigid prop: the optical tracking can obtain the position of a constellation of 3 markers embedded on 3D-printed attachments placed at the back of the finger as shown on Fig. B.4. These attachments are designed to be put behind the nail while slightly tightening the users' phalanx with gripping parts around the joint, and the border of finger pad. The nail and the pad of the finger remain free, as they are the most sensitive parts of the phalanx [25]. When the attachment fits the phalanx, it holds well enough not to fall, while not being too tight. Just in case, we also added on the back of the phalanx a little piece of wig-tape which is a double-sided tape specially made for the skin.

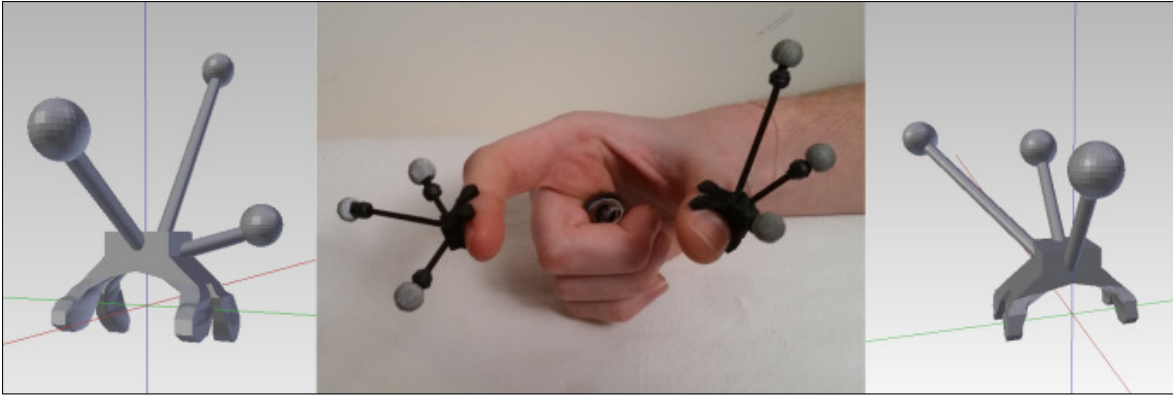


Figure B.4: 3D-printed attachments with constellations of markers. CADs of the thumb and index attachments respectively on the left and right side. A user wearing both in the middle.

The thumb and index have different constellations, so they can be differentiated from one-another. As the users pinch tangibles with horizontal grasps and the cameras are facing downward, the normal of the plans crossing the 3 markers of each constellation are tilted toward the vertical as to limit occlusion and ease the reconstruction process of the Blade software.

Design of the Attachment Sets

Since human hands come in various size, we made a whole set of attachments for index and thumb (see Fig. B.5).

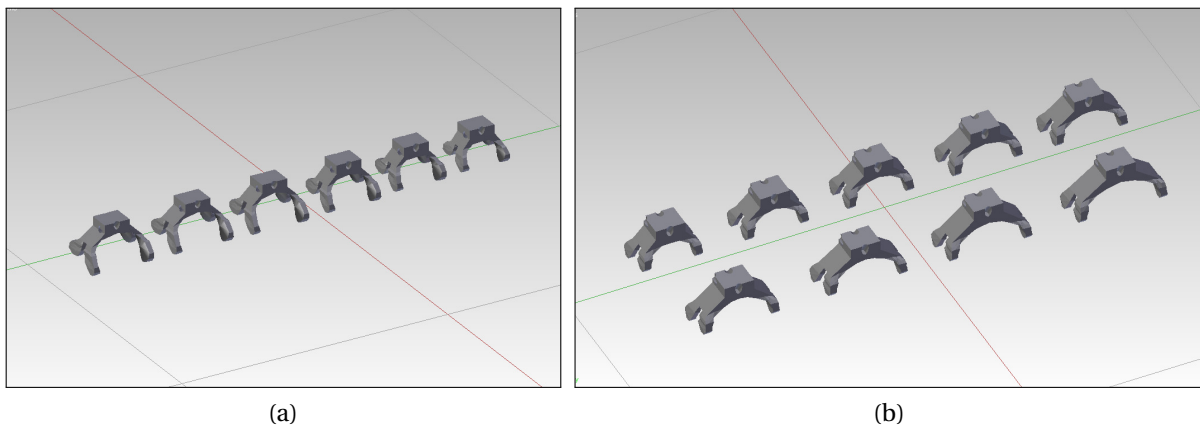


Figure B.5: Attachments Sets. Right: 6 index attachments. Left: 9 thumb attachments.

The bases onto which the constellations are built has standard dimensions, as specified in Fig. B.6. These cubic parts also have 3 holes into which we placed 3D-printed sticks of the specific length. At the end of these sticks are thin washers onto which are glued plastic screws for the markers. Below the base are the 4 arm parts which change in proportions through the sets. The smallest and largest sizes were set with the smallest and largest hand size we could find, then intermediary size where designed with incremental steps. We noticed that, the smaller a phalanx is, the thinner and shorter it is; thus the arm parts should not extend too much in any direction. As a consequence, we adjusted these parts along 6 different parameters highlighted in Fig. B.6.

- Width pincer: the width of the closing extremities which pinch the phalanx around the joint.
- Width joint: the largest width of the joint, which is actually the largest diameter of the bone.
- Width pad: the largest width of the pad, which is soft, thus the arm parts are flat.
- Length: the length of the attachment, which is kept as small as possible in order to avoid hindering the tip when touching a tangible.
- Thickness joint: the length of the arm parts partially circling the bone.
- Thickness pad: the length of the arm parts on the side of the pad, they are kept as short as possible in order to avoid colliding with the tangibles the users are touching.

The in-between parts of the attachments were just interpolated in order to provide an overall smooth shape.

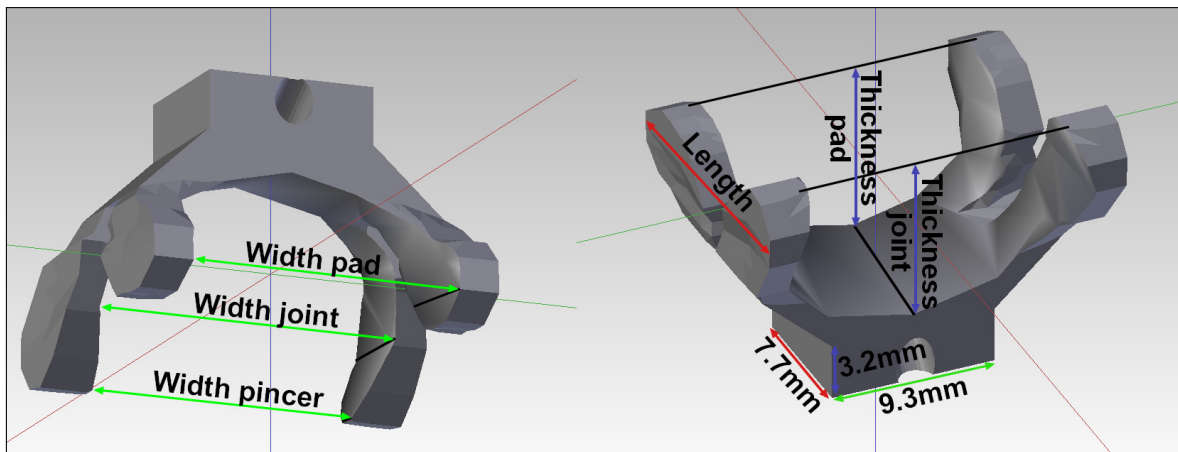


Figure B.6: Varying parameters of the sets.

The measurement of the index and thumb sets are given in Tab. B.1 and Tab. B.2.

Table B.1: Measurements of the attachments of the index set.

Parameters	I1	I2	I3	I4	I5	I6
width pincer	12.3	13.3	14.3	15.3	16.3	17.3
width bone	14.5	15.5	16.5	17.5	18.5	19.5
width pad	12	13	14	15	16	17
longueur	14.1	15.1	16.3	17	17.1	17.3
thickness bone	8.3	9.8	10.4	11.3	11.3	11.4
thickness pad	5	6	7	8	8	8

Virtual avatar registration

The tracking system is able to reconstruct the position and orientation of the constellations. However, it does not know where the surface of the users' pad is and the virtual fingers need to be positioned correctly with respect to the reconstructed position.

Table B.2: Measurements of the attachments of the thumb set.

Parameters	T1	T2	T3	T4	T5	T6	T7	T8	T9
width pincer	16	17	18	19	20	21	22	23	25
width bone	16.8	17.8	18.8	19.8	20.8	21.8	22.8	23.8	25.8
width pad	14.5	15.5	16.5	17.5	18.5	19.5	20.5	21.5	23.5
length	12	12	12	12	12	12	12	12	12
thickness bone	8.2	8.8	8.8	8.8	9.4	9.8	9.8	10.3	10.8
thickness pad	6.6	7.3	7.3	7.3	7.8	8.3	8.3	8.8	9.3

Hence, to compute the position and orientation offsets which need to be applied to the virtual fingers, we used a simple calibration process: We ask users to touch a specific point which is known in the support's frame, and simply position the virtual fingers, at the same time, at the exact same location in the virtual space. The position and orientation offsets are computed by knowing the targeted positions and orientations of the contact areas and the actual positions and orientations of the constellations, all of them into the same frame.

In Chap. 4 and Chap. 5, we tracked the users' thumb and index as to enable a pinching interaction. Thus, to calibrate their virtual thumb and index, we asked them to pinch a cylindrical prop on two indents. One of them is visible in Fig. B.7.

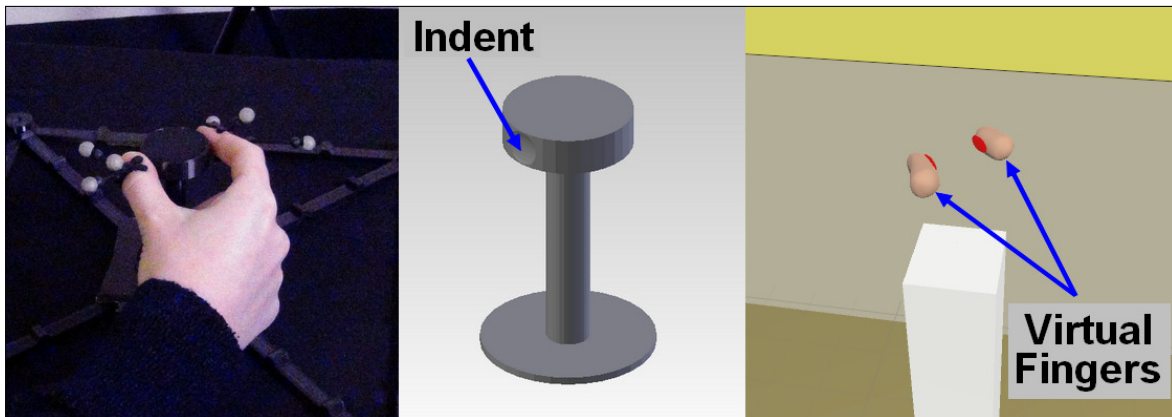


Figure B.7: Calibration procedure of the virtual fingers for pinching. Left: a user grasping the calibration prop. Middle: CAD of the calibration prop with two indents (second behind). Right: Virtual fingers positioned accordingly.

In Chap. 6, we only tracked the index as users only had to touch the surface of a tangible cube. Thus, to calibrate their virtual hand, we asked them to touch the upper surface of the cube while resting their finger along the slope a 3D-printed prop visible in Fig. B.8 in order to have the correct position and orientation.

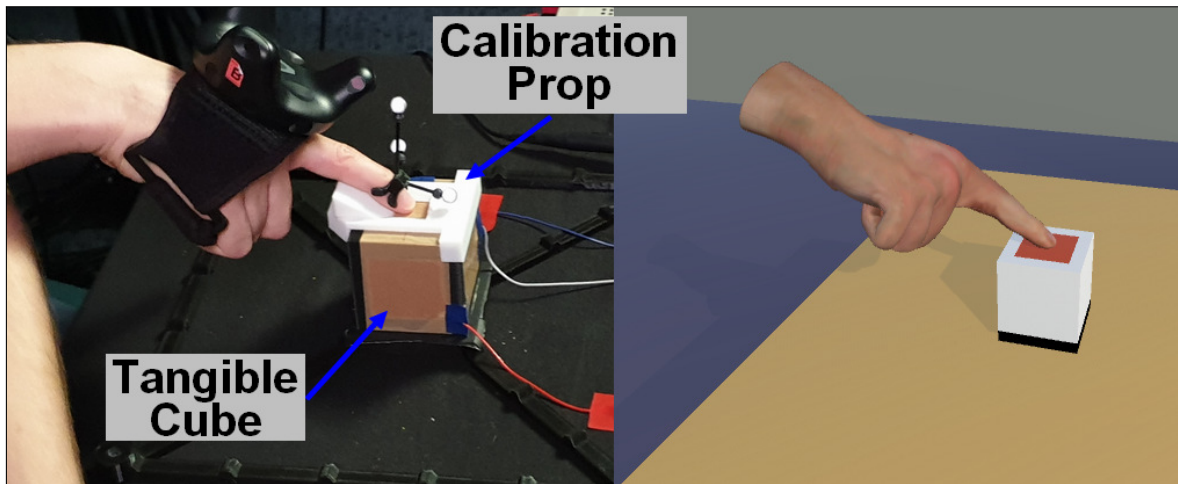


Figure B.8: Calibration procedure of the virtual hand for touching. Left: a user touching the upper while pressing against the slope of the calibration prop. Right: Virtual hand positioned accordingly.

Bibliography

- [1] I. E. Sutherland, “A head-mounted three dimensional display,” in *Proc. of the Fall Joint Computer Conference, Part I*, pp. 757–764, Association for Computing Machinery, 1968. [xiii](#), [1](#)
- [2] H. G. Hoffman, “Physically touching virtual objects using tactile augmentation enhances the realism of virtual environments,” in *Proc. of IEEE Virtual Reality Annual International Symposium*, pp. 59–63, 1998. [xiii](#), [4](#), [33](#), [35](#), [37](#), [47](#), [63](#), [154](#)
- [3] B. E. Insko, *Passive Haptics Significantly Enhances Virtual Environments*. PhD thesis, 2001. [xiii](#), [4](#), [15](#), [33](#), [34](#), [44](#), [47](#), [48](#), [63](#), [67](#)
- [4] P. Fuchs, G. Moreau, and P. Guitton, *Virtual Reality: Concepts and Technologies*. CRC Press, 2011. [2](#), [130](#)
- [5] P. Fuchs, *Les interfaces de la réalité virtuelle*. AJIIMD, 1996. [2](#)
- [6] P. Rajeswaran, T. Kesavadas, P. Jani, and P. Kumar, “Airwayvr: Virtual reality trainer for endotracheal intubation-design considerations and challenges,” in *Proc. of IEEE Conference on Virtual Reality and 3D User Interfaces*, pp. 1130–1131, 2019. [2](#)
- [7] M.-S. Bracq, M. Le Duff, E. Michinov, B. Arnaldi, V. Gouranton, J. Descamps, and P. Jannin, “Training situation awareness through error recognition in an immersive virtual operating room,” in *Proc. International Conference for Multi-Area Simulation*, pp. 208–216, 2019. [3](#)
- [8] A.-S. Dris, F. Lehericey, V. Gouranton, and B. Arnaldi, “Risk-Hunting Training in Interactive Virtual Environments,” in *Proc. of the 24th CIB W99 Conference*, pp. 1–8, 2018. [3](#)
- [9] S. A. Osimo, R. Pizarro, B. Spanlang, and M. Slater, “Conversations between self and self as Sigmund Freud—A virtual body ownership paradigm for self counselling,” *Scientific Reports*, vol. 5, no. 1, p. 13899, 2015. [3](#)
- [10] S. Seinfeld, J. Arroyo-Palacios, G. Iruretagoyena, R. Hortensius, L. E. Zapata, D. Borland, B. de Gelder, M. Slater, and M. V. Sanchez-Vives, “Offenders become the victim in virtual reality: Impact of changing perspective in domestic violence,” *Scientific Reports*, vol. 8, no. 1, 2018. [3](#)
- [11] M. V. Sanchez-Vives and M. Slater, “From presence to consciousness through virtual reality,” *Nature Reviews Neuroscience*, vol. 6, no. 4, pp. 332–339, 2005. [3](#), [4](#)
- [12] M. Slater, “Place illusion and plausibility can lead to realistic behaviour in immersive virtual environments,” *Philosophical Transactions of the Royal Society B: Biological Sciences*, vol. 364, no. 1535, pp. 3549–3557, 2009. [3](#), [4](#)

- [13] P. Fuchs, *Le traité de la réalité virtuelle*. Presses des MINES, 2006. 3
- [14] K. Kaspar, S. König, J. Schwandt, and P. König, “The experience of new sensorimotor contingencies by sensory augmentation,” *Consciousness and Cognition*, vol. 28, pp. 47–63, 2014. 4
- [15] H. Culbertson, S. B. Schorr, and A. M. Okamura, “Haptics: The Present and Future of Artificial Touch Sensation,” *Annual Review of Control, Robotics, and Autonomous Systems*, vol. 1, no. 1, pp. 385–409, 2018. 4, 16, 17, 34
- [16] C. C. Berger, M. Gonzalez-Franco, E. Ofek, and K. Hinckley, “The uncanny valley of haptics,” *Science Robotics*, vol. 3, p. eaar7010, 2018. 4, 67, 170
- [17] O. Shaer, “Tangible User Interfaces: Past, Present, and Future Directions,” *Foundations and Trends® in Human–Computer Interaction*, vol. 3, no. 1-2, pp. 1–137, 2009. 6
- [18] B. Ullmer and H. Ishii, “Emerging Frameworks for Tangible User Interfaces,” *IBM Systems Journal*, vol. 39, no. 3-4, pp. 915–931, 2000. 6, 34
- [19] K. P. Fishkin, “A taxonomy for and analysis of tangible interfaces,” *Personal and Ubiquitous Computing*, vol. 8, no. 5, 2004. 6
- [20] M. O. Ernst and M. S. Banks, “Humans integrate visual and haptic information in a statistically optimal fashion,” *Nature*, vol. 415, no. 6870, pp. 429–433, 2002. 8, 64, 91, 96
- [21] S. J. Lederman and R. L. Klatzky, “Haptic perception: A tutorial,” *Attention, Perception & Psychophysics*, vol. 71, no. 7, pp. 1439–1459, 2009. 15, 107
- [22] F. McGlone and D. Reilly, “The cutaneous sensory system,” *Neuroscience & Biobehavioral Reviews*, vol. 34, no. 2, pp. 148–159, 2010. 15
- [23] D. F. Collins, K. M. Refshauge, G. Todd, and S. C. Gandevia, “Cutaneous Receptors Contribute to Kinesthesia at the Index Finger, Elbow, and Knee,” *Journal of Neurophysiology*, vol. 94, no. 3, pp. 1699–1706, 2005. 15
- [24] D. Purves, G. J. Augustine, and D. Fitzpatrick, *Neuroscience*. Sinauer Associates, second ed., 2001. 15
- [25] R. S. Johansson and A. B. Vallbo, “Tactile sensibility in the human hand: Relative and absolute densities of four types of mechanoreceptive units in glabrous skin,” *The Journal of Physiology*, vol. 286, pp. 283–300, 1979. 15, V
- [26] W. Bergmann Tiest and A. Kappers, “Cues for Haptic Perception of Compliance,” *IEEE Transactions on Haptics*, vol. 2, no. 4, pp. 189–199, 2009. 15, 73, 80
- [27] W. M. Bergmann Tiest and A. M. L. Kappers, “Kinaesthetic and cutaneous contributions to the perception of compressibility,” in *Proc. of Haptics: Perception, Devices and Scenarios*, pp. 255–264, Springer Berlin Heidelberg, 2008. 15
- [28] E. R. Serina, E. Mockensturm, C. D. Mote, and D. Rempel, “A structural model of the forced compression of the fingertip pulp,” *Journal of biomechanics*, vol. 31, no. 7, pp. 639–646, 1998. 15

- [29] C. Giachritsis, R. Wright, and A. Wing, "The Contribution of Proprioceptive and Cutaneous Cues in Weight Perception: Early Evidence for Maximum-Likelihood Integration," in *Proc. of Haptics: Generating and Perceiving Tangible Sensations, EuroHaptics*, vol. 6191, pp. 11–16, Springer Berlin Heidelberg, 2010. [16](#)
- [30] J. Voisin, Y. Lamarre, and C. E. Chapman, "Haptic discrimination of object shape in humans: Contribution of cutaneous and proprioceptive inputs," *Experimental Brain Research*, vol. 145, no. 2, pp. 251–260, 2002. [16](#)
- [31] G. A. Gescheider, *Psychophysics: The Fundamentals*. Psychology Press, 2013. [16](#)
- [32] K. Shimoga, "A survey of perceptual feedback issues in dexterous telemanipulation. II. Finger touch feedback," in *Proc. of IEEE Virtual Reality Annual International Symposium*, pp. 271–279, 1993. [16](#), [17](#)
- [33] M. Benali-Khoudja, M. Hafez, J.-M. Alexandre, and A. Kheddar, "Tactile interfaces: A state-of-the-art survey," *International Symposium on Robotics*, vol. 31, pp. 23–26, 2004. [16](#), [17](#)
- [34] H. Seifi, F. Fazlollahi, M. Oppermann, J. A. Sastrillo, J. Ip, A. Agrawal, G. Park, K. J. Kuchenbecker, and K. E. MacLean, "Haptipedia: Accelerating Haptic Device Discovery to Support Interaction & Engineering Design," in *Proc. of CHI Conference on Human Factors in Computing Systems*, pp. 1–12, 2019. [16](#)
- [35] M. Sarac, M. Solazzi, and A. Frisoli, "Design Requirements of Generic Hand Exoskeletons and Survey of Hand Exoskeletons for Rehabilitation, Assistive, or Haptic Use," *IEEE Transactions on Haptics*, vol. 12, no. 4, pp. 400–413, 2019. [17](#), [30](#)
- [36] C. Pacchierotti, S. Sinclair, M. Solazzi, A. Frisoli, V. Hayward, and D. Prattichizzo, "Wearable haptic systems for the fingertip and the hand: Taxonomy, review, and perspectives," *IEEE Transactions on Haptics*, vol. 10, no. 4, pp. 580–600, 2017. [17](#), [28](#), [30](#), [72](#), [154](#)
- [37] D. Wang, M. Song, A. Naqash, Y. Zheng, W. Xu, and Y. Zhang, "Toward Whole-Hand Kinesthetic Feedback: A Survey of Force Feedback Gloves," *IEEE Transactions on Haptics*, vol. 12, no. 2, pp. 189–204, 2019. [17](#)
- [38] W. A. McNeely, "Robotic graphics: A new approach to force feedback for virtual reality," in *Proc. of IEEE Virtual Reality Annual International Symposium*, pp. 336–341, 1993. [17](#), [154](#)
- [39] H. Hoshino, R. Hirata, T. Maeda, and S. Tachi, "A construction method of virtual haptic space," in *Proc. of the 4th International Conference on Artificial Reality and Tele-Existence*, pp. 131–138, 1994. [18](#)
- [40] T. Furukawa, K. Inoue, T. Takubo, and T. Arai, "Encountered-type Visual Haptic Display Using Flexible Sheet," in *Proc. of IEEE International Conference on Robotics and Automation*, pp. 479–484, 2007. [18](#)
- [41] J. Posselt, R. Sas, L. Dominjon, and A. Bouchet, "Toward virtual touch: Investigating encounter-type haptics for perceived quality assessment in the automotive industry," in *Proc. of 14th annual EuroVR conference*, p. 3, 2017. [18](#)

- [42] E. Vonach, C. Gatterer, and H. Kaufmann, "VRRobot: Robot actuated props in an infinite virtual environment," in *Proc. of IEEE Virtual Reality*, pp. 74–83, 2017. [18](#), [60](#)
- [43] Y. Kim, H. J. Kim, and Y. J. Kim, "Encountered-type haptic display for large VR environment using per-plane reachability maps," *Computer Animation and Virtual Worlds*, vol. 29, no. 3-4, p. e1814, 2018. [18](#), [154](#)
- [44] M. Yafune and Y. Yokokohji, "Haptically rendering different switches arranged on a virtual control panel by using an encountered-type haptic device," in *Proc. of IEEE World Haptics Conference*, pp. 551–556, 2011. [18](#), [19](#), [65](#)
- [45] B. Araujo, R. Jota, V. Perumal, J. X. Yao, K. Singh, and D. Wigdor, "Snake Charmer: Physically Enabling Virtual Objects," in *Proc. of the 10th ACM International Conference on Tangible, Embedded, and Embodied Interaction*, pp. 218–226, 2016. [18](#), [19](#), [60](#), [61](#), [154](#)
- [46] V. R. Mercado, M. Marchal, and A. Lécuyer, "ENTROPiA: Towards Infinite Surface Haptic Displays in Virtual Reality Using Encountered-Type Rotating Props," *IEEE Transactions on Visualization and Computer Graphics*, 2019. [18](#), [19](#), [60](#)
- [47] E. Ruffaldi, "Haptic Rendering of Juggling with Encountered Type Interfaces," *Presence*, vol. 20, no. 5, pp. 480–501, 2011. [18](#), [19](#), [60](#), [154](#)
- [48] V. Mercado, M. Marchai, and A. Lécuyer, "Design and Evaluation of Interaction Techniques Dedicated to Integrate Encountered-Type Haptic Displays in Virtual Environments," in *Proc. of IEEE Conference on Virtual Reality and 3D User Interfaces*, pp. 230–238, 2020. [19](#), [60](#)
- [49] P. Knierim, T. Kosch, V. Schwind, M. Funk, F. Kiss, S. Schneegass, and N. Henze, "Tactile Drones - Providing Immersive Tactile Feedback in Virtual Reality through Quadcopters," in *Proc. of CHI Conference on Human Factors in Computing Systems*, pp. 433–436, 2017. [19](#), [20](#), [60](#)
- [50] M. Abdullah, M. Kim, W. Hassan, Y. Kuroda, and S. Jeon, "HapticDrone: An encountered-type kinesthetic haptic interface with controllable force feedback: Example of stiffness and weight rendering," in *Proc. of IEEE Haptics Symposium*, pp. 334–339, 2018. [19](#), [20](#), [60](#)
- [51] M. Hoppe, P. Knierim, T. Kosch, M. Funk, L. Futami, S. Schneegass, N. Henze, A. Schmidt, and T. Machulla, "VRHapticDrones: Providing Haptics in Virtual Reality through Quadcopters," in *Proc. of the 17th ACM International Conference on Mobile and Ubiquitous Multimedia*, pp. 7–18, 2018. [19](#), [20](#), [60](#)
- [52] P. Knierim, T. Kosch, A. Achberger, and M. Funk, "Flyables: Exploring 3D Interaction Spaces for Levitating Tangibles," in *Proc. of the 12th ACM International Conference on Tangible, Embedded, and Embodied Interaction*, pp. 329–336, 2018. [19](#), [20](#), [60](#), [154](#)
- [53] K. Yamaguchi, G. Kato, Y. Kuroda, K. Kiyokawa, and H. Takemura, "A Non-grounded and Encountered-type Haptic Display Using a Drone," in *Proc. of ACM Symposium on Spatial User Interaction*, pp. 43–46, 2016. [19](#), [20](#), [35](#), [36](#), [60](#)
- [54] Z. He, F. Zhu, A. Gaudette, and K. Perlin, "Robotic Haptic Proxies for Collaborative Virtual Reality," *CoRR*, 2017. [19](#), [21](#), [41](#), [43](#), [60](#), [62](#)

- [55] Z. He, F. Zhu, and K. Perlin, “Physhare: Sharing physical interaction in virtual reality,” in *Proc. of the 30th Annual ACM Symposium on User Interface Software and Technology*, p. 17–19, Association for Computing Machinery, 2017. [20](#), [21](#), [60](#), [62](#), [63](#), [155](#)
- [56] A. F. Siu, E. J. Gonzalez, S. Yuan, J. Ginsberg, A. Zhao, and S. Follmer, “shapeShift: A Mobile Tabletop Shape Display for Tangible and Haptic Interaction,” in *Proc. of the 30th Annual ACM Symposium on User Interface Software and Technology*, pp. 77–79, 2017. [20](#), [21](#), [55](#), [56](#), [60](#), [64](#)
- [57] Y. Wang, Z. T. Chen, H. Li, Z. Cao, H. Luo, T. Zhang, K. Ou, J. Raiti, C. Yu, S. Patel, and Y. Shi, “MoveVR: Enabling Multifform Force Feedback in Virtual Reality using Household Cleaning Robot,” in *Proc. of CHI Conference on Human Factors in Computing Systems*, pp. 1–12, 2020. [20](#), [21](#), [60](#)
- [58] R. Suzuki, H. Hedayati, C. Zheng, J. L. Bohn, D. Szafir, E. Y.-L. Do, M. D. Gross, and D. Leithinger, “RoomShift: Room-scale Dynamic Haptics for VR with Furniture-moving Swarm Robots,” in *Proc. of CHI Conference on Human Factors in Computing Systems*, pp. 1–11, 2020. [20](#), [21](#), [60](#)
- [59] H.-Y. Huang, C.-W. Ning, P.-Y. Wang, J.-H. Cheng, and L.-P. Cheng, “Haptic-go-round: A Surrounding Platform for Encounter-type Haptics in Virtual Reality Experiences,” in *Proc. of CHI Conference on Human Factors in Computing Systems*, pp. 1–10, 2020. [20](#), [21](#), [60](#), [61](#), [67](#), [170](#)
- [60] T. Feix, J. Romero, H.-B. Schmiedmayer, A. M. Dollar, and D. Kragic, “The GRASP Taxonomy of Human Grasp Types,” *IEEE Transactions on Human-Machine Systems*, vol. 46, no. 1, pp. 66–77, 2016. [21](#), [22](#), [170](#)
- [61] E. Fujinawa, S. Yoshida, Y. Koyama, T. Narumi, T. Tanikawa, and M. Hirose, “Computational design of hand-held VR controllers using haptic shape illusion,” in *Proc. of the 23rd ACM Symposium on Virtual Reality Software and Technology*, pp. 1–10, 2017. [22](#), [23](#), [56](#), [57](#), [64](#)
- [62] R. A. Montano-Murillo, C. Nguyen, R. H. Kazi, S. Subramanian, S. DiVerdi, and D. Martinez-Plasencia, “Slicing-Volume: Hybrid 3D/2D Multi-target Selection Technique for Dense Virtual Environments,” in *Proc. of IEEE Conference on Virtual Reality and 3D User Interfaces*, pp. 53–62, 2020. [22](#), [23](#), [52](#), [53](#), [67](#)
- [63] D. Matsumoto, K. Hasegawa, Y. Makino, and H. Shinoda, “Displaying variable stiffness by passive nonlinear spring using visuo-haptic interaction,” in *Proc. of IEEE World Haptics Conference*, pp. 587–592, 2017. [22](#), [23](#), [58](#), [64](#), [66](#)
- [64] M. Achibet, M. Marchal, F. Argelaguet, and A. Lécuyer, “The Virtual Mitten: A novel interaction paradigm for visuo-haptic manipulation of objects using grip force,” in *Proc. of IEEE Symposium on 3D User Interfaces (3DUI)*, pp. 59–66, 2014. [22](#), [23](#), [58](#), [64](#), [66](#)
- [65] A. Zenner and A. Kruger, “Shifty: A Weight-Shifting Dynamic Passive Haptic Proxy to Enhance Object Perception in Virtual Reality,” *IEEE Transactions on Visualization and Computer Graphics*, vol. 23, no. 4, pp. 1285–1294, 2017. [23](#), [55](#), [56](#), [64](#)

- [66] J. Shigeyama, T. Hashimoto, S. Yoshida, T. Aoki, T. Narumi, T. Tanikawa, and M. Hirose, "Transcalibur: Dynamic 2D haptic shape illusion of virtual object by weight moving VR controller," in *ACM SIGGRAPH*, pp. 1–2, 2018. [23](#), [55](#), [56](#), [64](#)
- [67] J. Shigeyama, T. Hashimoto, S. Yoshida, T. Narumi, T. Tanikawa, and M. Hirose, "Demonstration of Transcalibur: A VR Controller that Presents Various Shapes of Handheld Objects," in *Proc. of CHI Conference on Human Factors in Computing Systems*, pp. 1–4, 2019. [23](#)
- [68] Y. Liu, T. Hashimoto, S. Yoshida, T. Narumi, T. Tanikawa, and M. Hirose, "ShapeSense: A 2D shape rendering VR device with moving surfaces that controls mass properties and air resistance," in *Proc. of ACM SIGGRAPH 2019*, pp. 1–2, 2019. [23](#), [55](#), [56](#), [64](#)
- [69] A. Zenner, D. Degraen, F. Daiber, and A. Krüger, "Demonstration of Drag: on - A VR Controller Providing Haptic Feedback Based on Drag and Weight Shift," in *Proc. of CHI Conference on Human Factors in Computing Systems*, pp. 1–4, 2020. [23](#), [55](#), [56](#), [64](#)
- [70] C. Swindells, A. Unden, and T. Sang, "TorqueBAR: An ungrounded haptic feedback device," in *Proc. of the 5th ACM International Conference on Multimodal Interfaces*, pp. 52–59, 2003. [24](#), [25](#)
- [71] H. Yano, M. Yoshie, and H. Iwata, "Development of a non-grounded haptic interface using the gyro effect," in *Proc. of the 11th Symposium on Haptic Interfaces for Virtual Environment and Teleoperator Systems*, pp. 32–39, 2003. [24](#), [25](#)
- [72] K. N. Winfree, J. Gewirtz, T. Mather, J. Fiene, and K. J. Kuchenbecker, "A high fidelity ungrounded torque feedback device: The iTorqU 2.0," in *Proc. of IEEE World Haptics - Third Joint EuroHaptics conference and Symposium on Haptic Interfaces for Virtual Environment and Teleoperator Systems*, pp. 261–266, 2009. [24](#), [25](#)
- [73] E. Strasnick, C. Holz, E. Ofek, M. Sinclair, and H. Benko, "Haptic Links: Bimanual Haptics for Virtual Reality Using Variable Stiffness Actuation," in *Proc. of CHI Conference on Human Factors in Computing Systems*, pp. 1–12, 2018. [24](#), [25](#), [62](#), [63](#)
- [74] K. Kataoka, T. Yamamoto, M. Otsuki, F. Shibata, and A. Kimura, "A New Interactive Haptic Device for Getting Physical Contact Feeling of Virtual Objects," in *Proc. of IEEE Conference on Virtual Reality and 3D User Interfaces (VR)*, pp. 1323–1324, 2019. [24](#), [25](#)
- [75] S. Lu, Y. Chen, and H. Culbertson, "Towards Multisensory Perception: Modeling and Rendering Sounds of Tool-Surface Interactions," *IEEE Transactions on Haptics*, vol. 13, no. 1, pp. 94–101, 2020. [24](#), [25](#), [32](#), [59](#), [64](#)
- [76] A. L. Guinan, M. N. Montandon, A. J. Doxon, and W. R. Provancher, "Discrimination thresholds for communicating rotational inertia and torque using differential skin stretch feedback in virtual environments," in *Proc. of IEEE Haptics Symposium*, pp. 277–282, 2014. [24](#), [26](#)
- [77] D. K. Chen, J.-B. Chossat, and P. B. Shull, "HaptiVec: Presenting Haptic Feedback Vectors in Handheld Controllers using Embedded Tactile Pin Arrays," in *Proc. of CHI Conference on Human Factors in Computing Systems*, pp. 1–11, 2019. [25](#), [26](#)

- [78] S. Yoshida, Y. Sun, and H. Kuzuoka, “PoCoPo: Handheld Pin-based Shape Display for Haptic Rendering in Virtual Reality,” in *Proc. of CHI Conference on Human Factors in Computing Systems*, pp. 1–13, 2020. [25](#), [26](#)
- [79] Y. Sun, S. Yoshida, T. Narumi, and M. Hirose, “PaCaPa: A Handheld VR Device for Rendering Size, Shape, and Stiffness of Virtual Objects in Tool-based Interactions,” in *Proc. of CHI Conference on Human Factors in Computing Systems*, pp. 1–12, 2019. [25](#), [26](#), [66](#)
- [80] S. Kamuro, K. Minamizawa, and S. Tachi, “An ungrounded pen-shaped kinesthetic display: Device construction and applications,” in *Proc. of IEEE World Haptics Conference*, pp. 557–562, 2011. [25](#), [26](#)
- [81] H. Culbertson and K. J. Kuchenbecker, “Ungrounded Haptic Augmented Reality System for Displaying Roughness and Friction,” *IEEE/ASME Transactions on Mechatronics*, vol. 22, no. 4, pp. 1839–1849, 2017. [26](#), [59](#), [64](#)
- [82] G. Kato, Y. Kuroda, I. Nisky, K. Kiyokawa, and H. Takemura, “HapSticks: A novel method to present vertical forces in tool-mediated interactions by a non-grounded rotation mechanism,” in *Proc. of IEEE World Haptics Conference*, pp. 400–407, 2015. [26](#), [62](#), [66](#), [154](#)
- [83] G. Kato, Y. Kuroda, I. Nisky, K. Kiyokawa, and H. Takemura, “Design and Psychophysical Evaluation of the HapSticks: A Novel Non-Grounded Mechanism for Presenting Tool-Mediated Vertical Forces,” *IEEE Transactions on Haptics*, vol. 10, no. 3, pp. 338–349, 2017. [26](#), [62](#), [63](#)
- [84] H. Benko, C. Holz, M. Sinclair, and E. Ofek, “NormalTouch and TextureTouch: High-fidelity 3D Haptic Shape Rendering on Handheld Virtual Reality Controllers,” in *Proc. of the 29th Annual ACM Symposium on User Interface Software and Technology*, pp. 717–728, 2016. [26](#), [27](#)
- [85] E. Whitmire, H. Benko, C. Holz, E. Ofek, and M. Sinclair, “Haptic Revolver: Touch, Shear, Texture, and Shape Rendering on a Reconfigurable Virtual Reality Controller,” in *Proc. of CHI Conference on Human Factors in Computing Systems*, pp. 1–12, 2018. [27](#)
- [86] I. Choi, E. Ofek, H. Benko, M. Sinclair, and C. Holz, “CLAW: A Multifunctional Handheld Haptic Controller for Grasping, Touching, and Triggering in Virtual Reality,” in *Proc. of CHI Conference on Human Factors in Computing Systems*, pp. 1–13, 2018. [27](#), [28](#), [62](#), [63](#), [65](#), [66](#)
- [87] M. Sinclair, E. Ofek, M. Gonzalez-Franco, and C. Holz, “CapstanCrunch: A Haptic VR Controller with User-supplied Force Feedback,” in *Proc. of the 32nd Annual ACM Symposium on User Interface Software and Technology*, pp. 815–829, 2019. [27](#), [28](#), [62](#), [63](#), [65](#), [66](#)
- [88] P. Dills, N. Colonnese, P. Agarwal, and M. Zinn, “A Hybrid Active-Passive Actuation and Control Approach for Kinesthetic Handheld Haptics,” in *Proc. of IEEE Haptics Symposium*, pp. 690–697, 2020. [27](#), [28](#), [62](#), [63](#), [65](#), [66](#)
- [89] J. M. Walker, N. Zemiti, P. Poignet, and A. M. Okamura, “Holdable Haptic Device for 4-DOF Motion Guidance,” in *Proc. of IEEE World Haptics Conference*, pp. 109–114, 2019. [27](#), [28](#)

- [90] J. Lee, M. Sinclair, M. Gonzalez-Franco, E. Ofek, and C. Holz, "TORC: A Virtual Reality Controller for In-Hand High-Dexterity Finger Interaction," in *Proc. of CHI Conference on Human Factors in Computing Systems*, pp. 1–13, 2019. [27](#), [28](#), [58](#), [62](#), [63](#), [64](#), [66](#)
- [91] V. Hayward, O. R. Astley, M. Cruz-Hernandez, D. Grant, and G. Robles-De-La-Torre, "Haptic interfaces and devices," *Sensor Review*, vol. 24, no. 1, pp. 16–29, 2004. [28](#), [72](#)
- [92] A. Frisoli, M. Solazzi, F. Salsedo, and M. Bergamasco, "A Fingertip Haptic Display for Improving Curvature Discrimination," *Presence: Teleoperators and Virtual Environments*, vol. 17, no. 6, pp. 550–561, 2008. [28](#), [29](#)
- [93] M. Solazzi, A. Frisoli, and M. Bergamasco, "Design of a novel finger haptic interface for contact and orientation display," in *Proc. of IEEE Haptics Symposium*, pp. 129–132, 2010. [28](#), [29](#)
- [94] M. Gabardi, M. Solazzi, D. Leonardis, and A. Frisoli, "A new wearable fingertip haptic interface for the rendering of virtual shapes and surface features," in *Proc. of IEEE Haptics Symposium*, pp. 140–146, 2016. [28](#), [29](#)
- [95] K. Minamizawa, S. Fukamachi, H. Kajimoto, N. Kawakami, and S. Tachi, "Gravity grabber: Wearable haptic display to present virtual mass sensation," in *Proc. of ACM SIGGRAPH*, p. 8, 2007. [28](#), [29](#), [32](#), [58](#), [59](#), [64](#), [73](#), [74](#), [155](#)
- [96] C. Pacchierotti, G. Salvietti, I. Hussain, L. Meli, and D. Prattichizzo, "The hRing: A wearable haptic device to avoid occlusions in hand tracking," in *Proc. of IEEE Haptics Symposium*, pp. 134–139, 2016. [29](#), [30](#), [73](#), [74](#), [85](#)
- [97] D. Prattichizzo, F. Chinello, C. Pacchierotti, and K. Minamizawa, "RemoTouch: A system for remote touch experience," in *Proc. of the 19th International Symposium in Robot and Human Interactive Communication*, pp. 676–679, 2010. [29](#)
- [98] M. Bianchi, E. Battaglia, M. Poggiani, S. Ciotti, and A. Bicchi, "A Wearable Fabric-based display for haptic multi-cue delivery," in *Proc. of IEEE Haptics Symposium*, pp. 277–283, 2016. [29](#)
- [99] M. Bianchi, "A Fabric-Based Approach for Wearable Haptics," *Electronics*, vol. 5, p. 44, 2016. [29](#)
- [100] D. Prattichizzo, F. Chinello, C. Pacchierotti, and M. Malvezzi, "Towards Wearability in Fingertip Haptics: A 3-DoF Wearable Device for Cutaneous Force Feedback," *IEEE Transactions on Haptics*, vol. 6, no. 4, pp. 506–516, 2013. [29](#), [31](#)
- [101] D. Leonardis, M. Solazzi, I. Bortone, and A. Frisoli, "A wearable fingertip haptic device with 3 DoF asymmetric 3-RSR kinematics," in *Proc. of IEEE World Haptics Conference*, pp. 388–393, 2015. [29](#), [31](#)
- [102] D. Leonardis, M. Solazzi, I. Bortone, and A. Frisoli, "A 3-RSR Haptic Wearable Device for Rendering Fingertip Contact Forces," *IEEE Transactions on Haptics*, vol. 10, no. 3, pp. 305–316, 2017. [29](#)
- [103] F. Chinello, C. Pacchierotti, M. Malvezzi, and D. Prattichizzo, "A Three Revolute-Revolute-Spherical Wearable Fingertip Cutaneous Device for Stiffness Rendering," *IEEE Transactions on Haptics*, vol. 11, no. 1, pp. 39–50, 2018. [30](#), [31](#), [74](#), [97](#)

- [104] F. Chinello, M. Malvezzi, D. Prattichizzo, and C. Pacchierotti, "A Modular Wearable Finger Interface for Cutaneous and Kinesthetic Interaction: Control and Evaluation," *IEEE Transactions on Industrial Electronics*, vol. 67, no. 1, pp. 706–716, 2020. [30](#)
- [105] M. Maisto, C. Pacchierotti, F. Chinello, G. Salvietti, A. D. Luca, and D. Prattichizzo, "Evaluation of wearable haptic systems for the fingers in Augmented Reality applications," *IEEE Transactions on Haptics*, vol. 10, no. 4, pp. 511–522, 2017. [30](#), [85](#)
- [106] L. Meli, C. Pacchierotti, G. Salvietti, F. Chinello, M. Maisto, A. De Luca, and D. Prattichizzo, "Combining Wearable Finger Haptics and Augmented Reality: User Evaluation Using an External Camera and the Microsoft HoloLens," *IEEE Robotics and Automation Letters*, vol. 3, no. 4, pp. 4297–4304, 2018. [30](#)
- [107] S. B. Schorr and A. M. Okamura, "Three-Dimensional Skin Deformation as Force Substitution: Wearable Device Design and Performance During Haptic Exploration of Virtual Environments," *IEEE Transactions on Haptics*, vol. 10, no. 3, pp. 418–430, 2017. [30](#)
- [108] S. B. Schorr and A. M. Okamura, "Fingertip Tactile Devices for Virtual Object Manipulation and Exploration," in *Proc. of CHI Conference on Human Factors in Computing Systems*, pp. 3115–3119, 2017. [30](#), [31](#)
- [109] A. Girard, M. Marchal, F. Gosselin, A. Chabrier, F. Louveau, and A. Lécuyer, "HapTip: Displaying Haptic Shear Forces at the Fingertips for Multi-Finger Interaction in Virtual Environments," *Frontiers in ICT*, vol. 3, 2016. [30](#), [31](#)
- [110] Y.-L. Feng, C. L. Fernando, J. Rod, and K. Minamizawa, "Submerged haptics: A 3-DOF fingertip haptic display using miniature 3D printed airbags," in *Proc. of ACM SIGGRAPH*, pp. 1–2, 2017. [30](#), [31](#)
- [111] S. Laycock and A. Day, "A Survey of Haptic Rendering Techniques," *Computer Graphics Forum*, vol. 26, no. 1, pp. 50–65, 2007. [31](#), [32](#)
- [112] C. B. Zilles and J. K. Salisbury, "A constraint-based god-object method for haptic display," in *Proc. of IEEE/RSJ International Conference on Intelligent Robots and Systems. Human Robot Interaction and Cooperative Robots*, vol. 3, pp. 146–151, 1995. [31](#)
- [113] A. G. Perez, D. Lobo, F. Chinello, G. Cirio, M. Malvezzi, J. S. Martin, D. Prattichizzo, and M. A. Otaduy, "Optimization-Based Wearable Tactile Rendering," *IEEE Transactions on Haptics*, vol. 10, no. 2, pp. 254–264, 2017. [32](#)
- [114] E. M. Young, D. Gueorguiev, K. J. Kuchenbecker, and C. Pacchierotti, "Compensating for Fingertip Size to Render Tactile Cues More Accurately," *IEEE Transactions on Haptics*, vol. 13, no. 1, pp. 144–151, 2020. [32](#)
- [115] C. Pacchierotti, E. M. Young, and K. J. Kuchenbecker, "Task-Driven PCA-Based Design Optimization of Wearable Cutaneous Devices," *IEEE Robotics and Automation Letters*, vol. 3, no. 3, pp. 2214–2221, 2018. [32](#)
- [116] H. Culbertson, J. Unwin, and K. J. Kuchenbecker, "Modeling and Rendering Realistic Textures from Unconstrained Tool-Surface Interactions," *IEEE Transactions on Haptics*, vol. 7, no. 3, pp. 381–393, 2014. [32](#)

- [117] C. Pacchierotti, D. Prattichizzo, and K. J. Kuchenbecker, “Displaying Sensed Tactile Cues with a Fingertip Haptic Device,” *IEEE Transactions on Haptics*, vol. 8, no. 4, pp. 384–396, 2015. [33](#)
- [118] C. Pacchierotti, L. Meli, F. Chinello, M. Malvezzi, and D. Prattichizzo, “Cutaneous haptic feedback to ensure the stability of robotic teleoperation systems,” *The International Journal of Robotics Research*, vol. 34, no. 14, pp. 1773–1787, 2015. [33](#)
- [119] V. Hayward, “A brief taxonomy of tactile illusions and demonstrations that can be done in a hardware store,” *Brain Research Bulletin*, vol. 75, no. 6, pp. 742–752, 2008. [33](#)
- [120] S. J. Lederman and L. A. Jones, “Tactile and Haptic Illusions,” *IEEE Transactions on Haptics*, vol. 4, no. 4, pp. 273–294, 2011. [33](#)
- [121] G. Von Békésy, “Neural funneling along the skin and between the inner and outer hair cells of the cochlea,” *Journal of the Acoustical Society of America*, vol. 31, pp. 1236–1249, 1959. [33](#)
- [122] F. Biocca, J. Kim, and Y. Choi, “Visual Touch in Virtual Environments: An Exploratory Study of Presence, Multimodal Interfaces, and Cross-Modal Sensory Illusions,” *Presence*, vol. 10, no. 3, pp. 247–265, 2001. [33](#)
- [123] A. Lécuyer, “Simulating Haptic Feedback Using Vision: A Survey of Research and Applications of Pseudo-Haptic Feedback,” *Presence: Teleoperators and Virtual Environments*, vol. 18, no. 1, pp. 39–53, 2009. [34](#)
- [124] Y. Ban, T. Kajinami, T. Narumi, T. Tanikawa, and M. Hirose, “Modifying an identified curved surface shape using pseudo-haptic effect,” in *Proc. of IEEE Haptics Symposium*, pp. 211–216, 2012. [35](#), [36](#), [59](#), [60](#), [64](#)
- [125] Y. Ban, T. Narumi, T. Tanikawa, and M. Hirose, “MagicPot360: Free viewpoint shape display modifying the perception of shape,” in *Proc. of IEEE Virtual Reality*, pp. 321–322, 2015. [35](#), [36](#), [60](#), [96](#)
- [126] M. Suhail, S. P. Sargunam, D. T. Han, and E. D. Ragan, “Redirected reach in virtual reality: Enabling natural hand interaction at multiple virtual locations with passive haptics,” in *Proc. of IEEE Symposium on 3D User Interfaces*, pp. 245–246, 2017. [35](#), [36](#)
- [127] M. Suhail, S. P. Sargunam, D. T. Han, and E. D. Ragan, “Physical hand interaction for controlling multiple virtual objects in virtual reality,” in *Proc. of the 3rd ACM International Workshop on Interactive and Spatial Computing*, pp. 64–74, 2018. [35](#), [36](#), [53](#), [54](#), [65](#), [67](#)
- [128] D. T. Han, M. Suhail, and E. D. Ragan, “Evaluating Remapped Physical Reach for Hand Interactions with Passive Haptics in Virtual Reality,” *IEEE Transactions on Visualization and Computer Graphics*, vol. 24, no. 4, pp. 1467–1476, 2018. [35](#), [36](#), [54](#), [65](#), [67](#), [151](#), [155](#)
- [129] M. Azmandian, M. Hancock, H. Benko, E. Ofek, and A. D. Wilson, “Haptic retargeting: Dynamic repurposing of passive haptics for enhanced virtual reality experiences,” in *Proc. of CHI Conference on Human Factors in Computing Systems*, p. 1968–1979, 2016. [35](#), [36](#), [53](#), [54](#), [65](#), [67](#), [151](#), [155](#)

- [130] J. Spillmann, S. Tuchs Schmid, and M. Harders, "Adaptive Space Warping to Enhance Passive Haptics in an Arthroscopy Surgical Simulator," *IEEE Transactions on Visualization and Computer Graphics*, vol. 19, no. 4, pp. 626–633, 2013. [35](#), [36](#), [59](#), [60](#), [64](#), [66](#)
- [131] K. Hinckley, R. Pausch, J. C. Goble, and N. F. Kassell, "Passive real-world interface props for neurosurgical visualization," in *Proc. of SIGCHI Conference on Human Factors in Computing Systems*, pp. 452–458, 1994. [35](#), [37](#), [52](#), [53](#)
- [132] T. Ohshima, K. Satoh, H. Yamamoto, and H. Tamura, "Ar2 hockey: A case study of collaborative augmented reality," in *Proc. of IEEE Virtual Reality Annual International Symposium*, p. 268, 1998. [35](#), [37](#), [48](#), [49](#)
- [133] J. Sheng, R. Balakrishnan, and K. Singh, "An interface for virtual 3D sculpting via physical proxy," in *Proc. of the 4th ACM International Conference on Computer Graphics and Interactive Techniques*, p. 213–220, 2006. [35](#), [37](#)
- [134] A. Miller, B. White, E. Charbonneau, Z. Kanzler, and J. J. L. Jr, "Interactive 3D Model Acquisition and Tracking of Building Block Structures," *IEEE Transactions on Visualization and Computer Graphics*, vol. 18, no. 4, pp. 651–659, 2012. [35](#), [37](#)
- [135] M. Billinghurst, H. Kato, and I. Poupyrev, "The magicbook-moving seamlessly between reality and virtuality," *IEEE Computer Graphics and applications*, vol. 21, no. 3, pp. 6–8, 2001. [35](#), [37](#), [48](#), [49](#)
- [136] H. Kato, K. Tachibana, M. Tanabe, T. Nakajima, and Y. Fukuda, "MagicCup: A tangible interface for virtual objects manipulation in table-top augmented reality," in *Proc. of IEEE International Augmented Reality*, pp. 75–76, 2003. [35](#), [37](#), [49](#), [50](#)
- [137] T. Kashiwagi and K. Sumi, "Manipulating Virtual World with Props in Real-world," in *Proc. of IEEE Conference on Virtual Reality and 3D User Interfaces*, pp. 836–837, 2020. [35](#), [37](#), [66](#)
- [138] P. L. Strandholt, O. A. Dogaru, N. C. Nilsson, R. Nordahl, and S. Serafin, "Knock on Wood: Combining Redirected Touching and Physical Props for Tool-Based Interaction in Virtual Reality," in *Proc. of CHI Conference on Human Factors in Computing Systems*, pp. 1–13, 2020. [35](#), [37](#), [60](#), [66](#)
- [139] A. L. Simeone, E. Velloso, and H. Gellersen, "Substitutional reality: Using the physical environment to design virtual reality experiences," in *Proc. of the 33rd Annual ACM Conference on Human Factors in Computing Systems*, p. 3307–3316, 2015. [36](#), [38](#), [42](#), [43](#), [55](#), [57](#), [64](#), [65](#), [67](#), [96](#)
- [140] A. Hettiarachchi and D. Wigdor, "Annexing Reality: Enabling Opportunistic Use of Everyday Objects as Tangible Proxies in Augmented Reality," in *Proc. of CHI Conference on Human Factors in Computing Systems*, pp. 1957–1967, 2016. [36](#), [38](#), [55](#), [57](#), [64](#), [170](#)
- [141] Z. Yang, D. Weng, Z. Zhang, Y. Li, and Y. Liu, "Perceptual Issues of a Passive Haptics Feedback Based MR System," in *Proc. of IEEE International Symposium on Mixed and Augmented Reality*, pp. 310–317, 2016. [36](#), [38](#), [50](#), [51](#)

- [142] D. Lowe and Z. Liu, “Potential for utilising head-mounted displays (HMDs) for augmenting laboratories,” in *Proc. of 4th Experiment@International Conference*, pp. 165–170, 2017. [36](#), [38](#), [50](#), [51](#)
- [143] Q. Zhou, S. Sykes, S. Fels, and K. Kin, “Gripmarks: Using Hand Grips to Transform In-Hand Objects into Mixed Reality Input,” in *Proc. of CHI Conference on Human Factors in Computing Systems*, pp. 1–11, 2020. [36](#), [38](#), [66](#)
- [144] E. Kwon, G. J. Kim, and S. Lee, “Effects of sizes and shapes of props in tangible augmented reality,” in *Proc. of IEEE International Symposium on Mixed and Augmented Reality*, pp. 201–202, 2009. [37](#), [39](#), [96](#)
- [145] Y. Song, N. Zhou, Q. Sun, W. Gai, J. Liu, Y. Bian, S. Liu, L. Cui, and C. Yang, “Mixed Reality Storytelling Environments Based on Tangible User Interface: Take Origami as an Example,” in *Proc. of IEEE Conference on Virtual Reality and 3D User Interfaces*, pp. 1167–1168, 2019. [37](#), [39](#), [49](#)
- [146] K. J. Kruszyński and R. van Liere, “Tangible props for scientific visualization: Concept, requirements, application,” *Virtual Reality*, vol. 13, no. 4, p. 235, 2009. [37](#), [52](#)
- [147] J. Spence, D. P. Darzentas, Y. Huang, H. R. Cameron, E. Beestin, and S. Benford, “VRtefacts: Performative Substitutional Reality with Museum Objects,” in *Proc. of ACM Designing Interactive Systems Conference*, pp. 627–640, 2020. [37](#), [39](#), [66](#)
- [148] D. Clergeaud, J. Sol Roo, M. Hachet, and P. Guitton, “Towards Seamless Interaction between Physical and Virtual Locations for Asymmetric Collaboration,” in *Proc. of the 23rd ACM Symposium on Virtual Reality Software and Technology*, pp. 1–5, 2017. [37](#), [39](#), [49](#), [50](#)
- [149] J. Dong, J. Zhang, X. Ma, P. Ren, Z. C. Qian, and Y. V. Chen, “Virtual Reality Training with Passive Haptic Feedback for CryoEM Sample Preparation,” in *Proc. of IEEE Conference on Virtual Reality and 3D User Interfaces*, pp. 892–893, 2019. [37](#), [39](#), [50](#), [51](#), [64](#)
- [150] S. Gainer, S. Eadara, J. Haskins, W. Huse, B. Zhu, B. Boyd, C. Laird, J. Farantatos, and J. Jerald, “A Customized Input Device for Simulating the Detection of Hazardous Materials,” in *Proc. of IEEE Conference on Virtual Reality and 3D User Interfaces*, pp. 7–12, 2020. [38](#), [39](#), [50](#), [51](#), [66](#)
- [151] D. J. Zielinski, D. Nankivil, and R. Kopper, “Specimen Box: A tangible interaction technique for world-fixed virtual reality displays,” in *Proc. of IEEE Symposium on 3D User Interfaces*, pp. 50–58, 2017. [38](#), [39](#)
- [152] D. Englmeier, J. Dörner, A. Butz, and T. Höllerer, “A tangible spherical proxy for object manipulation in augmented reality,” in *Proc. of IEEE Conference on Virtual Reality and 3D User Interfaces*, pp. 221–229, 2020. [38](#), [39](#), [66](#)
- [153] T. Muender, A. V. Reinschluessel, S. Drewes, D. Wenig, T. Döring, and R. Malaka, “Does It Feel Real?: Using Tangibles with Different Fidelities to build and explore scenes in virtual reality,” in *Proc. of CHI Conference on Human Factors in Computing Systems*, pp. 1–12, 2019. [38](#), [39](#), [49](#), [50](#), [55](#), [57](#), [64](#)

- [154] A. Villegas, P. Perez, R. Kachach, F. Pereira, and E. Gonzalez-Sosa, “Realistic training in VR using physical manipulation,” in *Proc. of IEEE Conference on Virtual Reality and 3D User Interfaces*, pp. 109–118, 2020. [38](#), [39](#), [48](#), [49](#), [66](#)
- [155] L. Aguerreche, T. Duval, and A. Lécuyer, “Reconfigurable tangible devices for 3D virtual object manipulation by single or multiple users,” in *Proc. of the 17th ACM Symposium on Virtual Reality Software and Technology*, pp. 227–230, 2010. [39](#), [40](#), [55](#), [56](#), [64](#)
- [156] J. C. McClelland, R. J. Teather, and A. Girouard, “Haptobend: Shape-changing passive haptic feedback in virtual reality,” in *Proc. of the 5th Symposium on Spatial User Interaction*, pp. 82–90, 2017. [39](#), [40](#), [55](#), [56](#), [64](#)
- [157] Y. Zhao, L. H. Kim, Y. Wang, M. Le Goc, and S. Follmer, “Robotic Assembly of Haptic Proxy Objects for Tangible Interaction and Virtual Reality,” in *Proc. of ACM International Conference on Interactive Surfaces and Spaces*, pp. 82–91, 2017. [39](#), [40](#), [55](#), [56](#), [64](#)
- [158] S. Wang, W. He, B. Zheng, S. Feng, S. Wang, X. Bai, and M. Billingham, “Holding Virtual Objects Using a Tablet for Tangible 3D Sketching in VR,” in *Proc. of IEEE International Symposium on Mixed and Augmented Reality*, pp. 156–157, 2019. [40](#), [41](#), [67](#)
- [159] A. G. de Siqueira and A. Bhargava, “Tangibles within VR: Tracking, Augmenting, and Combining Fabricated and Commercially Available Commodity Devices,” [40](#), [41](#), [66](#)
- [160] P. Issartel, L. Besançon, T. Isenberg, and M. Ammi, “A tangible volume for portable 3D interaction,” in *Proc. of IEEE Symposium on Mixed and Augmented Reality*, pp. 215–220, 2016. [40](#), [41](#)
- [161] E. Callens, F. Danieau, A. Costes, and P. Guillotel, “A Tangible Surface for Digital Sculpting in Virtual Environments,” in *Proc. of Haptics: Science, Technology, and Applications, EuroHaptics*, vol. 10894, pp. 157–168, Springer International Publishing, 2018. [40](#), [41](#)
- [162] B. Panchaphongsaphak, R. Burgkart, and R. Riener, “Three-Dimensional Touch Interface for Medical Education,” *IEEE Transactions on Information Technology in Biomedicine*, vol. 11, no. 3, pp. 251–263, 2007. [40](#), [41](#), [52](#), [53](#)
- [163] H. Iwata, H. Yano, and N. Ono, “Volflex,” in *Proc. of ACM SIGGRAPH*, pp. 31–es, 2005. [40](#), [41](#)
- [164] A. Otte, D. Schneider, T. Menzner, T. Gesslein, P. Gagel, and J. Grubert, “Evaluating Text Entry in Virtual Reality using a Touch-sensitive Physical Keyboard,” in *Proc. of IEEE International Symposium on Mixed and Augmented Reality Adjunct*, pp. 387–392, 2019. [40](#), [41](#), [62](#), [63](#)
- [165] L. Zhao, Y. Liu, D. Ye, Z. Ma, and W. Song, “Implementation and Evaluation of Touch-based Interaction Using Electro-vibration Haptic Feedback in Virtual Environments,” in *Proc. of IEEE Conference on Virtual Reality and 3D User Interfaces*, pp. 239–247, 2020. [40](#), [42](#), [67](#)

- [166] A. Adilkhanov, A. Yelenov, R. S. Reddy, A. Terekhov, and Z. Kappassov, “VibeRo: Vibrotactile Stiffness Perception Interface for Virtual Reality,” *IEEE Robotics and Automation Letters*, vol. 5, no. 2, pp. 2785–2792, 2020. [40](#), [42](#), [58](#), [64](#), [66](#)
- [167] M. Sun, W. He, L. Zhang, and P. Wang, “Smart Haproxy: A Novel Vibrotactile Feedback Prototype Combining Passive and Active Haptic in AR Interaction,” in *Proc. of IEEE International Symposium on Mixed and Augmented Reality Adjunct*, pp. 42–46, 2019. [41](#), [42](#), [53](#), [54](#), [65](#)
- [168] D. Harley, A. P. Tarun, D. Germinario, and A. Mazalek, “Tangible VR: Diegetic Tangible Objects for Virtual Reality Narratives,” in *Proc. of the 2017 ACM Conference on Designing Interactive Systems*, pp. 1253–1263, 2017. [41](#), [42](#), [49](#), [66](#)
- [169] T. Amemiya and T. Maeda, “Asymmetric Oscillation Distorts the Perceived Heaviness of Handheld Objects,” *IEEE Transactions on Haptics*, vol. 1, no. 1, pp. 9–18, 2008. [41](#), [42](#), [58](#), [59](#), [64](#)
- [170] Y. Tanaka, S. Masataka, K. Yuka, Y. Fukui, J. Yamashita, and N. Nakamura, “Mobile Torque Display and Haptic Characteristics of Human Palm,” in *Proc. of International Conference on Artificial Reality and Tele-Existence*, p. 6, 2001. [41](#), [42](#)
- [171] D. Guinness, D. Szafir, and S. K. Kane, “GUI Robots: Using Off-the-Shelf Robots as Tangible Input and Output Devices for Unmodified GUI Applications,” in *Proc. of the 2017 ACM Conference on Designing Interactive Systems*, pp. 767–778, 2017. [41](#), [43](#), [66](#)
- [172] A. Inoue, T. Fukunaga, and R. Ishikawa, “Transformable Game Controller and Its Application to Action Game,” in *Proc. of IEEE Conference on Virtual Reality and 3D User Interfaces*, pp. 1317–1318, 2019. [41](#), [43](#), [55](#), [56](#)
- [173] J. Arora, A. Saini, N. Mehra, V. Jain, S. Shrey, and A. Parnami, “VirtualBricks: Exploring a Scalable, Modular Toolkit for Enabling Physical Manipulation in VR,” in *Proc. of CHI Conference on Human Factors in Computing Systems*, pp. 1–12, 2019. [42](#), [43](#), [56](#), [57](#), [64](#), [151](#)
- [174] M. Feick, S. Bateman, A. Tang, A. Miede, and N. Marquardt, “TanGi: Tangible Proxies for Embodied Object Exploration and Manipulation in Virtual Reality,” pp. 195–206, 2020. [42](#), [43](#), [57](#), [64](#)
- [175] K. Zhu, T. Chen, F. Han, and Y.-S. Wu, “HapTwist: Creating Interactive Haptic Proxies in Virtual Reality Using Low-cost Twistable Artefacts,” in *Proc. of CHI Conference on Human Factors in Computing Systems*, pp. 1–13, 2019. [42](#), [43](#), [57](#), [64](#)
- [176] A. L. Simeone, I. Mavridou, and W. Powell, “Altering User Movement Behaviour in Virtual Environments,” *IEEE Transactions on Visualization and Computer Graphics*, vol. 23, no. 4, pp. 1312–1321, 2017. [43](#)
- [177] L. Wang, Z. Zhao, X. Yang, H. Bai, A. Barde, and M. Billinghurst, “A Constrained Path Redirection for Passive Haptics,” in *Proc. of IEEE Conference on Virtual Reality and 3D User Interfaces*, pp. 650–651, 2020. [43](#)
- [178] L.-P. Cheng, L. Chang, S. Marwecki, and P. Baudisch, “iTürk: Turning Passive Haptics into Active Haptics by Making Users Reconfigure Props in Virtual Reality,” in *Proc. of the 2018 CHI Conference on Human Factors in Computing Systems*, pp. 1–10, 2018. [43](#), [53](#), [54](#), [65](#)

- [179] K. Matsumoto, T. Hashimoto, J. Mizutani, H. Yonahara, R. Nagao, T. Narumi, T. Tanikawa, and M. Hirose, “Magic table: Deformable props using visuo haptic redirection,” in *Proc. of SIGGRAPH Asia*, pp. 1–2, 2017. [43](#), [59](#), [60](#)
- [180] L. Kohli, E. Burns, D. Miller, and H. Fuchs, “Combining passive haptics with redirected walking,” in *Proc. of ACM International Conference on Augmented Tele-Existence*, pp. 253–254, 2005. [44](#), [53](#), [54](#), [65](#), [67](#)
- [181] S. Follmer, D. Leithinger, A. Olwal, A. Hogge, and H. Ishii, “inFORM: Dynamic physical affordances and constraints through shape and object actuation,” in *Proc. of the 26th Annual ACM Symposium on User Interface Software and Technology*, pp. 417–426, 2013. [44](#), [55](#), [56](#)
- [182] D. Degraen, A. Reindl, A. Makhsadov, A. Zenner, and A. Krüger, “Envisioning Haptic Design for Immersive Virtual Environments,” in *Proc. of ACM Designing Interactive Systems Conference*, pp. 287–291, 2020. [44](#)
- [183] A. Zenner, A. Makhsadov, S. Klingner, D. Liebemann, and A. Krüger, “Immersive Process Model Exploration in Virtual Reality,” *IEEE Transactions on Visualization and Computer Graphics*, vol. 26, no. 5, pp. 2104–2114, 2020. [44](#), [49](#), [50](#), [67](#)
- [184] B. J. Matthews, B. H. Thomas, S. Von Itzstein, and R. T. Smith, “Remapped Physical-Virtual Interfaces with Bimanual Haptic Retargeting,” in *Proc. of IEEE Conference on Virtual Reality and 3D User Interfaces*, pp. 19–27, 2019. [44](#), [45](#), [54](#), [65](#), [67](#)
- [185] R. Viciano-Abad, A. R. Lecuona, and M. Poyade, “The Influence of Passive Haptic Feedback and Difference Interaction Metaphors on Presence and Task Performance,” *Presence*, vol. 19, no. 3, pp. 197–212, 2010. [44](#), [45](#), [48](#)
- [186] D. Zielasko, M. Krüger, B. Weyers, and T. W. Kuhlen, “Menus on the Desk? System Control in DeskVR,” in *Proc. of IEEE Conference on Virtual Reality and 3D User Interfaces*, pp. 1287–1288, 2019. [45](#), [48](#)
- [187] L. Kohli, “Exploiting perceptual illusions to enhance passive haptics,” in *Proc. of IEEE VR*, pp. 22–24, 2009. [45](#), [59](#), [60](#), [64](#)
- [188] L. Kohli, “Redirected touching: Warping space to remap passive haptics,” in *Proc. of IEEE Symposium on 3D User Interfaces*, pp. 129–130, 2010. [45](#)
- [189] L. Kohli, M. C. Whitton, and F. P. Brooks, “Redirected Touching: Training and adaptation in warped virtual spaces,” in *Proc. of IEEE Symposium on 3D User Interfaces*, pp. 79–86, 2013. [45](#), [54](#), [65](#), [67](#), [90](#)
- [190] A. Kotranza and B. Lok, “Virtual human+ tangible interface= mixed reality human an initial exploration with a virtual breast exam patient,” in *Proc. of IEEE Virtual Reality Conference*, pp. 99–106, 2008. [45](#), [50](#), [51](#)
- [191] S. Hasanzadeh, N. F. Polys, and J. M. de la Garza, “Presence, Mixed Reality, and Risk-Taking Behavior: A Study in Safety Interventions,” *IEEE Transactions on Visualization and Computer Graphics*, vol. 26, no. 5, pp. 2115–2125, 2020. [45](#), [46](#), [51](#), [52](#), [63](#)
- [192] S. Aoyagi, A. Tanaka, S. Fukumori, and M. Yamamoto, “VR system to simulate tightrope walking with a standalone VR headset and slack rails,” in *Proc. of IEEE Conference on Virtual Reality and 3D User Interfaces*, pp. 1293–1294, 2019. [45](#), [46](#), [51](#), [52](#)

- [193] K. Vasylevska, B. I. Kovács, and H. Kaufmann, “VR Bridges: Simulating Smooth Uneven Surfaces in VR,” in *Proc. of IEEE Conference on Virtual Reality and 3D User Interfaces*, pp. 388–397, 2020. [45](#), [46](#)
- [194] C. Kasarda, M. Swartz, K. Mitchell, R. Khadka, and A. Banić, “Effects of Physical Prop Shape on Virtual Stairs Travel Techniques,” in *Proc. of IEEE Conference on Virtual Reality and 3D User Interfaces*, pp. 672–673, 2020. [45](#), [46](#)
- [195] R. Nagao, K. Matsumoto, T. Narumi, T. Tanikawa, and M. Hirose, “Infinite stairs: Simulating stairs in virtual reality based on visuo-haptic interaction,” in *Proc. of ACM SIGGRAPH*, pp. 1–2, 2017. [45](#), [46](#)
- [196] R. Nagao, K. Matsumoto, T. Narumi, T. Tanikawa, and M. Hirose, “Ascending and Descending in Virtual Reality: Simple and Safe System Using Passive Haptics,” *IEEE Transactions on Visualization and Computer Graphics*, vol. 24, no. 4, pp. 1584–1593, 2018. [45](#), [46](#)
- [197] K. Matsumoto, Y. Ban, T. Narumi, T. Tanikawa, and M. Hirose, “Curvature manipulation techniques in redirection using haptic cues,” in *Proc. of IEEE Symposium on 3D User Interfaces*, pp. 105–108, 2016. [46](#), [47](#)
- [198] K. Matsumoto, T. Narumi, Y. Ban, Y. Yanase, T. Tanikawa, and M. Hirose, “Unlimited Corridor: A Visuo-haptic Redirection System,” in *Proc. of the 17th International ACM Conference on Virtual-Reality Continuum and Its Applications in Industry*, pp. 1–9, 2019. [46](#), [47](#)
- [199] A. U. Batmaz, A. K. Mutasim, M. Malekmakan, E. Sadr, and W. Stuerzlinger, “Touch the Wall: Comparison of Virtual and Augmented Reality with Conventional 2D Screen Eye-Hand Coordination Training Systems,” in *Proc. of IEEE Conference on Virtual Reality and 3D User Interfaces*, pp. 184–193, 2020. [46](#), [47](#)
- [200] B. Eckstein, E. Krapp, and B. Lugrin, “Towards Serious Games and Applications in Smart Substitutional Reality,” in *Proc. of IEEE International Conference on Virtual Worlds and Games for Serious Applications*, pp. 1–8, 2018. [46](#), [47](#), [55](#), [64](#)
- [201] M. Tiator, B. Fischer, L. Gerhardt, D. Nowottnik, H. Preu, and C. Geiger, “Cliffhanger-VR,” in *Proc. of IEEE Conference on Virtual Reality and 3D User Interfaces*, pp. 1–2, 2018. [46](#), [47](#), [51](#), [52](#)
- [202] F. Ahmed, J. D. Cohen, K. S. Binder, and C. L. Fennema, “Influence of tactile feedback and presence on egocentric distance perception in virtual environments,” in *Proc. of IEEE Virtual Reality Conference*, pp. 195–202, 2010. [46](#), [47](#)
- [203] J.-R. Chardonnet, C. Di Loreto, J. Ryard, and A. Housseau, “A Virtual Reality Simulator to Detect Acrophobia in Work-at-Height Situations,” in *Proc. of IEEE Conference on Virtual Reality and 3D User Interfaces*, pp. 747–748, 2018. [46](#), [47](#), [51](#), [52](#)
- [204] L.-P. Cheng, T. Roumen, H. Rantzsch, S. Köhler, P. Schmidt, R. Kovacs, J. Jasper, J. Kemper, and P. Baudisch, “TurkDeck: Physical Virtual Reality Based on People,” in *Proc. of the 28th Annual ACM Symposium on User Interface Software and Technology*, pp. 417–426, 2015. [46](#), [47](#), [55](#), [56](#), [64](#)

- [205] S. Bovet, H. G. Debarba, B. Herbelin, E. Molla, and R. Boulic, "The Critical Role of Self-Contact for Embodiment in Virtual Reality," *IEEE Transactions on Visualization and Computer Graphics*, vol. 24, no. 4, pp. 1428–1436, 2018. [48](#)
- [206] H. Tamura, H. Yamamoto, and A. Katayama, "Mixed reality: Future dreams seen at the border between real and virtual worlds," *IEEE Computer Graphics and Applications*, vol. 21, no. 6, pp. 64–70, 2001. [48](#), [49](#)
- [207] A. D. Cheok, X. Yang, Z. Z. Ying, M. Billinghurst, and H. Kato, "Touch-space: Mixed reality game space based on ubiquitous, tangible, and social computing," *Personal and ubiquitous computing*, vol. 6, no. 5-6, pp. 430–442, 2002. [48](#)
- [208] H. G. Hoffman, A. Garcia-Palacios, A. Carlin, T. A. Furness III, and C. Botella-Arbona, "Interfaces That Heal: Coupling Real and Virtual Objects to Treat Spider Phobia," *International Journal of Human-Computer Interaction*, vol. 16, no. 2, pp. 283–300, 2003. [51](#), [52](#)
- [209] S. Jeon and S. Choi, "Stiffness modulation for Haptic Augmented Reality: Extension to 3D interaction," in *Proc. of IEEE Haptics Symposium*, pp. 273–280, 2010. [58](#), [64](#)
- [210] S. Jeon, S. Choi, and M. Harders, "Rendering Virtual Tumors in Real Tissue Mock-Ups Using Haptic Augmented Reality," *IEEE Transactions on Haptics*, vol. 5, no. 1, pp. 77–84, 2012. [58](#), [64](#)
- [211] L. Dominjon, A. Lecuyer, J. M. Burkhardt, P. Richard, and S. Richir, "Influence of control/display ratio on the perception of mass of manipulated objects in virtual environments," in *Proc. of IEEE Virtual Reality*, pp. 19–25, 2005. [58](#), [59](#), [64](#), [155](#), [167](#)
- [212] S. Asano, S. Okamoto, and Y. Yamada, "Vibrotactile Stimulation to Increase and Decrease Texture Roughness," *IEEE Transactions on Human-Machine Systems*, vol. 45, no. 3, pp. 393–398, 2015. [58](#), [59](#), [64](#)
- [213] C. W. Borst and R. A. Volz, "Evaluation of a Haptic Mixed Reality System for Interactions with a Virtual Control Panel," *Presence*, vol. 14, no. 6, pp. 677–696, 2005. [59](#), [60](#), [64](#)
- [214] H. Jiang and D. Weng, "HiPad: Text entry for Head-Mounted Displays Using Circular Touchpad," in *Proc. of IEEE Conference on Virtual Reality and 3D User Interfaces*, pp. 692–703, 2020. [62](#), [63](#)
- [215] M. Sinclair, E. Ofek, C. Holz, I. Choi, E. Whitmire, E. Strasnick, and H. Benko, "Three Haptic Shape-Feedback Controllers for Virtual Reality," in *Proc. of IEEE Conference on Virtual Reality and 3D User Interfaces*, pp. 777–778, 2018. [62](#)
- [216] J.-W. Lin, P.-H. Han, J.-Y. Lee, Y.-S. Chen, T.-W. Chang, K.-W. Chen, and Y.-P. Hung, "Visualizing the keyboard in virtual reality for enhancing immersive experience," in *Proc. of ACM SIGGRAPH*, pp. 1–2, 2017. [62](#), [63](#)
- [217] B. Benda, S. Esmaili, and E. D. Ragan, "Determining Detection Thresholds for Fixed Positional Offsets for Virtual Hand Remapping in Virtual Reality," 2020. [67](#), [155](#), [IV](#)
- [218] C. Pacchierotti, A. Tirmizi, G. Bianchini, and D. Prattichizzo, "Enhancing the Performance of Passive Teleoperation Systems via Cutaneous Feedback," *IEEE Transactions on Haptics*, vol. 8, no. 4, pp. 397–409, 2015. [82](#)

- [219] S. Kodaganur, I. R. Hosamani, M. Doddamani, and K. V. Udaykumar, "Mass in the Left Iliac Fossa-a Diagnostic Dilemma," *The Indian Journal of Surgery*, vol. 78, no. 1, pp. 54–56, 2016. [83](#)
- [220] M. J. Zigler, "Pressure Adaptation-Time: A Function of Intensity and Extensity," *The American Journal of Psychology*, vol. 44, no. 4, p. 709, 1932. [85](#)
- [221] K. Fujita and H. Ohmori, "A new softness display interface by dynamic fingertip contact area control," in *Proc. of 5th World Multiconference on Systemics, Cybernetics and Informatics*, pp. 78–82, 2001. [85](#)
- [222] J. Park, J. Kim, Y. Oh, and H. Z. Tan, "Compensation of perceived hardness of a virtual object with cutaneous feedback," in *Proc. of IEEE World Haptics Conference*, pp. 101–106, IEEE, 2017. [85](#)
- [223] S. V. Salazar, C. Pacchierotti, X. de Tinguy, A. Maciel, and M. Marchal, "Altering the Stiffness, Friction, and Shape Perception of Tangible Objects in Virtual Reality Using Wearable Haptics," *IEEE Transactions on Haptics*, vol. 13, no. 1, pp. 167–174, 2020. [85](#)
- [224] F. Argelaguet, L. Hoyet, M. Trico, and A. Lecuyer, "The role of interaction in virtual embodiment: Effects of the virtual hand representation," in *Proc. of IEEE Virtual Reality*, pp. 3–10, 2016. [89](#), [117](#)
- [225] A. L. Simeone, "Substitutional reality: Towards a research agenda," in *Proc. of IEEE 1st Workshop on Everyday Virtual Reality*, pp. 19–22, 2015. [96](#)
- [226] T. Feix, J. Romero, H.-B. Schmiedmayer, A. M. Dollar, and D. Kragic, "The GRASP Taxonomy of Human Grasp Types," *IEEE Transactions on Human-Machine Systems*, vol. 46, no. 1, pp. 66–77, 2016. [103](#)
- [227] M. R. Cutkosky, "On grasp choice, grasp models, and the design of hands for manufacturing tasks," *IEEE Transactions on Robotics and Automation*, vol. 5, no. 3, pp. 269–279, 1989. [103](#)
- [228] F. Cazals and M. Pouget, "Estimating differential quantities using polynomial fitting of osculating jets," *Computer Aided Geometric Design*, vol. 22, no. 2, pp. 121–146, 2005. [105](#), [110](#)
- [229] W. A. Hershberger and G. F. Misceo, "Touch dominates haptic estimates of discordant visual-haptic size," *Perception & Psychophysics*, vol. 58, no. 7, pp. 1124–1132, 1996. [106](#)
- [230] J. R. Flanagan and C. A. Bandomir, "Coming to grips with weight perception: Effects of grasp configuration on perceived heaviness," *Perception & Psychophysics*, vol. 62, no. 6, pp. 1204–1219, 2000. [106](#)
- [231] S. Yoshizawa, A. Belyaev, and H.-P. Seidel, "Fast and robust detection of crest lines on meshes," in *Proc. of ACM Symposium on Solid and Physical Modeling*, pp. 227–232, 2005. [113](#), [114](#)
- [232] M. Prachyabrued and C. W. Borst, "Visual feedback for virtual grasping," in *Proc. of IEEE Symposium on 3D User Interfaces*, pp. 19–26, 2014. [118](#)

- [233] M. Di Luca and A. Mahnan, “Perceptual Limits of Visual-Haptic Simultaneity in Virtual Reality Interactions,” in *Proc. of IEEE World Haptics Conference*, pp. 67–72, 2019. [130](#)
- [234] M. Di Luca, B. Knörlein, M. O. Ernst, and M. Harders, “Effects of visual-haptic asynchronies and loading-unloading movements on compliance perception,” *Brain Research Bulletin*, vol. 85, no. 5, pp. 245–259, 2011. [131](#)
- [235] B. Knörlein, M. Di Luca, and M. Harders, “Influence of visual and haptic delays on stiffness perception in augmented reality,” in *Proc. of IEEE International Symposium on Mixed and Augmented Reality*, pp. 49–52, 2009. [131](#), [167](#)
- [236] C. Jay, M. Glencross, and R. Hubbard, “Modeling the effects of delayed haptic and visual feedback in a collaborative virtual environment,” *ACM Transactions on Computer-Human Interaction*, vol. 14, no. 2, p. 8, 2007. [131](#)
- [237] T. Grosse-Puppenthal, C. Holz, G. Cohn, R. Wimmer, O. Bechtold, S. Hodges, M. S. Reynolds, and J. R. Smith, “Finding Common Ground: A Survey of Capacitive Sensing in Human-Computer Interaction,” in *Proc. of CHI Conference on Human Factors in Computing Systems*, pp. 3293–3315, 2017. [131](#)
- [238] K. Hinckley and M. Sinclair, “Touch-sensing input devices,” in *Proc. of ACM Conference on Human Factors in Computing Systems*, pp. 223–230, 1999. [131](#)
- [239] M. Sato, I. Poupyrev, and C. Harrison, “Touché: Enhancing touch interaction on humans, screens, liquids, and everyday objects,” in *Proc. of ACM Annual Conference on Human Factors in Computing Systems*, p. 483, 2012. [131](#), [132](#)
- [240] C. Honigman, J. Hochenbaum, and A. Kapur, “Techniques in Swept Frequency Capacitive Sensing: An Open Source Approach,” *NIME*, 2014. [132](#)
- [241] D. Marioli, E. Sardini, and A. Taroni, “Measurement of small capacitance variations,” in *Prof. of Conference on Precision Electromagnetic Measurements*, pp. 22–23, 1990. [132](#)
- [242] X. Lü, K. Xie, D. Xue, F. Zhang, L. Qi, Y. Tao, T. Li, W. Bao, S. Wang, X. Li, and R. Chen, “Capacitance variation measurement method with a continuously variable measuring range for a micro-capacitance sensor,” *Measurement Science and Technology*, vol. 28, no. 10, p. 105009, 2017. [132](#)
- [243] G. Barrett and R. Omote, “Projected-Capacitive Touch Technology,” *Information Display*, vol. 26, no. 3, pp. 16–21, 2010. [132](#)
- [244] N.-H. Yu, P. Huang, Y.-P. Hung, L.-W. Chan, S. Y. Lau, S.-S. Tsai, I.-C. Hsiao, D.-J. Tsai, F.-I. Hsiao, L.-P. Cheng, and M. Chen, “TUIC: Enabling tangible interaction on capacitive multi-touch displays,” in *Proc. of Annual Conference on Human Factors in Computing Systems*, p. 2995, ACM Press, 2011. [132](#)
- [245] J. Rekimoto, “SmartSkin: An infrastructure for freehand manipulation on interactive surfaces,” in *Proc. of SIGCHI Conference on Human Factors in Computing Systems*, pp. 113–120, 2002. [132](#), [170](#)

- [246] J. Novak and I. Feddema, "A capacitance-based proximity sensor for whole arm obstacle avoidance," in *Proc. of IEEE International Conference on Robotics and Automation*, vol. 2, pp. 1307–1314, 1992. [132](#)
- [247] H.-K. Lee, S.-I. Chang, and E. Yoon, "Dual-Mode Capacitive Proximity Sensor for Robot Application: Implementation of Tactile and Proximity Sensing Capability on a Single Polymer Platform Using Shared Electrodes," *IEEE Sensors Journal*, vol. 9, no. 12, pp. 1748–1755, 2009. [132](#)
- [248] V. Giordano and E. Rubiola, "Synthèse de fréquence," *Techniques de l'Ingénieur Électronique Analogique*, p. 16, 2002. [139](#)
- [249] Y. Yokokohji, N. Muramori, Y. Sato, and T. Yoshikawa, "Designing an Encountered-type Haptic Display for Multiple Fingertip Contacts Based on the Observation of Human Grasping Behaviors," *The International Journal of Robotics Research*, vol. 24, no. 9, pp. 717–729, 2005. [154](#)
- [250] S. Nakagawara, H. Kajimoto, N. Kawakami, S. Tachi, and I. Kawabuchi, "An Encounter-Type Multi-Fingered Master Hand Using Circuitous Joints," in *Proc. of IEEE International Conference on Robotics and Automation*, pp. 2667–2672, 2005. [154](#)
- [251] I. Poupyrev, T. Nashida, and M. Okabe, "Actuation and Tangible User Interfaces: The Vaucanson Duck, Robots, and Shape Displays," p. 205–212, 2007. [155](#)
- [252] J.-B. Chossat, D. K. Y. Chen, Y.-L. Park, and P. B. Shull, "Soft Wearable Skin-Stretch Device for Haptic Feedback Using Twisted and Coiled Polymer Actuators," *IEEE Transactions on Haptics*, vol. 12, no. 4, pp. 521–532, 2019. [155](#)

AVIS DU JURY SUR LA REPRODUCTION DE LA THESE SOUTENUE

Titre de la thèse:

Haptic Rendering in Virtual Reality During Interaction with Tangibles

Nom Prénom de l'auteur : DE TINGUY DE LA GIROULIERE XAVIER

Membres du jury :

- Monsieur COOPERSTOCK Jeremy
- Monsieur HARDERS Matthias
- Madame MARCHAL Maud
- Monsieur ROBUFFO GIORDANO Paolo
- Monsieur CHINELLO Francesco
- Monsieur PACCHIEROTTI Claudio

Président du jury : Paolo ROBUFFO GIORDANO

Date de la soutenance : 14 Décembre 2020

Reproduction de la these soutenue

- Thèse pouvant être reproduite en l'état
 Thèse pouvant être reproduite après corrections suggérées

Fait à Rennes, le 14 Décembre 2020

Signature du président de jury



Le Directeur,



Abdellatif MIRAOU



Titre : Rendu haptique en Réalité Virtuelle lors de l'interaction avec des objets tangibles

Mots clés : Réalité Virtuelle, Haptique, Objets Tangible, Interaction Virtuelle, Rendu Haptique

Résumé : Ce doctorat porte sur la conception de retour haptique lors de l'utilisation d'objets tangibles en réalité virtuelle. Lorsqu'il porte un visiocasque, l'utilisateur ne peut pas voir les objets tangibles et se retrouve à confronter les objets virtuels qu'il voit aux objets tangibles qu'il peut ressentir. Deux axes principaux de recherche ont été définis :

I) améliorer le rendu des objets virtuels en utilisant des objets tangibles différents, et II) améliorer le positionnement relatif entre les objets tangibles et les objets virtuels.

Tout d'abord, comme un objet tangible restitue une partie de l'environnement virtuel, nous étudierons comment et dans quelle mesure une différence entre les deux peut être introduite sans rompre l'immersion de l'utilisateur suivant trois stratégies : 1) en modifiant la perception que l'utilisateur a du tangible en ajoutant un stimulus tactile à l'aide d'un dispositif haptique

portable, 2) en introduisant intentionnellement des différences imperceptibles entre le tangible et sa représentation virtuelle sans que l'utilisateur ne s'en rende compte, et, 3) en associant un unique tangible à de multiples éléments de l'environnement virtuel tout en maximisant les similitudes entre eux.

Ensuite, étant donné que la superposition d'un objet tangible à un objet virtuel s'accompagne de limites en termes de précision ou de contraintes d'espace de travail, deux stratégies sont proposées pour résoudre certaines limitations du processus de superposition 1) à petite échelle, en compensant les erreurs de positionnement pour obtenir une synchronisation des contacts entre les mains et les objets réels et virtuels, et 2) à grande échelle, en fournissant un objet tangible à saisir et à relâcher n'importe où dans l'espace de travail, sans aucune restriction spatiale.

Title : Haptic rendering in Virtual Reality during interaction with Tangibles

Keywords : Virtual Reality, Haptics, Tangible Objects, Virtual Interaction, Haptic Rendering

Abstract : This thesis is centered around the usage of tangible objects in Virtual Reality. While wearing a Head Mounted Display, the user is unable see the tangibles and end up confronting the virtual objects he sees to the tangible ones he can feel. Two main axes were research upon this objective: I) improving the rendering of virtual objects using discrepant tangibles, and II) improving the registration between tangibles and virtual objects.

First, as a tangible object renders a part of the virtual environment, we will study how and to what extent a discrepancy between the two can be introduced without breaking the user's immersion with three strategies: 1) by altering the perception the user has of the tangible by adding an tactile stimuli using a wearable haptic

device, 2) by intentionally inducing unnoticeable discrepancies between the tangible and its virtual representation without the users noticing, and, 3) by pairing a single tangible to multiple elements of the virtual environment while maximizing the similitudes between them.

Second, as registering a tangible to a virtual object comes with limitation in terms of accuracy or workspace constraints, two strategies are proposed to solve some limitations of the registration process: 1) on a finer scale, by compensating setup errors to achieve contact synchronization between both real and virtual hand/object contacts, and, 2) on a large scale, by providing a tangible to grasp and release anywhere in the workspace, without any spatial restriction.